Universitat Autònoma de Barcelona

Contributions to the development of a bio-electronic regenerative interface for the injured peripheral nerve

Daniel Santos

Contributions to the development of a bio-electronic regenerative interface for the injured peripheral nerve

Daniel Santos

Group of Neuroplasticity and Regeneration. Department of Cellular Biology, Physiology and Immunology

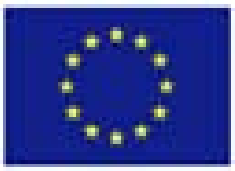

Contributions to the development of a bio-electronic regenerative interface for the injured peripheral nerve

Memòria de la Tesi Doctoral presentada per **Daniel Santos Rojas** per optar al grau de Doctor en Neurociències per la Universitat Autònoma de Barcelona

Aquesta tesi doctoral ha estat realitzada sota la dirección del

Dr. Xavier Navarro Acebes i Dr. **Jaume del Valle Macià**.

Director de Tesi
Dr. Xavier Navarro Acebes

Director de Tesi
Dr. Jaume del Valle Macià

Doctorand

Daniel Santos Rojas

Bellaterra, juny del 2016

Unitat de Fisiologia Mèdica. Departament de Biologia Cel·lular, Fisiologia i Immunologia. Institut de Neurociències

The research described in this thesis was conducted at the Department of Cellular Biology, Physiology and Immunology – Institute of Neuroscience, of the Universitat Autònoma de Barcelona in the Group of Neuroplasticity and Regeneration.

This research was supported by the European Union FP7-NMP project MERIDIAN under contract number 280778 and CIBERNED funds from the Fondo de Investigación Sanitaria of Spain.

I. INTRODUCTION

I. INTRODUCTION

1. Peripheral Nervous System

The peripheral nervous system (PNS) interconnects the central nervous system (CNS) with the limbs and different internal organs by means of the different cranial and spinal nerves. The PNS can be divided into the somatic and the autonomic nervous system. The somatic nervous system coordinates body movements and also receives information from external stimuli; it basically regulates activities that are under conscious control. On the other hand, the autonomic nervous system acts largely unconsciously and controls functions of internal organs, it is subdivided into the sympathetic, the parasympathetic and the enteric divisions.

Peripheral nerves are composed by axons extended from motor neurons located in the ventral horn of the spinal cord, from sensory neurons located in dorsal root ganglia (DRG) and from autonomic neurons, which innervate different target organs (Fig. 1A). Motor neurons can be divided in alpha motor neurons, that innervate skeletal muscle fibers, and gamma motor neurons that innervate muscle spindles. The sensory neurons can be mainly classified in proprioceptive, which provide information about the position of different parts of the body, mechanoreceptive, that code information on contacts or pressure, thermosensitive, that provide inputs on temperature, nociceptive, which process pain stimuli, and itch sensitive, that transmit inputs on irritation and tingling sensations (Usoskin et al., 2014). Motor and sensory neurons extend their axons that reside in a connective tissue matrix called endoneurium and are assembled together into bundles or fascicles defined by a second connective tissue layer called the perineurium. Groups of fascicles are then gathered together in a third connective tissue layer called epineurium (Fig. 1B).

Axons conduct electrical signals in the form of action potentials from target organs to CNS (afferent conduction) or from CNS to target organs (efferent conduction). In peripheral nerves, axons can be unmyelinated or myelinated by Schwann cells. Myelin is a concentrically laminated membrane constituted by lipids and proteins that surround some axons to electrically isolate them and thus increase the conduction velocity. In addition to myelination state, the caliber of axons and their conduction velocity is also variable and this has been used to classify axons in different groups (Erlanger and Gasser, 1937) (Table 1).

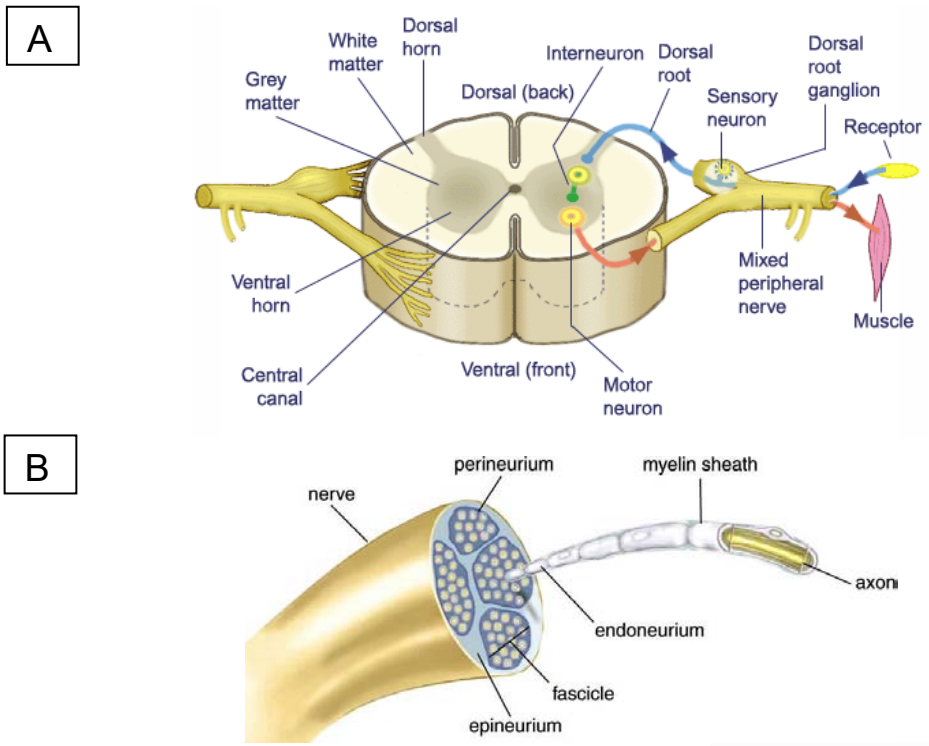

Figure 1. Anatomy of peripheral nervous system. (A) Peripheral nerves contain both sensory and motor axons that innervate skin receptors and muscles. Sensory neurons are located in dorsal root ganglia, whereas motoneurons are located in the ventral zone of spinal cord. (B) Transverse section of a peripheral nerve composed by epineurium, perineurium and endoneurium. Axons can be ensheathed by myelin and gathered together with other axons in fascicles. Adapted from people.eku.edu/ritchisong/342notes11.html (A) and classes.midlandstech.edu/carterp/Courses/bio110/ (B).

	Fiber	Diameter (µm)	Conduction Velocity (m/s)	Myelin	Function
Motor fibers	Aα	12-22	60-120	Yes	MN alpha control skeletal muscle
	Aγ	3-5	30-45	Yes	MN gamma control muscle spindle
Sensory Fibers	(Ia) Aα	12-22	60-120	Yes	Proprioception from muscle spindle
	(Ib) Aα				Proprioception from golgi tendon organs
	(II) Aβ	6-12	45-80	Yes	Fine touch and proprioception
	(III) Aδ	1-5	5-30	Yes	Light touch, fast pain and temperature
	(IV) C	0.3-1.5	0.5-2	No	Slow pain and temperature
Autonomic Fibers	B	6-12	45-80	Yes	Simpathetic preganglionic
	C	0.3-1.5	0.5-2	No	Simpathetic postganglionic

Table 1. Classification of peripheral nerve fibers. Adapted from Erlanger & Gasser (1937).

2. Nerve injury and regeneration

The incidence of peripheral nerve injury (PNI) is estimated between 13 and 23 per 100,000 persons per year in the developed countries, and in United States it results in approximately $150 billion spent in annual health-care (Taylor et al., 2008).

There are different etiologies of peripheral nerve injury such as direct mechanical trauma, laceration, compression, ischemia or stretch-related injuries (Campbell, 2008). After injury, there is a partial or total loss of motor, sensory and autonomic functions produced by interruption of axon continuity and consequently, the disconnection of the target organ from the nervous system. This situation results in a decreased quality of life because of permanently impaired sensory and motor functions and secondary problems, such as phantom limb or neuropathic pain phenomena, and has major social consequences in terms of health care and long periods of sick-leave (Jaquet et al., 2006; Rosberg et al., 2005). Such injuries have also a profound and permanent impact on patients and their ability to perform activities of daily living, as well as preventing return to work (Faroni et al., 2015).

Transected fibers distal to the lesion are disconnected from the neuronal body leaving the target organs denervated. Moreover, disconnected distal fibers undergo Wallerian degeneration, a process that helps to create a microenvironment that favors axonal regrowth (Stoll and Müller, 1999). In parallel, several molecular and cellular changes known as retrograde reaction and chromatolysis occur at the soma of axotomized neurons and leads to metabolic changes necessary for regeneration and axonal elongation (Navarro et al., 2007). The functional significance of axonal regeneration is to replace the distal nerve segment lost during degeneration, allowing reinnervation of target organs and restitution of their corresponding functions.

Still, not all the regenerating axons reinnervate their original targets and functional recovery is usually poor (Lundborg and Rosén, 2001; Valero-Cabré and Navarro, 2002). In addition, several factors affect axon regeneration and functional reinnervation such as patient's age, the nerve trunk affected, the site and type of lesion, the type and delay of surgical repair and the distance over which axons must regrow to span the injury (Navarro et al., 2007).

In the next sections, different events involved in nerve regeneration and target reinnervation are further described.

2.1.Types of Nerve Injury

The prognosis for functional return and timing of the peripheral nerve repair depends on the severity of nerve injury and the eventual distance between nerve stumps. Moreover, the nerve trunk injured, and the type and severity of the lesion will determine the need for surgical repair and which technique to apply. The classifications of mechanical nerve lesions of Seddon (Seddon, 1943) and of Sunderland (Sunderland, 1990) are based upon the morphology of the lesion and the nerve sheaths damaged (Fig. 2). Seddon divided nerve injuries by severity into three broad categories: neurapraxia, axonotmesis, and neurotmesis. On the other hand, Sunderland performed a most detailed classification that differentiates five degrees of injury:

1- The first degree (neurapraxia of Seddon) usually corresponds to a compression that causes a focal blocking of impulse conduction. By histology, there are no signals of degeneration in the distal stump as damage only affects myelin sheaths and nerve continuity is maintained. This lesion reverts within short time once the cause is eliminated.

2- In second degree injuries (axonotmesis of Seddon) the axons are interrupted, but the endoneurium remains intact. Nerve fibers distal to the lesion degenerate and recovery requires regeneration of the severed axons. Recovery is usually good because intact endoneurial tubes and basal lamina of Schwann cells guide regenerative axons towards their original target organ and allow an adequate reinnervation

3- The third degree of nerve lesion implies only the disruption of axons and of endoneurial tubes, whereas the perineurium or epineurium remains intact. This results in wallerian degeneration of injured axons and also in internal disorganization of the nerve fascicles.

4- In the fourth degree injury, the perineurium is also damaged remaining intact only the epineurium. This results in disorganization of the fascicular architecture, intraneural scar formation, and loss of directional guidance for regenerating axons.

5- The fifth degree of lesion (neurotmesis of Seddon) involves the complete transection of the nerve, with degeneration and disarrangement of the distal segment. In all cases there is separation of the nerve stumps due to the elastic forces.

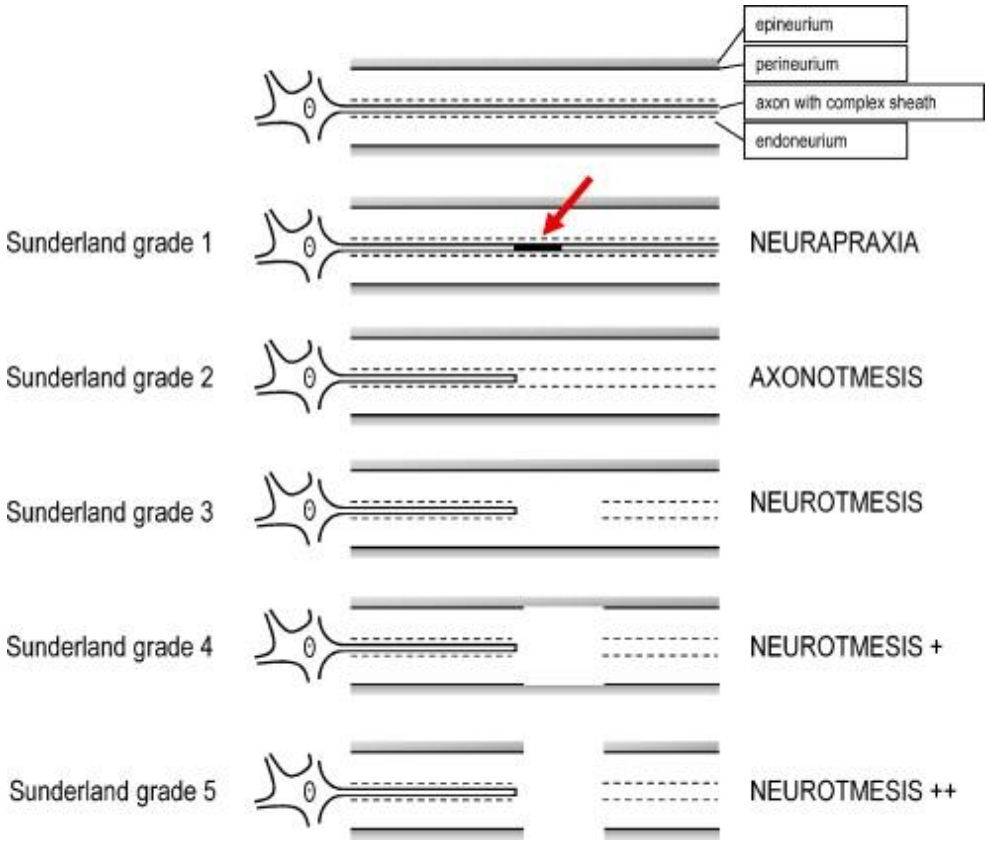

Figure 2. Classification of nerve injuries. Schematic representation of the five degrees of nerve injury according to Sunderland (Sunderland, 1990). Grade 1: conduction block indicated by red arrow (neurapraxia), Grade 2: transection of axon with an intact endoneurium (axonotmesis), Grade 3: transection of the nerve fiber (axon and endoneurium) within an intact perineurium (neurotmesis), Grade 4: transection of funiculi, epineurial tissue maintains nerve trunk continuity (neurotmesis +), Grade 5: transection of the whole nerve trunk (neurotmesis ++). (Extracted from Deumens et al., 2010).

After neurapraxia and axonotmesis (grade 1 and 2), functional recovery is usually good whereas from the third degree of injury, prognosis for recovery is poor and surgical repair may be indicated, being mandatory in grade 4 and 5 injuries as structural and fascicular alterations hinder the adequate regeneration and reconstitution of the nerve spontaneously. Moreover, after nerve transection endoneurial tubes loss their continuity and surgical repair will need to reestablish the gross continuity of the nerve trunk, avoiding the formation of scar tissue at the lesion site and providing the injured axons with a proper terrain for regrowth. However, although it has been described that in certain conditions motor axons will grow through muscular pathways and preferentially reinnervate distal muscles (Brushart, 1993), it is widely accepted that

regenerating axons are often misdirected and reinnervate incorrect target organs even if refined repair is applied (Bodine-Fowler et al., 1997; Sunderland, 1990; Valero-Cabré and Navarro, 2002).

2.2. Types of repair after neurotmesis

After neurotmesis or complete transection, both nerve stumps have to be reapposed in order to facilitate that proximal axons invade distal stump and reinnervate the target organs. The different types of nerve repair (Navarro and Verdú, 2004) are described below:

Direct Suture

The ideal method is to reappose both nerve stumps by epineural sutures; however this is only possible if the lesion is a clean cut and the repair takes place soon after the injury to avoid an excessive retraction of nerve stumps (Papalia et al., 2007). Nevertheless, although microsurgical identification and coaptation of individual fascicles is possible by means of perineurial sutures, direct suture does not still ensure correct matching of the fascicular organization of the nerve trunk.

Fibrin Glue

Fibrin glue is a blood-derived adhesive product that can be also used to directly reappose both nerve stumps without sutures. The main advantages of glues to seal nerve endings are reduced surgical and recovery time, decreased fibrosis and inflammation in addition to providing coaptation of severed nerve fascicles with minimal induced trauma and neural scar tissue. A systematic review on the use of fibrin glue for peripheral nerve repair showed less granulomatous inflammation in fibrin glue groups in comparison with conventional suturing methods. On the other hand, overall axonal regeneration, fiber alignment, and recovery of nerve conduction velocities of fibrin glue were equal to that of microsuturing (Sameem et al., 2011).

Nerve graft

A transplanted nerve from the same patient (autograft) or from a donor (allograft) can be implanted to physically connect the proximal with the distal nerve stump. This approach is mainly used when the length of the gap created by tissue destruction and nerve retraction is too long to allow a direct suture without tension and a nerve graft between the nerve stumps of a transected nerve will offer mechanical guidance as well as a stimulating environment for the advancing axons (Gómez et al., 1996). It is

generally agreed that gaps in injured nerves are most successfully bridged by the use of autologous nerve grafts than with other materials as grafts behave in the same way as does the distal segment of the own severed nerve.

In comparison with direct suture, regenerating axons have to cross two suture lines and the chances for misdirection increase. However, experimental studies (Ray and Mackinnon, 2010) have shown that autograft repair allows for similar number of regenerated axons and functional recovery than direct suture repair. Nevertheless, autograft repair may also imply some problems such as the need of a second surgical step, elimination of the donor nerve function, a limited supply of donor nerves and the mismatch between nerve and graft dimensions (Deumens et al., 2010). Moreover, donor nerves are limited to those with small caliber and pure sensory function, such as sural and antebrachial cutaneous nerves, causing lesser promotion of regeneration (Navarro and Verdú, 2004). On the other hand, if an allograft is used to circumvent these problems, the immunosupression treatment may restrain the use of this treatment for some patients (Navarro et al., 2001).

Tube repair

In this type of repair, proximal and distal nerve stumps are introduced a few millimeters within the ends of a tube and hold in place by means of one or a few epineurial sutures, leaving a gap between nerve stumps. The implantation of a tube or guide to bridge a nerve gap has provided a useful model for studying the cellular and biochemical events during peripheral nerve regeneration, and it has been also successfully applied for repairing injured nerves in different animal models, and in human patients (Arslantunali et al., 2014). The development of an artificial nerve graft, composed by a conduit filled with exogenous elements that promote axonal regeneration, has been pursued to provide for an effective alternative to solve the secondary problems of autograft and allograft repairs.

Nerve guides offer thus a closed space where neurotrophic elements provided by the injured nerve stumps accumulate and support axonal growth. Accordingly, tubulization allows successful regeneration over longer gaps than in unrepaired nerves. However, a limit to regeneration also exists within nerve guides depending upon the length of the gap (Navarro and Verdú, 2004). It is generally considered that in humans, for nerve gaps of less than 2 cm neurological recovery is moderate, but for gaps longer than 4 cm recovery is minimal to non-existent (Reyes et al., 2005). Likewise, tubes does not ensure the repair of gaps longer than 10 mm in rat (Butí et al., 1996).

There are several advantages of tubulization versus classical nerve repair methods. Tube repair involve an easier implantation, avoids tension, limits excessive collagen

and scar formation at the suture lines, provides directional guidance to the regenerating axons and prevents axonal escape into the surrounding tissues. In addition, nerve guides offer a controlled microenvironment, where different adjuncts may be applied in situ to promote axonal regeneration. Nerve guides may be produced in different dimensions and lengths to match different lesions, and stored for use when needed. However, regeneration outcomes are not as good as in autograft repair. Thus, the physico-chemical characteristics of the tube, mainly in terms of dimension, permeability, durability and wall composition, also influence the chances of regeneration, and further advances in biomaterials will likely improve the effectiveness of tubulization repair in order to reach autograft outcomes (Deumens et al., 2010).

2.3. Neuronal reaction after nerve injury

The success of nerve regeneration and functional reinnervation of targets depends at a first instance on the capacity of axotomized neurons to switch from a synaptic state to a regenerative state known as neuronal reaction and chromatolysis. These shifts in the neuronal soma promote a set of phenotypic changes that consist in the dissolution of the Nissl bodies, nuclear eccentricity, nuclear and nucleolar enlargement, cell swelling, and retraction of dendrites (Lieberman, 1971).

After axotomy, the rapid arrival of injury-induced signals in the soma is followed by the induction of transcription factors, adhesion molecules, growth-associated proteins and structural components, all of them needed for axonal regrowth (Rishal and Fainzilber, 2014) (Fig. 3). First, when the axoplasm comes into contact with the extracellular environment, a back-propagating calcium wave (Cho et al., 2013) and a high frequency burst of action potentials generated at the lesion site rapidly inform the cell body about distant axon injury contributing to activate several protein kinase pathways (Ghosh and Greenberg, 1995). A second set of signals includes the early deprivation of target derived trophic factors (Lee et al., 1998; Raivich et al., 1991) and the arrival of activating signals not only from the own injured axons but also from other non-neuronal cells. Finally, when the axoplasm is sealed, it expresses different receptors for neurotrophic factors or cytokines that can be activated, internalized and reach the neuronal body by retrograde transport when Schwann cells and infiltrating macrophages release these molecules in the degenerating environment that contribute to sustain the regenerative program of the neuron (Curtis et al., 1998, 1994, 1993).

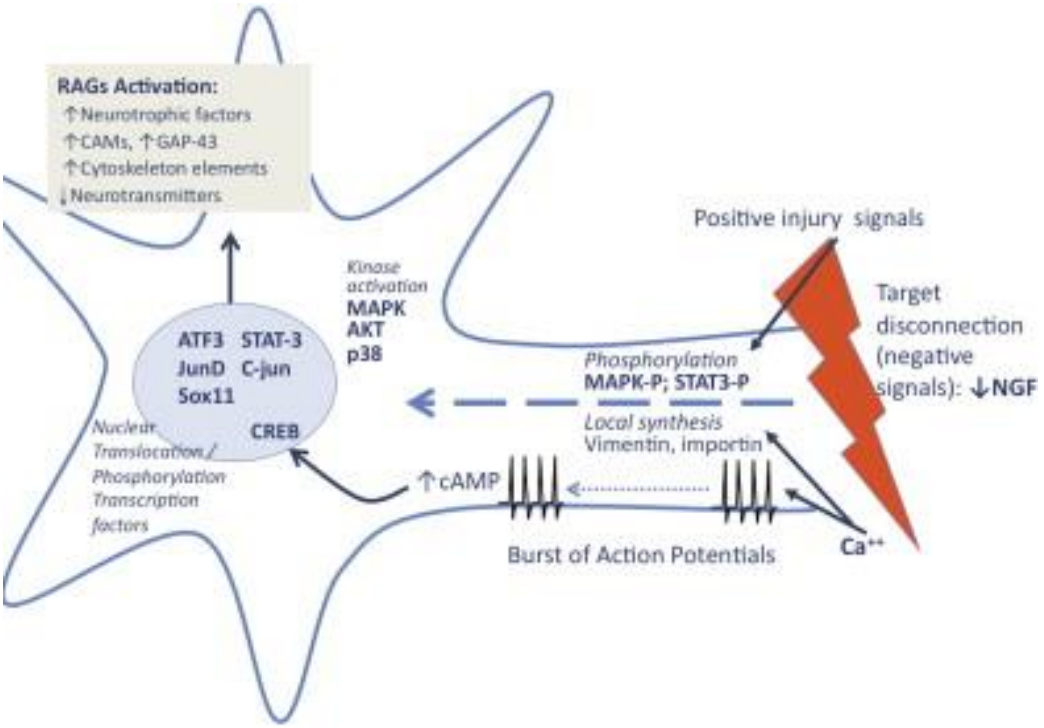

Figure 3. Events in axon and soma after nerve injury. Signals from the injury site arrive to the soma and switch the neuron to a pro- regenerative state, activating a set of transcription factors. Three main signaling mechanisms contribute: the burst of action potentials generated by the lesion, the interruption of the normal retrograde transport of trophic molecules provided by the end organs, and the retrograde transport of phosphorylated proteins, such as MAPK, which are positive injury signals. All these factors activate regeneration associated genes (RAGs), inducing the increased production of GAP43 and BDNF among other factors. (Extracted from Allodi I et al., 2012).

These signals of neuronal activation also trigger several signaling pathway genes in neuronal cell bodies that may lead to two opposing consequences: cell death or regenerative response. Amongst these are some kinases such as the MAPKs Erk1 and Erk2, c-jun N-terminal kinase (JNK) and p38 kinases. Gene expression changes affect the encoding of transcription factors, different receptors, cytoskeletal proteins, cell adhesion and guidance molecules, trophic factors, cytokines, neuropeptides and neurotransmitter synthesizing enzymes, ion channels, and membrane transporters.

Finally, One of the prominent changes after peripheral axotomy consists in the increase of regenerative-associated proteins, such as the growth-associated protein (GAP)-43 (Skene, 1989), tubulins and neurofilaments (Hoffman et al., 1987), ion channels (Goldberg, 2003) and different neuropeptides (Hökfelt et al., 2000). GAP-43 is up-regulated from the first day after axonal lesion, and is usually labeled to identify growing axonal profiles. GAP-43 is rapidly transported along the axon to the growth cones, where the protein accumulates regulating neurite formation and synaptic

plasticity (Li et al., 1997). Tubulins are significantly increased in axotomized motor and sensory neurons whereas neurofilament proteins NF-L, NF-M and NF-H are decreased, probably reflecting an increase in axoplasm fluidity in order to facilitate axonal transport (Hoffman et al., 1987; Tetzlaff et al., 1996; Wong and Oblinger, 1990). Several studies have also focused in the regulation of ion channels expression and receptors potentially involved also in the development of neuropathic pain (Goldberg, 2003; Hökfelt and Zhang, 2006; Makwana and Raivich, 2005). Furthermore, there are also marked changes in the expression of neuropeptides not only in the axotomized neurons and in their axonal projections but also in the spinal cord. These neuropeptides may exert different actions and contribute to neural signaling when the nervous system is stressed or injured (Hökfelt et al., 2000; Palkovits, 1995).

2.4. Wallerian degeneration

The environment that the axons find distal to the lesion site is crucial for their regeneration, they have to through a complicated milieu formed by the contents of the endoneurial tubes that may be filled with glial cells, other axons, and debris from the former axons and/or their myelin ensheathment (Kang and Lichtman, 2013). An intact nerve does not support axonal growth due to the presence of inhibitory factors for regeneration (Mueller, 1999; Tang, 2003) such as chondroitin sulfate proteoglycans (CSPGs) of the extracellular matrix and myelin-associated inhibitors of regeneration (Mukhopadhyay et al., 1994). However, when the distal nerve stump undergoes Wallerian degeneration, the activation of Schwann cells and the infiltration of hematogenous macrophages (Stoll and Müller, 1999) eliminate distal axons and myelin debris to clear all the inhibitory factors. Besides, a short segment of the proximal nerve stump may also suffer some retrograde degeneration that can be minimal (ranging from the injury site back to the next node of Ranvier) or it can extend all the way back to the cellular body. If the cellular body actually degenerates, which may occur in severe trauma, the entire proximal segment undergoes Wallerian degeneration and is phagocytized.

The first signs of wallerian degeneration are observed within 24 hours after nerve injury, and they are prolonged for about two weeks. First, Schwann cells of the distal nerve segment are stimulated to proliferate after injury by loss of axonal contact and by cytokines secreted by macrophages, (Fig. 4). By 48 hours, all axons show complete disruption of their internal structure with disintegration of the cytoskeleton. Afterwards, between 48 and 72 hours after injury, there is an important infiltration of macrophages into the degenerating nerve attracted by chemotactic and inflammatory cytokines such as leukaemia inhibitory factor (LIF), interleukin 1α or interleukin 1β secreted by reactive Schwann cells (Tofaris et al., 2002). This recruitment of hematogenous macrophages is the main pathway for myelin and axonal debris phagocytosis although denervated Schwann cells may also phagocyte myelin remnants to some extent (Tanaka et al., 1992). Furthermore, Schwann cells are also de-differentiated and lined up within the endoneurial tubes to form the bands of Büngner that will provide support for regenerating axons later. The highest rate of Schwann cell multiplication is reached by 3 days after lesion, and then continues with decreasing frequency for 2-3 weeks to reach a more than a three-fold increase in number (Salonen et al., 1988).

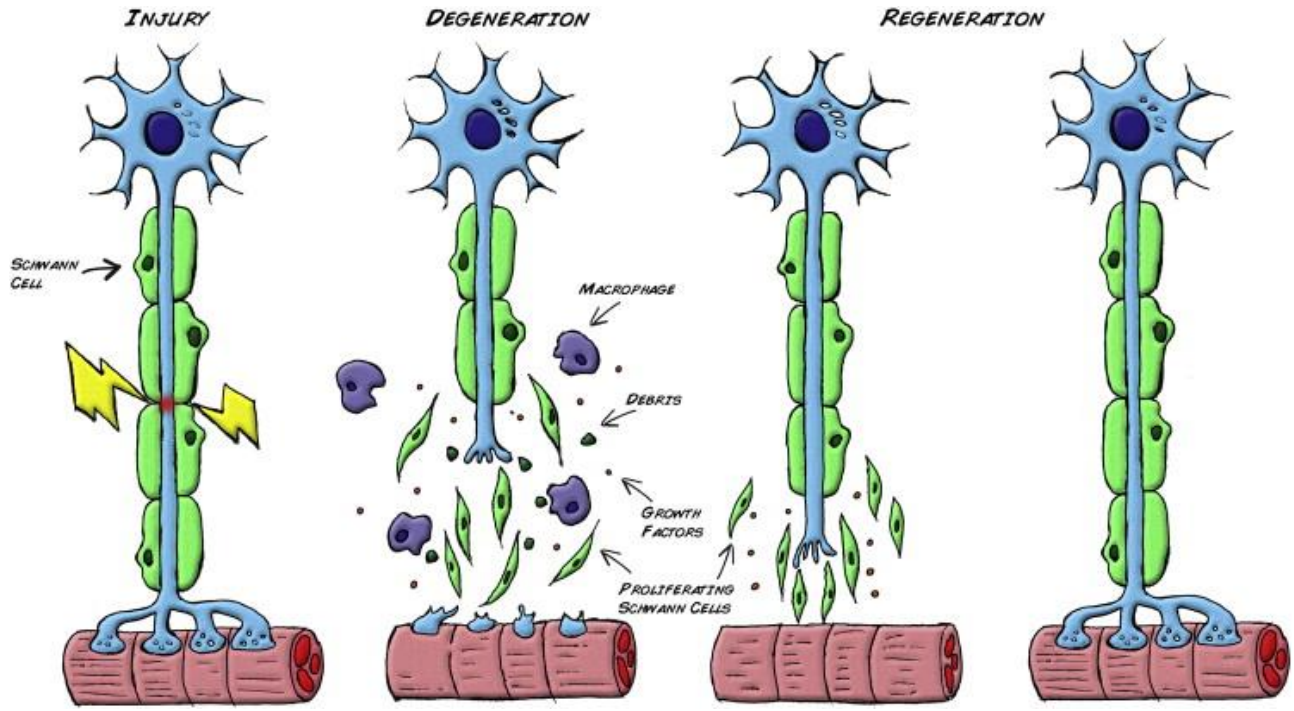

Figure 4. Wallerian degeneration. Following injury, Schwann cells detach from the axons, start proliferating and help the recruited macrophages to clear the cellular and myelin debris. At the same time, expression of stimulating factors by SCs create a favorable environment for nerve regrowth towards the target organ. (Extracted from Faroni A et al., 2015).

2.5. Axonal regeneration

Throughout the regeneration process, axonal sprouts grow down the distal nerve segment and, if successful, reinnervate their correct targets. However, axonal outgrowth is slow and occurs at a rate of around 1-2 mm per day (Gutmann et al., 1942; Kang and Lichtman, 2013). Each regenerating axon may give rise initially to over 10 axonal sprouts (Witzel et al., 2005), but the number of branches decreases with time in the distal segment, as sprouts that do not make peripheral connections undergo atrophy and eventually disappear, whereas axons reinnervating target organs mature and enlarge in size. If nerve regeneration is unsuccesful, axons may sprout within the proximal stump and form a neuroma. In the distal stump, denervated Schwann cells proliferate on the basal membrane of the endoneurial tubes and form columns, the so-called bands of Büngner, over which growth cones advance (Bunge et al., 1982).

The regeneration of a sectioned axon involves the transformation of a stable axonal segment into a highly motile tip, called growth cone, which senses the surrounding environment and leads the elongation of the regenerating axon (Mueller, 1999). The orientation of the advancing tip is guided by gradients of neurotrophic and chemotactic factors produced mainly by nonneuronal cells (Song and Poo, 1999) (Fig. 5). The molecular cues that the regenerating axons will find at the lesion site and into the distal nerve stump can have both chemoattractive and chemorepulsive properties, and can be diffusible or membrane-bound (Dickson, 2002). Indeed, the different signals may create a permissive environment for axonal growth or constitute a molecular barrier that impairs axonal elongation (Tessier-Lavigne and Goodman, 1996).

The chemotaxis and advance of growth cone involves mainly distinct steps: protrusion, engorgement and consolidation (Mortimer et al., 2008). On the other hand, growth cones consist of three specific domains: a central domain (C-domain) located at the base of growth cone with stable microtubules (MTs), a peripheral domain (P-domain) that is composed by filamentous (F)-actin bundles extended into the growth cone periphery forming the filopodia, and a transition zone (T-zone) placed between MTs rich C-domain and actin rich P-domain (Bouquet and Nothias, 2007) (Fig. 5A). Actin polymerization triggers the protrusion of growth cone membrane and this facilitates the delivery of new microtubule segments at the P-domain, as well as their stabilization along actin bundles. This allows the displacement of the C-domain forward (engorgement) and the further consolidation of the nascent axon. The most distal part of the growth cone, the P-domain bears lamellipodia, membranous protrusions from which extend several expansions called filopodia, mainly formed by actin filament

bundles. Equilibrium between actin polymerization and depolymerization generates constant protrusion forces that give the ability to explore the microenvironment.

Guidance cues of the external environment also play a key role in the elongation of the growth cone (Fig. 5B). These cues interact with specific receptors on the surface of the growth cone, and trigger a cascade of cytoplasmic events that eventually lead to the cytoskeletal rearrangement associated with oriented neurite extension (Letourneau and Shattuck, 1989). Neurotrophins, for instance, can exert their chemoattractive gradient acting through the activation of their receptors that are expressed in the tip of growth cones. Calcium signal pathways have an important role in axonal guidance as individual filopodia respond to alterations in the environment by changing internal calcium concentration, and filopodia on different parts of the growth cone respond independently via local changes in actin metabolism (Bixby and Harris, 1991).

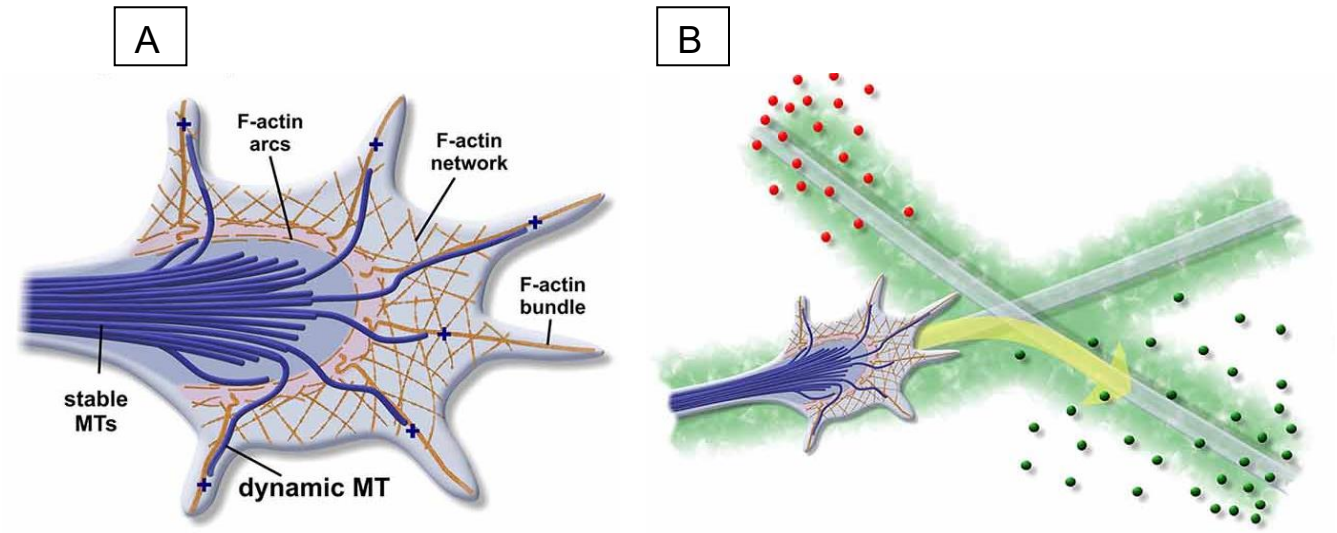

Figure 5. The growth cone cytoskeleton. (A) Structural organization of the growth cone cytoskeleton: Bundled, stable Microtubules (MTs) extend through the axon, entering the growth cone "wrist." These terminate in the growth cone "central" domain, surrounded by a cage of F-actin arcs. F-actin bundles extend into the growth cone "fingers" (filopodia) to sample the environment. Between the filopodia there exist a series of cortical actin networks which create the lamellipodial veils. A subset of MTs can escape the central domain, to trace along F-actin structures and explore the growth cone periphery. The dynamic plus-ends of MTs are decorated by set of proteins called plus-end tracking proteins (+TIPs) (not shown). Concentration of +TIPs at the dynamic leading edge is particularly important as they come in close contact with signaling cascades that are triggered by external cues. (B) The axon has to travel a complex landscape which presents a multitude of external chemotropic cues (e.g., red and green circles represent diffusible cues, light green represents substrate-bound cues). To properly interpret and navigate these signals, the axon is equipped with a dynamic cytoskeletal vehicle called the growth cone. (Adapted from Bearce E.A et al., 2015).

2.6. Axonal reinnervation and functional recovery

Motor and sensory axons of the PNS are able to regenerate after injury, and may reinnervate distal targets if the conditions are optimal. However, full functional recovery does not always occur after nerve injuries from grade III to V because axons may be misdirected and lead to unaccurate reinnervation (Lundborg and Rosén, 2001; Valero-Cabré and Navarro, 2002). After axonotmesis, where the connective sheaths of the nerve are preserved and only the axons are injured, functional recovery is usually good. In contrast, after neurotmesis (nerve transection), when the endoneurial tubes loss their continuity, axons are often misdirected and may reinnervate incorrect target organs even if refined repair is applied (Bodine-Fowler et al., 1997; Valero-Cabré and Navarro, 2002). Indeed, only a low percentage of adult patients regain normal function after complete transection and surgical repair of a major peripheral nerve, and the occurrence of a postparalytic syndrome, such as paresis, synkinesis, and dysreflexia, is often present (Kerrebijn and Freeman, 1998).

The mechanisms through which motor and sensory axons specifically reinnervate their corresponding targets are still poorly understood. Different mechanisms have been described as possible contributors in axonal guidance in order to facilitate accurate reinnervation. Some studies defend a preferential muscle reinnervation by motor axons, the so-called preferential motor reinnervation (PMR) (Brushart et al., 1998; Brushart, 1993, 1988). Pruning of the axons that reinnervated an erroneous target may contribute to produce the PMR effect (Madison et al., 1996). Other studies also identified the existence of the peptide L2/HNK1 (Martini et al., 1992) expressed in motor but not sensory Schwann cells and the presence of NCAM on Schwann cells of sensory but not in motor fascicle fractions (Franz et al., 2005) that may contribute to PMR. On the other hand, other authors argue that the key point for preferential attraction of axons to their targets is the expression of trophic factors by the own target organ and the distal stump (Madison et al., 2007).

Additional problems to reinnervation accuracy can be related with the generation of axonal sprouting in proximal growth cones and before target reinnervation. Axonal sprouting has been regarded as an adaptive mechanism to compensate for reduced functional capacity after injury. Each transected axon can sprout up to 25 branches (Mackinnon et al., 1991) and excessive sprouting leads to reinnervation of different muscles by a single motoneuron (Fig. 6), often with antagonizing action and leading to abnormally associated movements (Ito and Kudo, 1994). In addition, it will also

inevitably result in the enlargement of motor units (Gordon et al., 2004) and reinnervation of motor endplates by more than one axon, a state known as “polyinnervation” (Rich and Lichtman, 1989; Vleggeert-Lankamp et al., 2005), with muscle fibers being controlled by two or more asynchronously firing motoneurons (Fig. 6). Furthermore, some problems are also found related with inaccurate sensory reinnervation. For example, injury-induced sprouting of A-, C- or sympathetic fibers is likely to be involved in the generation of pain at the level of the peripheral nociceptor or within affected dorsal root ganglia (Ramer et al., 1999). Sensory aberrant reinnervation can result in mistaken localization of stimuli (Kimura et al., 1975) and misinnervation of proprioceptive sensory axons and the reorganization of spinal motor reflexes also limit locomotor recovery by altering the ordered recruitment of flexor and extensor motor units (Wasserschaff, 1990).

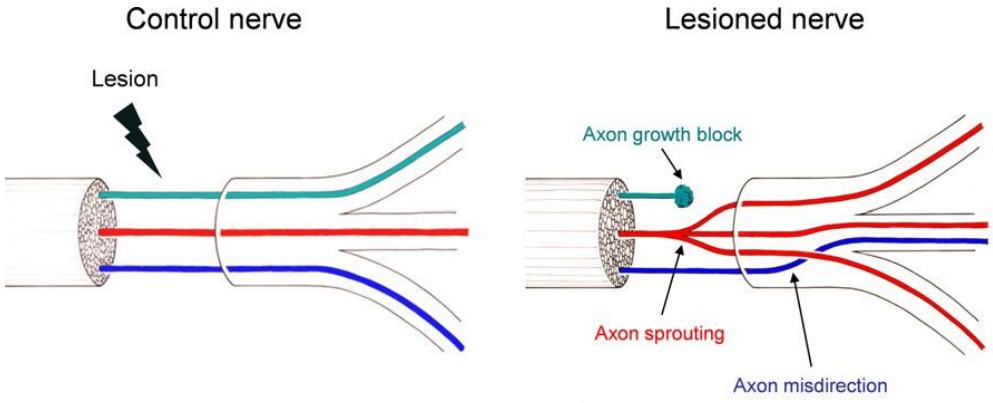

Figure 6. Misdirection in axon regeneration. After peripheral nerve injuries, only _60% of patients regain useful function. Three main problems have been identified. First, axons stop elongating and form local sprouts, resulting in neuroma formation. Second, axons elongate but form sprouts that innervate more than one peripheral nerve branch. Third, false regeneration into the wrong nerve can occur, leading to unsuccessful regeneration, for example, if motor axons grow into sensory nerves or vice versa. Current research efforts attempt to identify the relevant neuronal signaling mechanisms and specifically enhance axon elongation without promoting axonal sprouting at the lesion site. (Extracted from Klimaschewski L et al., 2013)

Besides, the time of nerve regeneration and the state of end target organs also contribute to reinnervation and functional recovery. End organs undergo characteristic histological changes with nerve degeneration and subsequent reinnervation. Although the synaptic folds of motor endplates are preserved for at least 1 year after denervation, muscle fibers atrophy quite rapidly (a mean 70% reduction of cross-sectional area by 2 months) and cell nuclei assume a central rather than the normal peripheral position (Gordon et al., 2011). Furthermore, there is a massive proliferation of fibroblasts that characterize the histological picture of denervation, and this

intramuscular fibrosis may limit the efficacy of the contraction produced by a nerve impulse. Hence, axonal development and maturation are aborted if the end organ, due to prolonged denervation, has undergone degenerative changes that do not allow the establishment of functional connections. If the entry of regenerating axons into the distal segment is delayed more than approximately 4 months, the axons may enter endoneurial tubes of small diameter, generally 3 μm or less. This shrinkage can make it more difficult for axon sprouts to locate and enter endoneurial tubes, but this does not appear to impede axonal regrowth once sprouts are inside the tubes (Burnett and Zager, 2004).

3. Strategies to increase axonal regeneration after tube repair

Nerve regeneration through a nerve guide requires the reconstitution a new neural structure that gives support to axon regeneration. During the first days after tube implantation, fluid mainly derived from blood extravasation invades the lumen of the tube. Then, a fibrin cable matrix is formed within the tube, bridging both nerve stumps. Afterwards, different non-neuronal cells such as fibroblasts or Schwann cells migrate from both stumps along the fibrin cable providing neovascularization, connective strands, basal lamina and secreting a variety of neurotrophic and extracellular matrix compounds that stimulates the growth of axonal sprouts from the proximal stump. Concurrently, the fluid surrounding the regenerative cable in the tubes contains also macromolecular factors, which display neurotrophic activity and promote Schwann cell migration and proliferation. By 3 weeks, depending on the gap length, nonneuronal cells can completely bridge the chamber, and unmyelinated and myelinated axons are found distally. As regeneration progresses, the nerve increases in caliber. Finally, the newly regenerated nerve is usually centered in the tube lumen surrounded by a thin perineurium and composed of small fascicles with myelinated and unmyelinated axons (Williams et al., 1983). Nevertheless, the success of intratubular regeneration depends upon the capability of the injured nerve to provide enough humoral and cellular elements that constitute the initial regenerative cable (Navarro and Verdú, 2004).

3.1. Synthesis of new biomaterials to develop nerve guide conduits

The first studies using tubulization to repair nerve sections date from the 19th century (Gluck, 1880; Vanlair, 1882). Remarkably, this technique has rather evolved on account of new materials available at the time than by practical application of advances in theory (Fields et al., 1989). Several studies have been aimed to develop and test new materials and fabrication techniques to produce new nerve guides that are able to enhance regeneration and allow to bridge difficult injuries (Arslantunali et al., 2014; Chiono and Tonda-Turo, 2015; Deumens et al., 2010).

Different type of tubes used in previous years can be divided in different groups: one group is composed by biologial materials like collagen (Archibald et al., 1991) or silk (Yang et al., 2007) with positive results in short but not in long gaps. On the other hand, chitosan tubes have shown promising results with some results similar to autograft outcomes (Meyer et al., 2016). In the family of synthetic materials, silicone has been used as standard material for tube repair for many years (Fields et al., 1989; Lundborg et al., 1982; Williams et al., 1983) providing the accepted interstump limits for successful peripheral nerve regeneration of up to 4 mm in the mouse, 10 mm in the rat and 30 mm in large primates (Navarro and Verdú, 2004; Yannas and Hill, 2004). Other materials such as poly-glycolic acid (PGA), poly-(lactic acid) (PLA), poly-caprolactone (PCL), poly-(lactide-coglycolide) (PLGA) copolymer, poly(3-hydroxybutyric acid (PHB) or poly(acrylonitrile-co-methylacrylate (PAN-MA) have also been used in different studies to repair peripheral nerve injury (Deumens et al., 2010; Konofaos, 2013; Nectow et al., 2012) with different outcomes.

With regard to clinical practice, the repair of peripheral nerve sections with nerve guides has been assessed as an alternative to direct nerve suture or to nerve autografts to bridge short (less than 2 cm) gap defects. In a prospective randomized study comparing primary suture versus silicone tube repair of transected median or ulnar nerves in the forearm, Lundborg and colleagues reported no differences between the two techniques after 1 or 5 years after surgery (Lundborg et al., 2004, 1997). In another randomized trial (Weber et al., 2000) a bioresorbable polyglycolic acid conduit was compared with standard repair, either end-to-end or with a short nerve graft, of digital nerve transection in the hand. The overall results showed no significant difference between the two groups, although the group with a conduit had improved recovery of sensory discrimination.

3.2. Filling nerve guides with biological molecules

3.2.1. Extracellular matrix (ECM)

The ECM is an intricate network of macromolecules (e.g. proteins or polysaccharides) that has mainly structural functions, providing support and maintaining cellular regulation. Moreover, many cells interact with the ECM through specific membrane receptors to modulate their behavior. The ECM components can be divided into two main categories: proteoglycans and glycoproteins. Among the latter, three of them have an important role in axonal regeneration and their effects have been proved both in vivo and in vitro: collagen (Babington et al., 2005), fibronectin (Gardiner et al., 2007) and laminin (Werner et al., 2000).

-*Collagens* are trimeric molecules formed by three α chains and can be divided into several sub-families according to the type of structure they form: fibrillar (types I, II, III, V, XI), facit-fibril associated collagens with interrupted triple helices (types IX, XII, XIV), short chain (types VIII, X), basement membrane (type IV) and other kinds with a different conformation (types VI, VII, XIII). It is interesting to highlight the role of those related to fibril formation (collagen type I) and the basement membrane (collagen type IV) with axon pathfinding in neural development and in synaptic connection and maintenance (Fox, 2008).

- *Laminins* are major proteins of the ECM participating in cell differentiation, migration, and adhesion activities. They are mainly found in the basal lamina and different isoforms can be secreted by Schwann cells such as laminin-2 (α2, β1, γ1) and laminin 8 (α4, β1, γ1) found in the peripheral nerves (Wallquist et al., 2002), or laminin 10 (α5, β1, γ1) that can be detected in sensory end organs (Caissie et al., 2006). Furthermore, laminin is the adhesive component that gives the regenerative promoting capability to basal lamina scaffolds after nerve injury (Wang et al., 1992) and has been shown to promote neuritogenesis in vitro (Agius and Cochard, 1998).

- *Fibronectin* is the other major component of noncollagen glycoproteins of the ECM (Singh et al., 2010). It forms a fibrillar network and maintains interactions with collagen IV and laminins, promoting cell proliferation and differentiation. Moreover, although fibronectin binds mainly to integrins, it contains also domains for fibrin, collagen, heparin and syndecan (Mao and Schwarzbauer, 2005). In the nervous system, fibronectin is up-regulated immediately after peripheral nerve injury (Lefcort et al.,

1992) and secreted by Schwann cells and fibroblasts (Chernousov and Carey, 2000; Evercooren et al., 1986).

As a matter of fact, it has been reported that ECM component in nerve guides promote formation of a larger-diameter matrix that enhance axonal growth compared with empty nerve guides (Gonzalez-Perez et al., 2015). However, gel substrates, even if containing neuritotropic factors, may impair regeneration by physically impeding the migration of non-neuronal cells and regenerating axons if they are too dense or provide too narrow pores network (Navarro and Verdú, 2004). It has also been reported that gels composed of collagen or laminin at the maximal dilution that still allows gelification, were the most successful in enhancing regeneration, but the improvement was limited and results still worse than those found with an autograft (Labrador et al., 1998). Hence, prefilling the lumen of nerve guides with ECM components such as collagen, fibronectin or laminin-containing gels can improve nerve regeneration not only through their neurotropic effects but also by creating porous scaffolds with longitudinally oriented pathways that mimic the endoneurial tubules of the nerve and thus enhance cellular and axonal migration (Gonzalez-Perez et al., 2015).

3.2.2. Neurotrophic Factos (NTFs)

As previously described, damage to the adult PNS induces cellular mechanisms that control neuronal differentiation, survival and axon growth (Allodi et al., 2012). Neurotrophic factors represent one of the most studied areas of research aimed at finding new and more effective treatments for nerve regeneration and axon guidance.

After injury, denervated Schwann cells increase the expression of several neurotrophic factors like glial cell-derived neurotrophic factor (GDNF), fibroblast growth factor (FGF-2) or other neurotrophic factors from the familiy of neurotrophins such as nerve growth factor (NGF), brain-derived neurotrophic factor (BDNF) or neurotrophin-3 (NT3). Studies from Höke and colleagues (Höke et al., 2006) describe that Schwann cells of sensory and motor (ventral roots) nerves exhibit differing growth factor profiles at baseline and, interestingly, respond differently during denervation and when reinnervated by cutaneous or motor axons. Specifically, mRNAs for NGF, BDNF, vascular endothelial growth factor (VEGF), insulin growth factor 1 (IGF-1) and hepatocyte growth factor (HGF) are expressed vigorously by denervated and reinnervated cutaneous nerves but minimally by ventral roots, whereas mRNAs for

GDNF and pleiotrophin are increased to a greater degree in motor than in cutaneous nerves. Such differences are maintained during Wallerian degeneration, although they tend to decline with time when reinnervation was induced by the wrong type of axons (Höke et al., 2006).

On the other hand, neurotrophins and other trophic factors play also a role in axonal guidance in development and after injury. The same intracellular mechanisms that regulate the effect of neurotrophins in nerve survival and axonal growth are also responsible for their attraction properties (Huang and Reichardt, 2001). For example, the presence of a specific concentration of either BDNF or NT-3 attracts the growth cone of spinal neurons in cultures (Song et al., 1997). Likewise, coactivation of PLC-γ and PI-3K via the receptor TrkA is responsible for the chemotactic effect of NGF on spinal cord neurons. The intracellular levels of this specific second messenger, which is activated into the growth cone, regulate whether the growth cone is going to turn to or turn away from the axonal guidance source (Ming et al., 1999).

Therefore, the addition of neurotrophic factors into nerve guides can enhance nerve regeneration, neuronal survival and axonal guidance; however, some efforts are still needed to optimize their application and their effects. A detailed description of the most studied neurotrophic factors and their effects on different populations are described below:

GDNF: Sensory, motor and autonomic neurons are responsive to trophic effects mediated by GDNF (Buj-Bello et al., 1995; Ebendal et al., 1995; Henderson et al., 1994). Two weeks after birth, some of the small-diameter non-peptidergic neurons of the DRG lose their sensitivity to NGF and become GDNF sensitive (Bennett et al., 1996; Molliver et al., 1997) but higher levels are expressed in cutaneous nerves than ventral roots in adulthood (Höke et al., 2006). However, after injury GDNF is similarly up-regulated both in ventral and dorsal roots (Höke et al., 2001) and overexpression of this factor in motoneurons improve neuronal survival after axotomy (Zhao et al., 2004). The up-regulation in both motor and sensory neurons of GDNF after injury triggers also the up-regulation of its receptor (GFRa-1) suggesting its important role for neurotrophic support (Höke et al., 2000). In fact, several studies have showed that external application of GDNF enhances regeneration of both motor and sensory axons. For example, sustained delivery of GDNF to the injury site in vivo by a synthetic nerve guide allowed regeneration of both sensory and motor axons over long gaps to a significantly higher number than with NGF delivery (Fine et al., 2002). Furthermore,

GDNF expression decline was associated with impaired regeneration after long-term denervation (Höke et al., 2002), whereas GDNF applied to the proximal stump of chronically sectioned nerves increased the number of motoneurons that were able to regenerate their axons (Boyd and Gordon, 2003a). On the other hand, GDNF has also important effects on Schwann cells, and when applied at high doses in adult rats it induces proliferation of Schwann cells and even myelination of normally unmyelinated small axons (Höke et al., 2003).

FGF: Different isoforms of this trophic factor are expressed in adult nervous tissue by glial cells and different neuronal populations and play a key role in signal transduction in central and peripheral nervous systems (Ornitz and Itoh, 2001). Among the 23 members of the FGF family, FGF-2 has been shown to be the most important contributor to nerve regeneration (Grothe and Nikkhah, 2001) and four different high affinity tyrosine transmembrane receptors have been described to which FGF-2 binds with different affinities (Ornitz et al., 1996). The main receptors in the nervous system, FGFR 1-3, are up-regulated after injury (Grothe et al., 1997) and in vitro studies have found enhanced sensory neuron outgrowth after FGFR-1 overexpression, mediated by activation of extracellular signal-regulated kinase (ERK) and Akt pathways (Hausott et al., 2008). FGF-2 isoforms seem to be differentially regulated after injury (Giordano et al., 1992; Grothe et al., 2000; Meisinger et al., 1996) and differential effects of FGF-2 isoforms have been reported. Transplantation of Schwann cells overexpressing the 21–23 kDa FGF-2 form supported sensory recovery through a long gap injury, whereas the 18 kDa isoform inhibited myelination of regenerated axons (Haastert et al., 2006). In contrast, in cultured DRG neurons both low- and high molecular weight FGF-2 isoforms increase the number of axonal branches from control rats. In addition, it has been also demonstrated that FGF-2 enhance motor neurite outgrowth both in vitro and in vivo(Allodi et al., 2014, 2013). Furthermore, it has also been reported that FGF-2 acts on Schwann cells stimulating their mitogenesis and proliferation (Davis and Stroobant, 1990).

Neurotrofins: The family of neurotrophins consists of NGF, BDNF, NT-3 and neurotrophin-4/5 (NT-4/ 5), which can bind to two structurally unrelated receptors: the neurotrophin receptor p75NTR and the tropomyosin receptor kinases (TrkA, -B, and -C). Binding of neurotrophins to the Trk receptors is selective with NGF binding to TrkA, BDNF and NT-4/5 to TrkB and NT-3 to TrkC (Chao, 2003). However, many neurons co-express Trk receptors and p75NTR, which together strengthen the affinity and

specificity of the neurotrophins for the Trk receptors probably through the formation of a receptor complex (Bibel et al., 1999; Hempstead et al., 1991; Wright and Snider, 1995). The neurotrophins bind to their respective Trk receptors to mediate survival and differentiation via extracellular signal-regulated kinase (ERK), phosphatidylinositol 3-kinase (PI3K) and phospholipase C-γ (PLC-γ) pathways. Neurotrophins can also provide survival signaling via p75NTR and the NF-κB pathway or affect cytoskeletal organization and neurite outgrowth via downstream RhoA kinase activity (Chao, 2003; Reichardt, 2006). Yet, p75NTR is better recognized for its ability to induce cell death signaling via binding of various intracellular adaptor proteins, ultimately activating the c-Jun N-terminal kinase (JNK) pathway and subsequently p53 leading to apoptosis (Vaegter, 2014).

NGF: This neurotrophin was first described to have remarkable growth promoting effects on sympathetic and spinal ganglia of the chick embryo (Cohen and Levi-Montalcini, 1956) and has long been characterized for its effects on sensory neurons as some studies report is required for the survival of developing sympathetic and sensory neurons (Freeman et al., 2004). In adult animals, neither NGF nor its mRNA are detected in the intact adult rat sciatic nerve but its expression is markedly induced in non-neuronal cells of the distal and the immediate proximal segment of transected nerves (Heumann et al., 1987a, 1987b). The levels of NGF mRNA exhibit a biphasic response to axotomy with an immediate early rise in NGF mRNA peaking 6 h after injury. The second increase in NGF mRNA expression is slower and is believed to be caused by IL-1, released by macrophages invading the site of injury during Wallerian degeneration and lasting several weeks (Heumann et al., 1987b; Lindholm et al., 1987). Several studies point to Schwann cells as the source of NGF (Funakoshi et al., 1993; Heumann et al., 1987a; Lindholm et al., 1987; Meyer et al., 1992) in the transected nerve by induction of p75NTR expression.
NGF is needed for collateral sprouting of nociceptive and sympathetic axons into denervated skin, but does not affect large sensory axons (Diamond et al., 1987; Gloster et al., 1992). However, it has been described that application of NGF after axotomy delays the onset of regeneration (Gold, 1997), probably by reducing the neuronal body response to injury (Mohiuddin et al., 1999), although without compromising the rate of subsequent regeneration. On another hand, focal administration of NGF or NT-3 to adult axotomized nerves inside a blinded impermeable chamber effectively prevented sensory neuronal loss, which mainly affects small DRG neurons (Groves et al., 1999; K.M Rich, J.R Luszczynski, P.A Osborne, 1987).

BDNF: In intact animals, BDNF is differently expressed in motor and sensory neurons, and after injury, it can be detected also at higher concentrations in cutaneous nerves than in ventral roots (Höke et al., 2006). Following nerve injury, some studies suggest that Schwann cells of the distal nerve stump synthesize BDNF and that they are responsible for the BDNF increase following injury (Acheson et al., 1991; Funakoshi et al., 1993; Meyer et al., 1992; Zhang et al., 2000). A continuous slow monophasic increase of BDNF mRNA is observed in the distal segment of the rat sciatic nerve starting 3 days after axotomy and reaching maximal levels after 2–4 weeks (Funakoshi et al., 1993; Meyer et al., 1992). The role of BDNF in nerve regeneration is controversial, although the presence of its receptor trkB seems crucial to sustain axonal regeneration (Boyd and Gordon, 2001).

By depriving endogenous BDNF with BDNF-neutralizing antibodies it was observed a reduced elongation of regenerating axons and myelination following sciatic nerve crush injury, which indicates that endogenous BDNF is important for stimulating axonal elongation (Zhang et al., 2000), whereas local infusion of BDNF improved nerve regeneration in neural conduits (Vögelin et al., 2006). Interestingly, (Boyd and Gordon, 2001) described no effects on axonal regeneration when BDNF was administered acutely after a cut and suture of the sciatic nerve, although it enhanced regeneration in a dose dependent manner when applied after chronic axotomy (Boyd and Gordon, 2003a). Similar results to BDNF deprivation were observed when the expression of TrkB receptor is significantly attenuated in heterozygous TrkB mutant mice, as it appears to be critical for motor neuron axonal regeneration as axonal regrowth. In contrast, function-blocking antibodies against p75NTR have been reported to increase motor neuron axonal regeneration and to reverse the inhibitory effect of BDNF at high doses, indicating an inhibitory role of p75NTR on motor neuron axonal regrowth (Boyd and Gordon, 2002).

On the other hand, the role of Schwann cell-derived BDNF in regeneration of motor neuron axons has recently been examined by analyzing regeneration of wild-type motor neuron axons through grafts of BDNF-deficient Schwann cells. The length of regenerating axons into grafts of BDNF-deficient Schwann cells have been found to be significantly shorter than those growing into wild type grafts. Addition of recombinant human BDNF at the site of repair were shown to rescue axon regeneration in absence of Schwann cell-derived BDNF as well as to enhance the length of regenerating axons into wild type grafts (Wilhelm et al., 2012), indicating that BDNF derived from Schwann cells is important for motor neuron axonal regeneration after nerve transection.

NT-3: In baseline conditions, neurotrophin-3 is present at higher concentration in cutaneous sensory than in motor nerves, but no great differences between roots have been found after injury (Höke et al., 2006). NT-3 is also present in adult skeletal muscles and has a trophic role on motoneurons and primary sensory neurons innervating muscles. Its trophic action on motoneurons has been shown in vitro (Braun et al., 1996), whereas in vivo it seems to exert a selective action on type 2b fast muscle fibers (Sterne et al., 1997; Sternel et al., 1997). On the other hand, other studies confirm its important role for the survival of proprioceptive and mechano-receptive sensory neurons (Airaksinen et al., 1996; Ernfors et al., 1993). Consistent with these effects, the impact on axonal regeneration of the rat peroneal nerve after injury has been investigated using genetically modified peripheral nerve grafts repopulated ex vivo with Schwann cells modified to express NT-3, which has been found to result in a significant increase in the number of sensory fibers (Godinho et al., 2013).

After nerve injury, NT-3 levels in nerve tissue has been shown to decrease shortly after nerve transection, but to return to the normal level 2 weeks post injury (Funakoshi et al., 1993; Meyer et al., 1992). As is the case for NGF, studies indicate Schwann cells as being the source of NT-3 in the transected nerve (Meier et al., 1999; Sahenk et al., 2008). Moreover, NT-3 is important for survival of denervated Schwann cells in the distal segment of the injured nerve. Mature Schwann cells in adult nerves are able to survive in absence of axons by establishing an autocrine survival loop (Meier et al., 1999) and NT-3 is one of the important factors of this autocrine regulatory mechanism that support long-term Schwann cell survival (Meier et al., 1999; Sahenk et al., 2008) and nerve regeneration and remyelination after peripheral nerve injury (Sahenk et al., 2008).

With regard to in vitro experiments, it is interesting to highlight that in chicken embryos, NT-3 responsive sensory neurons extend neurites well both on laminin and fibronectin coated coverslips, whereas NGF responsive neurons grow better only on laminin. Thus, differences seem to exist in substrate preference between NGF and NT-3 responsive sensory neurons (Guan et al., 2003). Moreover, some effects in axonal guidance have also been observed in mixed population of DRG neurons by using a compartmentalized delivery of NGF and NT-3. (Lotfi et al., 2011) found that the NGF channel attracted nociceptive axons, which elongated longer when compared to saline or NT-3 channels, whereas there were more proprioceptive fiber branches in the NT- 3 channels. However, the authors failed to corroborate these findings in vivo.

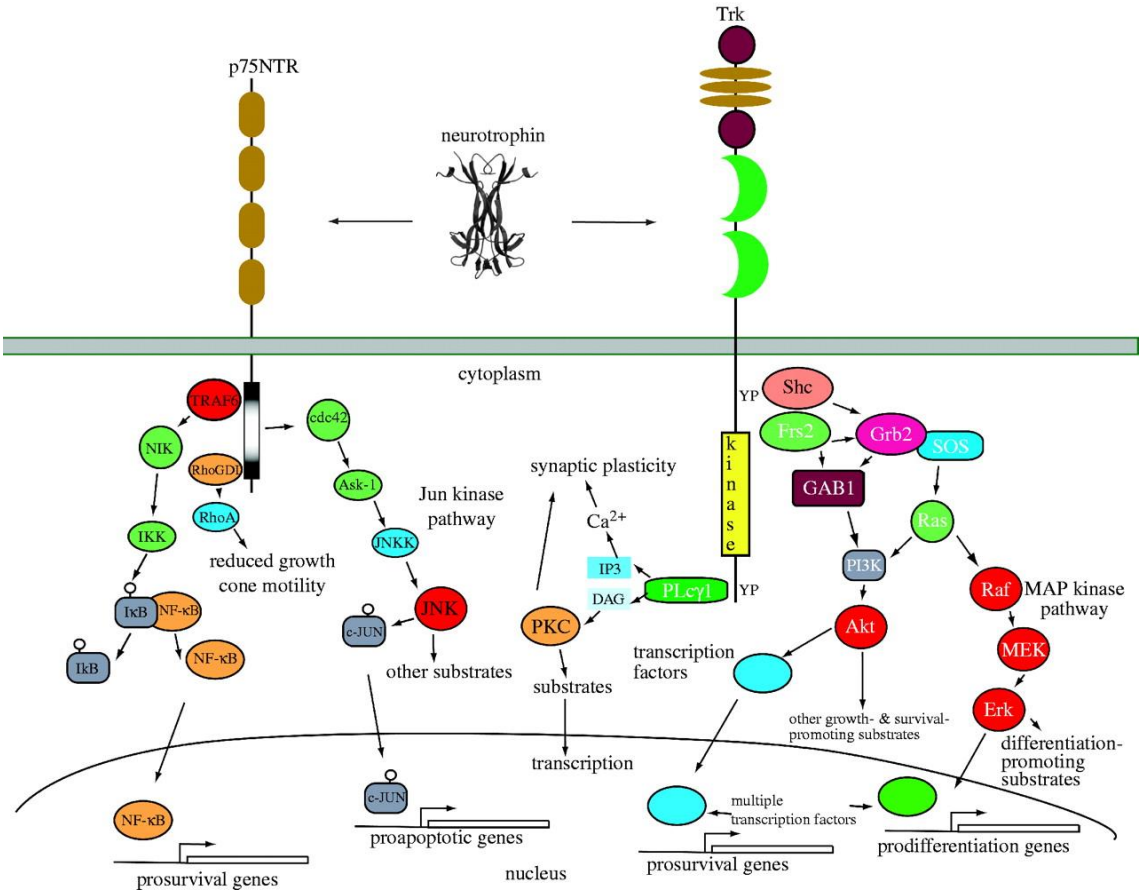

Figure 7. Neurotrophin signalling. Interactions of each neurotrophin with Trk and p75NTR receptors and major intracellular signalling pathways activated through each receptor. The p75NTR receptor regulates three major signalling pathways. NF-κB activation results in transcription of multiple genes, including neuronal survival promotion; or activation of the Jun kinase pathway which similarly controls activation of several genes, some of which promote neuronal apoptosis and the activation of Rho, which controls growth cone motility. Each Trk receptor also controls three major signalling pathways. Activation of Ras results in activation of the MAP kinase-signalling cascade, which promotes neuronal differentiation including neurite outgrowth. Activation of PI3 kinase through Ras or Gab1 promotes survival and growth of neurons and other cells. Activation of PLC-γ1 results in activation of Ca^{2+}- and protein kinase C-regulated pathways that promote synaptic plasticity. (Extracted from Reichardt LF et al., 2006).

3.3. Controlled release of biological molecules

Trophic factors can be administered either systemically or locally. Although intraperitoneal systemic administration is usually preferred for several treatments and a few studies show some good results (Sahenk et al., 1994) on nerve regeneration, the fact is that this type of administration is not usually used and a local delivery of the trophic factor is chosen (Johnson et al., 2008).

On the other hand, neurotrophic factors added within the nerve lesion environment can degrade rapidly (Ejstrup et al., 2010) or diffuse out of its site of action thus exerting

lower effects than expected (de Boer et al., 2012). In order to have an uninterrupted presence of the trophic factor within the axon regeneration milieu different approaches have been used such as by using repeated injections through catheters (Mcdonald and Zochodne, 2003), osmotic minipumps (Hontanilla et al., 2007), gene therapy (Haastert et al., 2006), binding the factors to extracellular matrix molecules (Sakiyama-Elbert and Hubbell, 2000; Sternel et al., 1997) or to the wall of nerve conduits (Madduri et al., 2010). However, each of these strategies still present some difficulties to reach optimal nerve regeneration.

In this context, strategies involving injectable biocompatible and biodegradable microspheres (MPs) associated to selected bioactive molecules may provide a sustained and controlled release of factors, offering valuable approaches for overcoming those limitations.

3.3.1. Osmotic minipumps and catheters

Osmotic minipumps are devices that can be chronically implanted in patients or animal models and consist in a reservoir for the drug solution and an adjacent or surrounding chamber filled with an osmotically active agent that is enclosed in a semipermeable membrane (Theeuwes and Yum, 1976). When exposed to an aqueous environment, water penetrates into the osmolyte chamber and exerts a pressure on the reservoir that delivers the drug solution generally at zero-order kinetics via a catheter. When used in nerve regeneration to deliver drugs within the regeneration environment, the catheter is directed towards the nerve conduit (NC) or nerve gap and osmotic minipumps can be used to deliver focally different drugs at constant rates for typically up to 4 weeks (Pfister et al., 2007). Indeed, to determine the therapeutic window of growth factors such as BDNF and GDNF, an osmotic minipump was used after nerve section and repairt with different nerve grafts. BDNF exhibited a bimodal dose response as high doses (8 mg/day) inhibited motor neuron survival in a dose-dependent manner whereas low doses (0.5–2 mg/day) had no detectable effect after immediate repair, but reversed the negative effects of chronic axotomy 2 months prior to nerve resuture (Boyd and Gordon, 2002). In contrast, GDNF showed no dose dependency within the tested range (0.1–10 mg/day), but a synergistic effect in combination with BDNF was observed (Boyd and Gordon, 2003).

However, the use of osmotic minipumps shows also some limitations. They are particularly unwieldy and the demanding microsurgical handling for placing the catheter may become problematic in locations where space is scarce, such as in hand surgery

or experimental surgery in small animals. Moreover, they are not biodegradable, thus a surgical explantation is required at the end of the therapy. Furthermore, the maintenance of the catheter in the correct position during nerve regeneration appears difficult (Santos et al., 1998). Therefore, their use in therapeutic applications is limited.

3.3.2. Microspheres

Polymeric biodegradable microspheres (MP) have been used for the sustained delivery of neuronal growth factors in the context of both the implantation in the brain (Menei et al., 2000; Péan et al., 2000) and the combination with nerve conduits for peripheral nerve repair (Whitehead and Sundararaghavan, 2014). The use of MP can extend the therapeutic window, decrease the dosing frequency and thus improve the therapeutic compliance. Particularly, it has been observed that the immobilization GDNF microspheres into a tube wall enhance sciatic nerve regeneration in 15 mm gaps in rats (Kokai et al., 2011) and GDNF microspheres mixed in fibrin glue enhance nerve regeneration (Tajdaran et al., 2015).

One of the main polymers used to synthetize MP is poly (lactic-co-glycolic acid) (PLGA) and it is approved as biodegradable polymer for *in vivo* use by the US Food and Drug Administration (FDA). Moreover, the application of a combination of different MP containing several neurotrophic factors is also plausible. In addition, the protocol for MP preparation can be adapted in order to modify the behaviour of the microspheres regarding both kinetics and dosage release for different periods (Jain, 2000). Hence, a patient individualized growth factor treatment (depending on nerve type, lesion degree, gap length, patient's age, etc…) could be achieved by loading the desired amount of different trophic factors in microspheres into a nerve conduit NC and thus personalize the treatment so as to improve the regeneration outcomes.

Moreover, in nerve conduits, MP can be loaded either into the wall or filling the lumen. In the lumen, the MP can be filled as aqueous suspension (Xu et al., 2002) or dispersed in a hydrogel or collagen matrix (Rosner et al., 2003). However, filling the guide with different matrices instead of saline assures an immobilization of MP into the lumen during the regeneration process and prevents the MPs to dilute out the lumen or result in sub-optimal concentrations after liquid infiltration.

Thus, the use of MP as a prolonged delivery system can be a powerful tool to enhance nerve regeneration. The lengthening of the trophic support will be of further relevance for the repair of long gaps with nerve conduits, a situation in which the endogenous

support is insufficient to sustain axonal regeneration, as well as for delayed repair of nerve injuries that need a reactivation of the pro-regenerative environment along the distal nerve.

4. Neuroprostheses and nerve interfaces

After loss of a body part, most commonly a limb, there is not only a major reduction of motor and sensory tasks but also psychological distress produced by the missing extremity disrupting patient's own image and self-assurance.
In order to solve this problem, the use of prosthesis to artificially replace the amputee limb has been a solution even in the ancient Egypt (Nerlich et al., 2000). The use of cosmetic prostheses can help to cope with the grief and improve self-esteem of the subject but with such devices no significant functionality and restoration of sensorimotor lost functions can be achieved. Myoelectric prostheses can help to modify the environment and still give some aid in the daily activities but still offer limited actions (Micera, 2016). Thus, an ideal prosthesis should substitute the missing parts of the body and recover its previous normal roles by resembling as much as possible the lost extremity, being operated by the own patient and also offering the ability to perform different complex movements and providing the patient with information sensed from the environment (del Valle and Navarro, 2013).

With this regard, several neuroprostheses have been designed that are able to perform different movements with multifold degrees of freedom (Kwok, 2013) and that incorporate several sensors that are able to perceive (Raspopovic et al., 2014) and even discriminate (Oddo et al., 2016) small variations of the environment and provide the patient with useful sensory information. However, a critical part of the neuroprosthesis is the electrode that interfaces the nervous system and interconnects the human with the mechanical device.

An interface includes all the elements of a system between the machine processor and the human tissues. Thus, an interface entails an electrode or sensor in direct contact with the biological target and the internal wires that link the inner body with the outer processor, the data-acquisition circuitry, and the command unit for controlling the artifact or effector (Navarro et al 2005). Hence, in a neurosprosthesis, the electrode will need to selectively record efferent bioelectrical activity in peripheral nerves that stems from commands of the brain and transform these impulses into electrical signals that activate the motors of the prosthesis. Ideally, the electrode should also be able to

translate the signals of the sensors in the device into electrical inputs and properly transform this information into biological activity that will provide sensory feedback through afferent pathways to the patient (del Valle and Navarro, 2013). Furthermore, inside electrodes several active sites (AS) placed at different points of the surface electrode may increase the probability to stimulate/record different groups of axons and thus provide and exert different and complementary actions. (Micera and Navarro, 2009).

Thus, nerve electrodes should bidirectionally and selectively interface different specific motor and sensory pathways with the best possible long-term biocompatibility.

Peripheral nerve interfaces are of interest because of their reduced invasivity compared with central neural interfaces, and the possibility of delivering an appropriate bidirectional communication by means of a single device, since peripheral nerves contain both motor and sensory fibers (Navarro and del Valle, 2014). Selective electrical interfacing aims at contacting nerve fibers as selectively as possible, requiring devices and fabrication technology in the size of micrometers (Rutten, 2002). However, the use of many small electrodes does not always grant the expected selectivity within the praxis. For example, nerve fibers are recruited by electrical stimulation according to their thickness, therefore large motor fibers innervating the fast-fatigue and strong motor units are activated earlier than the physiologically first-recruited thinner fibers controlling slow fatigue-resistant motor units in what is called inverse recruitment with electrical stimulation (Navarro et al., 2005). In addition, it should also be taken into consideration that a neural interface implanted in a mixed nerve may also lead to a low selective stimulation, as one AS could stimulate at the same time both motor and sensory axons. However, with increasing invasiveness of the implant, higher selectivity of interfacing individual nerve fibers may be reached, lower intensity of stimulation is needed and better signal recording is achieved as the interposition of tissue between the electrode and the axons is reduced (del Valle and Navarro, 2013).

Different types of electrodes have been developed to interface the PNS for different biomedical applications (Navarro et al., 2005; Schultz and Kuiken, 2011). Nerve electrodes can be classified into three main categories depending on nerve invasiveness: extraneural, intraneural and regenerative. (Figure 8).

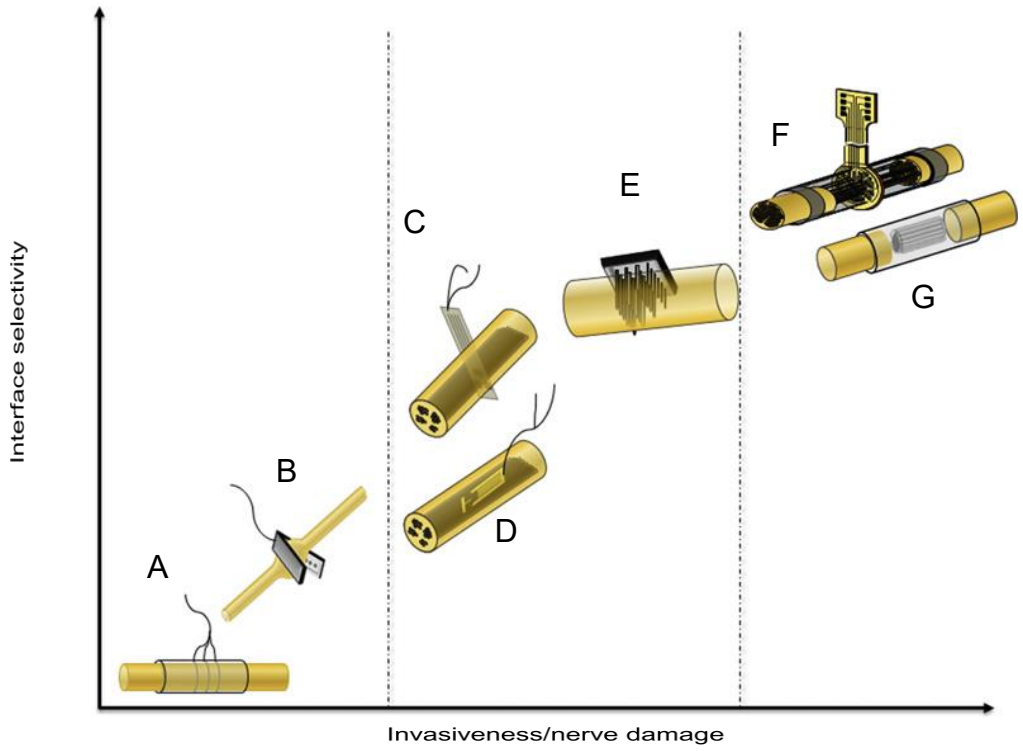

Figure 8. Peripheral nerve electrodes. Electrodes used to interface peripheral nerves classified according to their invasiveness and selectivity. Images show examples of (A) cuff electrode, (B) flat interface nerve electrode (FINE), (C) longitudinal intrafascicular electrode (LIFE), (D) transverse intrafascicular multichannel electrode (TIME), (E) multielectrode array (USEA), (F) sieve electrode, and (G) microchannel electrode. (Extracted from del Valle J et al., 2013)

Extraneural electrodes, such as cuff and FINE (Fig. 8 A-B) (Micera and Navarro, 2009) or the new design neural ribbon (Xiang et al., 2016) are implanted wrapping the nerve with two or more electrode sites in facing the axons (Tan et al., 2014). The ensheathing design of extraneural electrodes reduces their selectivity, thus large myelinated fibers located at superficial locations will preferentially be interfaced (Badia et al., 2011) and those axons located in deep fascicles will remain as if they were silent. However, the reduced invasiveness of these electrodes makes them easier to handle and safer to implant for different biomedical applications (del Valle and Navarro, 2013).

On the other hand, in order to improve the selectivity with respect to extraneural electrodes, intrafascicular electrodes (Fig. 8 C-E) are invasively implanted in the nerve and thus are in close contact with the axons of different fascicles. In fact, these electrodes have been used in several studies in rats to stimulate different muscles and record ENG signals elicited generated after tactile or propioceptive stimuli (Cutrone et al., 2015). Moreover, electrodes like LIFE have been implanted in humans for control of a distal neuroprosthesis and for sensory feed-back (Rossini et al., 2010), MEAs to pilot a wheelchair (Warwick et al., 2003) and USEAs to command virtual robotic fingers and

induce sensory percepts (Davis et al., 2016) and, finally, TIMEs to govern an implanted neurosprosthesis being it able to perform distinct movements and distinguish several stiffness (Raspopovic et al., 2014) and even discriminate between different coarseness of objects (Oddo et al., 2016).

Regenerative electrode

Regenerative electrodes represent a different approach to interface the PNS and are probably the most invasive electrodes but also the ones that are envisioned to offer the highest level of selectivity (del Valle and Navarro, 2013). Regenerative electrodes are not designed to be implanted in an intact nerve but they are thought to be implanted between the cut stumps of a peripheral nerve. They are envisioned to interface a high number of nerve fibers by using an array of contacts covered by the axons as they regrow over or within them, thus, making it possible to record action potentials from and to stimulate small groups of axons (Navarro and del Valle, 2014). The first and most investigated design of a regenerative electrode was the sieve electrode (Akin et al., 1994) (Fig. 8F), composed of an array of via holes with electrodes built around them and placed in the gap between stumps of a transected nerve. Thus, the axons regenerate through the holes, and the electrodes can interface the small bunch of axons of every single hole reaching a high level of selectivity.
The most ambitious utilization of sieve electrodes is the implantation in the sectioned nerves of an amputee so as to interface the axons that formerly innervated the severed limb for a bidirectional interface with the prosthetic limb. Regenerative electrodes not only grant selective stimulation of small groups of regenerated fibers (Lago et al., 2007) but also allow providing receptive signals from different sensory areas to the interface (Navarro et al., 1998). Despite full nerve regeneration is not achieved due to the obstacle of the sieve for growing axons, sieve electrodes have shown promising results after 30 months implant in cats, as only minor electrical changes were found in regenerated nerves and sound levels of functionality were reached (Panetsos et al., 2008). However, extensive research done with these electrodes has raised some questions that still need to be solved. Sieve electrodes are thought to make the axons grow through small holes limiting the possibility to use these electrodes in acute experiments (Navarro et al., 2005). On the other hand, long-term studies have shown some signs of axonopathy in several regenerated fibers due to compression after 6 months in rats (Lago et al., 2005) as well as compromise nerve regeneration because of their reduced transparency.

Several alternative designs have been proposed for improving the amount of axonal regeneration through non-obstructive design. One of them was a facilitating regenerative scaffold in which, instead of growing through holes, the axons grow via thin, narrow parallel tubes with embedded electrodes (Fig. 8G) (Lacour et al., 2009; Srinivasan et al., 2011) or regenerative scaffold electrodes (RSE) inserted along the tube (Clements et al., 2007). Some studies in rats reported that these new approaches may offer a high selectivity in recording and stimulation of the regenerated axons (Clements et al., 2013; Delivopoulos et al., 2012). However, regeneration occurred only in a low proportion of the animals and reinnervation of distal targets is still not well accomplished when gap defects are longer than 2 mm (Clements et al., 2013; Fitzgerald et al., 2012; Musick et al., 2015). In addition, RSE have not still clearly demonstrated that they are able to activate motor fibers to provide a muscular contraction nor to register sensory activity after tactile stimuli of the distal targets.

II. OBJECTIVES

II. OBJECTIVES

Neuroprosthetic devices are a good approach to restore the control of different target organs after peripheral nerve injuries. While different interfaces have been studied, regenerative electrodes are considered to be able to interface the highest number of nerve fibers. However, more efforts are still needed in terms of design and functionality as selective stimulation and/or recording of neural signals from different types of axons are difficult in nerves of high caliber containing a mixed population of motor and sensory axons. Furthermore, implant of regenerative electrodes requires that nerve fibers regenerate through the regenerative scaffold and different strategies can be applied to modulate specifically motor and sensory axons regeneration in order to improve functional selectivity.

In the mainframe of the Europeran project MERIDIAN we aimed to develop and optimize a new design of pluricompartment conduit containing a planar multielectrode array (Fig. 9A), and functionalize the contents of each aisle to favor preferential motor or sensory neurons regeneration (Fig. 9B).

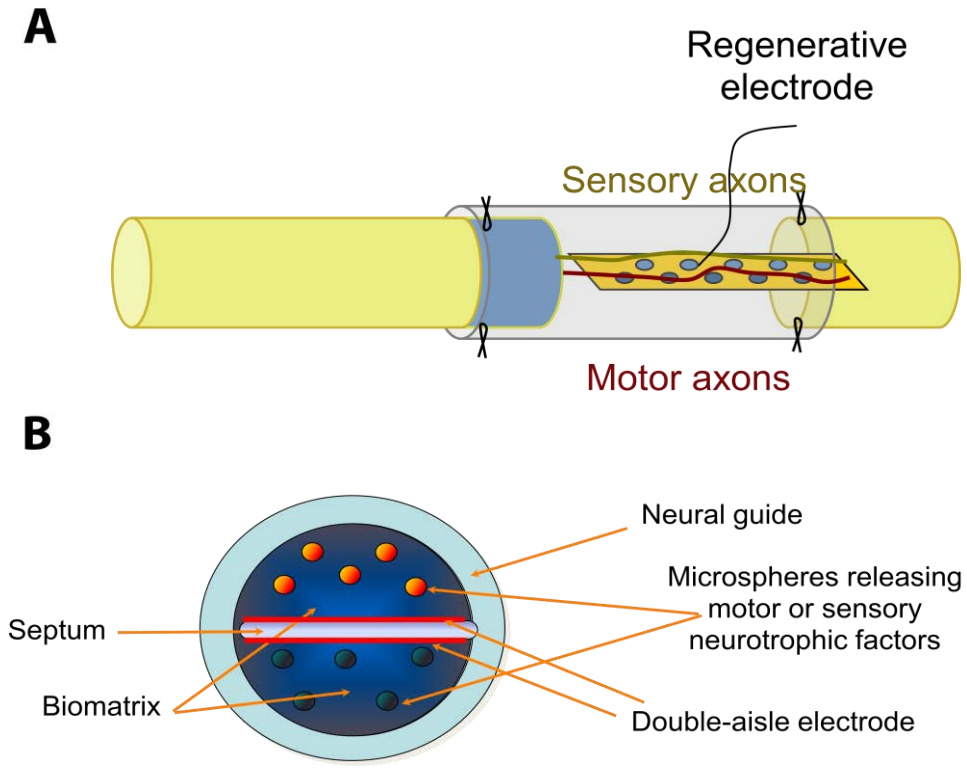

Figure 9. Final objective of the thesis. Double-aisle electrode scaffold into a conduit used for bridge proximal with distal stumps after nerve transection (A). Crossview of the device with a planar electrode that divides the lumen of the conduit in two aisles, which will be filled with specific matrix containing NTFs to attract motor or sensory regenerating axons (B).

For this purpose, the main objectives of this thesis are:

-To investigate new strategies to selectively promote and guide motor and sensory axons regeneration.

-To optimize the design and functionality of double-aisle electrodes for interfacing injured peripheral nerves.

The specific objectives of the thesis are:

- To study the regenerative potential of poly(ethylene glycol terephthalate) and poly(butylene terephthalate) (PEOT/PBT) tubes for repairing long gap defects, and determine if they can be used as a tube scaffold for a regenerative electrode.

- To evaluate whether NTFs encapsulated in PLGA microspheres enhance nerve regeneration by allowing sustained delivery to the regenerating axons.

- To study the role different NTFs at different doses have to selectively promote regeneration of motor or sensory axons.

- To combine selected NTFs and ECM components to selectively and synergistically enhance motor or sensory axon regeneration.

- To optimize the regeneration process in a bicompartment conduit, mimicking the presence of the regenerative electrode, by adding within each compartment the most effective combinations tested in order to separately guide regenerating sensory from motor axons.

- To optimize the design and test in vivo the functionality of double-aisle electrodes both in acute and in chronic animal models.

III. RESULTS

CHAPTER 1

PEOT/PBT Guides Enhance Nerve Regeneration in Long Gap Defects

Daniel Santos[1#], Paul Wieringa[2#], Lorenzo Moroni[2], Xavier Navarro[1], Jaume del Valle[1*]

[1] Institute of Neurosciences, Department of Cell Biology, Physiology and Immunology, Universitat Autònoma de Barcelona, and CIBERNED, Bellaterra, Spain.
[2] Department of Complex Tissue Regeneration, MERLN Institute, Maastricht University, Maastricht, The Netherlands.
[#] Both authors contributed equally to this work

*** Corresponding author:** Dr. Jaume del Valle, Unitat de Fisiologia Mèdica, Facultat de Medicina, Universitat Autònoma de Barcelona, E-08193 Bellaterra, Spain. E-mail: jaume.delvalle@uab.cat

Keywords: peripheral nerve injury; PEOT/PBT; nerve conduit; nerve regeneration; motor, skin and autonomic reinnervation.

Abstract

The development of new nerve guides is required for replacing autologous nerve grafts for the repair of long gap defects after nerve injury. In this study we tested nerve guides made of electrospun fibers of PEOT/PBT, a biocompatible copolymer composed of alternating amorphous, hydrophilic poly(ethylene glycol terephthalate) and crystalline, hydrophobic poly(butylene terephthalate) segments known commercially as Polyactive™ (PA). SEM analysis of the tube reveals that the guides are porous and that PA fibers are aligned in the longitudinal axis of the guide. In vitro studies show that both neurites and Schwann cells grow aligned with the longitudinally oriented PA fibers. In vivo studies reveal that, after rat sciatic nerve transection and repair with PA guides, axons grow more dispersed and occupying a larger area compared to silicone tubes. Moreover, after repair of a limiting (10 mm) and a critical (15 mm) nerve gap, PA guides significantly increased the percentage of regenerated nerves, the number of regenerated myelinated axons, and improved motor, sensory and autonomic reinnervation in both gap lengths. Therefore, these results demonstrate that synthetic PA is a promising biomaterial to build new nerve conduits that promote nerve regeneration through long gaps.

1. Introduction

After peripheral nerve transection due to injury, a gap between proximal and distal nerve stumps is often created as a result of nerve retraction, tissue loss, or the need to remove neuromas [1,2].

The capacity of the peripheral nervous system to regenerate is well known, as evidenced by reports showing that reanastomosed nerve ends successfully undergo axon regeneration and functional reinnervation of target organs. However, this requires tension-free direct suturing of lacerated nerves and, therefore, cannot be applied to the nerve defects that result from a large proportion of transection injuries [3]. The common clinical practice to bridge a nerve defect is the use of an autologous nerve graft. However, autograft repair presents several disadvantages, such as the use of sensory-only nerves, mismatches in size and fascicular pattern regarding both proximal and distal stumps, donor site morbidity, and possible requirement of a second surgical procedure caused by painful neuroma formation or scarring [4,5]. These drawbacks have driven the development of alternative solutions to repair peripheral nerve discontinuities, with a promising approach being the development of synthetic nerve guides.

Entubulation procedures for repairing nerve lesions have already been used clinically as an alternative to autograft using a variety of different conduits [6,7]. This technique has some advantages in comparison with the autograft, such as limiting fibroblast invasion at the repair site, avoiding donor site morbidity, neuroma and scar formation, and facilitating the accumulation of neurotrophic factors within the tube lumen [8]. Although this approach holds promise, more efforts are needed to obtain similar or better outcomes with a nerve conduit than with autograft repair. The main limitation of entubulation is the length of the gap. Nerve regeneration through hollow tubes made of silicone or other synthetic materials fails if the gap is longer than 4 mm in the mouse [9], 10 mm in the rat [10,11], and 30 mm in large primates [12]. Clinically, nerve injury often results in far-reaching gap lengths, necessitating new nerve guides capable of promoting regeneration over these long distances.

Towards this goal, the current study evaluates a purposely designed nerve conduit produced by electrospinning a poly(ethylene glycol terephthalate) and poly(butylene terephthalate) (PEOT/PBT) copolymer, representing the first time this material has been used for neural repair. Several studies have tested nerve conduits made of different biomaterials that enhance nerve regeneration both in short and long gaps [8,13,14]. PEOT/PBT, known commercially as Polyactive™ (PA), is a unique biodegradable copolymer comprised of random blocks of amorphous, hydrophilic PEOT segments and crystalline, hydrophobic PBT segments. While PEOT/PBT

polymers have satisfactory biocompatibility, these materials can be uniquely tuned to elicit a desired biological response by changing the copolymer ratio of PBT to PEOT [15]. With limited adverse effects to the surrounding tissue and flexibility in terms of processing methods, PEOT/PBT has been used in various strategies for repairing different tissues, including tissue scaffolds for tympanic membrane replacement [16] and cartilage regeneration [17], coatings on dental and hip implants, and as bone cement restrictor which has been approved by the US Food and Drug Administration [18] for clinical use in humans. The composition used in this study (PEOT/PBT 300 55/45) has been selected based on proven cell adhesive properties and long resorption time (>6 months), suitable for providing long-term support for cell growth [15].

Continued advances in biofabrication have also shown that material selection in combination with a tailored conduit design can improve nerve regeneration through long gaps. This includes modifying the surface structure of the conduit wall to promote cellular adhesion and guidance [19] and incorporating pores within the conduit, optimally ranging from 5 to 30 μm, to improve nutrients exchange while limiting the invasion of inflammatory cells [20]. This current work capitalizes on the ability to electrospin the PEOT/PBT polymer [16,17] in order to create microfiber nerve guides that exhibit pores that are 8 to 10 μm in diameter and incorporate topographical cues via aligned PA microfibers; electrospinning has been previously shown to produce polymeric fibrous meshes that can impart topographical guidance for neurite growth and glial cell migration [21] and can realize tissue scaffolds with tailored porosity [22].

To our knowledge, there are no reports that studied electrospun PA nerve guides and how they influence peripheral nerve regeneration. In this work we have characterized the structure of a PA nerve guide, and evaluated the PA properties in vitro to examine the role PA nerve guides exert on axonal regeneration. Moreover, we have tested whether PA nerve guides are able to improve regeneration in comparison with a standard silicone tube in both a limiting (10 mm) and a critical (15 mm) gap in the rat sciatic nerve.

Our results show that PA nerve guides not only increase the proportion of regeneration success (i.e. percentage of regenerated nerves over all the repaired nerves), but also enhance nerve regeneration and reinnervation in both gaps at long term. The behavior of the PA conduits to provide an internal milieu-bridge-scaffold that supports and guides regenerating axons represents a novel advance compared with the majority of nerve conduits tested so far. Hence, PA is a promising alternative to be used in clinics for repair of peripheral nerve transection.

2. Results

2.1. Characterization of the PA guides

Nerve guides were examined under SEM, confirming an inner diameter of 2 mm (**Figure 1**A) and an approximate wall thickness of 75 µm (Figure 1B). Closer examination of this nerve guide cross section (Figure 1B) revealed a large porous internal structure (Figure 1C) with an estimated porosity of 62.7 ± 1.3%. Measured pore diameters on the inner and outer surfaces ranged from 2 to 24 µm, with respective average values of 8.02 ± 3.35 µm (Figure 1E) and 10.22 ± 3.8 µm (not shown). SEM examination under higher magnification (Figure 1D) revealed that the electrospun

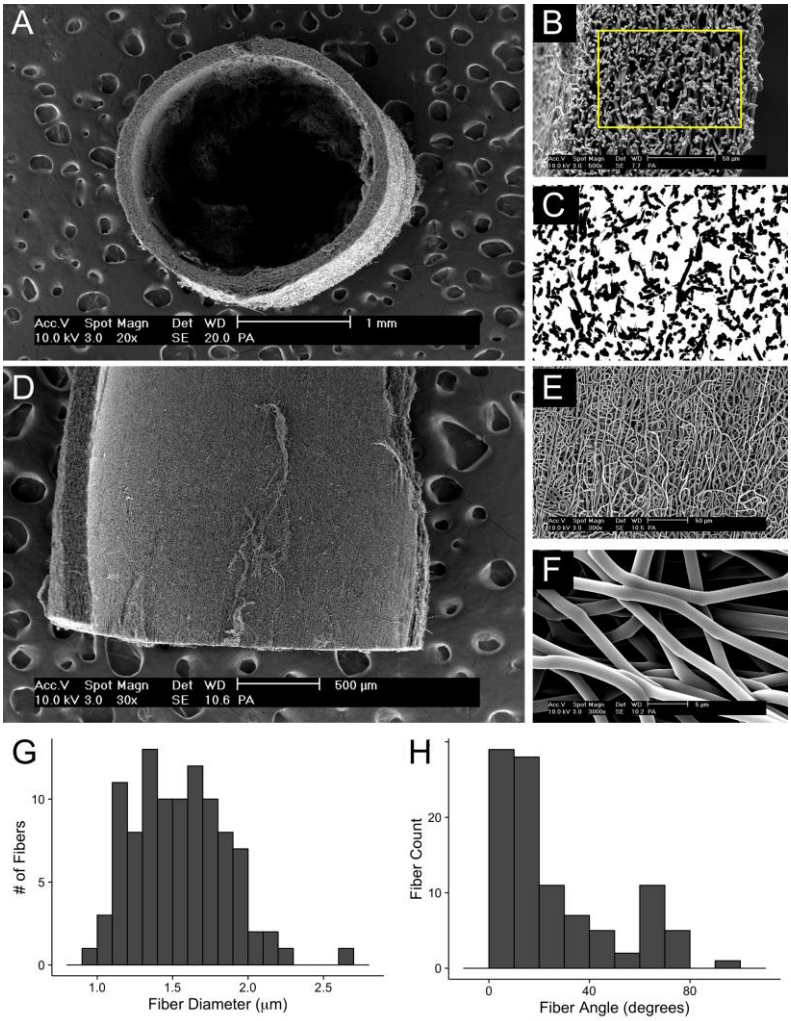

Figure 1. Scanning electron micrographs of PA nerve guides produced with an inner diameter of 2 mm (A) and a wall thickness of 75 µm (B). Image analysis of the wall cross-section (C) indicated nerve guides had a void space, or volume porosity, of 67%. Cutting the nerve guides in half (D) exposed well-formed fibers with a general orientation in the direction of the longitudinal axis and average pore diameter of 8.02 ± 3.35 µm (E). Closer inspection also revealed that fibers were merged at specific locations (F), enhancing the overall physical stability of the fibrous conduit. Plots with the distribution of fiber diameters (G) and angle deviation from the longitudinal axis (H) forming the wall of the PA tube.

nanofibers were consistently well formed and had a smooth morphology (Figure 1E-F) with a range of diameters from 1 to 2 μm and an average diameter of 1.44 ± 0.29 μm (Figure 1G). Fibers showed a general orientation of 1.4 ± 0.37 degrees (Figure 1H) from the longitudinal axis of the nerve guide, creating topographical guidance cues for guiding cell growth in the direction of regeneration. Also observed under SEM were distinct locations where overlapping fibers had slightly fused with one another (Figure 1F). Fiber fusion could be attributed to the retention of small amounts of solvent that allowed fibers to merge when coming in contact during deposition and form physical crosslinks after complete evaporation of the solvent.

2.2. In vitro neurite growth results

Over a 5 day period, in vitro studies of explanted DRG maintained on nerve guides showed directed neurite outgrowth (**Figure 2**B) as well as Schwann cell migration (Figure 2C). Figure 2D shows the calculated neurite growth distribution around the explanted DRG, with the average neurite distribution of three samples shown in Figure 2F. The mean neurite distance was 290 ± 38 μm. The neurite length on laminin-coated glass surface (Figure 2A) was not significantly different from the nerve guide substrate, with a mean neurite length of 487 ± 219 μm ($p = 0.26$; Figure 2E).

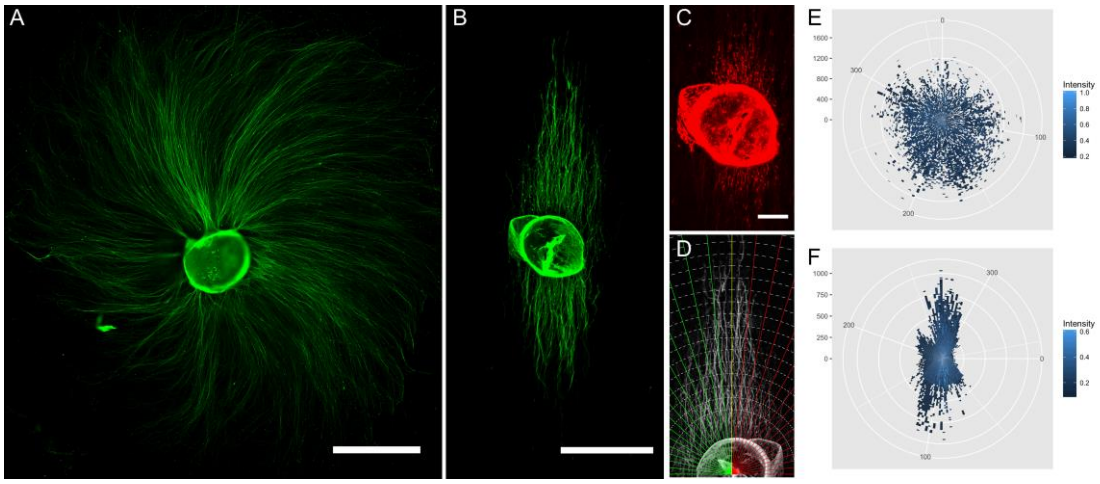

Figure 2. Outgrowth of an explanted DRG on a flat glass substrate (A) and on the inside surface of a PA nerve guide (B). The nerve guide also supports Schwann cell migration (C). Neurite growth was evaluated by applying spatial bins in a radial fashion from the center of the DRG, as shown in (D). The angular frequency of the bins was 2 degrees with a fixed bin area of 50 μm^2. Images of DRG outgrowth were measured for both flat glass substrates and nerve guide substrates (n = 3), with the resulting binned values averaged over each sample for an indication of mean growth.

Further examination showed that the general direction of neurite growth on PA (Figure 2B) differs from the underlying fiber orientation by an average of only 2.67 ± 3.61 degrees. In contrast, no discernable orientation was observed for neurite growth on glass substrate. To quantify the overall pattern of neurite extension, the relative dispersion of neurite extension from a radial axis was calculated to produce a value between 0 and 1; a value of 1 indicates growth that has maximal deviation (90º) from the chosen axis, while growth which overlaps with the axis results in a 0 value. The longitudinal axis of the nerve guide was used to calculate an average dispersion of 0.173 ± 0.034, indicating highly oriented growth (Figure 2B, F). By comparison, neurite growth on glass substrate (Figure 2A, E) exhibits an average dispersion of 0.594 ± 0.05, indicating no directionality.

2.3. Morphological results of short term regenerated nerves

The first in vivo studies were conducted on 6 mm nerve defects, as it has been reported that all nerves regenerate through a silicone guide in such relatively short gap [10,23]. This was performed to establish that PA guides produced similar or better outcomes in terms of nerve regeneration compared to silicone tubulation, before investigating the more challenging conditions of critical nerve gaps. Two weeks after repairing a 6mm sciatic nerve gap with silicone or PA tubes, a regenerating cable was found in all the animals. Surprisingly, in contrast to the classical thin nerve cable formed in the center of the standard silicone tubes (**Figure 3**A) [11], a distinct regenerated nerve was observed in the PA guides, which showed a cellularized structure occupying all the internal lumen of the tube (Figure 3B).

Immunohistochemical labeling showed that as early as two weeks after repair a high number of dot-shaped and densely packed axons can be seen in the nerves repaired with silicone tubes (Figure 3A) whereas axons in PA tubes appeared more dispersed (Figure 3B). Similarly, four weeks after repair, nerves regenerated inside silicone tubes showed an organized structure with an outer layer of cells and small axons with a dotted shape in the core of the nerve cable (Figure 3C) and axons in PA guides were spread over the whole lumen of the conduit (Figure 3D). Moreover, axons were ensheathed by Schwann cells without difference in both groups indicating similar progression of axonal regeneration and remyelination (Figure 3E, F). Measurement of the transverse area of the regenerated cable at 2 and 4 weeks indicated that PA guides supported a larger regenerating area compared to silicone tubes (Figure 3G, H).

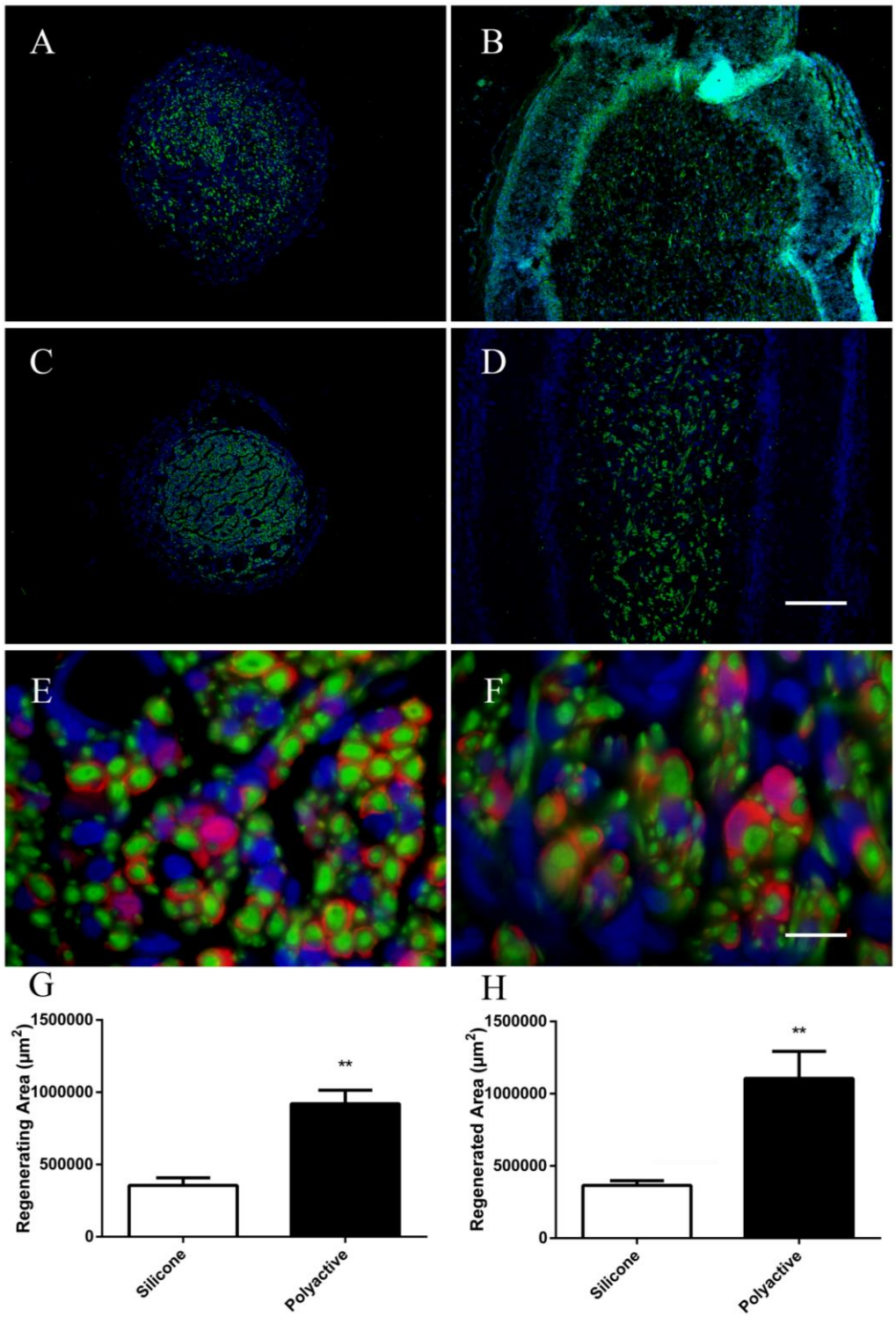

Figure 3. Representative cross section images of the regenerated nerve taken 3 mm distal to the proximal stump of nerves regenerated through a 6 mm gap in silicone (A, C) or PA (B, D) guides 2 (A, B) and 4 (C, D) weeks after repair. Axons are stained with βIII-tubulin (green) and nuclei with DAPI (blue). **E-F:** Close view of C (G) and D (F) with Schwann cells stained with S100 (red). **G-H:** Area of the regenerated nerve at the mid tube (3 mm from the proximal stump) in silicone and PA groups after 2 (G) and 4 (H) weeks of regeneration. Data presented as mean ± SEM, **p<0.01 vs silicone group. Scale bar 200 µm (A-D) and 10 µm (E-F).

2.4. Target reinnervation in long term regeneration studies

Nerve conduction tests performed 1 week after sciatic nerve injury demonstrated complete denervation of the hind limb muscles. At 60 dpo all PA10 animals showed evidence of reinnervation with recordable CMAPs in TA and GM muscles whereas only 37.5% of S10 animals showed positive values. In animals with 15 mm gap defect, CMAPs in TA and GM muscles were recorded in half of the PA15

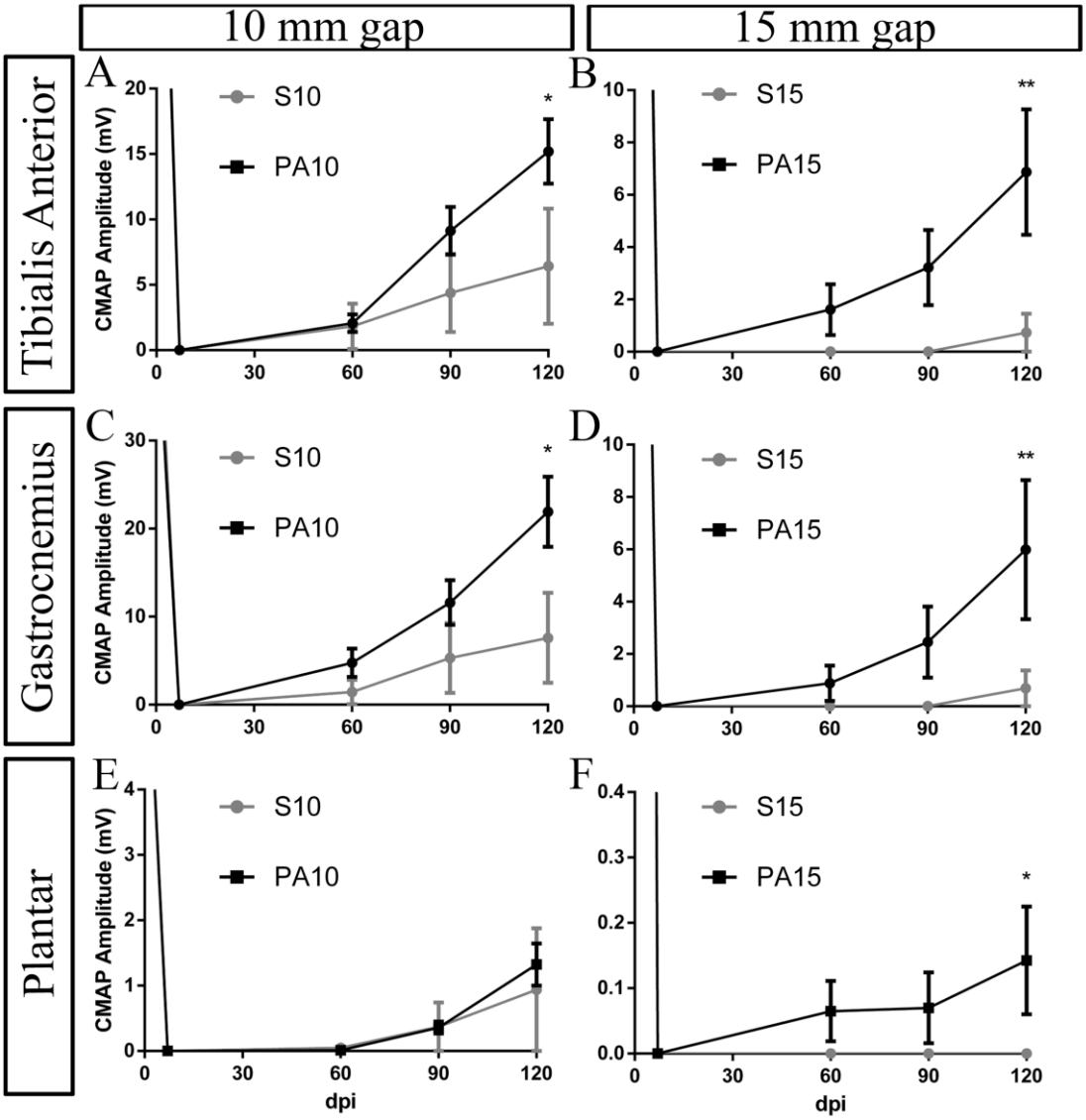

Figure 4. Mean amplitude of the compound muscle action potential (CMAP) of tibialis anterior (A, B), gastrocnemius (C, D) and plantar interossei (E, F) muscles in rats with 10 (A, C, E) and 15 (B, D, F) mm gap defect during 4 months after sciatic nerve lesion and repair with silicone or PA tubes. Data presented as mean ± SEM. *p<0.05, **p<0.01 vs S10 and S15 groups.

animals but in none of S15 animals. At 90 dpo, although non-significant, the differences in CMAP amplitude between the PA10 and S10 groups increased and still no signs of regeneration for the S15 rats appeared. At the end of the follow up (120 dpo) the mean CMAP amplitude of the TA (15.2 ± 2.4 mV) and the GM (17.7 ± 4.1 mV) muscles in the PA10 group were significantly higher than in the S10 group (6.4 ± 4.4 mV and 7.6 ± 5.1 mV respectively) (**Figure 4** A, C), while no statistical difference was found for the PL muscle (Figure 4E). On the other hand, the PA15 group had significantly higher CMAP amplitudes in all the three tested muscles (Figure 4B, D, F) (6.1 ± 2.2 mV for TA, 6.0 ± 2.6 mV for GM and 0.14 ± 0.10 mV for PL muscles) compared to the S15 group (1.2 ± 1.2 mV, 0.7 ± 0.7 mV and 0 mV, respectively; $p < 0.05$).

2.5. Histological results

Macroscopic evaluation of the regenerated nerves at 4 months after injury and repair (**Figure** 5) demonstrated that three of eight animals (37.5%) in group S10 presented a regenerative cable at the center of the tube (Figure 5B), whereas only one regenerated nerve (16.6%) was found in group S15 (**Figure 6**I).

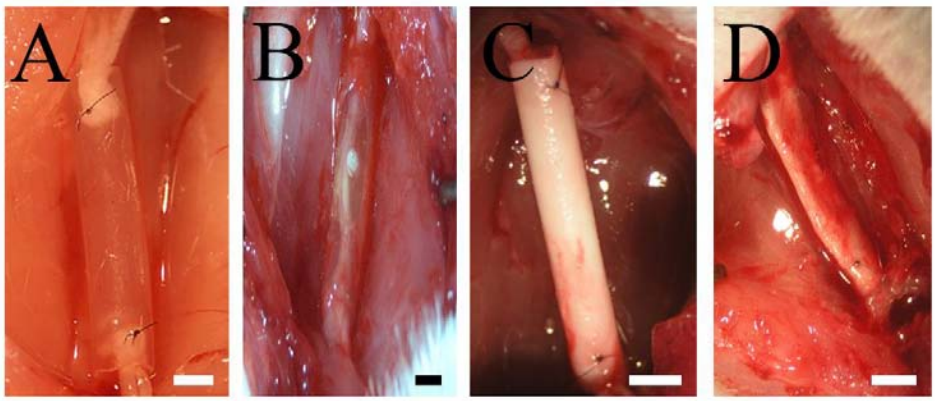

Figure 5. Representative images of silicone (A, C) and PA (B, D) tubes before (A, B) and after (C, D) 120 days of regeneration. Scale bar 2 mm.

The PA tubes were partially degraded at this time but still opaque (Figure 5D), so macroscopic visualization of the regenerated tissue was not possible. All the tubes showed a thick structure filling the lumen. Histological evaluation at the midpoint of the PA tubes indicated that all the animals presented a regenerated nerve in group PA10 (100%) and five of nine animals in group PA15 (55.5%) (Figure 6I).

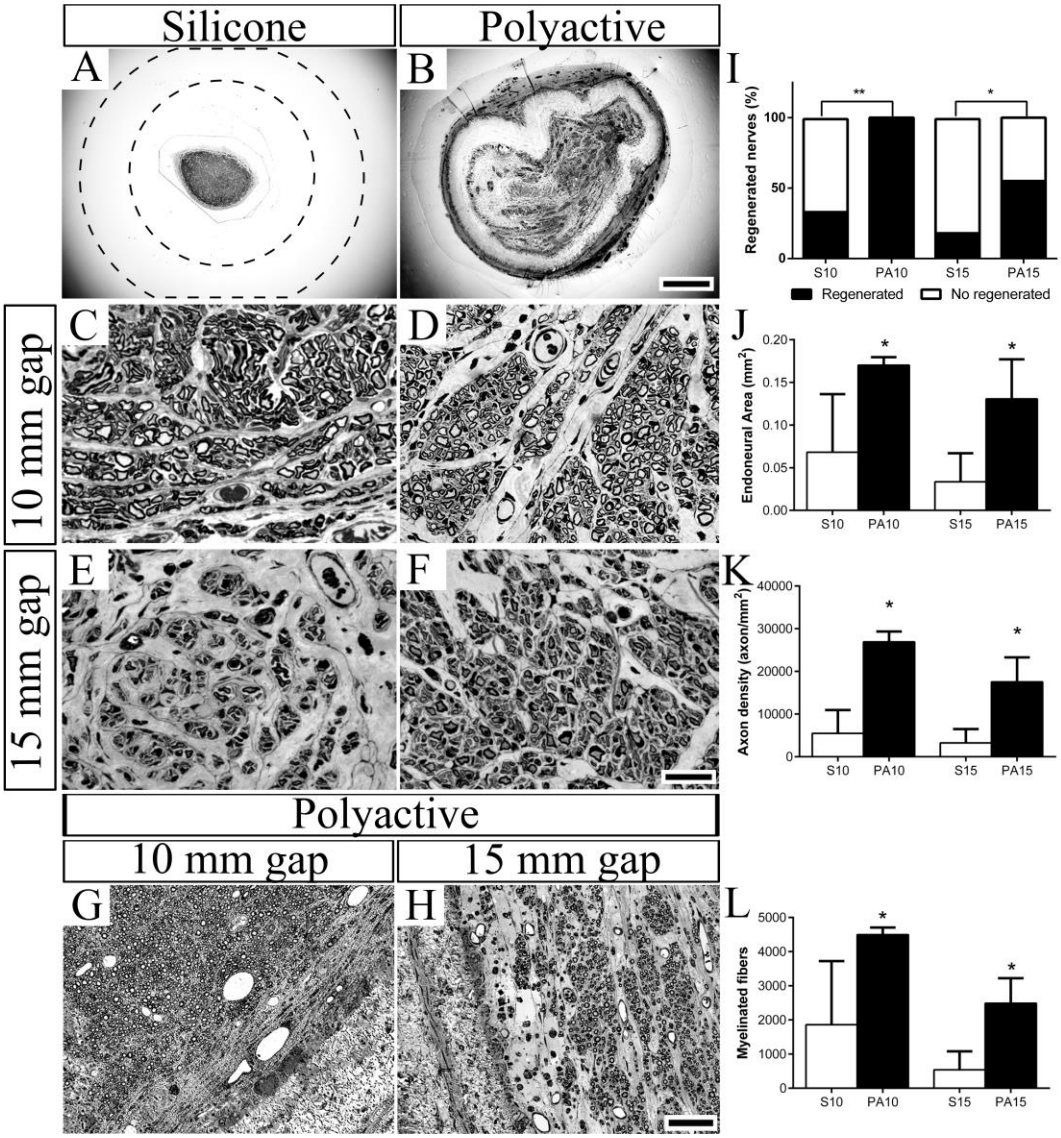

Figure 6. Representative semithin transverse sections of S10 (A) and PA15 (B) regenerated nerves, the contour of the silicone tube is drawn as a dotted line in A. **C-F:** Representative micrographs at higher magnification of transverse sections of S10 (C), PA10 (D), S15 (E) and PA15 (F) groups 120 days after repair. **G-H:** Representative images of myelinated axons growing close to the wall in PA10 (G) and PA15 (H) rats. **I-L:** Plots comparing success of nerve regeneration (I), endoneurial area (J), axon density (K) and number of regenerated myelinated fibers at the mid-tube (L) in groups with 10 and 15 mm gap repaired with silicone or PA tubes. All images were taken 5 and 7.5 mm distal to proximal stump for the 10 and 15 mm gap groups respectively. Data presented as mean ± SEM. *p<0.05 vs S10 and S15 groups; **p<0.01 vs S10 group. Scale bar 500 μm (A, B), 25 μm (C-F) and 50 μm (G-H).

Nerves that regenerated in S10 rats showed a centered cable containing a dense core of tissue with numerous small blood vessels and regenerative units with myelinated axons (Figure 6A, C), whereas the only regenerated nerve in S15 rats had fewer myelinated fibers than in S10 nerves (Figure 6E). On the other hand, PA tubes showed a thick wall and the inner area of regeneration occupied by axons, extracellular matrix and non-neuronal cells (Figure 6B, D, F). Axons can be seen in direct contact

with the inner surface of the PA tubes (Figure 6G, H) indicating that the PA conduits also provide a guiding longitudinal structure to the regenerating axons. Morphometrical analysis demonstrated that the mean value of endoneurial area (Figure 6J), axon density (Figure 6K) and number of myelinated axons (Figure 6L) at the midpoint of the tubes was higher in both PA groups in comparison with silicone tube repaired animals.

2.6. Cutaneous reinnervation of plantar pads

Immunostaining of intact plantar pads with anti-PGP antibody reveal a complex network of nerve trunks that penetrate the skin and are divided into several bundles of fibers that form subepidermal nerve plexuses (SNP), create central bundles that innervate the epidermis (**Figure 7**A-B) and also innervate the sweat glands (SGs) (Figure 7C-D) [24]. In animals with a 10 mm gap lesion there was reduced innervation of the dermis, epidermis and the SGs in comparison with intact animals. In animals with a 15 mm gap defect, no innervation was found in S15 group whereas PA15 animals showed some nerve bundles in the SNP, and spare innervation of the epidermis.

Quantitative analysis indicated that the number of intraepidermal nerve fibers (IENF) and innervated SGs were higher in the PA10 group in comparison with the S10 group (Figure 7E, F), although not significantly due to the large variability. The PA15 showed significantly higher reinnervation of the epidermis and the SGs compared with the S15 group that was completely denervated.

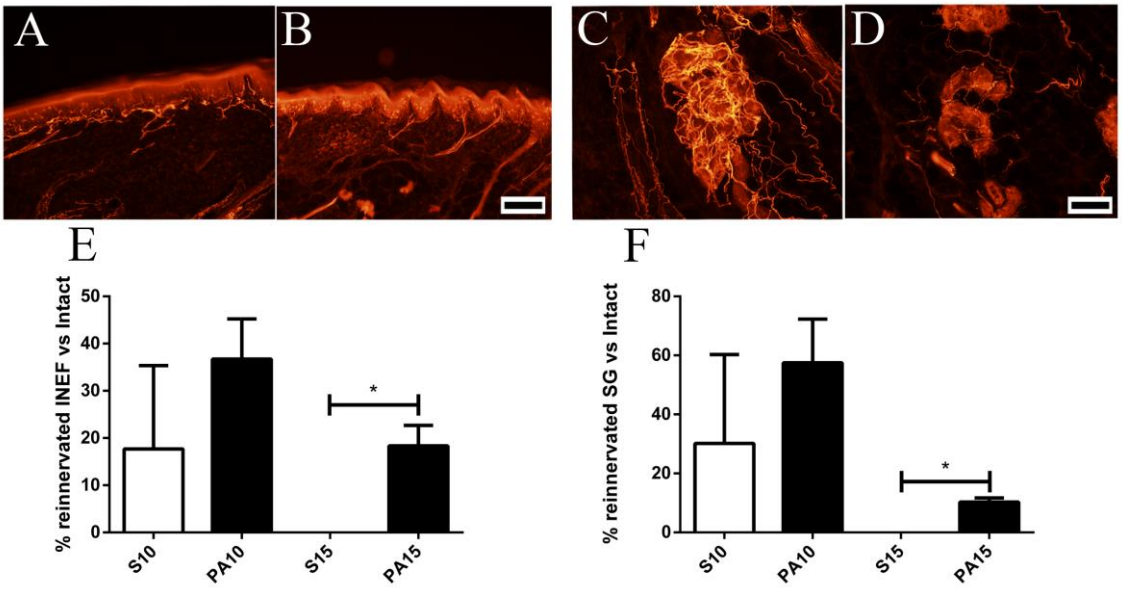

Figure 7. Representative images of footpads stained with PGP showing the innervation of epidermis (A, B) and of sweat glands (C, D) of intact (A, C) and PA15 (B, D) samples. **E:** Percentage of reinnervated IENF with respect to control values. **F:** Percentage of reinnervated SGs with respect to control values. Data presented as mean ± SEM. *p<0.05 vs S15 group. Scale bar 100 μm.

3. Discussion

After peripheral nerve injury, coaptation of nerve stumps to promote axonal regeneration is not always possible because of nerve retraction or tissue loss. Tube repair is an accepted approach to solve this issue; however, more efforts are needed to improve regeneration through nerve conduits in order to match the performance of autografts. Since the first attempts with tube repair [25], different strategies have been tested to enhance regeneration in long gaps including the use of different materials in tube manufacturing[14], addition of extracellular matrix filling the tube [26] or application of neurotrophic factors [27].

Fibrous nerve conduits produced via electrospinning represent a promising biofabrication approach to achieve this aim, with initial studies reporting moderate success [28,29]. One of the major benefits of this technique is the flexibility over the design and composition that can be obtained. Electrospun nerve guides have been created from synthetic polymers [28,30], natural proteins [31], or a synthetic/natural blend[29], which allows for the tuning of surface chemistry, bioactivity, and degradation properties. Electrospun fibers can also incorporate neurotrophic growth factors, either via controlled release [30,32,33] or conjugated to the fiber surface [31]. Nerve guides incorporating Schwann cells is another strategy employed to enhance axonal growth[34], and since the first studies reporting the integration of living cells in the electrospinning process [35] this technique has been widely used for the fabrication of a wide range of living scaffolds [36,37].

Current regulations restrict the immediate clinical application of incorporated biological components [34], which has motivated the development of electrospun nerve guides that intrinsically improve nerve growth through optimal material selection and construct design. To this end, fibrous nerve guides have been created with pores ranging from 5 to 30 μm in diameter [28,38]; this is considered optimal for the influx of nutrients while providing a sufficient barrier to minimize the invasion of detrimental inflammatory cells [20]. Electrospun constructs with oriented fibers have also been shown to enhance *in vitro* neurite elongation and Schwann cells migration[39]. Similarly, aligned fibers have been incorporated within nerve guides[32,40] and have been shown to promote nerve regeneration *in vivo* [30,41,42]. However, alignment and the subsequent packing density of the oriented fibers can also reduce the pore size below the recommended diameter [38]. Evidence also suggests that smaller nanofibers exhibit higher packing densities that restrict cell infiltration, limiting Schwann cell migration and neurite extension; fibers 1.5 μm in diameter are reported to provide optimal guidance of sensory neurons [43].

In the present study, we characterized a novel nerve guide fabricated from PA through an optimized electrospinning process that realizes an ideal combination of fiber size, fiber alignment, and porosity. To the best of our knowledge, this is the first study to determine the efficacy of electrospun nerve guides in the repair of the rat sciatic nerve with a critical nerve gap greater than 10 mm. PA belongs to a family of biocompatible copolyethers which have been used to realize a variety of implantable biomedical devices approved by the FDA [18]. The polymer used in this study (PEOT/PBT 300 55/45) was selected because it promotes cell adhesion and can be readily processed by electrospinning. SEM analysis of the resulting nerve guides revealed well-formed fibers with an average diameter of 1.44 μm and a generally aligned, longitudinal orientation. *In vitro* studies (**Figure 2**) confirmed that both neurites and Schwann cells were able to adhere on the surface of the nerve guide and that the aligned fibers of the nerve guide resulted in highly oriented neurite extension, similar to other studies with electrospun fibers loaded with trophic factors [32]. The nerve guides produced in this study had an estimated void space, or volume porosity, of 62% and an average pore diameter between 8 and 10 μm, which is within the recommended range [20].

Closer inspection revealed that microfibers slightly fused with one another during the fabrication process, where such physical crosslinks are known to improve mechanical properties of electrospun constructs [44]. This likely correlates with the observed physical stability of this nerve guide, which was able to maintain integrity despite having compliant walls with an approximate thickness of 75 μm and a high degree of porosity for nutrient diffusion. The fibrous network was able to easily accommodate suturing as well as retain the 10-0 suture for up to 120 days. Reports have shown that highly porous nerve guides can also be degraded too rapidly to be effective for long nerve defects[45]. Polymer degradation often occurs via surface-mediated bulk fragmentation and, therefore, the greater surface area of a porous nerve guide can result in proportionally faster degradation compared to a solid nerve guide of the same material. However, the PA nerve guides in this current study were observed to be mostly intact when explanted; this is in line with previous reports on the degradation of this polymer, which also showed that degradation products are not cytotoxic [15,46]. The relatively slow rate of PA absorption allows these electrospun nerve guides to be highly porous while remaining physically intact, leading to a balance between nutrient influx and sustained directed growth for overall improved nerve regeneration.

Although the nerve guides remained relatively intact at 4 months after implantation, we also observed that fibers began to progressively invade the luminal

cavity and appeared to provide an unexpected benefit to the regenerative process. This is attributable to the erosion of physical crosslinks between fibers, allowing fibers to serve as additional ECM-like guidance structure for Schwann cell migration and neurite extension. The benefits of explicitly including an intraluminal structure to improve neural regeneration have been widely explored, with a number of strategies incorporating fibrous elements to improve growth [33,47,48]. However, this strategy often necessitates increased manufacturing complexity[19] and intralumen structures can also obstruct regenerative growth, reducing effectiveness [47,49]. In the current study, the appearance of an internal structure is an intrinsic property of the PA nerve guide and is limited to the periphery of the lumen, where it provides additional support for cell adhesion while not obstructing growth through the guide. Furthermore, this partial degradation over time also suggests that this nerve guide becomes progressively more accommodating to maturing neural tissue, thus circumventing the risk of compression of the regenerated nerve that has been observed within traditional solid nerve guides [19,50].

With regard to characterization of the regenerative process, across a short 6 mm gap at two or four weeks, axons were present in both tubes, but, in contrast to the usual regenerated nerve centered in the silicone tube, the PA guides showed axons spread throughout the internal lumen and also in contact with the wall (see **Figure 4**). This is a novel observation regarding tube repair of nerve defects. We can hypothesize that the permeability of the PA wall and the longitudinal cues offered by PA fibers account for the larger regenerative scaffold inside the PA guide. The formation of a connective cable that connects both nerve stumps over which fibroblasts and Schwann cells migrate to form a new nerve structure that provides support for axonal elongation, are the first steps in the regeneration process in nerve conduits [11]. Axonal regeneration fails to occur in long gaps, over a critical length, because the regenerative capabilities of the nerve stumps are exceeded and the initial cable is not formed. In this situation, the inflow through the porous tube wall of extraneural diffusible factors or of repairing cells may represent an additional support [51,52]. The nerve growth observed in contact with the PA wall indicates that PA guides may serve not only as a tube concentrating the regenerative microenvironment but also as a bridge enhancing the first step of nerve regeneration and facilitating cell migration along and within the tube.

Concerning the more challenging 10 and 15 mm nerve gaps in the rat sciatic nerve, a separation of 10 mm has been reviewed to account for about 50% of regeneration success with silicone and other plastic tubes, whereas a 15 mm gap is considered critical since no regeneration occurs in those tubes [8,23]. In this study, PA guides allowed for a significantly higher success of regeneration compared to silicone

tubes; all the animals regenerated in group PA10, and 55% in group PA15 (**Figure 6**l), demonstrating that PA guides are adequate to bridge critical gaps and ensure improved outcome of nerve regeneration. Functional and histological evaluations showed that PA guides had more myelinated axons in comparison with silicone tubes, and allowed higher motor, sensory and autonomic reinnervation, demonstrating that PA guides enhance nerve regeneration in both limiting and critical long gaps. Although our results are still far from those obtained with autograft repair in a 15mm critical gap in the same animal model [53], it should be taken into account that the length of the gap in the autograft repair has not the same influence as it has in regeneration with tube repair. While regeneration is limited in tube repair over critical gaps (e.g. 6 mm in mice, 15 mm in rats) when using silicone or other synthetic tubes [23], similar levels of regeneration take place irrespective of permissive or critical gap lengths after autograft repair [54,55]. The present results are comparable with studies that used other advanced hollow synthetic nerve guides to repair a 15 mm nerve defect in the rat, such as poly-L-lactide-e-caprolactone [56], poly D,L-lactic acid [57] or chitosan [53] tubes, that obtained acceptable outcomes of nerve regeneration but still below to autograft. However, PA guides act both as a tube and as a scaffold that is able to bridge long gaps without the need to use an exogenous matrix, providing a promising platform for further development. A multifactorial approach has been claimed to be necessary to bridge long gaps providing a real alternative to the nerve autograft [8]. The flexibility of the electrospinning technology used to fabricate PA guides makes it possible to not only realize topographical cues, but also to improve guide design by incorporating adhesive and encapsulated chemical signals [58,59] as well as living cells [37], opening an opportunity to take peripheral nerve regeneration a step further.

4. Conclusions

PEOT/PBT emerge as a new biomaterial in the field of peripheral nerve regeneration with high perspectives because of their intrinsic properties that include biocompatibility, bioresorption, cell adherence and cell viability. Our results demonstrate that the PA guide is a promising synthetic conduit to promote nerve regeneration through critical length defects in the injured peripheral nerve.

5. Materials and methods

5.1. PEOT/PBT conduit preparation

PA nerve guides were prepared using a custom electrospinning apparatus, supporting XY translation of the spinneret needle over a collector and maintaining humidity at 30% and temperature at 25ºC. Polymer solution preparations

300PEOT55PBT45, known commercially as Polyactive™ 30055/45, were provided by PolyVation B.V. (Groningen, Netherlands). The chemical composition is represented by the notation aPEOTbPBTc, where a is the molecular weight, in g/mol, of the starting PEG segments used in the polymerization process, whilst b and c are the weight ratio between PEOT and PBT blocks, respectively. PA was prepared as a 25% w/v solution dissolved overnight in a mixture of chloroform ($CHCl_3$, Sigma Aldrich) and 1,1,1,3,3,3-hexafluoro-2-propanol (HFIP, Biosolve, Netherlands) at a volume ratio of 7:3.

A PA nerve guide formulation with thin, porous walls was produced. For the electrospinning of the PA guide a 2 mm diameter, 3 cm long brass mandrel collector was used, rotated at a speed of 50 rpm. A 0.8 mm diameter spinneret was mounted onto a charge parallel plate suspended above the mandrel, held at a working distance of 13.5 cm and programmed to translate along the axis of the mandrel (120 mm/min) to ensure even distribution of fiber deposition. A polymer solution flow rate of 1 ml/h was maintained using a KD Scientific syringe pump. A voltage of 20 kV was applied using a DC high voltage supply (Gamma High Voltage Research, USA). Fibers were deposited onto the mandrel for 10 minutes. After deposition, the mandrel was placed in 70% ethanol to ease removal of the nerve guides, and they were left to air dry. Nerve guides were gold sputter-coated with a Polaron E5600 sputter-coater and examined with a XL 30 ESEM-FEG (Phillips) operating at 10 kV (**Figure 1**A). The resulting images were used within ImageJ (NIH, Bethesda, MD) to assess approximately 100 fibers, measuring the fiber diameter and fiber orientation angle with respect to the nerve guide longitudinal axis. The pore diameters on the inner and outer guide surfaces were similarly evaluated. To analyze the void space, or volume porosity, of the nerve guide wall, samples were placed in liquid nitrogen and cut with a scalpel for a precise ‘snap freeze‘ section (**Figure 1**B). Subsequent SEM images of the cross-section were processed using the default ImageJ threshold method, producing a binary image (**Figure 1**C) with the fiber area shown in black and void space shown in white. The ratio of the void space to the overall area was calculated as a measure of porosity.

5.2 In vitro studies

In vitro assessment of the neurite outgrowth on the internal surface of the PA nerve guides was first performed. The PA tubes were longitudinally cut and opened to create flat sheets. These were placed in a 24 well plate with the internal surface of the guide facing up and held in place with the help of appropriately sized Viton o-rings (Eriks). Dorsal root ganglia (DRG) were excised from 2-day-old Wistar rat pups; following a procedure approved by the Utrecht Animal Use Committee (DEC) according to Dutch law (as stated in the “Wet op de dierproeven”). DRG were cut in half and

placed on the nerve guide. DRG cultures were maintained in Neural Basal Medium (Invitrogen) with B27 supplement, 0.2 mM glutamine, penicillin/streptomycin and 50 ng/ml of recombinant human NGF-β (Sigma Aldrich). As a control, DRG were also seeded on glass coverslips (VWR) previously coated with 20 µg/ml of poly-d-lysine (Sigma Aldrich) and 10 µg/ml of laminin (Sigma Aldrich) [60]. Medium was refreshed every 2 to 3 days and cultures were maintained for a total of 5 days. Cultures were then fixed in 4% paraformaldehyde for 20 min at 4ºC, followed by permeabilitization with 0.1% TritonX (Sigma Aldrich) for 15 min at room temperature. Immunofluorescence was employed to visualize DRG neurite outgrowth. First, a blocking solution of 5% goat serum was applied for 1 h at room temperature, followed by 12 h incubation at 4ºC with primary antibodies mouse anti-βIII-tubulin antibody (1:1000; Sigma Aldrich) and rabbit anti-S100 antibody (1:500; Sigma Aldrich), and a secondary 1 h incubation at room temperature with anti-mouse Atto 647N antibody (Sigma Aldrich) and anti-rabbit Alexa 488 antibody produced in Goat (Invitrogen). Imaging was performed with either a Nikon A1 confocal or a BD Pathway 435 Imager, with the resulting collection of overlapping images finally stitched to form a large image using the ImageJ Grid Stitching Plug-in [61]. To evaluate pattern of neurite outgrowth, a polar histogram was created that represents the associated distribution of fluorescence intensity centered around the DRG. The average intensity of neurite immunofluorescence was measured per histogram bin with an angular 'width' of 2 degrees and a fixed area of 500 µm per bin (**Figure 2**D). To determine the orientation of neurite growth on nerve guides, the intensity of neurite immunofluorescence was evaluated to produce a 'center of mass' of the neurite growth per radius. Calculating this point for every radius resulted in a line emanating from the DRG, with the orientation of neurite growth calculated as the average angle of this resulting line. This orientation was compared to the visually assessed orientation of the underlying nerve guide fibers.

5.3. In vivo studies

Adult female Sprague Dawley rats (250–300 g) were used in this study. All animals were kept on standard laboratory conditions with a light-dark cycle of 12:12 h and *ad libitum* access to food and tap water. The experimental procedures were approved by the ethical committee of the Universitat Autonoma de Barcelona in accordance with the European Directive 2010/63/EU on the use of animals for scientific purposes. All efforts were made to minimize pain and animal discomfort during surgery and treatments.

Animals were anaesthetized with an i.p. injection of sodium pentobarbital (40 mg/kg), the right sciatic nerve was then exposed at the midthigh and sectioned 92 mm from the tip of the third toe, and a distal nerve segment resected. Before implantation, nerves guides were sterilized in 70% ethanol and washed in sterile water. In order to assess whether PEOT/PBT could be a good material to sustain peripheral nerve regeneration, a short term study (15 and 30 days after repair) was conducted with silicone or PA nerve guides that were sutured with 10-0 monofilament sutures (Alcon) to the nerve stumps leaving a 6 mm gap between both nerve ends (n=4 per group). Once the proof of concept was set, a long term reinnervation study (120 days after repair) was conducted in different groups of rats with the aim to repair either a limiting gap of 10 mm with silicone (S10, n=8) or PA (PA10, n=9) guides or a longer 15 mm critical gap with silicone (S15, n=6) or PA (PA15, n=9) guides (see **Figure 3**A, C). After implanting the tubes, the wound was closed by planes with silk sutures and animals were left to recover from the anesthesia on a warming pad before being housed again.

5.4. Morphological evaluation of nerve regeneration

After 15, 30 or 120 days post operation (dpo) animals were deeply anesthetized and perfused with 4% paraformaldehyde in PBS. Before nerve processing, silicone tubes were carefully removed and only the regenerated cable was processed, whereas in PA groups the regenerated nerve and tube were processed together because the strong adherence between them. The regenerated sciatic nerves were divided in two halves, proximal sections were post-fixed in the same perfusion solution for 4 h and then cryoprotected in PBS-sucrose 30% with azide 0.1% at 4ºC before cryosectioning. The distal parts were post-fixed with 3% glutaraldehyde–3% paraformaldehyde in cacodylate-buffer solution (0.1 M, pH 7.4) before their processing for morphological evaluation.

For immunostaining, the regenerated nerves were serially cut into 15µm thick sections on a cryostat (Leica Microsystems, Germany) and collected on gelatin-coated slides. The sections were blocked and permeabilized with 0.3% Triton-X100 and 5% normal donkey or goat serum for 30 min. Then, slides were incubated with rabbit anti-βIII-tubulin (1:500, Covance) to stain all axons and rabbit anti-S100 (1:200, Immunostar) to stain Schwann cells overnight at 4ºC in 0.1% Triton-PBS. After washes in PBS, slides were incubated with Alexa 488 or Alexa 594-conjugated secondary antibodies (1:200; Life Sciences) for 1h. For S100 biotin amplification, samples were incubated with biotinylated anti-rabbit antibody (1:200, Vector) and, after washes, with Alexa Fluor 488 streptavidin (1:200; Life Sciences). The sections were coverslipped

with Mowiol containing DAPI (0.1 µg/ml, Sigma). Image acquisition was performed with an epifluorescence microscope BX51 (Olympus) and a DP73 digital camera (Olympus).

For light microscopy analysis, nerves were postfixed in OsO_4 (2%, 2h) and dehydrated through ethanol series prior to embedding in Epon resin. Semithin sections (0.5 µm thick) taken at the mid tube level were stained with toluidine blue and examined by light microscopy. Images of the whole sciatic nerve were acquired with an Olympus DP50 camera attached to computer. Sets of images for analysis obtained at 100X were chosen by systematic sampling of squares representing at least 30% of the nerve cross-sectional area. Measurements of cross-sectional area of the whole nerve and counts of the number of myelinated nerve fibers were carried out using ImageJ software.

5.5. Evaluation of distal target reinnervation

In the long term study, noninvasive nerve conduction tests of the sciatic nerve were performed at 60, 90 and 120 dpo to assess functional reinnervation of distal muscles. Briefly, animals were anesthetized, placed on a warm plate and the sciatic nerve was stimulated percutaneously through a pair of monopolar needle electrodes at the sciatic notch with single electrical pulses at supramaximal intensity. The compound muscle action potentials (CMAP) were recorded from the tibialis anterior (TA), gastrocnemius medialis (GM) and plantar interossei (PL) muscles with small needle electrodes placed into the muscle belly [56]. The tests were performed using an electromyograph (Sapphire 4M, Medelec Vickers). Control values for each rat were obtained from the intact left hind limb.

At the end of follow-up, footpads were harvested and processed as indicated above (2.4), but with primary antibody against protein gene product 9.5, (PGP, 1:500, ABD Serotec) a cytoplasmic peptide selectively found in practically all neurons to stain axons innervating the skin [24]. For analysis, images of three sections of each sample were collected with an Olympus DP50 digital camera to count the number of IENF per mm skin and the number of reinnervated SGs in the pad.

5.6. Data analysis

Data are presented as mean ± SEM unless otherwise stated. Analysis of statistical significance was performed using GraphPad Prism (GraphPad Software version 6.0, USA) software. Student's t-test, two-way ANOVA followed by Bonferroni's post hoc test or chi-square test for comparisons between groups were used when appropriate. Statistical significance was considered when P value was <0.05.

Acknowledgments

This research was supported by the European Union FP7-NMP project MERIDIAN under contract number 280778 and FPT-ICT project NEBIAS under contract number 611687, TERCEL and CIBERNED funds from the Instituto de Salud Carlos III of Spain, FEDER funds, and the Natural Science and Engineering Research Council of Canada (NSERC). This research has also been made possible with the support of the Dutch Province of Limburg. The authors acknowledge the support of Prof. Silvestro Micera, from Scuola Superiore Sant'Anna, Pisa, throughout this study and thank the technical help of Monica Espejo, Jessica Jaramillo and Marta Morell.

References

[1] G. A. Georgeu, E. T. Walbeehm, R. Tillett, A. Afoke, R. A. Brown, J. B. Phillips, *Cell Tissue Res.* **2005**, *320*, 229.

[2] S. Hall, *J. Bone Joint Surg. Br.* **2005**, *87*, 1309.

[3] R. Robinson, *Muscle Nerve* **2000**, *23*, 863.

[4] W. Daly, L. Yao, D. Zeugolis, A. Windebank, A. Pandit, *J. R. Soc. Interface* **2012**, DOI 10.1098/rsif.2011.0438.

[5] E. O. Johnson, P. N. Soucacos, *Injury* **2008**, *39*, S30.

[6] M. E. H. Boeckstyns, A. I. Sørensen, J. F. Viñeta, B. Rosén, X. Navarro, S. J. Archibald, J. Valss-Solé, M. Moldovan, C. Krarup, *J. Hand Surg. Am.* **2013**, *38*, 2405.

[7] G. Lundborg, *J. Peripher. Nerv. Syst.* **2003**, *226*, 209.

[8] R. Deumens, A. Bozkurt, M. F. Meek, M. A. E. Marcus, E. A. J. Joosten, J. Weis, G. A. Brook, *Prog. Neurobiol.* **2010**, *92*, 245.

[9] M. Butí, E. Verdú, R. O. Labrador, J. Vilches, J. Forés, X. Navarro, *Exp. Neurol.* **1996**, *33*, 26.

[10] G. Lundborg, L. B. Dahlin, N. Danielsen, R. H. Gelberman, F. M. Longo, H. C. Powell, S. Varon, *Exp. Neurol.* **1982**, *76*, 361.

[11] L. R. Williams, F. M. Longo, H. C. Powell, G. Lundborg, S. Varon, *J. Comp. Neurol.* **1983**, *218*, 460.

[12] S. J. Archibald, J. Shefner, C. Krarup, R. D. Madison, *J. Neurosci.* **1995**, *15*, 4109.

[13] D. Arslantunali, T. Dursun, D. Yucel, N. Hasirci, V. Hasirci, **2014**, 405.

[14] W. T. Daly, A. M. Knight, H. Wang, R. de Boer, G. Giusti, M. Dadsetan, R. J. Spinner, M. J. Yaszemski, A. J. Windebank, *Biomaterials* **2013**, *34*, 8630.

[15] E. J. P. Jansen, J. Pieper, M. J. J. Gijbels, N. A. Guldemond, J. Riesle, L. W. Van Rhijn, S. K. Bulstra, R. Kuijer, *J. Biomed. Mater. Res. - Part A* **2009**, *89*, 444.

[16] S. Danti, C. Mota, D. D'alessandro, L. Trombi, C. Ricci, S. L. Redmond, A. De Vito, R. Pini, R. J. Dilley, L. Moroni, S. Berrettini, *Hear. Balanc. Commun.* **2015**, *13*, 133.

[17] L. Moroni, R. Schotel, D. Hamann, J. R. de Wijn, C. A. van Blitterswijk, *Adv.*

Funct. Mater. **2008**, *18*, 53.

[18] D. Henley, *Food Drug Adm. Drug Eval. Res.* **2002**, *K023680*.

[19] G. C. W. de Ruiter, M. J. A. Malessy, M. J. Yaszemski, A. J. Windebank, R. J. Spinner, *Neurosurg. Focus* **2009**, *26*, E5.

[20] S. Kehoe, X. F. Zhang, D. Boyd, *Injury* **2012**, *43*, 553.

[21] W. Liu, S. Thomopoulos, Y. Xia, *Adv. Healthc. Mater.* **2012**, *1*, 10.

[22] V. Milleret, B. Simona, P. Neuenschwander, H. Hall, *Eur. Cell. Mater.* **2011**, *21*, 286.

[23] I. V. Yannas, B. J. Hill, *Biomaterials* **2004**, *25*, 1593.

[24] X. Navarro, E. Verdu, W. R. Kennedy, *J. Neurosci. Res.* **1995**, *41*, 111.

[25] F. F. A. IJpma, R. C. Van De Graaf, M. F. Meek, *J. Hand Surg. Eur. Vol.* **2008**, *33*, 581.

[26] F. Gonzalez-Perez, E. Udina, X. Navarro, *Int. Rev. Neurobiol.* **2013**, *108*, 257.

[27] I. Allodi, E. Udina, X. Navarro, *Prog. Neurobiol.* **2012**.

[28] S. Panseri, C. Cunha, J. Lowery, U. Del Carro, F. Taraballi, S. Amadio, A. Vescovi, F. Gelain, *BMC Biotechnol.* **2008**, *8*, 39.

[29] W. Yu, W. Zhao, C. Zhu, X. Zhang, D. Ye, W. Zhang, Y. Zhou, X. Jiang, Z. Zhang, *BMC Neurosci.* **2011**, *12*, 68.

[30] S. Y. Chew, R. Mi, A. Hoke, K. W. Leong, *Adv. Funct. Mater.* **2007**, *17*, 1288.

[31] T. M. Dinis, R. Elia, G. Vidal, Q. Dermigny, C. Denoeud, D. L. Kaplan, C. Egles, F. Marin, *J. Mech. Behav. Biomed. Mater.* **2015**, *41*, 43.

[32] S. Madduri, M. Papaloïzos, B. Gander, *Biomaterials* **2010**, *31*, 2323.

[33] H. S. Koh, T. Yong, W. E. Teo, C. K. Chan, M. E. Puhaindran, T. C. Tan, A. Lim, B. H. Lim, S. Ramakrishna, *J. Neural Eng.* **2010**, *7*, 1.

[34] J. H. A. Bell, J. W. Haycock, *Tissue Eng. Part B* **2012**, *18*, 116.

[35] A. Townsend-Nicholson, S. N. Jayasinghe, *Biomacromolecules* **2006**, *7*, 3364.

[36] J. J. Stankus, J. Guan, K. Fujimoto, W. R. Wagner, *Biomaterials* **2006**, *27*, 735.

[37] S. N. Jayasinghe, *Analyst* **2013**, *138*, 2215.

[38] A. Subramanian, U. M. Krishnan, S. Sethuraman, *Biomed. Mater.* **2011**, *6*, 025004.

[39] E. Schnell, K. Klinkhammer, S. Balzer, G. Brook, D. Klee, P. Dalton, J. Mey,

Biomaterials **2007**, *28*, 3012.

[40] Y. Panahi-Joo, A. Karkhaneh, A. Nourinia, B. Abd-Emami, B. Negahdari, P. Renaud, S. Bonakdar, *Biomed. Mater.* **2016**, *11*, 025017.

[41] B. S. Jha, R. J. Colello, J. R. Bowman, S. A. Sell, K. D. Lee, J. W. Bigbee, G. L. Bowlin, W. N. Chow, B. E. Mathern, D. G. Simpson, *Acta Biomater.* **2011**, *7*, 203.

[42] Y. Zhu, A. Wang, S. Patel, K. Kurpinski, E. Diao, X. Bao, G. Kwong, W. L. Young, S. Li, *Tissue Eng. Part C. Methods* **2011**, *17*, 705.

[43] H. B. Wang, M. E. Mullins, J. M. Cregg, C. W. McCarthy, R. J. Gilbert, *Acta Biomater.* **2010**, *6*, 2970.

[44] Y. Li, G. A. Thouas, Q. Chen, *J. Mech. Behav. Biomed. Mater.* **2014**, *40*, 210.

[45] M. F. Meeks, W. F. A. den Dunnen, *Microsurgery* **2009**, *29*, 473.

[46] A. A. Deschamps, M. B. Claase, W. J. Sleijster, J. D. De Bruijn, D. W. Grijpma, J. Feijen, *J. Control. Release* **2002**, *78*, 175.

[47] I. P. Clements, Y. Kim, A. W. English, X. Lu, A. Chung, R. V Bellamkonda, *Biomaterials* **2009**, *30*, 3834.

[48] W. Huang, R. Begum, T. Barber, V. Ibba, N. C. H. Tee, M. Hussain, M. Arastoo, Q. Yang, L. G. Robson, S. Lesage, T. Gheysens, N. J. V Skaer, D. P. Knight, J. V. Priestley, *Biomaterials* **2012**, *33*, 59.

[49] T. T. B. Ngo, P. J. Waggoner, A. A. Romero, K. D. Nelson, R. C. Eberhart, G. M. Smith, *J. Neurosci. Res.* **2003**, *72*, 227.

[50] M. Merle, A. L. Dellon, J. N. Campbell, P. S. Chang, *Microsurgery* **1989**, *10*, 130.

[51] S. H. Oh, J. H. Kim, K. S. Song, B. H. Jeon, J. H. Yoon, T. B. Seo, U. Namgung, I. W. Lee, J. H. Lee, *Biomaterials* **2008**, *29*, 1601.

[52] F. J. Rodriguez, N. Gomez, G. Perego, X. Navarro, *Biomaterials* **1999**, *20*, 1489.

[53] F. Gonzalez-Perez, S. Cobianchi, S. Geuna, C. Barwig, T. Freier, E. Udina, X. Navarro, *Microsurgery* **2015**, *35*, 300.

[54] N. Gómez, J. Cuadras, M. Butí, X. Navarro, *Restor Neurol Neurosci.* **1996**, *10*, 187.

[55] F. J. Rodríguez, N. Gómez, R. O. Labrador, M. Butí, D. Ceballos, J. Cuadras, E. Verdú, X. Navarro, *Restor. Neurol. Neurosci.* **1999**, *14*, 65.

[56] A. Valero-Cabré, K. Tsironis, E. Skouras, G. Perego, X. Navarro, W. F. Neiss, *J.*

Neurosci. Res. **2001**, *223*, 214.

[57] H.-C. Ni, T.-C. Tseng, J.-R. Chen, S.-H. Hsu, I.-M. Chiu, *Biofabrication* **2013**, *5*, 035010.

[58] T. J. Whitehead, H. G. Sundararaghavan, *J. Vis. Exp.* **2014**, 1.

[59] D. Santos, G. Giudetti, S. Micera, X. Navarro, J. del Valle, *Brain Res.* **2016**, *1636*, 93.

[60] S. A. Malin, B. M. Davis, D. C. Molliver, *Nat. Protoc.* **2007**, *2*, 152.

[61] S. Preibisch, S. Saalfeld, P. Tomancak, *Bioinformatics* **2009**, *25*, 1463.

CHAPTER 2

Available online at www.sciencedirect.com

ScienceDirect

www.elsevier.com/locate/brainres

Research Report

Focal release of neurotrophic factors by biodegradable microspheres enhance motor and sensory axonal regeneration in vitro and in vivo

Daniel Santos[a,b], *Guido Giudetti*[c], *Silvestro Micera*[c,d], *Xavier Navarro*[a,b], *Jaume del Valle*[a,b,*]

[a]*Institute of Neurosciences and Department of Cell Biology, Physiology and Immunology, Universitat Autònoma de Barcelona, Bellaterra, Spain*
[b]*Centro de Investigación Biomédica en Red sobre Enfermedades Neurodegenerativas (CIBERNED), Bellaterra, Spain*
[c]*The BioRobotics Institute, Scuola Superiore Sant'Anna, Viale Rinaldo Piaggio 34, 56025 Pontedera, Italy*
[d]*Translational Neural Engineering Laboratory, Center for Neuroprosthetics and Institute of Bioengineering, School of Engineering, Ecole Polytechnique Federale de Lausanne (EPFL), Lausanne, Switzerland*

ARTICLE INFO

Article history:
Accepted 31 January 2016
Available online 4 February 2016

Keywords:
Growth factors
Microspheres
Motor axons
Nerve conduit
Nerve regeneration
Sensory axons

ABSTRACT

Neurotrophic factors (NTFs) promote nerve regeneration and neuronal survival after peripheral nerve injury. However, drawbacks related with administration and bioactivity during long periods limit their therapeutic application. In this study, PLGA microspheres (MPs) were used to locally release different NTFs and evaluate whether they accelerate axonal regeneration in comparison with free NTFs or controls. ELISA, SEM, UV/visible light microscopy, organotypic cultures of DRG explants and spinal cord slices were used to characterize MP properties and the bioactivity of the released NTFs. Results of organotypic cultures showed that encapsulated NTFs maintain longer bioactivity and enhance neurite regeneration of both sensory and motor neurons compared with free NTFs. For in vivo assays, the rat sciatic nerve was transected and repaired with a silicone tube filled with collagen gel or collagen mixed with PBS encapsulated MPs (control groups) and with free or encapsulated NGF, BDNF, GDNF or FGF-2. After 20 days, a retrotracer was applied to the regenerated nerve to quantify motor and sensory axonal regeneration. NTF encapsulation in MPs improved regeneration of both motor and sensory axons, as evidenced by increased numbers of retrolabeled neurons. Hence, our results show that slow release of NTFs with PLGA MP enhance nerve regeneration.

*Correspondence to: Unitat de Fisiologia Mèdica, Facultat de Medicina, Universitat Autònoma de Barcelona, E-08193 Bellaterra, Spain.
E-mail address: jaume.delvalle@uab.cat (J. del Valle).

http://dx.doi.org/10.1016/j.brainres.2016.01.051
0006-8993/

1. Introduction

Peripheral neurons are able to regenerate their axons after nerve injuries and reinnervate end organs, although functional recovery is often poor. After nerve transection, surgical repair is mandatory to rejoin the nerve stumps allowing axons to find an adequate substrate to grow distally. Direct suture of the two stumps or interposition of an autologous graft when the inter-stump defect is long are considered the standard option for repairing a nerve transection. The use of nerve conduits to bridge short or mid length gaps is a good alternative to autografts (Arslantunali et al., 2014), although regeneration is slowed during the initial phase compared to autograft (Boeckstyns et al., 2013). Several parameters affect the rate of axonal regeneration, including the distance between stumps (Scherman et al., 2001), the age of the subject (Kang and Lichtman, 2013; Painter et al., 2014; Verdú et al., 2008), the time after repair and the distance between the lesion site and end organ (Gordon et al., 2003). Indeed, the time from injury to target reinnervation is the most important predictor of the degree of functional recovery (Krarup et al., 2002), emphasizing that factors that control early axonal outgrowth influence the final level of recovery attained even years later. Therefore, strategies to accelerate the rate of axonal growth could be useful to stimulate nerve regeneration through longer distances and improve the recovery outcome. In fact, different strategies have already been developed to solve this problem including the use of different neurotrophic factors (NTFs) (Allodi et al., 2012).

After nerve injury, NTFs are synthesized and secreted not only at the spinal cord (SC) and the dorsal root ganglia (DRG) where the somas of the injured neurons are located, but mainly at the site of the lesion by reactive Schwann cells. NTFs have been long studied for their positive effects on nerve regeneration, including their ability to promote neuronal survival, to increase axonal outgrowth and to improve target reinnervation. Different NTFs have been tested in vitro and in vivo to improve peripheral nerve regeneration, such as nerve growth factor (NGF) (Kemp et al., 2011; Lee et al., 2003), brain-derived neurotrophic factor (BDNF) (Vögelin et al., 2006), neurotrophin-3 (NT-3) (Sternel et al., 1997), glial cell-derived neurotrophic factor (GDNF) (Moore et al., 2010), fibroblast growth factors (FGF1, FGF2) (Midha et al., 2003; Allodi et al., 2013) or insulin like growth factors (IGF1, IGF2) (Ishi et al., 1993; Kanje et al., 1989).

The induction of an increased production of NTFs at the site of the lesion will stimulate axonal regeneration when the local environment is poor. Thus, the combination of a nerve conduit with NTFs appears as a good option to enhance nerve regeneration. However, NTFs added within a nerve conduit can be rapidly degraded (Ejstrup et al., 2010; Tria et al., 1994), diffuse outside the conduit or get diluted after liquid infiltration resulting in sub-optimal concentrations, and thus poor regeneration outcome (De Boer et al., 2012; Wood et al., 2013). Hence, a better way to apply NTFs and prolong their presence in close contact with regenerating axons and Schwann cells is still needed to optimize the effects of NTFs on regeneration. In attempts to increase the NTF availability at the site of injury over time, different approaches have been utilized by using repeated injections through catheters (Mcdonald and Zochodne, 2003), osmotic minipumps (Hontanilla et al., 2007), binding to extracellular matrix molecules (Sternel et al., 1997; Sakiyama-Elbert and Hubbell, 2000; Lee et al., 2003) or to the wall of nerve conduits (Madduri et al., 2010; Piquilloud et al., 2007) and gene therapy (Allodi et al., 2014; Eggers et al., 2013; Haastert et al., 2006). However, these strategies still present some (Fig. 1) difficulties to reach optimal nerve regeneration.

In (Fig. 2) this context, strategies involving biocompatible and biodegradable microspheres (MPs) associated to selected bioactive molecules may provide a sustained and controlled release of factors, offering valuable approaches for overcoming those limitations. Nanotechnology-based carrier technologies offer indeed a customizable approach for locally controlled delivery, by coupling the drug or molecule of interest to carrier particles such as MPs (Tam et al., 2014), nanoparticles, liposomes or dendrimers (Mura et al., 2013). Thanks to relatively simple fabrication protocols and fair requests in terms of equipment, such technologies have been extensively explored in the last decade, and applied in different fields, spanning from cancer research to nutritional sciences (Mozafari et al., 2008; Peer et al., 2007). The characteristics of carrier technologies have been developed to overcome hindrances arisen in the field of drug administration, thus to improve the selectivity of targeting, to increase the capability to control drug release via chemistry tailoring, and to obtain an increase of stability of otherwise labile payloads. Despite the myriad different chemistries and payloads, the recurring goal has been definitely to exert an otherwise difficult control of drug release and stability at the local level. Among polymer-based microsphere carrier systems that take advantage of the biocompatible character of bio-derived substances, such alginate, chitosan and silk fibroin, PLGA (Poly-lactic Co-Glycolic acid, a synthetic biodegradable polymer) based MPs (Makadia and Steven, 2011) are particularly attractive for neural regeneration applications, given their favorable biocompatible behavior in physiological environments, low immunogenicity and toxicity, the possibility of size control and predictable, highly tailorable degradation kinetics, not mentioning the fact that they are FDA approved for drug delivery use (Jain, 2000).

Finally, the chaotic reinnervation of distal targets due to misdirection of regenerating axons is the main factor that results in poor functional recovery after nerve transection and tube repair (Valero-Cabré and Navarro, 2002), thus study of strategies to improve motor and/or sensory specific reinnervation are still needed. Therefore, the objective of the present study was the initial evaluation of the potential advantages of sustained release from MPs versus acute supply of several neurotrophic factors and their possible selective effects on the regeneration of motor and sensory axons.

2. Results

2.1. MPs fabrication and characterization

To test the correct encapsulation of molecules during the MP fabrication process, fluorescent FITC-BSA was used as tracking dye and its fluorescence in the MP was checked by fluorescence microscopy (Fig. 3). These fluorescent MPs were

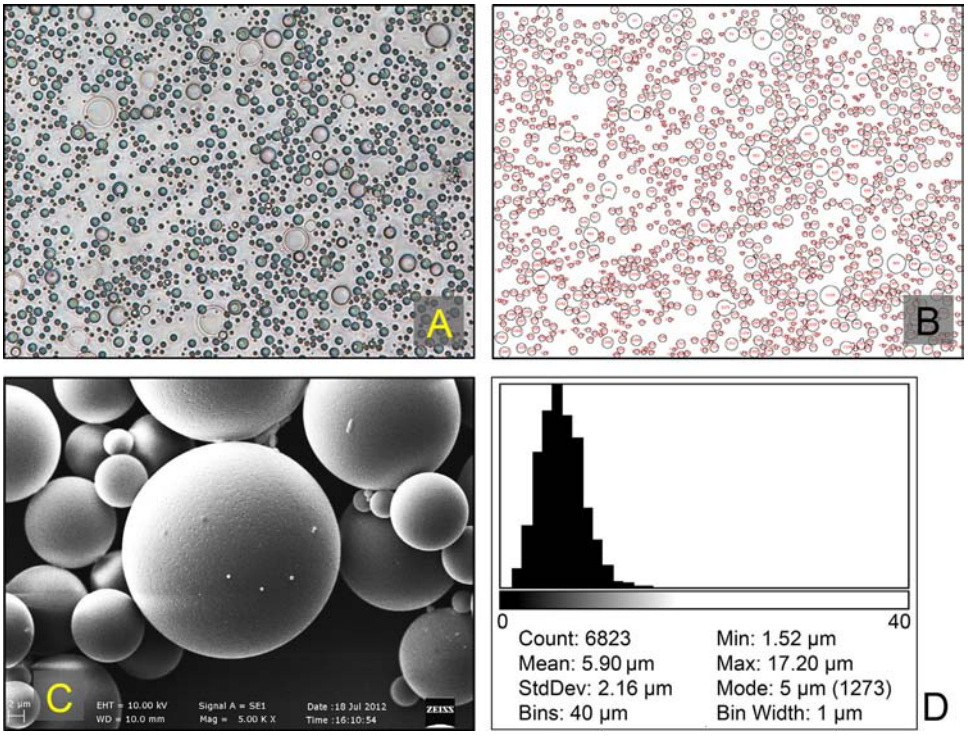

Fig. 1 – A, B: steps in image treatment for automated microspheres counting. A: starting, as-is, captured image of microspheres suspension in visible light; B: same image after normalization, thresholding, binarization and automatic recognition for counting. C: sample SEM micrograph of PLGA MPs showing regular surface roughness. D: statistical data distribution for MPs counted with the automated procedure from A, B.

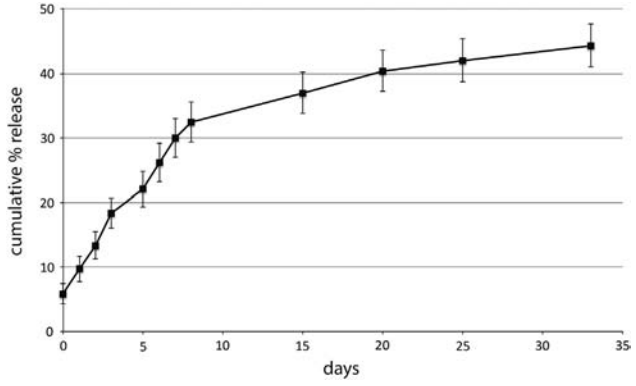

Fig. 2 – Cumulative release of NGF from PLGA MPs, measured by ELISA and expressed as percentage of an estimated starting total concentration of 50 ng/ml of neurotrophin. Data expressed as mean ± SEM.

also used as negative control to initially test their biocompatibility in the organotypic explant experiments (see 3.2).

SEM imaging of MPs showed a fairly rough surface (Fig. 1C) and was used also as a tool for rapid assessment of particle dispersion, allowing quick modifications of the synthesis protocol to obtain narrowly distributed microsphere size by protocol adjustment. A consistent change was observed using non-hydrolyzed PVA instead of hydrolyzed PVA as dispersant of the second emulsification stage in the fabrication protocol. Non-hydrolyzed PVA has higher viscosity and reasonably hampers coalescing of the microdroplets formed during the first homogenization phase, thus permitting smaller and narrowly distributed MP sizes.

To assess the mean MP size, as Dynamic Light Scattering (DLS) was not feasible due the micrometric size of the particles, an optical microscopy-based method was implemented as described. Fig. 1 shows the sequential steps of the software pipeline, from the starting image taken in visible light (Fig. 1A), proceeding through normalization, thresholding binarization, particle recognition and counting (Fig. 1B), with final summarization of statistical distribution of the measured diameters (expressed as Feret's diameter) of the MP (Fig. 1D). The particles produced by this protocol have a narrow size distribution with a mean size of 5.9 ± 2.1 µm (n = 6823). This is a desirable size range, as nanometer-sized MPs would likely be endocytosed by cells, while bigger ones would be difficult to handle due to quick precipitation after resuspension.

The encapsulation efficiency was calculated as the actual fraction of a theoretical 100% efficiency. By ELISA tests the estimated encapsulation efficiency resulted to be 64.1 ± 0.02%, that, while being lower than otherwise reachable high reported efficiencies (Péan et al., 1998), also in view of smaller mean particle size, compares with previous work with similar applications (De Boer et al., 2011). This estimate was used to calculate the mass of MP to use when assessing the release profile of NGF. Quantification of the released NGF was performed by ELISA, starting with an estimated 50 ng NGF-containing MP mass (equivalent to 62.5 µg) and measuring the NGF quantity in the supernatant of a suspension of MPs kept in cell culture-like conditions (37 °C, 5% CO_2 atmosphere) over one month. The

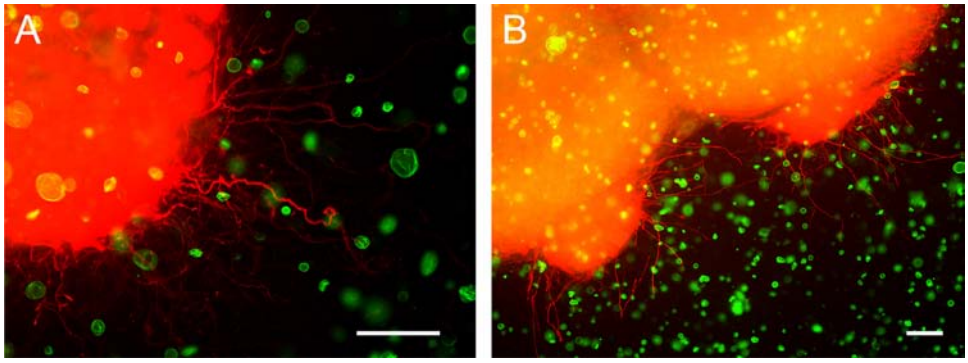

Fig. 3 – Neurite outgrowth stained with RT97 (red) from DRG (A) and SC (B) organotypic cultures in a collagen matrix filled with fluorescent MPs (green). Scale bar: 100 μm.

resulting data (shown in Fig. 2 as percentage quantity of the total initial estimated NGF) showed an initial small burst at day 0 (sampling was performed at the end of each considered day) and increasing release over the first 8–10 days of suspension, followed by sustained release until the end of the observation period.

2.2. *In vitro effects of NTF loaded MP on neurite outgrowth*

Although PLGA has been widely described to be biocompatible and biodegradable (Makadia and Steven, 2011), there are studies reporting some cell toxicity in culture (Grabowski et al., 2013). Thus, we first evaluated if PLGA MPs could affect neurite outgrowth by loading FITC-BSA in the MPs and embedding them within the collagen matrix surrounding DRG and SC cultures. In both cases neurites grew from the explants and were present in close proximity to the MPs (Fig. 3A, B), indicating no adverse effects caused by PLGA or PLGA degradation products that could interact with neurite outgrowth.

Organotypic cultures of DRG (Fig. 4A–F) and SC (Fig. 5A–F) were performed to test whether MPs loaded with NGF (MP-NGF) and with BDNF (MP-BDNF) increased neurite outgrowth in comparison with the same NTF placed as free protein in the collagen matrix. Without conditioning the collagen matrix, both free and encapsulated NTF increased the amount of neurites that grew from the explant in comparison with cultures without NTF (Figs. 4G and 5G), indicating that MPs released NTF. The longest neurite measured was significantly longer in DRG cultures with free NGF but not in cultures with MP-NGF than in control cultures (Fig. 4H). In SC cultures both free BDNF and MP-BDNF increased the maximal length of neurites with respect to control cultures (Fig. 5H).

After 1 week of conditioning the collagen matrix with no NTF, free NTF or encapsulated NTF, only the explants cultured with MPs increased the amount of neurites in comparison with the control and also free NTF (Figs. 4I and 5I), indicating that after 1 week there was still NTF within the matrix of the MP conditions being able to promote axon outgrowth but not in the free NTF cultures. Similarly, both MP-NGF (Fig. 4J) and MP-BDNF (Fig. 5J) cultures showed increase in the longest neurite measures with respect to control values, while no differences were seen between the free NTF and control conditions.

2.3. *NTFs enhance axon outgrowth of motor and sensory neurons in vivo*

All the rats showed evidence of axonal regeneration after section of the sciatic nerve and tube repair, as judged by the retrograde labeling of motor and sensory regenerated neurons with FG (Fig. 6). No differences were found between groups treated with collagen alone and with MP-PBS (Fig. 7A, B) indicating again lack of interaction of PLGA MPs with axon outgrowth.

GDNF and BDNF applied as free factor in the nerve conduit were the only NTFs that enhanced motor axon regeneration in comparison with the control group, whereas NT-3, FGF and NGF did not show differences (Fig. 7A). Similarly, free GDNF, BDNF and also FGF yielded significant differences in comparison with animals treated with MP-PBS. On the other hand, all the groups with NTFs encapsulated in MPs had higher number of regenerated motor neurons than the control group. Particularly, groups treated with MP-GDNF and MP-BDNF showed the highest increase in the number of regenerated motor axons. Concerning sensory neurons regeneration, only free NGF showed differences with the two control groups without NTF (Fig. 7B). In contrast, MP-NGF, MP-GDNF and MP-BDNF enhanced sensory axon growth with respect to control and MP-PBS groups.

With regard to the performance of MPs, a comparison of free NTF (dotted line, taken as 100%) with the same factor encapsulated in MPs is shown in Fig. 7C,D. For motor neurons, all the MP groups had higher numbers of neurons with regenerated axons in comparison with free NTF with the exception of FGF (Fig. 7C). For sensory neurons, all the MP groups had increased axon regeneration in comparison with free NTF, except for NGF and BDNF (Fig. 7D). These results indicate that the slow release of NTFs from MPs promoted nerve regeneration in vivo.

Finally, histologic quantification of MF inside the regenerating tube was performed. The biocompatibility of the PLGA MPs used in this study was confirmed, as MPs were in close proximity with regenerated myelinated and unmyelinated axons (Fig. 8D,F). The regenerated nerve inside the tube had a thin external layer of fibrous tissue and a central region with axons forming the typical morphology of a regenerated nerve inside a tube (Gómez et al., 1996; Lago and Navarro, 2006) in all the groups (Fig. 8A–C).

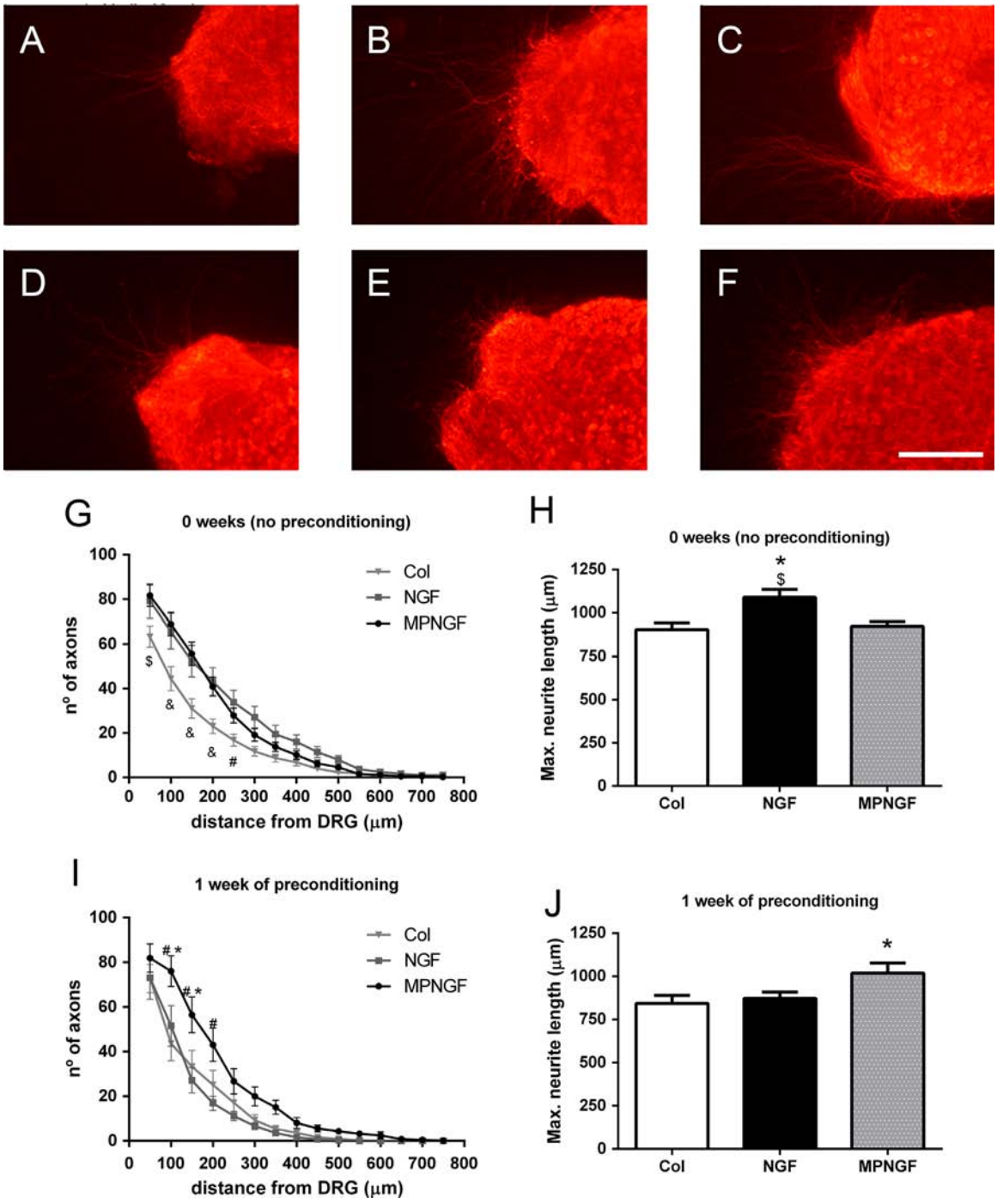

Fig. 4 – A–C: neurites stained with RT97 from DRG neurons cultured within non-conditioned collagen alone (A), with added free NGF (B), and MP-NGF (C). D–F: neurite outgrowth from DRG neurons cultured within 1 week-conditioned collagen matrix alone (D), with added free NGF (E), and MP-NGF (F). G, I: plot of the number of neurites grown at increasing distance from the DRG body in a collagen matrix non-conditioned (G) and after 1 week conditioning with free NGF or MP-NGF (I). H, J: measurement of the longest neurite in non-conditioned (H) and after 1 week conditioning with free NGF or MP-NGF (J). *$p<0.05$ vs Col; \$$p<0.05$ vs MP-NGF; #$p<0.05$ vs free NGF, &$p<0.05$ vs free NGF and MPNGF. Data expressed as mean ± SEM. Scale bar: 250 μm.

With regard to the number of MFs, control and MP-PBS groups showed similar values. On the other hand, only NGF and MP-NGF treated groups showed higher number of MFs than controls, whereas the other treated groups had similar values with no differences compared to the control groups (Fig. 8G).

3. Discussion

The results of this study demonstrate that different NTFs encapsulated in PLGA MPs enhance motor and sensory axons

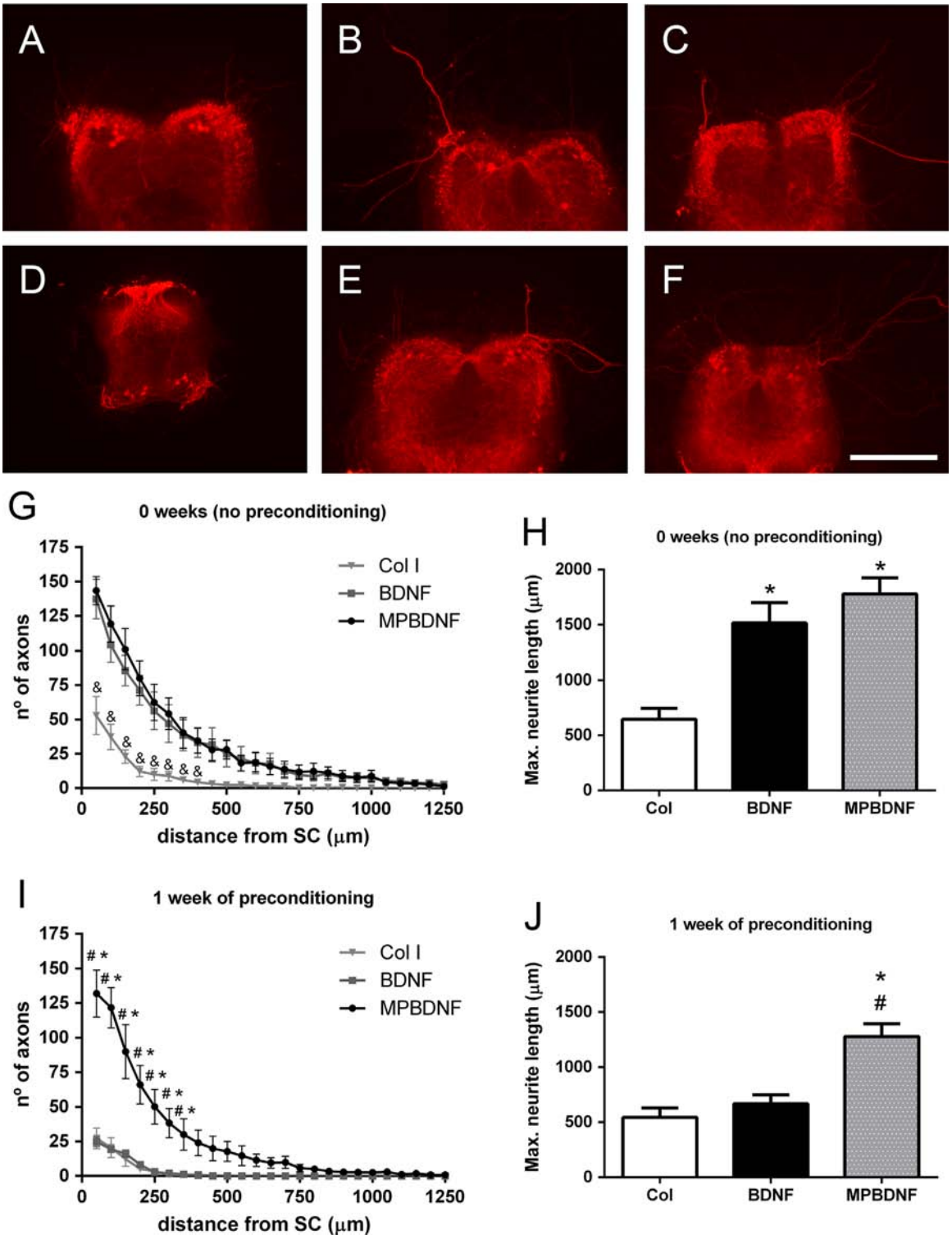

Fig. 5 – A–C: neurites stained with RT97 from SC neurons cultured within non-conditioned collagen alone (A), with added free BDNF (B), and MP-BDNF (C). D–F: neurite outgrowth from SC neurons cultured within 1 week-conditioned collagen matrix alone (D), with added free BDNF (E), and MP-BDNF. G, I: plot of the number of neurites grown at increasing distance from the SC body in a collagen matrix non-conditioned (G) and after 1 week conditioning with free BDNF or MP-BDNF (I). H, J: measurement of the longest neurite in non-conditioned (H) and after 1 week conditioning with free BDNF or MP-BDNF (J). *$p<0.05$ vs Col; \$$p<0.05$ vs MP-BDNF, #$p<0.05$ vs free BDNF, &$p<0.05$ vs free BDNF and MP-BDNF. Data expressed as mean ± SEM. Scale bar: 250 μm.

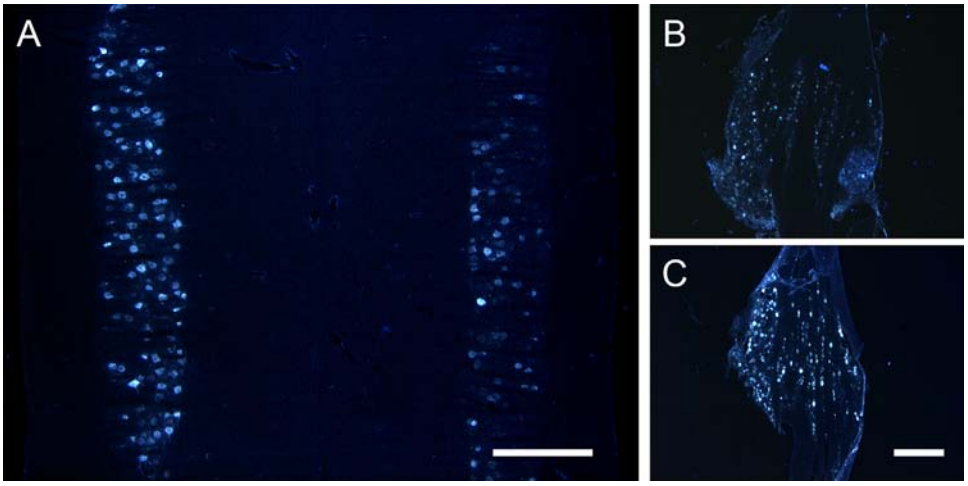

Fig. 6 – Representative micrographs of neurons retrolabeled with FG in the lumbar SC of rats after sciatic nerve section and repair with a nerve conduit filled with collagen plus MP-BDNF (A, left) and with collagen alone (A, right). Representative micrographs of neurons retrolabeled with FG in the lumbar DRG of rats after sciatic nerve section and repair with a nerve conduit filled with collagen alone (B) and with collagen plus MP-NGF (C). Scale bar: 500 μm.

regeneration both in vitro and in vivo in comparison with the same NTFs administered as free molecules without encapsulation. The encapsulation in controlled release systems has the advantage to allow a slow and sustained release of desired NTFs focally at selected areas of the nervous system as a therapeutical approach for neurodegenerative diseases and neural injuries (Benoit et al., 2000; Catrina et al., 2013). Due to their small size, MPs can be easily implanted in well localized areas without affecting the surrounding tissues (Figs. 3 and 8), thus avoiding also secondary effects. The controllable delivery of molecules from the MPs is advantageous as compared to a burst supply by direct injection and allows to overcome the limited therapeutic protein stability. Advantages of MPs (and conduits) as carriers for local, prolonged delivery of NTFs include that they are biocompatible and biodegradable, minimizing the foreign-body reaction, they avoid the implantation of catheters and external devices needed with injection ports and osmotic pumps, or the grafting of engineered cells with immunogenicity issues.

First, a characterization of the PLGA MPs was made before their in vitro and in vivo use. ELISA results demonstrate that 10 days after MP fabrication, 30% of the encapsulated NTF has been already released, and that slow release is maintained for more than a month. This releasing profile seems adequate for enhancing nerve regeneration, since the expression of different NTF receptors remains upregulated during the firsts months after injury (Boyd and Gordon, 2003a). Despite previous studies have used PLGA MPs to deliver NTFs, mechanical and chemical stresses during MP manufacturing may affect the structure and the stability of the encapsulated protein (Yeo and Park, 2004; Pfister et al., 2007). To address this issue, we first used organotypic cultures of DRG (Fig. 4) and SC (Fig. 5) to assess the bioactivity of NTFs released from the prepared MPs. The obtained results showed that the NTFs tested, NGF and BDNF, are released in effective concentration beyond one week, and after this period still keep bioactivity to promote neurite outgrowth in comparison with the application of free NTFs. The neurite growth observed in cultures without preconditioning (i.e. immediate use) was similarly enhanced by free NTFs and by NTFs loaded in MPs added within the collagen matrix, which can be explained by the initial burst release of enough amount of the NTFs (Fig. 2). However, after 1 week of preconditioning the medium, only NTFs encapsulated in MPs produced an increase in neurite outgrowth in comparison with control cultures, indicating that MPs were still releasing NTFs at a concentration high enough to stimulate the growing response. Thus, rather than an increased effect of encapsulated NTFs over free NTFs, it seems that the elution of the free NTFs outside the matrix or the loss of their activity is responsible of the low effect in the conditioned setting, while the NTFs continuously released from the MPs were still able to enhance neurite outgrowth to similar levels than in the non-conditioned matrix.

Second, after testing that the manufactured MPs did not interact with growing neurites and improved regeneration in vitro, the same preparations were applied in vivo. A silicone tube filled with a collagen gel containing either free or MPs encapsulated NTFs was implanted to repair a nerve gap. The NTFs applied were expected to act during the period of axonal regeneration across the tube, i.e. 2–3 weeks (Williams et al., 1983; Mcdonald and Zochodne, 2003). As the MP encapsulation increased the therapeutic window of NTFs delivery in vitro, its effects were presumed to be also higher in vivo than those of free NTFs. Thus, both retrotracer and histological analyses were conducted to test whether application of encapsulated NTF improved nerve regeneration in vivo.

The number of regenerated neurons (Fig. 7A–B) and MFs (Fig. 8G) in both control groups was similar, indicating that the presence of PLGA MPs did not interfere in the regeneration process. On the other hand, while retrotracer analysis demonstrates an enhancement of regeneration in all the groups with NTFs, this improvement is not seen in the histological analysis where only groups treated with NGF showed differences compared to control. Moreover, we found less regenerating neurons in the retrotracer study than MFs in the histology. Although this results could seem contradictory, it has been reported that neurons initially generate several axonal sprouts after axotomy

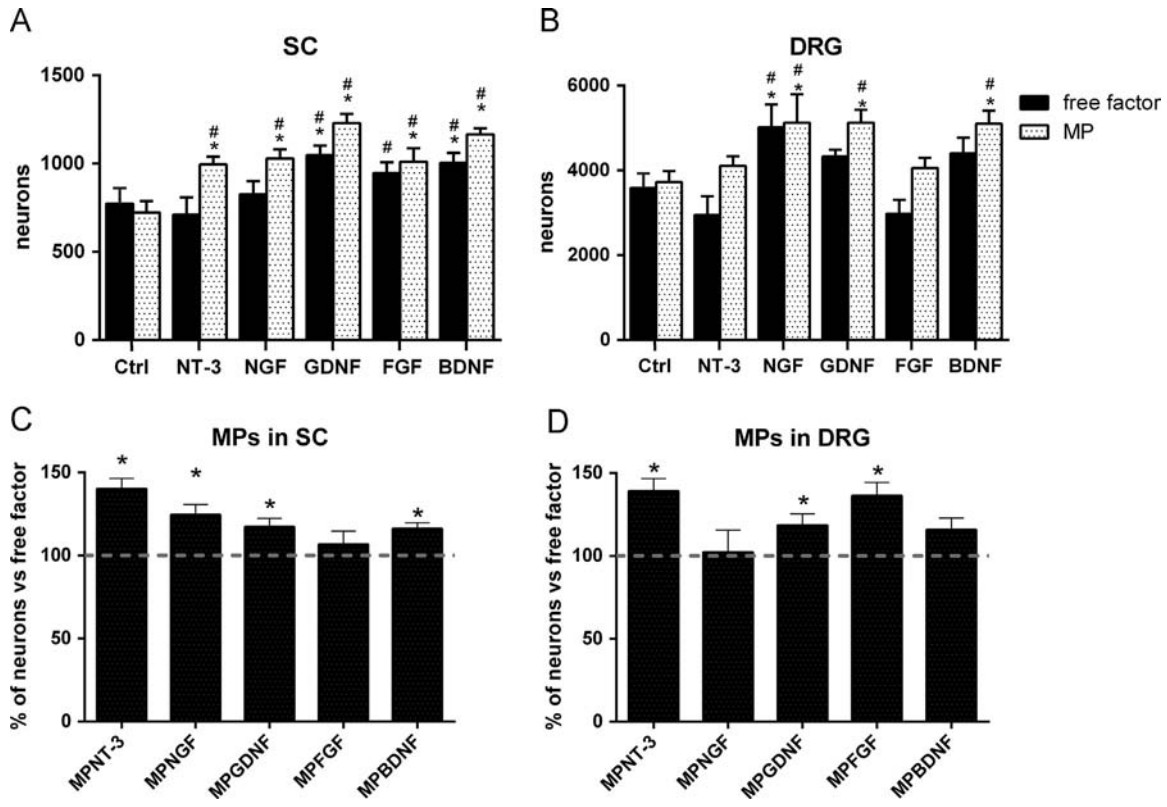

Fig. 7 – Histograms of the number of motor neurons in the SC (A) and of sensory neurons in the DRG (B) retrolabeled with FG after sciatic nerve section and conduit repair counted in the different groups compared, with and without NFs in free and in MP preparations. Percentage of retrolabeled motor (C) and sensory (D) neurons counted in rats with NTF loaded MPs with respect to rats with the same NTF applied as free factor in the collagen gel. Data expressed as mean ± SEM. *$p < 0.05$ vs Col; #$p < 0.05$ vs MP-PBS.

(Mackinnon et al., 1991), and even at long term each neuron may maintain more than a single regenerated axonal branch (Gómez et al., 1996; Jenq and Coggeshall, 1985). Furthermore, more regenerated axons (sprouts) do not necessarily indicate more neurons regenerating (Piquilloud et al., 2007) and may be also considered deleterious in terms of functional recovery (Guntinas-Lichius et al., 2005). Hence, the increase of MF in the NGF groups would be in accordance with other studies that describe an important role of NGF on axonal sprouting (Diamond et al., 1987; Gloster et al., 1992; Ruiz et al., 2004). Thus, histological quantification of MFs may result in an overestimation of the number of regenerated neurons (Navarro, 2015) and only the retrotracer study provides reliable information on the number of regenerating neurons. For these reasons, in our study the positive effects of the NTFs loaded MPs were indicated by the effective growth of axons that were able to capture the retrotracer placed distal to the nerve conduit.

The results found in this work indicate that an increased number of motor and sensory neurons regenerate distally to the nerve conduit in the groups with MP-encapsulated NTFs. This can be explained by an acceleration of axonal regeneration, as well as by an indirect effect inducing endogenous Schwann cells to a proregenerative state (Gordon et al., 2003). After nerve lesion reactive Schwann cells highly induce the expression of several NTFs, including NGF, BDNF, GDNF, and their receptors (Boyd and Gordon, 2003a; Allodi et al., 2012). The increased neurotrophic secretion peaks at about 1 week postaxotomy and declines with time. Our results give further support to the view that additional exogenous supply of NTFs may enhance the regenerative response of peripheral neurons. Nevertheless, the concentration and time window of the NTFs applied at the site of nerve injury, such as within a nerve conduit, need to be carefully investigated. Indeed, a small supply of a NTF at the site of injury does not always have beneficial effects, and on the opposite an excessive concentration may even hinder axonal growth. Thus, exogenous application of NGF to axotomized sensory neurons may interfere with the regenerative response and delay axonal regrowth (Gold et al., 1997; Mohiuddin et al., 1999). An increased supply of GDNF at the focal site has been shown to stimulate axonal sprouting, thus multiplying the number of regenerating fibers within a nerve conduit, but did not result in positive outcomes in terms of distal regeneration and return of motor function (Piquilloud et al., 2007). A further problem was reported after the injection in the injured nerve of viral vectors transducing the overexpression of NTFs. The high amount of GDNF secreted created a "candy-store" effect (Tannemaat et al., 2008), in which regenerating axons stay in areas with high GDNF concentration and fail to grow distally towards the target organs. Therefore, our results sustain that prolonged, controlled release of NTFs is beneficial to improve nerve regeneration.

Third, after fluorogold retrolabeling and quantification of regenerated neurons in DRG and SC (Fig. 7), we were able to

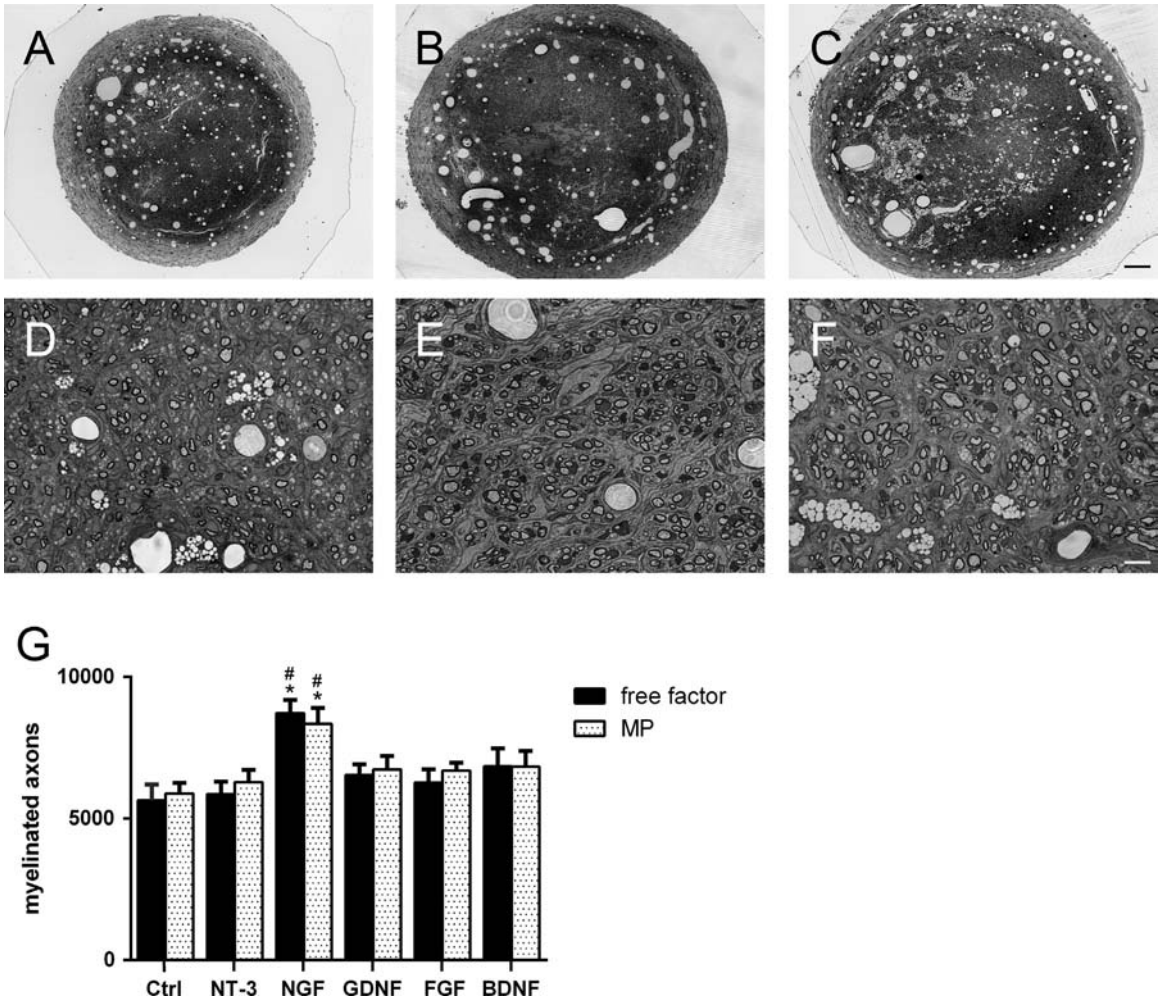

Fig. 8 – A–F: representative microphotographs of semithin transverse sections of the regenerated nerves in groups MP-PBS (A, D), NGF (B, E) and MP-NGF (C, F). G: histogram of myelinated fibers number in the different groups compared. Data expressed as mean ± SEM. *$p < 0.05$ vs Col; #$p < 0.05$ vs MP-PBS. Scale bar 100 μm in A–C and 10 μm in D–F.

distinguish if different NTFs exerted a selective effect on the axonal regeneration of motor or sensory neurons in vivo, an information that is not provided by standard microscopy methods. The in vivo results corroborated some results previously reported using the organotypic cultures in vitro. Thus, in cultures with NTFs added directly to the collagen matrix, NGF had a positive effect only on sensory neurons, BDNF mainly enhanced motoneurons growth, GDNF promoted neurite outgrowth in both types of neurons, whereas NT-3 did not have a noticeable effect (Allodi et al., 2011), similarly to our results in vivo with free NTFs. Nevertheless, we found that when applied encapsulated in MPs, the same NTFs had stronger effects on axonal regeneration of both populations of peripheral neurons, although the differential effects were maintained.

Previous studies demonstrated that an additional supply of GDNF and of BDNF exerts beneficial effects on motoneuron survival and regeneration (Boyd and Gordon, 2003b; Pajenda et al., 2014), but no positive effects were found for sensory neurons (Tannemaat et al., 2008). In agreement with those reports, we observed improved motor but not sensory neuron regeneration when BDNF and GDNF were embedded as free factors in the collagen filling the silicone tube. However, when they were encapsulated in MPs, regeneration was enhanced in both motor and sensory neurons. Although sensory neurons and Schwann cells express both BDNF and GDNF receptors (Boyd and Gordon, 2003a), it is likely that a single administration immediately after nerve injury is not enough to exert a significant effect on sensory regeneration.

FGF-2 is expressed in three isoforms that are upregulated after nerve injury (Klimaschewski et al., 2013). FGF-2 18 KDa isoform mainly enhances motor functional recovery with some effects on sensory functional recovery (Allodi et al., 2014; Haastert et al., 2006; Meyer et al., 2015). In accordance with these studies, we found an enhancement only of motor axon regeneration compared to both controls in the MP group.

On the other hand, as motoneurons do not express TrkA receptor and after sciatic nerve axotomy TrkC receptor levels remain relatively unchanged (Boyd and Gordon, 2003a), significant effects on motoneurons regeneration with the application of NGF and NT-3 were not expected. However, when encapsulated in MPs both NGF and NT-3 produced significant increase in the number of motoneurons that regenerated their axons distal to the conduit. A previous study described improvement of

motor regeneration with NGF administration in a fibrin depot (Jubran and Widenfalk, 2003). It may be hypothesized that the prolonged supply by the MPs might indirectly enhance axonal regeneration by stimulating Schwann cell proliferation and reactivity. Furthermore, a possible inhibition of NGF or NT-3 via p75 receptor activation (Boyd and Gordon, 2002) could also be compensated by the upregulation of other NTFs such as BDNF secreted by stimulated Schwann cells or fibroblasts (Acheson et al., 1991; Klein et al., 1991).

In conclusion, the results of this study indicate that the use of PLGA MPs as a prolonged delivery system within a nerve conduit is a good approach to enhance nerve regeneration in comparison with a single application of NTFs that have a limited effect due to degradation, leakage outside the conduit or dilution resulting in sub-optimal concentration. Despite some NTFs are able to enhance axonal regeneration when directly applied to the injured nerve, our in vitro and in vivo results support that the therapeutic effect in terms of increasing axon growth is significantly increased by a sustained release from PLGA MPs. The lengthening of trophic support will be of further relevance for the repair of long gaps with nerve conduits, a situation in which the endogenous support is insufficient to sustain axonal regeneration, as well as for delayed repair of nerve injuries (Wood et al., 2013) that need a reactivation of the pro-regenerative environment along the distal nerve. Further research to refine the MPs supply of NTFs should address on tuning the time-concentration rate of delivery, as well as the potential contribution of several factors simultaneously or sequentially.

4. Experimental procedure

4.1. *Microsphere fabrication and characterization*

The chosen material was Poly-lactic Co-Glycolic acid (PLGA, Sigma-Aldrich Co. LLC, cat# 719870), a synthetic biocompatible and biodegradable co-polymer widely used for controlled release applications (Makadia and Steven, 2011). Low molecular weight PLGA (M_w 24,000–38,000) was used because of its encapsulation efficiency (Blanco and Alonso, 1998) and a water-in-oil-in-water (WoW) protocol was followed, as already described (Ghaderi et al., 1996), with modifications to adapt to the application. Briefly, 30–35 mg of PLGA (50:50) were dissolved in 1 ml DCM. The first emulsion was created with 200 μl aqueous solution of the desired trophic factor (NGF, BDNF, GDNF, FGF-2 18 KDa, or NT-3, Peprotech, USA) with an immersion homogenizer. This water-in-oil emulsion was then poured in 7 ml PVA 5% aqueous solution to create the second emulsion. After 45 min in the magnetic stirrer the double emulsion was poured in 40 ml PVA 0.1% aqueous solution to allow for solidification and solvent evaporation over 16 h in the magnetic stirrer at RT. The MPs were washed with distilled water twice by centrifugation at 4650 RCF at 4 °C, finally resuspended in an aqueous solution with penicillin/streptomycin, to control possible downstream bacterial contamination and sent forth for in vitro/in vivo experiments.

MP surface and size distribution assessment was performed by SEM (EVO™MA10 Scanning Electron Microscope, Zeiss, Germany). Briefly, 1–3 μl of particles dispersion were spotted on silicone stubs, metallized with a sputter coater (Quorum Q150R ES, Quorum technologies, UK) and imaged with an acceleration voltage of 10 kV. Size distribution characterization was performed by means of an inverted microscope (Eclipse Ti; Nikon Instruments, Japan) equipped with a cooled CCD camera (DS-Fi1C; Nikon Instruments, Japan). MPs were imaged immediately after synthesis in 5 μl distilled water spotted on a clean glass coverslip, and snapshots of random fields were taken in visible light. Particle size was evaluated via image analysis with the Fiji software (Schindelin et al., 2013). Assessment of fluorescent proteins encapsulation and tracking was performed with same apparatus equipped with suitable fluorescent filters.

NGF was chosen to further characterize the performance of the microspheres system. NGF encapsulation efficiency of the fabrication protocol was calculated as the fraction between experimental load versus theoretical load. For efficiency testing, 4 μg of NGF were encapsulated in 30 mg PLGA MPs, following the above described protocol. The MPs were washed and dissolved by incubation overnight in 2 ml dissolution buffer (5% SDS, 0.1 N NaOH) at RT. Following microsphere dissolution, the released NGF was quantified with an ELISA test kit (Human beta-NGF ELISA kit, Sigma-Aldrich, USA), following the manufacturer's protocol.

For NGF release assessment, a tube containing 1 ml of phosphate buffered saline (PBS) was loaded with 62.5 μg of MPs coming from batches of 30 mg total mass, equivalent to an estimated 50 ng encapsulated NGF (based on previously calculated load efficiency). The tube was incubated at 37 °C and at specific time points (0, 1, 2, 3, 5, 6, 7, 8, 15, 20, 25, and 33 days), the mixture was centrifuged at 4650 RCF at 4 °C, the supernatant was collected and fresh PBS was then added to replace the withdrawn supernatant; the MPs were resuspended again and returned to 37 °C. Supernatants were frozen for subsequent quantification. Assessment of quantity of the released NGF in each supernatant at different time points was also performed by an ELISA kit (Human beta-NGF ELISA kit SIGMA-Aldrich, USA), following the manufacturer's protocol. Release experiments were all performed in duplicate.

4.2. *In vitro study on organotypic cultures*

The in vitro procedures were approved by the ethical committee of the Universitat Autonoma de Barcelona in accordance with the European Communities Council Directive 2010/63/EU. Organotypic cultures were prepared as previously described (Allodi et al., 2011). A volume of 392 μl of rat tail collagen type I solution (#354236, Corning) at a concentration of 3.83 mg/ml was mixed with 50 μl of 10 × basal Eagle's medium (Gibco) and 2 μl of 7.5% sodium bicarbonate solution. Moreover, 56 μl of PBS with MPs containing FITC-BSA for biocompatibility assessment or 56 μl of PBS with free or MP encapsulated NGF or BDNF for bioactivity experiments were added to the collagen solution. The same volume of MPs with PBS vehicle was used for the control group (Col). The final concentration of the NTF was 10 ng/ml of within a 3.0 mg/ml collagen gel.

Single drops of 30 μl were deposited on poly-D-lysine (PL, 1 g/ml, Sigma) coated coverslips, which were placed in Petri dishes or 24-well multidishes (Iwaki, Asahi Technoglass, Chiba, Japan) and kept in the incubator at 37 °C and 5% CO_2 for two hours to induce collagen gel formation. Three different sets of collagen-based matrices (containing MPs loaded with PBS, NTFs or free

NTFs) were prepared and used immediately or maintained for 1 week (conditioning) in the incubator to test if MPs released the factors over time and if the NTF was accumulated or eluted with time in each condition.

P7 rats were euthanised by cervical dislocation following AVMA Guidelines on Euthanasia (Leary et al., 2013), and spinal cord (SC, $n=6$–8/group) lumbar segments and lumbar DRG ($n=14$–24/group) were harvested, placed in cold Gey's balanced salt solution (Sigma) enriched with 6 mg/ml glucose and cleaned from blood and meningeal debris. SCs were cut with a McIlwain Tissue Chopper in 350 μm thick slices. SC slices and DRG explants were then placed on the gelled collagen droplets, prepared as indicated above, and covered by a second drop of 30 μl collagen matrix. The embedded samples were placed again in the incubator for 45 min before adding Neurobasal medium (NB, Invitrogen), supplemented with B27 (Invitrogen), glutamine and penicillin/streptomycin (Sigma). The medium volume delivered into Petri dishes and wells was 1.5 ml for SC slices and 0.5 ml for DRG. After one day in culture, the medium of SC cultures was removed and changed by a penicillin/streptomycin free medium. DRG explants were cultured for 2 days, and SC slices for 4 days.

SC and DRG cultures were fixed with 4% paraformaldehyde in PBS for 30 min. Afterwards, SC and DRG samples were incubated for 48 h with primary antibody mouse RT97 (1:200, Developmental Studies Hybridoma Bank) at 4 °C. After three hours washing, the sections were incubated with secondary antibodies AF594 conjugated donkey anti-mouse (1:200, Jackson IR) overnight at 4 °C. After two washes samples were mounted on slides with Mowiol containing DAPI (1:10,000, Sigma) nuclear counterstain. Cultures were visualized with an Olympus BX51 fluorescence microscope, images of different areas were taken with Cell A software (Olympus) and merged using Adobe Photoshop CS3 (Adobe System). Confocal images were obtained using a ZEISS LSM 700 microscope and the ZEN ZEISS software. Whole culture images were analyzed with the Neurite-J plug-in (Torres-Espín et al., 2014) for ImageJ software (NIH, available at http://rsb.info.nih.gov/ij/) and the number of neurites grown at different distances from the explant was compared between sets of cultures.

4.3. *In vivo study of peripheral nerve regeneration*

Female Sprague-Dawley rats (250–300 g) were used for the in vivo studies. They were kept on standard laboratory conditions with a light-dark cycle of 12:12 h and *ad libitum* access to food and tap water. All efforts were made to minimize pain and animal discomfort during surgery and treatments.

Animals were anaesthetized with pentobarbital sodium (40 mg/kg i.p.)., the sciatic nerve was exposed at the midthigh and sectioned 90 mm from the tip of the third toe, and a 6 mm nerve portion distal to the section was resected. A silicone tube was then sutured with 10–0 monofilament sutures to each nerve stump leaving a 6 mm gap between both nerve ends. Animals were kept for 20 days post-operation (dpo) to allow axonal regeneration before testing.

NGF, NT-3, GDNF and BDNF free or encapsulated in MPs were added to a collagen solution to reach a final concentration of 2 μg/ml; FGF free and encapsulated was used at 10 μg/ml. Each preparation of NTF was mixed with 50 μl of 10× basal Eagle's medium (Gibco), 2 μl of 7.5% sodium bicarbonate and 187 μl of PBS, and then kindly mixed with 261 μl of collagen type I solution at 3.83 mg/ml to a reach a final collagen concentration of 2 mg/ml. Silicone tubes 8 mm long with an external diameter of 3 mm and an internal diameter of 2 mm were filled with one of the collagen mixtures containing free or encapsulated NTFs. In order to promote fibril alignment, the collagen was left to gel vertically for 12 h before surgery (Verdú et al., 2002). Therefore, there were 10 experimental groups ($n=5$–6 per group), one for each NTF free and encapsulated in MPs. In addition, two control groups were implanted with tubes containing collagen alone or collagen with MPs containing only PBS. All in vivo procedures were approved by the ethical committee of the Universitat Autonoma de Barcelona in accordance with the European Communities Council Directive 2010/63/EU.

4.4. *Retrograde labeling and neuronal counting*

To quantify regenerated motor and sensory neurons, rats were anaesthetized at 20 days after lesion with pentobarbital sodium, the sciatic nerve was exposed and transected 8 mm distal to the distal end of the silicone tube. The tip of the severed nerve was soaked into 5 μl of Fluorogold (FG; 5%; Fluorochrome Inc.) for 1 h in a vaseline well. After retrieval of the well, the area was rinsed with saline to clean remnants of the tracer, and the wound sutured in planes. Animals were allowed to survive for 7 days to allow accumulation of the tracer in the soma of the spinal motoneurons and the DRG sensory neurons. Then, rats were deeply anesthetized with pentobarbital sodium overdose (200 mg/kg i.p.) following AVMA Guidelines on Euthanasia (Leary et al., 2013) and transcardially perfused with 4% paraformaldehyde in PBS. The lumbar segment (L3–L6) of the SC and L4 and L5 DRG were removed, postfixed in the same fixative solution for 1 h and transferred to 30% sucrose in PBS. The SC and DRG were cut longitudinally in 40 and 20 μm thick sections, respectively, in a cryostat and mounted on slides. Sections were observed with an Olympus BX51 fluorescence microscope under UV light and the number of labeled neurons were counted in every third section following the fractionation principle (Gundersen, 1986).

4.5. *Nerve histology*

After perfusion, the regenerated nerves inside the tubes were also harvested and fixed in glutaraldehyde-paraformaldehyde (3%/3%) in cacodylate-buffer solution (0.1 M, pH 7.4) overnight at 4 °C. Then, nerves were postfixed with osmium tetroxide (2%, 2 h) and dehydrated through ethanol series prior to embedding samples in epon resin. Semithin sections (0.5 μm thick) taken 3 mm distal from the proximal stump were stained with toluidine blue and examined by light microscopy. Images of the whole sciatic nerve were acquired at 10× with an Olympus DP73 camera attached to a computer. Sets of images for analysis obtained at 100× magnification were chosen by systematic random sampling of squares representing at least 30% of the nerve cross-sectional area and measurements of cross-sectional area of the whole nerve and counts of the number of myelinated nerve fibers (MF) were conducted.

4.6. *Data analysis and statistics*

Data are presented as mean ± SEM. Results were statistically analyzed by using GraphPad Prism (GraphPad Software, USA). One- or two-way ANOVA followed by Bonferroni's multiple comparison test was used in the in vitro studies for comparison between groups. Student's *t*-test or one-way ANOVA followed by post hoc Fisher's exact test were applied in the in vivo studies. Statistical significance was considered when *P* value was <0.05.

Acknowledgments

This research was supported by the European Union FP7-NMP project MERIDIAN under contract number 280778, and FPT-ICT project NEBIAS under contract number 611687, TERCEL and CIBERNED funds from the Fondo de Investigación Sanitaria of Spain. The authors thank the technical help of Francisco González-Pérez, Mónica Espejo, Jéssica Jaramillo and Marta Morell. The RT97 antibody was obtained from the Developmental Studies Hybridoma Bank developed under the auspices of the NICHD and maintained by the University of Iowa, Department of Biology.

REFERENCES

Acheson, A., Barker, P.A., Alderson, R.F., Miller, F.D., Murphy, R.A., 1991. Detection of brain-derived neurotrophic factor-like activity in fibroblasts and Schwann cells: inhibition by antibodies to NGF. Neuron 7, 265–275.

Allodi, I., Casals-Díaz, L., Santos-Nogueira, E., Gonzalez-Perez, F., Navarro, X., Udina, E., 2013. FGF-2 low molecular weight selectively promotes neuritogenesis of motor neurons in vitro. Mol. Neurobiol. 47, 770–781.

Allodi, I., Guzmán-Lenis, M.-S., Hernàndez, J., Navarro, X., Udina, E., 2011. In vitro comparison of motor and sensory neuron outgrowth in a 3D collagen matrix. J. Neurosci. Methods 198, 53–61.

Allodi, I., Mecollari, V., González-Pérez, F., Eggers, R., Hoyng, S., Verhaagen, J., Navarro, X., Udina, E., 2014. Schwann cells transduced with a lentiviral vector encoding Fgf-2 promote motor neuron regeneration following sciatic nerve injury. Glia 62, 1736–1746.

Allodi, I., Udina, E., Navarro, X., 2012. Specificity of peripheral nerve regeneration : interactions at the axon level. Prog. Neurobiol. 98, 16–37.

Arslantunali, D., Dursun, T., Yucel, D., Hasirci, N., Hasirci, V., 2014. Peripheral nerve conduits: technology update. Med. Devices 7, 405–424.

Benoit, J.-P., Faisant, N., Venier-Julienne, M.-C., Menei, P., 2000. Development of microspheres for neurological disorders: from basics to clinical applications. J. Control. Release 65, 285–296.

Blanco, D., Alonso, M.J., 1998. Protein encapsulation and release from poly(lactide-co-glycolide) microspheres: effect of the protein and polymer properties and of the co-encapsulation of surfactants. Eur. J. Pharm. Biopharm. 45, 285–294.

Boeckstyns, M.E.H., Sørensen, A.I., Viñeta, J.F., Rosén, B., Navarro, X., Archibald, S.J., Valss-Solé, J., Moldovan, M., Krarup, C., 2013. Collagen conduit versus microsurgical neurorrhaphy: 2-year follow-up of a prospective, blinded clinical and electrophysiological multicenter randomized, controlled trial. J. Hand Surg. Am. 38, 2405–2411.

Boyd, J.G., Gordon, T., 2002. A dose-dependent facilitation and inhibition of peripheral nerve regeneration by brain-derived neurotrophic factor. Eur. J. Neurosci. 15, 613–626.

Boyd, J.G., Gordon, T., 2003a. Neurotrophic factors and their receptors in axonal regeneration and functional recovery after peripheral nerve injury. Mol. Neurobiol. 27, 277–324.

Boyd, J.G., Gordon, T., 2003b. Glial cell line-derived neurotrophic factor and brain-derived neurotrophic factor sustain the axonal regeneration of chronically axotomized motoneurons in vivo. Exp. Neurol. 183, 610–619.

Catrina, S., Gander, B., Madduri, S., 2013. Nerve conduit scaffolds for discrete delivery of two neurotrophic factors. Eur. J. Pharm. Biopharm. 85, 139–142.

De Boer, R., Knight, A.M., Spinner, R.J., Malessy, M.J., Yaszemski, M.J., Windebank, A.J., 2011. In vitro and in vivo release of nerve growth factor from biodegradable poly-lactic-co-glycolic-acid microspheres. J. Biomed. Mater. Res. A 95, 1067–1073.

De Boer, R., Borntraeger, A., Knight, A.M., Hébert-Blouin, M.-N., Spinner, R.J., Malessy, M.J.A., Yaszemski, M.J., Windebank, A.J., 2012. Short- and long-term peripheral nerve regeneration using a poly-lactic-co-glycolic-acid scaffold containing nerve growth factor and glial cell line-derived neurotrophic factor releasing microspheres. J. Biomed. Mater. Res. A 100, 2139–2146.

Diamond, J., Coughlin, M., Macintyre, L., Holmes, M., 1987. Evidence that endogenous IU nerve growth factor is responsible for the collateral sprouting, but not the regeneration, of nociceptive axons in adult rats. Proc. Nat. Acad. Sci. USA 84, 6596–6600.

Eggers, R., de Winter, F., Hoyng, S.A., Roet, K.C.D., Ehlert, E.M., Malessy, M.J.A., Verhaagen, J., Tannemaat, M.R., 2013. Lentiviral vector-mediated gradients of GDNF in the injured peripheral nerve: effects on nerve coil formation, Schwann cell maturation and myelination. PLoS One 8, e71076.

Ejstrup, R., Kiilgaard, J.F., Tucker, B.A., Klassen, H.J., Young, M.J., La Cour, M., 2010. Pharmacokinetics of intravitreal glial cell line-derived neurotrophic factor: experimental studies in pigs. Exp. Eye Res. 91, 890–895.

Ghaderi, R., Sturesson, C., Carlfors, J., 1996. Effect of preparative parameters on the characteristics of poly (D,L-lactide-co-glycolide) microspheres made by the double emulsion method. Int. J. Pharm. 141, 205–216.

Gloster, A., Diamond, J., Ln, C., 1992. Sympathetic nerves in adult rats regenerate normally and restore pilomotor function during an anti-NGF treatment that prevents their collateral sprouting. J. Comp. Neurol. 326, 363–374.

Gold, B.G., 1997. Axonal regeneration of sensory nerves is delayed by continuous intrathecal infusion of nerve growth factor. Neuroscience 76, 1153–1158.

Gómez, N., Cuadras, J., Butí, M., Navarro, X., 1996. Histologic assessment of sciatic nerve regeneration following resection and graft or tube repair in the mouse. Restor. Neurol Neurosci. 10, 187–196.

Gordon, T., Sulaiman, O., Boyd, J.G., 2003. Experimental strategies to promote functional recovery after peripheral nerve injuries. J. Peripher. Nerv. Syst. 8, 236–250.

Grabowski, N., Hillaireau, H., Vergnaud, J., Santiago, L.A., Kerdine-Romer, S., Pallardy, M., Tsapis, N., Fattal, E., 2013. Toxicity of surface-modified PLGA nanoparticles toward lung alveolar epithelial cells. Int. J. Pharm. 454, 686–694.

Gundersen, H.J., 1986. Stereology of arbitrary particles. A review of unbiased number and size estimators and the presentation of some new ones, in memory of William R. Thompson. J. Microsc. 143, 3–45.

Guntinas-Lichius, O., Irintchev, A., Streppel, M., Lenzen, M., Grosheva, M., Wewetzer, K., Neiss, W.F., Angelov, D.N., 2005. Factors limiting motor recovery after facial nerve transection

in the rat: combined structural and functional analyses. Eur. J. Neurosci. 21, 391–402.
Haastert, K., Lipokatic, E., Fischer, M., Timmer, M., Grothe, C., 2006. Differentially promoted peripheral nerve regeneration by grafted Schwann cells over-expressing different FGF-2 isoforms. Neurobiol. Dis. 21, 138–153.
Hontanilla, B., Aubá, C., Gorría, O., 2007. Nerve regeneration through nerve autografts after local administration of brain-derived neurotrophic factor with osmotic pumps. Neurosurgery 61, 1268–1274.
Ishi, D.N., Glazner, G.W., Whalenc, L.R., 1993. Regulation of peripheral nerve regeneration by insulin-like growth factors. Ann. N. Y. Acad. Sci 692, 172–182.
Jain, R.A., 2000. The manufacturing techniques of various drug loaded biodegradable poly (lactide-co-glycolide) (PLGA) devices. Biomaterials 21, 2475–2490.
Jenq, C.-B., Coggeshall, R.E., 1985. Numbers of regenerating axons in parent and tributary peripheral nerves in the rat. Brain Res. 326, 27–40.
Jubran, M., Widenfalk, J., 2003. Repair of peripheral nerve transections with fibrin sealant containing neurotrophic factors. Exp. Neurol. 181, 204–212.
Kang, H., Lichtman, J.W., 2013. Motor axon regeneration and muscle reinnervation in young adult and aged animals. J. Neurosci. 33, 19480–19491.
Kanje, M., Skottner, A., Sjöberg, J., Lundborg, G., 1989. Insulin-like growth factor I (IGF-I) stimulates regeneration of the rat sciatic nerve. Brain Res. 486, 396–398.
Kemp, S.W.P., Webb, A., Dhaliwal, S., Syed, S., Walsh, S.K., Midha, R., 2011. Dose and duration of nerve growth factor (NGF) administration determine the extent of behavioral recovery following peripheral nerve injury in the rat. Exp. Neurol. 229, 460–470.
Klein, R., Nanduri, V., Jing, S., Lamballe, F., Tapley, P., 1991. The trkB tyrosine protein kinase is a receptor for brain-derived neurotrophic factor and neurotrophin-3. Cell 66, 395–403.
Klimaschewski, L., Hausott, B., Angelov, D.N., 2013. The pros and cons of growth factors and cytokines in peripheral axon regeneration. Int. Rev. Neurobiol. 108, 137–171.
Krarup, C., Archibald, S.J., Madison, R.D., 2002. Factors that influence peripheral nerve regeneration: an electrophysiological study of the monkey median nerve. Ann. Neurol. 51, 69–81.
Lago, N., Navarro, X., 2006. Correlation between target reinnervation and distribution of motor axons in the injured rat sciatic nerve. J. Neurotrauma 23, 227–240.
Leary, S., Underwood, W., Anthony, R., et al., 2013. AVMA Guidelines for the Euthanasia of Animals: 2013 edition.
Lee, A.C., Yu, V.M., Lowe, J.B., Brenner, M.J., Hunter, D.A., Mackinnon, S.E., Sakiyama-Elbert, S.E., 2003. Controlled release of nerve growth factor enhances sciatic nerve regeneration. Exp. Neurol. 184, 295–303.
Mackinnon, S.E., Dellon, A.L., O'Brien, J.P., 1991. Changes in nerve fibers distal to a nerve repair in the rat sciatic nerve model. Muscle Nerve 14, 1116–1122.
Madduri, S., Feldman, K., Tervoort, T., Papaloïzos, M., Gander, B., 2010. Collagen nerve conduits releasing the neurotrophic factors GDNF and NGF. J. Control. Release 143, 168–174.
Makadia, H.K., Steven, S.J., 2011. Poly lactic-co-glycolic acid (PLGA) as biodegradable controlled drug delivery carrier. J. Liposome Res. 3, 1377–1397.
Mcdonald, D.S., Zochodne, D.W., 2003. An injectable nerve regeneration chamber for studies of unstable soluble growth factors. J. Neurosci. Methods 122, 171–178.
Meyer, C., Wrobel, S., Raimondo, S., Rochkind, S., Heimann, C., Shahar, A., Ziv-Polat, O., Geuna, S., Grothe, C., Haastert-Talini, K., 2015. Peripheral nerveregeneration through hydrogel enriched chitosan conduits containing engineered Schwann cells for drug delivery. Cell transplantat 25, 159–182.
Midha, R., Munro, C.A., Dalton, P.D., Tator, C.H., Shoichet, M.S., 2003. Growth factor enhancement of peripheral nerve regeneration through a novel synthetic hydrogel tube. J. Neurosurg. 99, 555–565.
Mohiuddin, L., Delcroix, J.D., Fernyhough, P., Tomlinson, D.R., 1999. Focally administered nerve growth factor suppresses molecular regenerative responses of axotomized peripheral afferents in rats. Neuroscience 91, 265–271.
Moore, A.M., Wood, M.D., Chenard, K., Hunter, D.A., Mackinnon, S.E., Sakiyama-Elbert, S.E., Borschel, G.H., 2010. Controlled delivery of glial cell line-derived neurotrophic factor enhances motor nerve regeneration. J. Hand Surg. Am. 35, 2008–2017.
Mozafari, M.R., Johnson, C., Hatziantoniou, S., Demetzos, C., 2008. Nanoliposomes and their applications in food nanotechnology. J. Liposome Res. 18, 309–327.
Mura, S., Nicolas, J., Couvreur, P., 2013. Stimuli-responsive nanocarriers for drug delivery. Nat. Mater. 12, 991–1003.
Navarro, X., 2015. Functional evaluation of peripheral nerve regeneration and target reinnervation in animal models: a critical overview. Eur. J. Neurosci. http://dxdoi.org/10.1111/ejn.13033.
Painter, M.W., Brosius Lutz, A., Cheng, Y.-C., Latremoliere, A., Duong, K., Miller, C.M., Posada, S., Cobos, E.J., Zhang, A.X., Wagers, A.J., Havton, L.A., Barres, B., Omura, T., Woolf, C.J., 2014. Diminished Schwann cell repair responses underlie age-associated impaired axonal regeneration. Neuron 83, 331–343.
Pajenda, G., Hercher, D., Márton, G., Pajer, K., Feichtinger, G.A., Maléth, J., Redl, H., Nógrádi, A., 2014. Spatiotemporally limited BDNF and GDNF overexpression rescues motoneurons destined to die and induces elongative axon growth. Exp. Neurol. 261, 367–376.
Péan, J.M., Venier-Julienne, M.C., Boury, F., Menei, P., Denizot, B., Benoit, J.P., 1998. NGF release from poly (D, L-lactide-co-glycolide) microspheres. Effect of some formulation parameters on encapsulated NGF stability. J control release 56, 175–187.
Peer, D., Karp, J.M., Hong, S., Farokhzad, O.C., Margalit, R., Langer, R., 2007. Nanocarriers as an emerging platform for cancer therapy. Nat. Nanotechnol. 2, 751–760.
Pfister, L.A., Papaloïzos, M., Merkle, H.P., Gander, B., 2007. Nerve conduits and growth factor delivery in peripheral nerve repair. J. Peripher. Nerv. Syst. 12, 65–82.
Piquilloud, G., Christen, T., Pfister, L.A., Gander, B., Papaloïzos, M. Y., 2007. Variations in glial cell line-derived neurotrophic factor release from biodegradable nerve conduits modify the rate of functional motor recovery after rat primary nerve repairs. Eur. J. Neurosci. 26, 1109–1117.
Ruiz, G., Ceballos, D., Baños, J.-E., 2004. Behavioral and histological effects of endoneurial administration of nerve growth factor: possible implications in neuropathic pain. Brain Res. 1011, 1–6.
Sakiyama-Elbert, S.E., Hubbell, J.A., 2000. Controlled release of nerve growth factor from a heparin-containing fibrin-based cell ingrowth matrix. J. Control. Release 69, 149–158.
Scherman, P., Lundborg, G., Kanje, M., Dahlin, L.B., 2001. Neural regeneration along longitudinal polyglactin sutures across short and extended defects in the rat sciatic nerve. J. Neurosurg. 95, 316–323.
Schindelin, J., Arganda-carreras, I., Frise, E., Kaynig, V., Pietzsch, T., Preibisch, S., Rueden, C., Saalfeld, S., Schmid, B., Tinevez, J., White, D.J., Hartenstein, V., Tomancak, P., Cardona, A., 2013. Fiji – an open source platform for biological image analysis. Nat. Methods 9, 676–682.
Sternel, G.D., Brown, R.A., Green, C.J., Terenghi, G., 1997. Neurotrophin-3 delivered locally via fibronectin mats

enhances peripheral nerve regeneration. Eur. J. Neurosci. 9, 1388–1396.
Tam, R.Y., Fuehrmann, T., Mitrousis, N., Shoichet, M.S., 2014. Regenerative therapies for central nervous system diseases: a biomaterials approach. Neuropsychopharmacology 39, 169–188.
Tannemaat, M.R., Eggers, R., Hendriks, W.T., de Ruiter, G.C.W., van Heerikhuize, J.J., Pool, C.W., Malessy, M.J., Boer, G.J., Verhaagen, J., 2008. Differential effects of lentiviral vector-mediated overexpression of nerve growth factor and glial cell line-derived neurotrophic factor on regenerating sensory and motor axons in the transected peripheral nerve. Eur. J. Neurosci. 28, 1467–1479.
Torres-Espín, A., Santos, D., González-Pérez, F., del Valle, J., Navarro, X., 2014. Neurite-J: an image-J plug-in for axonal growth analysis in organotypic cultures. J. Neurosci. Methods 236, 26–39.
Tria, M.A., Fusco, M., Vantini, G., Mariot, R., 1994. Pharmacokinetics of nerve growth factor (NGF) following different routes of administration to adult rats. Exp. Neurol. 127, 178–183.
Valero-Cabré, A., Navarro, X., 2002. Functional impact of axonal misdirection after peripheral nerve injuries followed by graft or tube repair. J. Neurotrauma 19, 1475–1485.
Verdú, E., Labrador, R.O., Rodríguez, F.J., Ceballos, D., Forés, J., Navarro, X., 2002. Alignment of collagen and laminin-containing gels improve nerve regeneration within silicone tubes. Restor. Neurol. Neurosci. 20, 169–180.
Verdú, E., Ceballos, D., Vilches, J.J., Navarro, X., 2008. Influence of aging on peripheral nerve function and regeneration. J. Peripher. Nerv. Syst. 5, 191–208.
Vögelin, E., Baker, J.M., Gates, J., Dixit, V., Constantinescu, M.A., Jones, N.F., 2006. Effects of local continuous release of brain derived neurotrophic factor (BDNF) on peripheral nerve regeneration in a rat model. Exp. Neurol. 199, 348–353.
Williams, L.R., Longo, F.M., Powell, H.C., Lundborg, G., Varon, S., 1983. Spatial-temporal progress of peripheral nerve regeneration within a silicone chamber: parameters for a bioassay. J. Comp. Neurol. 218, 460–470.
Wood, M.D., Gordon, T., Kim, H., Szynkaruk, M., Phua, P., Lafontaine, C., Kemp, S.W., Shoichet, M.S., Borschel, G.H., 2013. Fibrin gels containing GDNF microspheres increase axonal regeneration after delayed peripheral nerve repair. Regen. Med. 8, 27–37.
Yeo, Y., Park, K., 2004. Control of encapsulation efficiency and initial burst in polymeric microparticle systems. Arch. Pharm. Res. 27, 1–12.

Dose-dependent differential effect of neurotrophic factors on in vitro and in vivo regeneration of motor and sensory neurons

Daniel Santos, Xavier Navarro, Jaume del Valle

Institute of Neurosciences, Department of Cell Biology, Physiology and Immunology, Universitat Autònoma de Barcelona and Centro de Investigación Biomédica en Red sobre Enfermedades Neurodegenerativas (CIBERNED), Bellaterra, Spain

Corresponding author: Dr. Jaume del Valle, Unitat de Fisiologia Mèdica, Facultat de Medicina, Universitat Autònoma de Barcelona, E-08193 Bellaterra, Spain. E-mail: jaume.delvalle@uab.cat

Abstract

Although axons can regenerate after peripheral nerve transection and repair, functional recovery is usually poor because misdirected regenerating axons lead to inaccurate reinnervation. Neurotrophic factors promote and offer directional guidance to regenerating axons and their selective application may help to improve functional recovery. Hence, we have characterized in organotypic cultures of spinal cord and dorsal root ganglia (DRG) the effect of GDNF, FGF-2, NGF, NT-3 and BDNF at different concentrations on motor and sensory neurite outgrowth. In vitro results show that GDNF and FGF-2 enhanced both motor and sensory neurite outgrowth, NGF and NT-3 were the most selective to enhance sensory neurite outgrowth and high doses of BDNF selectively enhanced motor neurite outgrowth. Then, different doses of NGF, NT-3 and BDNF selected as the most selective factors were delivered in a collagen matrix within a silicone tube to repair the severed sciatic nerve of rats. Fluorogold was applied to the regenerated nerve to quantify the number of motor and sensory neurons in the spinal cord and DRG respectively. In vivo, NGF and NT-3 did not show preferential effect on sensory regeneration whereas BDNF preferentially promoted motor axons regeneration. Therefore, our results indicate that the selective effect of NGF and NT-3 shown in vitro is lost when they are applied in vivo, but a high dose of BDNF is able to selectively enhance motor neuron regeneration both in vitro and in vivo.

1. Introduction

After peripheral nerve injury transected axons can regenerate and reinnervate target organs. However, reinnervation of distal organs and functional recovery is often deficient because random regeneration of axons results in aberrant target reinnervation (Valero-Cabré and Navarro, 2002). Thus, specificity of reinnervation is a key issue to improve functional recovery after peripheral nerve injuries.

Although some studies described that motor axons preferentially reinnervate muscular pathways (Brushart, 1988), this accuracy is compromised when optimal conditions such as pure muscular and cutaneous branches, matching distal nerve caliber, and short separation between nerve stumps are not met (Madison et al., 1996; Robinson and Madison, 2004). Actually, it has been suggested that although motor or sensory neurons tend to regenerate through its original pathway, axons sense the levels of trophic factors in distal branches and then grow towards the target that offers more trophic support (Robinson and Madison, 2005). In fact, some authors argue that the key point for preferential attraction of axons to their adequate targets is the expression of trophic factors by the own target organ and the distal stump (Brushart, 1988; Madison et al., 1996).

After nerve injury, in order to support neuronal survival and enhance regeneration, motoneurons in spinal cord (SC) and sensory neurons in dorsal root ganglia (DRG) synthesize and secrete neurotrophic factors (NTF). Furthermore, within the proximal and the distal nerve stumps, denervated Schwann cells become growth supportive and secrete several NTF and citokines that follow different patterns of expression, with an initial up-regulation of NGF, BDNF and GDNF, whereas others, such as NT-3 or CNTF, are down-regulated (Allodi et al., 2012). However, changes in NTF levels are several fold higher at the lesion area than in the SC or the DRG where the somata of the axotomized neurons are located (Boyd and Gordon, 2003). Moreover, it has been described that some NTF may influence the direction of regenerating axons on certain models of regeneration (Markus et al., 2002). Thus, modifying the regenerative microenvironment is a promising approach to modulate and selectively enhance sensory and motor regeneration.

However, high levels of NTF or a prolonged delivery over time can in fact induce no improvement or even result deleterious in terms of regeneration (Boyd and Gordon, 2002; Piquilloud et al., 2007; Tannemaat et al., 2008), inducing neurotoxicity (Kim et al., 2003), endoneurial sprouting and hyperalgesia (Ruiz et al., 2004). Therefore, as low levels of NTF may not reach therapeutical action and high levels may disrupt

regeneration, a comparative study of the concentrations and delivery of NTF to specifically improve regeneration of motor or sensory neurons was undertaken. We have analysed the effect of GDNF, FGF-2, NGF, NT-3 and BDNF at different concentrations on motor and sensory axonal regeneration using in vitro and in vivo models.

2. Materials and methods

2.1. Ethical guidelines

Both in vitro and in vivo experimental procedures were approved by the ethical committee of the Universitat Autonoma de Barcelona in accordance with the European Communities Council Directive 2010/63/EU. Adult rats were anaesthetized with pentobarbital sodium (40 mg/kg i.p.). P7 and adult rats were euthanized by pentobarbital sodium overdose (200 mg/kg i.p.).

2.2. DRG and SC organotypic cultures

Organotypic cultures were prepared as previously described (Santos et al., 2016). Briefly, collagen I (rat tail, #354236, Corning) diluted in basal Eagle's medium (Gibco) and sodium bicarbonate at 0.3 mg/mL was prepared as control condition., NGF, NT-3, GDNF and BDNF (Peprotech) were added to achieve concentrations of 5, 10, 50 or 100 ng/ml. As FGF-2 has been reported to work at higher concentrations (Allodi et al., 2013), FGF-2 18 kDa (Peprotech) was prepared at 25, 50, 250 and 500 ng/ml. Finally, 30 µl single drops of the prepared matrices were deposited on poly-d-lysine (1 g/ml, Sigma) coated 24-well multidishes (Iwaki, Asahi Technoglass, Chiba, Japan) and were left to gel for 2h at 37ºC and 5% CO_2 in the incubator.

SC lumbar segments and lumbar DRG were harvested from 7 days old Sprague–Dawley rats, placed in 4ºC Gey's balanced salt solution (Sigma) enriched with 6 mg/ml glucose and cleaned from blood and meningeal debris. SCs were cut with a McIlwain Tissue Chopper in 350 µm thick slices. SC slices and DRG explants were placed on top of the collagen matrix and covered by a second 30 µl drop of the same solution. After 45 min in the incubator, samples were embedded with 0.5 ml of Neurobasal medium (Life Technologies), supplemented with B27 (Life Technologies), glutamine and penicillin/streptomycin (Sigma). After one day in culture, the medium of SC cultures was removed and changed by a penicillin/streptomycin free medium. DRG explants were cultured for 2 days, and SC slices for 4 days. A detailed description of this protocol has been previously reported (Torres-Espín et al., 2016).

2.3. Neurite outgrowth analysis

SC and DRG cultures were fixed with 4% paraformaldehyde in PBS for 30 min. Afterwards, SC and DRG samples were incubated for 48 h with primary antibody mouse RT97 (1:200, Developmental Studies Hybridoma Bank) at 4ºC. After three hours washing, the sections were incubated with secondary antibody AF594 conjugated donkey anti-mouse (1:200, Life Technologies) overnight at 4ºC. After two more washes, samples were mounted on slides with Mowiol. Cultures were visualized with an Olympus BX51 fluorescence microscope, images of different areas were taken with a DP50 camera attached to a computer with Cell A software (Olympus) and merged using Adobe Photoshop CS3 (Adobe System). Whole culture images were analyzed with the Neurite-J plug-in (Torres-Espín et al., 2014) for ImageJ software (NIH, available at http://rsb.info.nih.gov/ij/) and the number of neurites grown at different distances from the explant was compared between different conditions of the cultures. The area under the curve (AUC) for each group was calculated by the linear trapezoidal method using the amount of neurites every 25 µm.

2.4. In vivo study of peripheral nerve regeneration

Only the NTFs which showed trophic selectivity for motor and sensory outgrowth were further tested in vivo. Thus, NGF, NT-3 and BDNF at 1, 2 and 10 µg/ml each were added to a 2 mg/ml collagen solution prepared as above. These mixtures were used to fill silicone tubes (8 mm long, 3 mm wide and 2mm i.d.) that were maintained vertically for 12 h to promote collagen fibril alignment during gel formation (Verdú et al., 2002). A collagen matrix without NTF was used in the control group.

Female Sprague-Dawley rats weighing 250–300 g (n=4 group) were anaesthetized, the sciatic nerve was exposed at the midthigh and sectioned 90 mm from the tip of the third toe, and a 6 mm nerve portion distal to the section was resected. The prepared tube was then sutured with 10-0 monofilament sutures to each nerve end leaving a 6 mm gap between nerve stumps. Animals were left to recover on a warming pad and then housed with littermates. They were kept on standard laboratory conditions with a light-dark cycle of 12:12 h and *ad libitum* access to food and tap water. All efforts were made to minimize pain and animal discomfort during surgery and recovery.

2.5 Retrograde labeling and neuronal counting

Rats were anesthetized at 20 dpo with pentobarbital sodium, the sciatic nerve was exposed and transected 8 mm distal to the distal end of the silicone tube. Then, the tip of the severed nerve was soaked into 5 µl Fluorogold (FG; 5%; Fluorochrome Inc.) for 1 h in a vaseline well. After retrieval of the well, saline was flushed to clean remnants of the tracer before suturing the wound in planes. Seven days later the rats were deeply

anesthetized and transcardially perfused with 4% paraformaldehyde in PBS. The lumbar segment (L3-L6) of the SC and L4 and L5 DRG were removed, postfixed in the same fixative solution for 1h and transferred to 30% sucrose in PBS. The SC and DRG were cut longitudinally in 40 and 20 μm thick sections respectively in a cryostat and mounted on slides. Sections were observed with an Olympus BX51 fluorescence microscope under UV light and the number of labeled neurons were counted in every third section following the fractionator principle (Gundersen et al., 1986).

2.6 Data analysis

Data are presented as mean ± SEM. Results were statistically analyzed by using GraphPad Prism (GraphPad Software, USA). A Student's t-test and one-way ANOVA followed by Bonferroni's post hoc test for comparison between groups was used when applicable. Statistical significance was considered when P value was <0.05.

3. Results and discussion

BDNF, NGF, NT-3, GDNF and FGF-2 at different concentrations were tested to elucidate the optimal concentration of each NTF that is able to enhance either motor or sensory neurite outgrowth without affecting the other neuronal population. For that purpose, 3D organotypic cultures of SC slices and DRG were used (Figs. 1-3).

3.1. GDNF and FGF-2 enhance both motor and sensory neurite outgrowth

Almost all doses of both FGF-2 and GDNF increased motor and sensory neurite outgrowth with respect to the control substrate (Fig. 1). Regarding motor neurite outgrowth, FGF-2 showed a progressive dose effect with the lowest concentrations not being able to reach significant differences versus the control group (Fig. 1 G, I), while GDNF enhanced motor neurite outgrowth with no dose-dependency as all the groups exhibit similar curves (Fig. 1H, J). On the other hand, sensory neurites growth from DRG increased similarly at all the tested concentrations of FGF-2 (Fig. 1K, M), while GDNF followed a dose-dependent increase showing the high doses even significantly larger AUC values than the low ones (Fig. 1N). Comparatively, using the data of the AUC in each culture condition, GDNF promoted a maximum increase of about 11 and 8 times in neurite growth of both motor and sensory neurites, whereas FGF-2 induced maximal increase of 9 and 3 times respectively (Fig. 4A,B).

These results in vitro reveal that neither GDNF nor FGF-2 show a preference for motor or sensory neuritogenesis, as both neuronal populations are enhanced at different concentrations used. While GDNF has already been reported to promote neurite

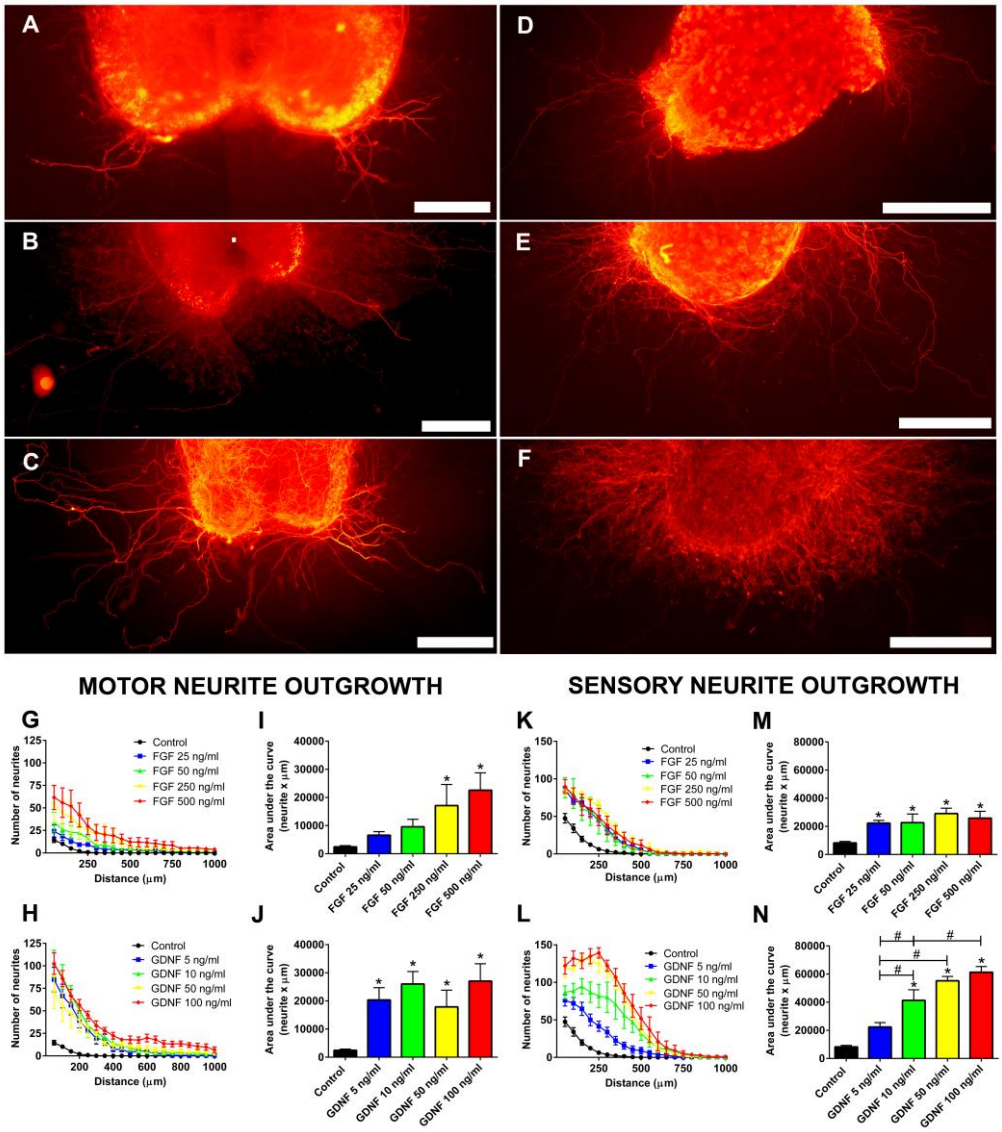

Figure 1. Representative images of RT97 stained neurites from spinal cord slices (A-C) and DRG neurons (D-F) cultured within a 3D collagen matrix alone (A, D), and with addition of 500 ng/ml of FGF-2 (B, E) or 100 ng/ml of GDNF (C, F). Quantification of the number of neurites grown at increasing distance from the spinal cord slices (G, H) and from DRG body (K, L) after the addition of FGF-2 and GDNF. Plots of the quantified AUC from G, H, K and L graphs for motor (I, J) or sensory (M, N) neurite outgrowth. Data expressed as mean ± SEM. *p<0.05 vs control; # p<0.05. Scale bar 100 µm (A), 200 µm (B-F).

outgrowth of both populations, FGF-2 was described to preferentially enhance motor neurite outgrowth when measuring the length of longest neurites (Allodi et al., 2013). Since reliable measurements of neurite outgrowth analysis in organotypic cultures is complicated (Al-Ali et al., 2016), we used a semiautomatic analysis that works as an adaption of the Sholl method (Torres-Espín et al., 2014) to improve accuracy and reproducibility as shown in other works (Parra et al., 2015; Tukmachev et al., 2016). Thus, the differences in methods and variables to quantify neurite outgrowth in these

studies may in fact explain some controversies. Hence, in accordance with our results, we discarded GDNF and FGF-2 for in vivo studies because of their lack of selective effect.

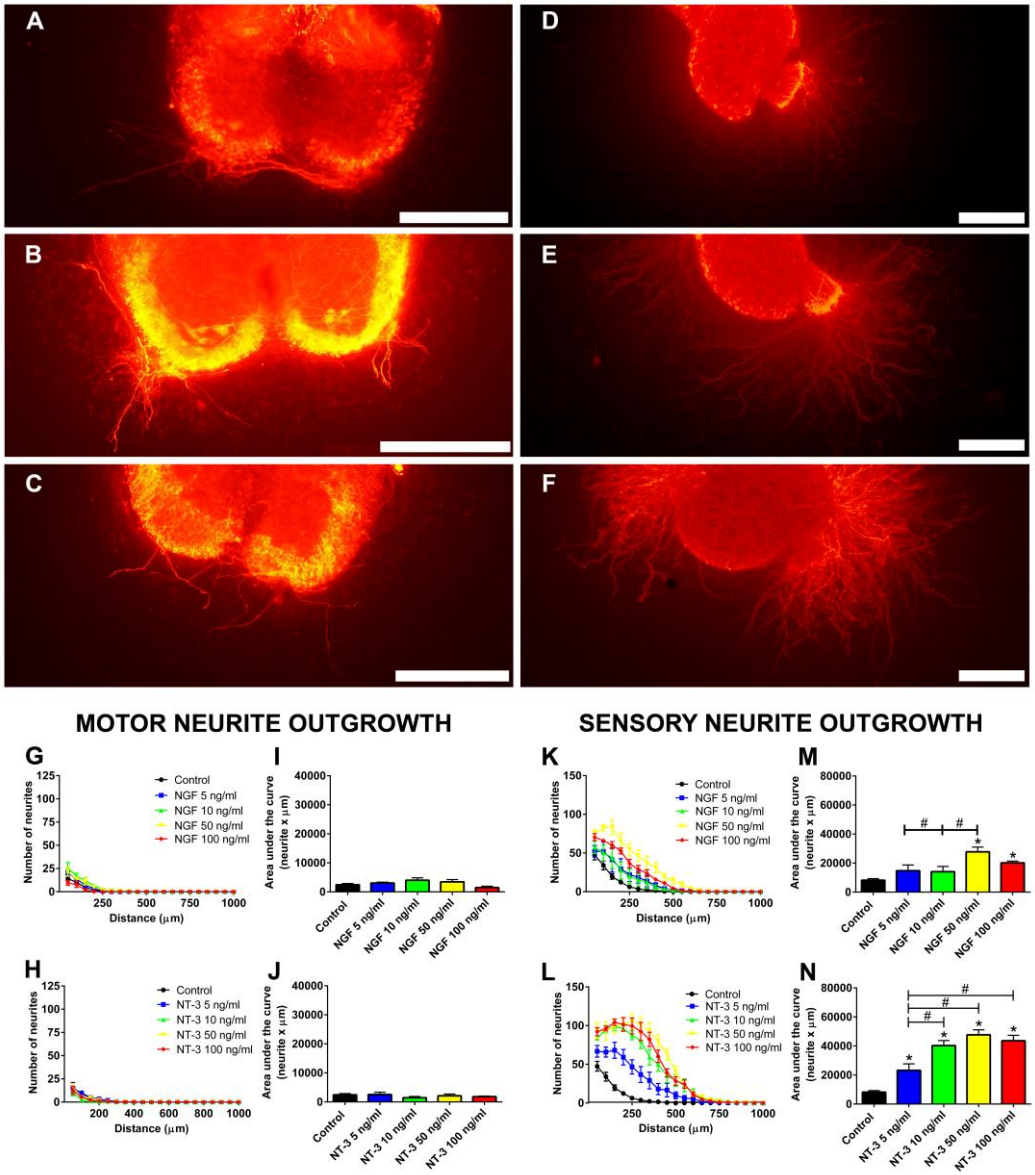

Figure 2. Representative images of RT97 stained neurites from spinal cord slices (A-C) and DRG neurons (D-F) cultured within a 3D collagen matrix alone (A, D), and with addition of 50 ng/ml of NGF (B, E) or NT-3 (C, F). Quantification of the number of neurites grown at increasing distance from the spinal cord slices (G, H) and from DRG body (K, L) after the addition of NGF and NT-3. Plots of the quantified AUC from G, H, K and L graphs for motor (I, J) or sensory (M, N) neurite outgrowth. Data expressed as mean ± SEM. *p<0.05 vs control; # p<0.05. Scale bar 200 μm (A-F).

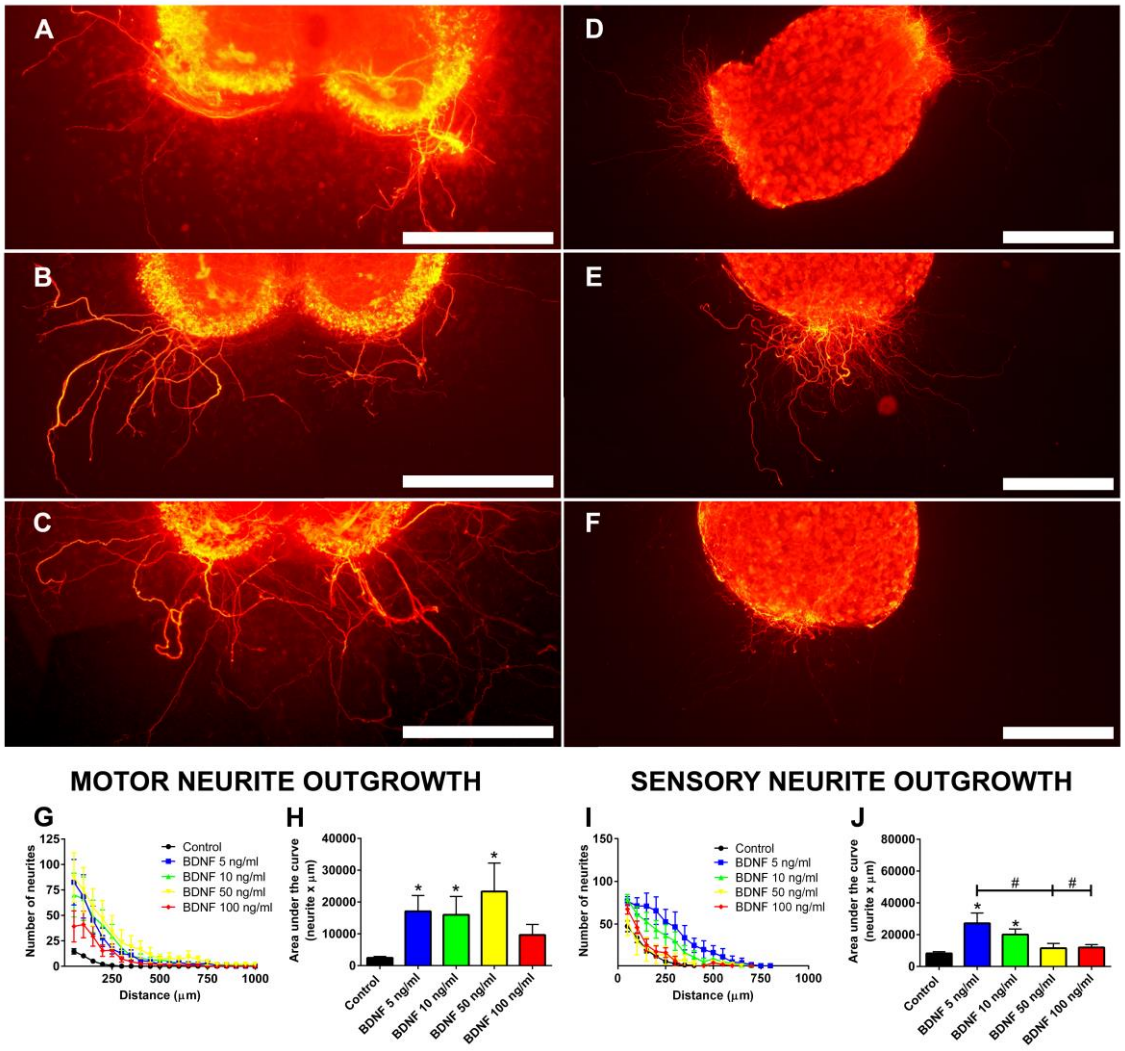

Figure 3. Representative images of RT97 stained neurites from spinal cord slices (A-C) and DRG neurons (D-F) cultured within a 3D collagen matrix alone (A, D), and with addition of 10 ng/ml (B, E) and 50 ng/ml of BDNF (C, F). Quantification of the number of neurites grown at increasing distance from the cord slices (G) and from DRG body (I) after the addition of different doses of BDNF. Plots of the quantified area under each curve from G and I graphs for motor (H) or sensory neurite outgrowth (J). Data expressed as mean ± SEM. *p<0.05 vs control; # p<0.05. Scale bar 200 µm (A-F).

3.2. NGF and NT-3 selectively enhance sensory regeneration in vitro but not in vivo

Observation of cultures of SC slices and DRG with NGF and NT-3 (Fig. 2 A-F) revealed they were the most selective tested factors for sensory regeneration. Motor neurite outgrowth was not affected by NGF or NT-3 at any of the concentrations compared to the control cultures (Fig. 2 G-J). In contrast, addition of NGF (Fig. 2K, M) or NT-3 (Fig. 2L, N) in the collagen matrix yielded more sensory neurites at different distances and larger values of the AUC in comparison with controls (Fig. 2 M, N), being the 50 ng/ml dose the one that showed the highest values for NGF and NT-3. In agreement with previous studies (Terenghi, 1999) NGF and NT-3 are able to promote exclusively

sensory neurite outgrowth, without enhancing motor axon regeneration from SC slices. This selective effect may be explained because motoneurons do not express TrkA receptor and after nerve injury the expression levels of TrkC receptor remain relatively unchanged (Boyd and Gordon, 2003).

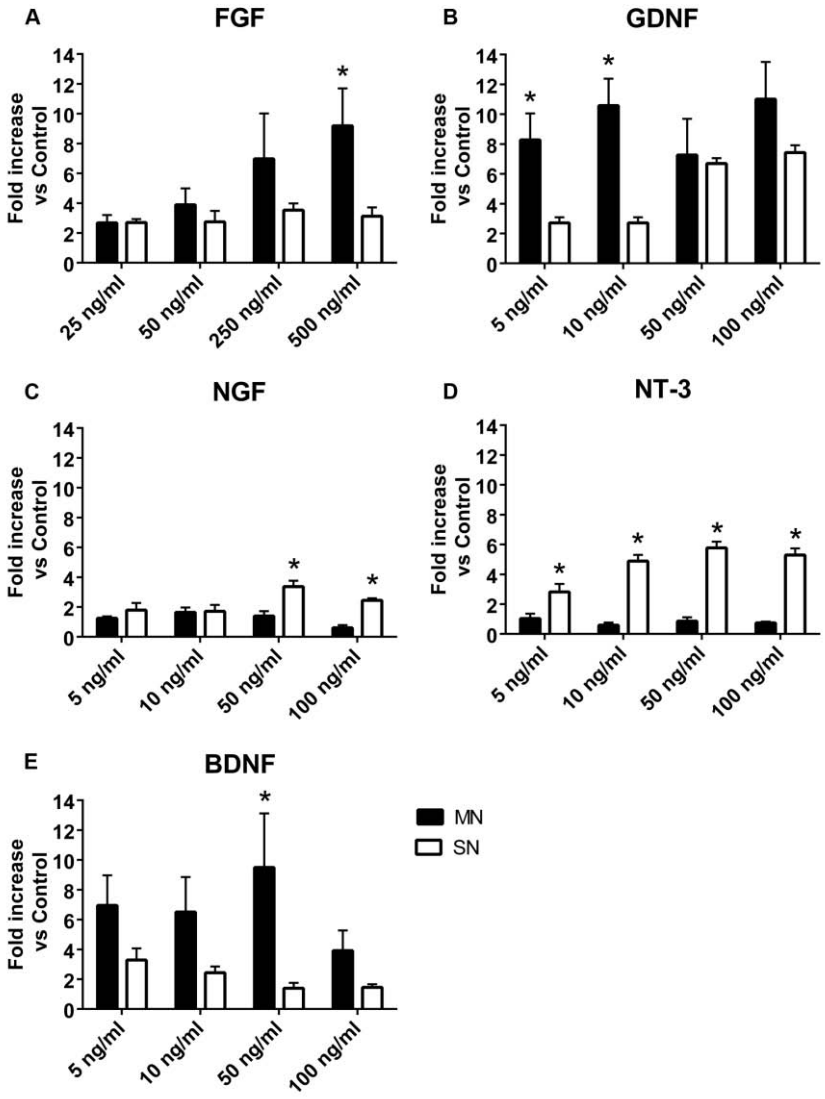

Figure 4. Histogram of the fold increase of the AUC for motor and sensory neurite outgrowth induced by FGF (A), GDNF (B), NGF (C), NT-3 (D) and BDNF (E) at the concentrations tested compared to the control collagen matrix. Data expressed as mean ± SEM. *p<0.05.

Taking advantage of the differential promotion of sensory but not motor neurite outgrowth, these NTF were tested in vivo in a model of nerve regeneration. 20 days after section of the sciatic nerve and tube repair, all the rats showed evidence of axonal regeneration, as judged by the retrograde labeling of motor (Fig. 5A,B) and sensory (Fig. 5C,D) regenerated neurons. Concerning motor axon regeneration, both NGF and

NT-3 groups unexpectedly improved motor axon regeneration at all doses (Fig. 5E). Although some studies have already described that NGF administration in a fibrin depot improves motor regeneration (Jubran and Widenfalk, 2003), the common belief is that NGF and NT-3 are pro-sensory NTFs (Allodi et al., 2012). Regarding sensory neurons, as expected, NGF and NT-3 groups showed a significantly increased number of regenerated neurons at all doses, except the lowest of NT-3 (1 µg/mL) (Fig. 5F).

Thus, in vivo results with NGF and NT-3 seem to contravene the in vitro observations where only sensory neurite outgrowth was improved. Differences between the in vitro and in vivo models should be first taken into account. Organotypic cultures are multicellular in vitro models, in which neurons remain embedded in contact with accompanying glial cells. Although Schwann cells and fibroblasts migrate outside the slice in organotypic cultures interacting with and giving structural support to the newborn neurites (Allodi et al., 2011), the amount and activation of these cells is probably different from in vivo conditions in which cells from the denervated distal stump migrate inside the tube to stimulate nerve regeneration. In addition, the recruitment of hematogenous inflammatory cells that plays an important role during Wallerian degeneration, is absent in vitro.

After nerve damage, levels of NGF mRNA rise rapidly in the nonneuronal cells of the damaged nerve (Meyer et al., 1992). It is also known that NGF and other neurotrophins interact not only with axons but also with Schwann cells and fibroblasts within the regenerative microenvironment (Matsuoka et al., 1991). Taking into account that Schwann cells de-differentiate after injury and change their phenotype to a pro-regenerative state (Jessen and Mirsky, 2005) secreting a variety of tropic and trophic molecules, both NGF and NT-3 might indirectly enhance indiscriminately axonal regeneration by stimulating Schwann cell proliferation and release of other NTFs such as BDNF or GDNF (Acheson et al., 1991; Klein et al., 1991).

3.3. BDNF selectively enhances motor regeneration in vitro and in vivo

BDNF was the NTF showing the most selective effect on motoneuron regeneration in vitro (Fig. 3). Addition of BDNF to the medium (Fig. 3 B, C) showed an increase in motor neurite outgrowth in comparison with control values (Fig. 3G), being the 50 ng/ml

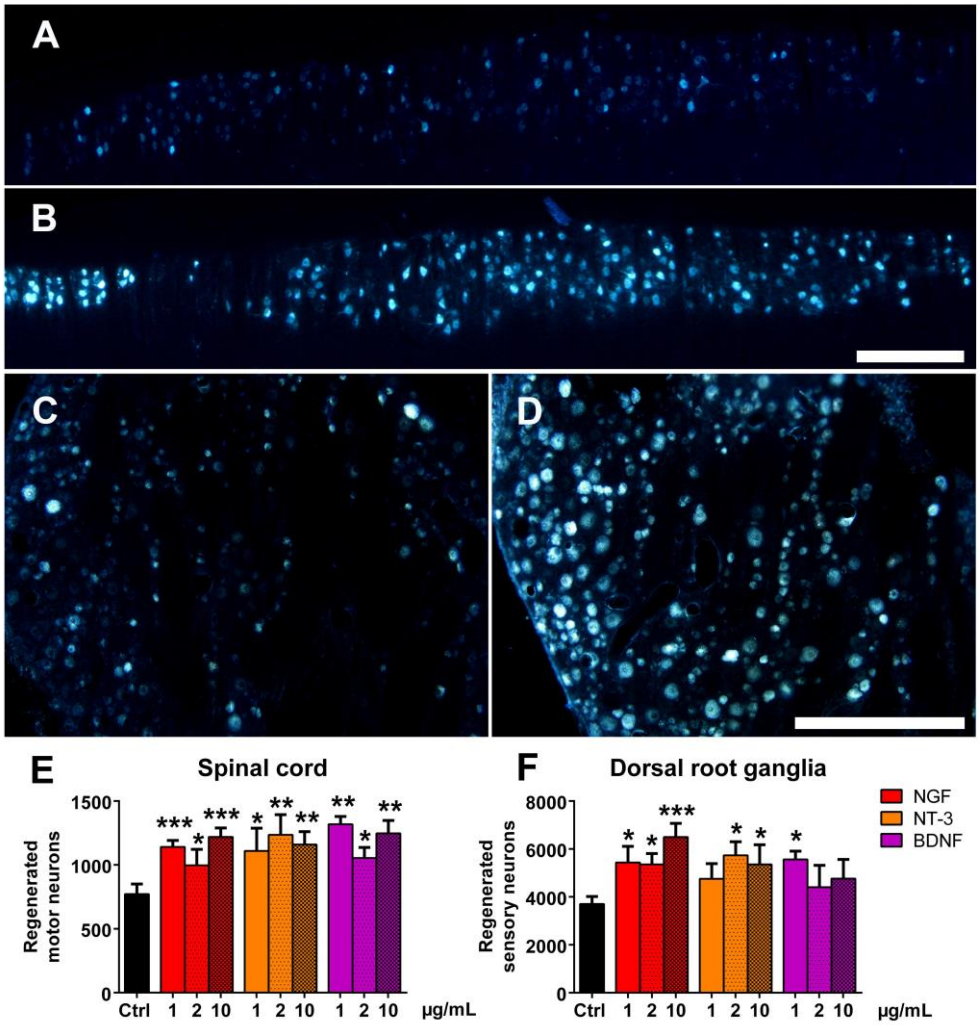

Figure 5. Representative micrographs of neurons retrolabeled with FG in the spinal cord (A,B) and DRG (C,D) growing in control conditions (A,C), with 10 µg/ml of BDNF (B) 10 µg/ml of NGF (D). Histogram of the number of regenerated motor (E) and sensory (F) neurons after ciatic nerve section and conduit repair with NGF, NT-3 and BDNF at diferent doses. Data expressed as mean ± SEM. *p<0.05. Scale bar 500 µm (A-D).

the concentration that produced the highest values in terms of neurites length (Fig. 3G) and AUC (Fig. 3H). Interestingly, a higher concentration of 100 ng/ml did not promote neurite growth, suggesting a window of dose-effect. On the other hand, BDNF slightly enhanced sensory neurite outgrowth only at low concentrations of 5 and 10 ng/ml (Fig. 3E, I, J) while higher levels reverted this increase. These results suggest a preferential motor profile for BDNF with a high dose of BDNF (50ng/ml) increasing about 10 fold the growth of motor neurites from SC slices but without effect on DRG neurite outgrowth (Fig. 4E).

Following the in vitro results, we tested if BDNF could selectively promote motor axon regeneration in vivo after nerve section and tube repair. Quantification of retrolabeled neurons revealed that 20 days after surgery all the groups treated with BDNF had higher number of regenerated motor neurons than the control group (Fig. 5E). In parallel to the in vitro results, BDNF only increased the number of regenerated sensory neurons at a low dose (1 μg/mL) while higher doses gave similar result to the control group (Fig. 5F).

The BDNF receptor TrkB is expressed constitutively in motoneurons and its levels increase after injury (Boyd and Gordon, 2003), while intact sensory neurons show low levels of TrkB, although its expression is also upregulated after injury (Karchewski et al., 2002). Similarly, the endogenous expression of BDNF is also upregulated in the distal stump after nerve injury (Boyd and Gordon, 2003). On the other hand, it has been suggested that BDNF upregulates TrkB expression at low doses (Ferrer et al., 1998), but high levels of this neurotrophin may downregulate this receptor in neuronal cells (Frank, 1996). Thus, it seems that BDNF can modulate motor axon growth under a bimodal profile. The low doses upregulate TrkB receptors and enhance both sensory and motor neurite growth promoting the expression of growth-associated genes such as tubulin or GAP-43 (Kobayashi et al., 1997). In contrast, high doses would downregulate TrkB receptors, minimizing the effect of BDNF on sensory neurites or even promoting an inhibitory effect via activation of the p75 receptor (Boyd and Gordon, 2001).

5. Conclusion

The results of this study provide a comparative analysis of the optimal doses for stimulating motor and sensory axonal regeneration both in vitro and in vivo for different NTFs (GDNF, FGF-2, NGF, NT-3 and BDNF). Optimal concentrations of GDNF and FGF-2 show the highest potentiation of both motor and sensory neuron regeneration. On the other hand, NGF and NT-3 show a selective enhancement of sensory neurite growth in vitro that is lost in our in vivo model. Finally, BDNF at selected doses selectively promotes motor axonal growth both in vitro and in vivo.

Acknowledgments

This research was supported by the European Union FP7-NMP project MERIDIAN under contract number 280778, and FPT-ICT project NEBIAS under contract number 611687, FEDEER funds, and TERCEL (RD12/0019/0011) and CIBERNED (CB06/05/1105) funds from the Instituto de Salud Carlos III of Spain. The authors thank the technical help of Monica Espejo and Marta Morell.

6. References

Acheson, A., Barker, P.A., Alderson, R.F., Miller, F.D., Murphy, R.A., 1991. Detection of brain-derived neurotrophic factor-like activity in fibroblasts and Schwann cells: inhibition by antibodies to NGF. Neuron 7, 265–275. doi:10.1016/0896-6273(91)90265-2

Al-Ali, H., Beckerman, S., Bixby, J.L., Lemmon, V.P., 2016. In vitro models of axon regeneration. Exp. Neurol. doi:10.1016/j.expneurol.2016.01.020

Allodi, I., Casals-Díaz, L., Santos-Nogueira, E., Gonzalez-Perez, F., Navarro, X., Udina, E., 2013. FGF-2 Low Molecular Weight Selectively Promotes Neuritogenesis of Motor Neurons In Vitro. Mol. Neurobiol. 47, 770–781. doi:10.1007/s12035-012-8389-z

Allodi, I., Guzmán-Lenis, M.-S., Hernàndez, J., Navarro, X., Udina, E., 2011. In vitro comparison of motor and sensory neuron outgrowth in a 3D collagen matrix. J. Neurosci. Methods 198, 53–61. doi:10.1016/j.jneumeth.2011.03.006

Allodi, I., Udina, E., Navarro, X., 2012. Specificity of peripheral nerve regeneration : Interactions at the axon level. Prog. Neurobiol. 98, 16–37.

Boyd, J., Gordon, T., 2003. Neurotrophic factors and their receptors in axonal regeneration and functional recovery after peripheral nerve injury. Mol. Neurobiol. 27, 277–324. doi:10.1385/MN:27:3:277

Boyd, J., Gordon, T., 2002. A dose-dependent facilitation and inhibition of peripheral nerve regeneration by brain-derived neurotrophic factor. Eur. J. Neurosci. 15, 613–626. doi:10.1046/j.1460-9568.2002.01891.x

Boyd, J., Gordon, T., 2001. The neurotrophin receptors, trkB and p75, differentially regulate motor axonal regeneration. J. Neurobiol. 49, 314–325. doi:10.1002/neu.10013

Brushart, T.M., 1988. Preferential Axons Reinnervation of Motor Nerves by Regenerating Motor 8.

Ferrer, I., Ballabriga, J., Marti, E., Perez, E., Alberch, J., Arenas, E., 1998. BDNF up-regulates TrkB protein and prevents the death of CA1 neurons following transient forebrain ischemia. Brain Pathol 8, 253–261.

Frank, L., 1996. BDNF down-regulates neurotrophin responsiveness, TrkB protein and TrkB mRNA levels in cultured rat hippocampal neurons. Eur. J. Neurosci. 8, 1220–1230. doi:10.1111/j.1460-9568.1996.tb01290.x

Gundersen, H.J., 1986. Stereology of arbitrary particles. A review of unbiased number

and size estimators and the presentation of some new ones, in memory of William R. Thompson. J. Microsc. 143, 3–45. doi:10.1111/j.1365-2818.1986.tb02764.x

Jessen, K.R., Mirsky, R., 2005. The origin and development of glial cells in peripheral nerves. Nat Rev Neurosci 6, 671–682. doi:nrn1746 [pii]\r10.1038/nrn1746

Jubran, M., Widenfalk, J., 2003. Repair of peripheral nerve transections with fibrin sealant containing neurotrophic factors. Exp. Neurol. 181, 204–212. doi:10.1016/S0014-4886(03)00041-4

Karchewski, L. a., Gratto, K. a., Wetmore, C., Verge, V.M.K., 2002. Dynamic patterns of BDNF expression in injured sensory neurons: differential modulation by NGF and NT-3. Eur. J. Neurosci. 16, 1449–1462. doi:10.1046/j.1460-9568.2002.02205.x

Kim, H.J., Hwang, J.J., Behrens, M.M., Snider, B.J., Choi, D.W., Koh, J.Y., 2003. TrkB mediates BDNF-induced potentiation of neuronal necrosis in cortical culture. Neurobiol. Dis. 14, 110–119. doi:10.1016/S0969-9961(03)00103-7

Klein, R., Nanduri, V., Jing, S., Lamballe, F., Tapley, P., 1991. The trkB Tyrosine Protein Kinase Is a Receptor for Brain-Derived Neurotrophic Factor and Neurotrophin-3. Cell 66, 395–403.

Kobayashi, N.R., Fan, D.P., Giehl, K.M., Bedard, a M., Wiegand, S.J., Tetzlaff, W., 1997. BDNF and NT-4/5 prevent atrophy of rat rubrospinal neurons after cervical axotomy, stimulate GAP-43 and Talpha1-tubulin mRNA expression, and promote axonal regeneration. J. Neurosci. 17, 9583–9595.

Madison, R.D., Archibald, S.J., Brushart, T.M., 1996. Reinnervation accuracy of the rat femoral nerve by motor and sensory neurons. J. Neurosci. 16, 5698–5703.

Markus, A., Patel, T.D., Snider, W.D., 2002. Neurotrophic factors and axonal growth. Curr. Opin. Neurobiol. 12, 523–531. doi:10.1016/S0959-4388(02)00372-0

Matsuoka, I., Meyer, M., Thoenen, H., 1991. Cell-type-specific regulation of nerve growth factor (NGF) synthesis in non-neuronal cells: comparison of Schwann cells with other cell types. J. Neurosci. 11, 3165–77.

Meyer, M., Matsuoka, I., Wetmore, C., Olson, L., Thoenen, H., 1992. Enhanced synthesis of brain-derived neurotrophic factor in the lesioned peripheral nerve: Different mechanisms are responsible for the regulation of BDNF and NGF mRNA. J. Cell Biol. 119, 45–54. doi:10.1083/jcb.119.1.45

Parra, L.M., Hartmann, M., Schubach, S., Li, Y., Herrlich, P., Herrlich, A., 2015. Distinct Intracellular Domain Substrate Modifications Selectively Regulate Ectodomain

Cleavage of NRG1 or CD44. Mol. Cell. Biol. 35, 3381–3395. doi:10.1128/MCB.00500-15

Piquilloud, G., Christen, T., Pfister, L. a, Gander, B., Papaloïzos, M.Y., 2007. Variations in glial cell line-derived neurotrophic factor release from biodegradable nerve conduits modify the rate of functional motor recovery after rat primary nerve repairs. Eur. J. Neurosci. 26, 1109–17. doi:10.1111/j.1460-9568.2007.05748.x

Robinson, G.A., Madison, R.D., 2005. Manipulations of the mouse femoral nerve influence the accuracy of pathway reinnervation by motor neurons. Exp. Neurol. 192, 39–45. doi:10.1016/j.expneurol.2004.10.013

Robinson, G.A., Madison, R.D., 2004. Motor neurons can preferentially reinnervate cutaneous pathways. Exp. Neurol. 190, 407–413. doi:10.1016/j.expneurol.2004.08.007

Ruiz, G., Ceballos, D., Baños, J.-E., 2004. Behavioral and histological effects of endoneurial administration of nerve growth factor: possible implications in neuropathic pain. Brain Res. 1011, 1–6. doi:10.1016/j.brainres.2004.02.001

Santos, D., Giudetti, G., Micera, S., Navarro, X., del Valle, J., 2016. Focal release of neurotrophic factors by biodegradable microspheres enhance motor and sensory axonal regeneration in vitro and in vivo. Brain Res. 1636, 93–106. doi:10.1016/j.brainres.2016.01.051

Tannemaat, M.R., Eggers, R., Hendriks, W.T., de Ruiter, G.C.W., van Heerikhuize, J.J., Pool, C.W., Malessy, M.J. a, Boer, G.J., Verhaagen, J., 2008. Differential effects of lentiviral vector-mediated overexpression of nerve growth factor and glial cell line-derived neurotrophic factor on regenerating sensory and motor axons in the transected peripheral nerve. Eur. J. Neurosci. 28, 1467–79. doi:10.1111/j.1460-9568.2008.06452.x

Terenghi, G., 1999. Peripheral nerve regeneration and neurotrophic factors. J. Anat. 194, 1–14.

Torres-Espín, A., Allodi, I., Santos, D., González-Pérez, F., Udina, E., del Valle, J., Navarro, X., 2016. Analysis of axonal growth in organotypic neural cultures.

Torres-Espín, A., Santos, D., González-Pérez, F., del Valle, J., Navarro, X., 2014. Neurite-J: An Image-J plug-in for axonal growth analysis in organotypic cultures. J. Neurosci. Methods 236, 26–39. doi:10.1016/j.jneumeth.2014.08.005

Tukmachev, D., Forostyak, S., Zaviskova, K., Koci, Z., Vackova, I., Vyborny, K., Sandvig, I., Sandvig, A., Medberry, C., Badylak, S., Sykova, E., Kubinova, S.,

2016. Injectable extracellular matrix hydrogels as scaffolds for spinal cord injury repair. Tissue Eng. Part A 22, 306–317. doi:10.1089/ten.TEA.2015.0422

Valero-Cabré, A., Navarro, X., 2002. Functional Impact of Axonal Misdirection after Peripheral Nerve Injuries followed by Graft or Tube Repair. J. Neurotrauma 19, 1475–1485. doi:10.1089/089771502320914705

Verdú E, Labrador RO, Rodríguez FJ, Ceballos D, Forés J, N.X., 2002. Alignment of collagen and laminin-containing gels improve nerve regeneration within silicone tubes. Restor Neurol Neurosci. 20, 169–180.

Preferential enhancement of sensory and motor axon regeneration by combining extracellular matrix components with neurotrophic factors

Daniel Santos* [1,2], Francisco Gonzalez-Perez* [1,2], Guido Giudetti [3], Silvestro Micera [3,4], Esther Udina [1,2], Jaume del Valle [1,2], Xavier Navarro [1,2]

[1] Institute of Neurosciences and Department of Cell Biology, Physiology and Immunology, Universitat Autònoma de Barcelona

[2] Centro de Investigación Biomédica en Red sobre Enfermedades Neurodegenerativas (CIBERNED), Bellaterra, Spain

[3] The BioRobotics Institute, Scuola Superiore Sant'Anna, Viale Rinaldo Piaggio 34, 56025 Pontedera, Italy

[4] Translational Neural Engineering Laboratory, Center for Neuroprosthetics and Institute of Bioengineering, School of Engineering, Ecole Polytechnique Federale de Lausanne (EPFL), Lausanne, Switzerland

*Both authors contributed equally to the work

Corresponding author: Dr. Xavier Navarro, Unitat de Fisiologia Mèdica, Facultat de Medicina, Universitat Autònoma de Barcelona, E-08193 Bellaterra, Spain. E-mail: xavier.navarro@uab.cat

Running title: Combined effects of ECM and NTFs on motor and sensory axon regeneration

Abstract

After peripheral nerve injury, motor and sensory axons are able to regenerate but inaccuracy of target reinnervation leads to poor functional recovery. Extracellular matrix (ECM) components and neurotrophic factors (NTFs) exert their effect on different neuronal populations creating a suitable environment to promote axonal growth. In the present study, we assess the selective effects of combining different ECM components with NTFs on regeneration of motor and sensory axons and reinnervation of the target organs. We observed *in vitro* that addition of laminin and NGF/NT3 (LM + NGF/NT3) within a collagen matrix selectively enhanced neurite outgrowth of dorsal root ganglia (DRG) neurons, whereas addition of fibronectin and BDNF (FN + BDNF) mainly enhanced motor axon outgrowth from organotypic spinal cord slices (SC). For *in vivo* studies, the rat sciatic nerve was transected and repaired with a silicone tube filled with a collagen matrix, enriched with laminin, fibronectin, laminin with NGF/NT3 encapsulated in PLGA microspheres, or fibronectin with BDNF in PLGA microspheres. By applying retrograde tracers distally to the tube 20 days after the surgery, we found that the group with the collagen matrix enriched with laminin and encapsulated NGF/NT3 (LM + MP.NGF/NT3) had the highest number of regenerated sensory neurons, whereas addition of fibronectin and encapsulated BDNF (FN + MP.BDNF) preferentially increased the number of regenerated motor neurons. Moreover, long term results showed that motor functional recovery was improved in FN + MP.BDNF group and sensory functional recovery was improved in LM + MP.NGF/NT3 group. Therefore, our study demonstrates that combining ECM molecules with NTFs may be a good approach to selectively enhance motor and sensory axons regeneration and appropriate tissue reinnervation.

Keywords: neurotrophic factors, extracellular matrix, motor axons, sensory axons, nerve regeneration, reinnervation.

1. Introduction

Peripheral nerves are composed of sensory and motor axons that link peripheral organs with the central nervous system. After peripheral nerve injury, transected axons in the distal stump are disconnected from the neuronal body and undergo Wallerian degeneration, thus, leading to denervation of peripheral organs (Hall, 2005). Axotomized neurons switch from a neurotransmission state to a growth state, and non-neuronal cells in the distal stump undergo activation and dedifferentiation to sustain nerve regeneration (Allodi et al., 2012; Richardson et al., 2009). Despite axons are able to regenerate after a nerve transection, axons grow randomly among the endoneurial tubules in the distal nerve, so that the accuracy of target reinnervation is usually poor, resulting in limited functional recovery (Aldskogius and Molander, 1990; Valero-Cabré and Navarro, 2002; Valero-Cabré et al., 2004; Lundborg, 2003). Therefore, creating a pro-regenerative environment to selectively promote motor and sensory axon regeneration into different branches of the injured nerve may facilitate specific target reinnervation. Furthermore, selective regeneration of different populations could be also useful in the field of neuroprosthetics, as separating motor axons from sensory axons in mixed nerves will improve functionally selective recording and stimulation (Clements et al., 2013; Lotfi et al., 2011).

Previous studies demonstrate that neurotrophic factors (NTFs) and extracellular matrix (ECM) components secreted by Schwann cells of different phenotypes, and also factors released from target organs play a role in promoting regeneration of different axonal populations and may improve subsequent accurate reinnervation (Brushart et al., 2013; Höke et al., 2006; Martini and Brushart, 1994; Robinson and Madison, 2004). The activation of the regenerative neuronal state and the generation of a pro-regenerating environment involves the upregulation and secretion of ECM components, such as collagen type IV, laminin and fibronectin, by non-neuronal cells, and the secretion of different NTFs, such as nerve growth factor (NGF), brain-derived neurotrophic factor (BDNF), neurotrophin-3 (NT3), among others (Allodi et al., 2012). ECM components interact with integrin heterodimer receptors that are highly expressed in growth cones and non-neuronal cells, both during development and after injury (Gardiner, 2011; Lemons and Condic, 2008), promoting axonal guidance, cell adhesion and migration. For instance, laminin substrates enhance elongation of sensory neurites in vitro when compared to collagen or fibronectin containing scaffolds, whereas fibronectin substrates promote neurite elongation of motor neurons from spinal cord slices in vitro (Gonzalez-Perez et al., 2015; Plantman et al., 2008). On the other hand, the interaction between NTFs and their different receptors, such as Trk/p75 receptors or GDNFR/RET receptors, promotes survival and

axonal regeneration of different neuronal populations. For example, NGF selectively promotes sensory neurite outgrowth, whereas BDNF preferentially increases motor neurite outgrowth in vitro (Allodi et al., 2011).

In the present study we tested whether the combination of different NTFs and ECM components was able to produce synergistic and selective pro-regenerative effects on either motor or sensory neurons in vitro, using organotypic cultures, and also in vivo after peripheral nerve injury in the adult animal.

2. Materials and methods

2.1. Ethics statement

In vitro (procedure #1963) and in vivo (procedure #1162M) experimental procedures were approved by the ethical committee of the Universitat Autonoma de Barcelona in accordance with the European Communities Council Directive 2010/63/EU. Adult rats were anaesthetized with ketamine/xylazine (90/10 mg/kg i.p.). Rats were euthanized by pentobarbital sodium overdose (200 mg/kg i.p.) following AVMA Guidelines on Euthanasia (Leary et al., 2013).

2.2. In vitro study on organotypic cultures

Organotypic cultures were prepared as previously described in detail (Torres-Espín et al., 2016). Briefly, a 3 mg/ml collagen solution was prepared by mixing rat tail collagen type I (#354236, Corning) with PBS (D8537, Sigma) and sodium bicarbonate at 0.3 mg/ml, and diluting 1:10 with basal Eagle's medium (10x, Gibco). NTF enriched substrates were prepared by adding BDNF at 50 ng/ml (Peprotech) or NGF and NT3 (Peprotech) at 25 ng/ml each, and fibronectin (BD Bioscences) or laminin type I (Sigma) to a 20% final volume. Single 30 µl drops of the prepared matrices were deposited on poly-d-lysine (Sigma) coated coverslips, which were placed in Petri dishes or 24-well multidishes (Iwaki, Asahi Technoglass, Chiba, Japan), and kept in the incubator at 37ºC and 5% CO_2 for two hours to induce collagen gel formation. Collagen gel was mixed with PBS (COL) and used as control. Collagen gels were also combined with NGF/NT3 (COL+NGF/NT3) or BDNF (COL+BDNF). Similarly, laminin and fibronectin-enriched gels were combined with PBS (LM and FN, respectively), NGF+NT3 (LM+NGF/NT3 and FN+NGF/NT3, respectively) or BDNF (LM+BDNF and FN+BDNF, respectively; Table 1).

The lumbar spinal cord (SC, n=6-8/group) and dorsal root ganglia (DRG, n=7-8/group) were harvested from 7 days old Sprague–Dawley rats, placed in cold Gey's balanced salt solution (Sigma) enriched with 6 mg/ml glucose and cleaned. SC 350 µm thick slices and DRG explants were placed on gelled collagen droplets, prepared as

indicated above, and covered with a second 30 µl drop. The embedded samples were placed in the incubator for 45 min before adding Neurobasal medium (NB, Life Technologies), supplemented with B27 (Life Technologies), glutamine and penicillin/streptomycin (Sigma).

Table 1. Experimental conditions compared in the in vitro experiments

***In vitro* condition**	**Abbreviation**	**N**	**Description**
Collagen	COL	8	Collagen type I (3 mg/ml) gel
Collagen + NGF/NT3	COL+NGF/NT3	7	Collagen type I (3 mg/ml) gel supplemented with NGF and NT3 (25 + 25 ng/ml)
Collagen + BDNF	COL+BDNF	6	Collagen type I (3 mg/ml) gel supplemented with BDNF (50 ng/ml)
Laminin	LM	8	Collagen type I (3 mg/ml) gel containing 20% laminin type I
Laminin + NGF/NT3	LM+NGF/NT3	7	Collagen type I (3 mg/ml) gel containing 20% laminin type I and NGF+NT3 (25 + 25 ng/ml)
Laminin + BDNF	LM+BDNF	7	Collagen type I (3 mg/ml) gel containing 20% laminin type I and BDNF (50 ng/ml)
Fibronectin	FN	6	Collagen type I (3 mg/ml) gel containing 20% fibronectin
Fibronectin + NGF/NT-3	FN+NGF/NT3	6	Collagen type I (3 mg/ml) gel containing 20% fibronectin and NGF+NT3 (25 + 25 ng/ml)
Fibronectin + BDNF	FN+BDNF	7	Collagen type I (3 mg/ml) gel containing 20% fibronectin and BDNF (50 ng/ml)

SC slices were cultured for 4 days, and DRG explants for 2 days. Then, cultures were fixed with 4% paraformaldehyde in PBS for 30 min, and incubated for 48 h with primary antibody mouse RT97 (1:200, Developmental Studies Hybridoma Bank) at 4ºC. After washes, the sections were incubated with secondary antibody AF594 conjugated donkey anti-mouse (1:200, Life Technologies) overnight at 4ºC. Samples were mounted on slides with Mowiol containing DAPI (1:10000, Sigma) nuclear counterstain. Cultures were visualized with an Olympus BX51 fluorescence microscope, images of different areas were taken with Cell A software (Olympus) and merged using Adobe Photoshop CS3 (Adobe System). To analyze the length of neurites, ImageJ software (NIH, available at http://rsb.info.nih.gov/ij/) resolution

parameters were fixed and the three longest neurites were followed from the ventral horn (spinal cord) or ganglion boundary (DRG) to their ending projections. Whole culture images were analyzed with the Neurite-J plug-in (Torres-Espín et al., 2014) for ImageJ software, and the number of neurites grown at different distances from the explant was compared between sets of cultures. To facilitate the visualization of differences between groups, the area under the curve of each group was converted to a bar plot.

2.3. In vivo study of peripheral nerve regeneration

Female Sprague-Dawley rats (250–300 g) were used for the in vivo studies. They were kept on standard laboratory conditions with a light-dark cycle of 12:12 h and *ad libitum* access to food and tap water. All efforts were made to minimize pain and animal discomfort during surgery and treatments.

Animals were anaesthetized with ketamine/xylacine, the sciatic nerve was exposed at the midthigh and sectioned 90 mm from the tip of the third toe, and a nerve portion resected. A silicone tube was then sutured with 10-0 monofilament sutures to each nerve stump leaving a 6 mm gap between both nerve ends for the short term study or 8 mm gap for the long term study. Animals were kept for 20 days post-injury (dpi) (short term) or 75 dpi (long term) to allow axonal regeneration before testing.

NGF, NT3, and BDNF were encapsulated in microspheres (MPs) as previously described (Giudetti et al., 2014) and added to a collagen solution to reach a final concentration of 2 µg/ml for BDNF and 1 µg/ml for NGF and NT3 respectively. Each preparation of NTF was then added to ECM solutions prepared as for the cultures, i.e. collagen at 3 mg/ml, collagen supplemented with laminin 20% (V/V), and collagen supplemented with fibronectin 20% (V/V). Silicone tubes 8 or 10 mm long with an internal diameter of 2 mm were filled with one of the mixtures containing different combinations of substrates and NTF. In order to promote fibril alignment, the collagen solution was left to gel vertically for 12 hours before surgery (Verdú et al., 2002). Therefore, there were 5 experimental groups for short and long term experiments (n=6 per group). Collagen group (COL) used as control group, laminin (LM), fibronectin (FN), laminin combined with encapsulated NGF/NT3 (LM+MP.NGF/NT3) and fibronectin combined with encapsulated BDNF (FN+MP.BDNF) (Table 2).

Table 2. Experimental groups for in vivo experiments

***In vivo* condition**	**Abbreviation**	**N**	**Description**
Collagen	COL	6	Collagen type I (3 mg/ml) gel
Laminin	LM	6	Collagen type I (3 mg/ml) gel containing 20% laminin type I
Laminin + NGF/NT3	LM + MP.NGF/NT3	6	Collagen type I (3 mg/ml) gel containing 20% laminin type I and NGF+NT3 (1 + 1 µg/ml) encapsulated in PLGA microspheres
Fibronectin	FN	6	Collagen type I (3 mg/ml) gel containing 20% fibronectin
Fibronectin + BDNF	FN + MP.BDNF	6	Collagen type I (3 mg/ml) gel containing 20% fibronectin and 2 µg/ml of BDNF encapsulated in PLGA microspheres

2.4. Retrograde labeling and neuronal counting

To quantify motor and sensory regenerated neurons at short term (20 dpi), rats were anaesthetized with ketamine/xylacine, the sciatic nerve was exposed and transected 8 mm distal to the distal end of the silicone tube. The tip of the severed nerve was soaked into 5 µl of Fluorogold (FG; 5%; Fluorochrome Inc.) for 1 hr in a vaseline well. After retrieval of the well, the area was rinsed with saline to clean any remnants of the tracer and the wound sutured in planes. Similarly, for the long term study (75 dpi) FG was also applied to the tibial nerve at the ankle level. After tracer application, animals were allowed to survive for 7 days for accumulation of the tracer in the soma of the spinal motoneurons and the DRG sensory neurons. Then, rats were deeply anesthetized and transcardially perfused with 4% paraformaldehyde in PBS. The lumbar segment (L3-L6) of the SC and the L4 and L5 DRG were removed, postfixed at 4ºC in the same fixative solution for 1h and transferred to 30% sucrose in PBS. The SC and DRG were cut in a cryostat longitudinally in 40 and 20 µm thick sections respectively, mounted on slides, heated at 35ºC for 1h and stored at -20ºC in the dark. Finally, sections were observed with an Olympus BX51 fluorescence microscope under UV light and the number of labeled neurons was counted in every third section following the fractionator principle (Gundersen, 1986).

2.5. Assessment of muscle reinnervation

Functional reinnervation of target muscles was assessed at 7, 30, 45, 60 and 75 dpi by means of nerve conduction tests. Animals were anesthetized with ketamine/xylacine and the sciatic nerve was stimulated by transcutaneous electrodes placed at the sciatic notch. The compound muscle action potential (CMAP) of tibialis

anterior (TA) and plantar interosseus muscles (PL) was recorded using monopolar needle electrodes placing the active one in the muscle belly and the reference in the fourth toe (Valero-Cabré and Navarro, 2002). The amplitude and the latency of the M-wave were measured. Values of the contralateral intact limb were used as control. During the tests, the rat body temperature was maintained by means of a thermostated warming flat coil.

2.6. Assessment of skin nociceptive reinnervation

The progression of nociceptive reinnervation of the hindpaw was assessed by means of the pinprick test and thermal sensitivity at 7, 30, 45 60 and 75 dpi. For the pinprick test, animals were gently kept in a cloth with the sole of the injured paw facing upward, and the skin was stimulated with a needle progressively from proximal to distal at specific sites of the lateral side of the hindpaw plantar surface (Cobianchi et al., 2014). Positive responses were taken as sign of skin functional reinnervation and recorded only when clear pain reaction (as fast withdrawal) was triggered by the stimulation. A composite score was calculated as the mean number of responses per group at each day of testing.

Thermal sensitivity was assessed with a Plantar test algesimeter (Ugo Basile). Rats were placed into a plastic box with an elevated plexiglass floor. The beam of a lamp was pointed to the lateral part in the hindpaw plantar surface. Intensity was set to low power (40 mW/cm^2) with a heating rate of 1°C/s to elicit activation of unmyelinated fibers. A cutoff time for the stimuli was set at 20 seconds to prevent tissue damage. Heat pain threshold was calculated as the mean of 3 trials per test site, with a 5-minute resting period between each trial and expressed as the latency (in seconds) of paw withdrawal response.

2.7. Evaluation of skin and sweat gland reinnervation

For assessing skin reinnervation, plantar pads corresponding to the lateral side were removed at the end of the functional follow-up. Cryotome sections 60 µm thick were processed for immunolabeling against protein gene product (PGP) 9.5 (rabbit; 1:1000; UltraClone), a pan-neuronal marker. Secondary antibodies were conjugated to Cy3. Sections were observed with an Olympus BX51 fluorescence microscope to visualize immunoreactive nerve fibers that had reinnervated the epidermis and the sweat glands (SG). For analysis, images of three sections of each sample were collected with an Olympus DP73 digital camera, the number of intraepidermal nerve fibers (IENFs) was counted in a 1-mm-long segment of the

footpad epidermis and the number of reinnervated SGs in the whole pad was also quantified (Navarro et al., 1997).

2.8. Data analysis

Data are presented as mean ± SEM. Results were statistically analyzed by using GraphPad Prism (GraphPad Software). One and two-way ANOVA followed by Bonferroni's post hoc test for comparison between groups were used. Statistical significance was considered when P value was <0.05.

3. Results

3.1. In vitro effects of combining NTFs and ECM substrates on neurite outgrowth

To study the effect of different combinations of NTFs and ECM components on motor and sensory neurons outgrowth, we first performed an in vitro screening using SC slices and DRG explants. In cultures of SC slices (Fig. 1), addition of FN to the matrix doubled the maximum neurite length whereas addition of LM did not increase it compared to the control COL matrix (Fig. 1J). Addition of BDNF but not of NGF/NT3 to the different substrates enhanced neurite length. Furthermore, the combination of FN+BDNF significantly enhanced maximum neurite length and density of neurites compared to the other single and combined groups. Thus, while groups with either FN or BDNF present an increase in the amount and length of neurites, the combination of the two factors shows a synergistic effect with significant differences with respect to all the other groups. On the other hand, LM or NGF/NT3 alone or combined did not show any improvement (Fig. 1J-L).

In DRG explants (Fig. 2), addition of LM or FN into the collagen matrix similarly enhanced maximum neurite length (Fig. 2J) compared to collagen alone. The addition of NGF/NT3 or BDNF into COL, LM and FN substrates enhanced maximum neurite length compared with COL substrates except COL+BDNF cultures. It is noteworthy that only LM+NGF/NT3 group showed differences in maximum neurite length with respect to all the other culture conditions except with LM+BDNF. The addition of NGF and NT3 enhanced significantly the density of neurites in all the substrates, being LM+NGF/NT3 the most prominent. In contrast, addition of BDNF only promoted neurite growth with LM but not when combined with COL or FN (Fig. 2L).

These results indicate that combination of FN+BDNF shows synergistic effects on motor neurons promoting neurite elongation and arborization, with weaker effect on sensory elongation, whereas LM+NGF/NT3 is the only condition that exhibits a synergistic effects on sensory but not on motor neurons based on the enhancement observed in neurite elongation and arborization.

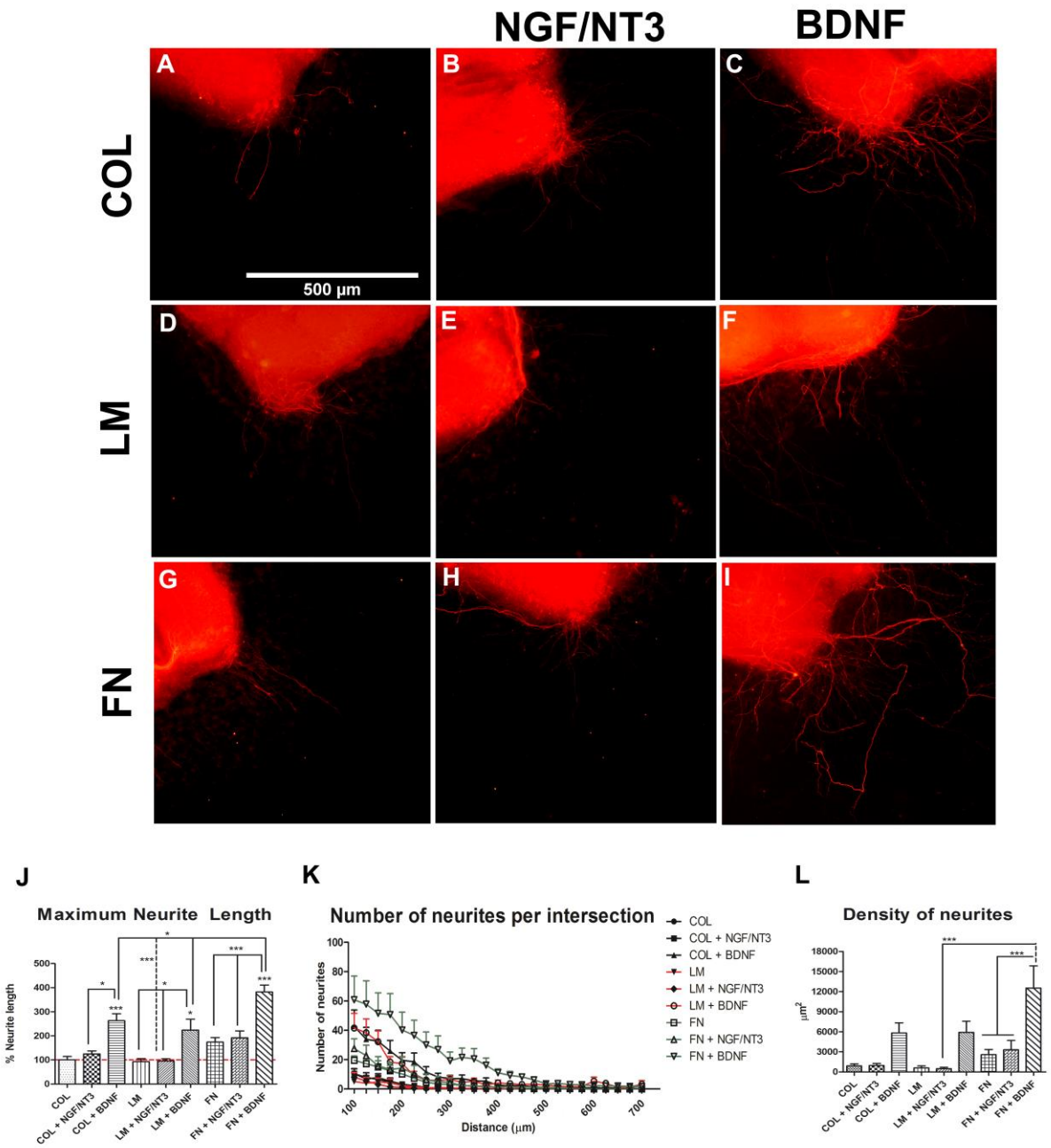

Figure 1. RT97 stained neurites from DRG neurons cultured within a 3D collagen matrix alone, and with addition of NGF/NT3 or BDNF (A-C); with 20% laminin, plus NGF/NT3 or BDNF (D-F); with 20% fibronectin, plus NGF/NT3 or BDNF (G-I). Plots representing maximum neurite length in the different DRG culture conditions (J). Quantification of the number of neurites grown at increasing distance from the DRG body (K). Plots of the quantified area under each curve of K graph (L). Data expressed as mean ± SEM. *p<0.05, **p<0.01 and ***p<0.001.

3.2. In vivo effects of combination of NTF and ECM substrates on nerve regeneration

We performed first an in vivo study in which the sciatic nerve was transected and repaired with silicone tubes filled with matrices composed of COL, LM, LM+MP.NGF/NT3, FN and FN+MP.BDNF to elucidate if the effects found in vitro were relevant also in vivo. The NTFs were encapsulated in PLGA microspheres to allow a sustained release during the time that axons regenerate across the tube (Santos et al., 2016). All the rats showed evidence of axonal regeneration, as judged by the retrograde labeling of motor and sensory neurons with FG (Fig. 3A-F).

Regarding the number of regenerated motor neurons, all groups with addition of ECM and NTFs showed significant differences with respect to the COL group ($p<0.001$, Fig. 3G), being the FN+MP.BDNF group the one with the highest effect, that was also significantly higher compared to LM ($p<0.01$) and LM+MP.NGF/NT3 groups ($p<0.05$). For sensory neurons, the group LM+MP.NGF/NT3 showed the highest number of regenerated neurons, and also groups LM, FN and FN+MP.BDNF had better results than the COL control ($p<0.05$, Fig. 3H).

In the longer term in vivo study, FG retrotracer was applied to the tibial nerve at the ankle at 75 dpi. In this case, no significant differences in the number of regenerated motor neurons were observed between groups (Fig. 3I). However, more regenerated sensory neurons were counted in LM+MP.NGF/NT3 group compared to the other four groups (Fig. 3J).

Despite the preferential effects observed in vitro appear less marked in vivo, these results indicate that FN+MP.BDNF mainly favors motor axon regeneration, whereas LM+MP.NGF/NT3 is more effective to promote sensory axon regeneration. In the long term evaluation, these differences were reduced, likely because most axons have passed the site of tracer application at 75 dpi.

3.3. Combination of FN and BDNF promotes motor functional recovery at long term

We then tested whether this preferential effect is maintained in a long term study and how it could affect muscle reinnervation and functional recovery. For this purpose, we compared groups of rats similar to the short term study but leaving an 8 mm gap between stumps, since this more challenging gap allows to better elucidate differences between groups (Valero-Cabré et al., 2001).

These results suggest that an intratubular matrix containing FN and BDNF promotes motor axon regeneration and reinnervation of target muscles, whereas LM and LM+NGF/NT3 groups showed values similar to the COL control group. The faster

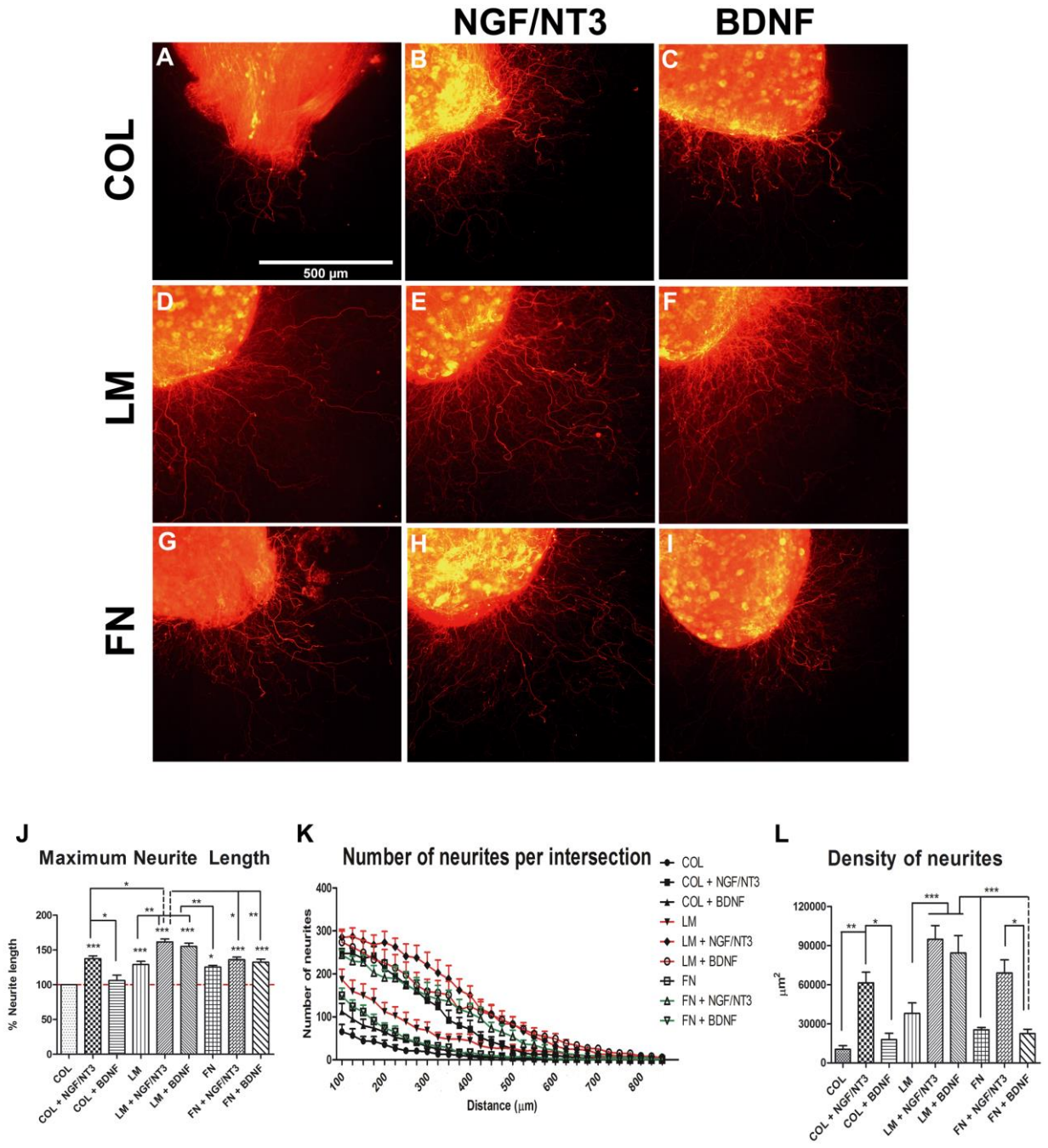

Figure 2. RT97 stained neurites from spinal cord slices cultured within a 3D collagen matrix alone, and with addition of NGF/NT3 or BDNF (A-C); with 20% laminin, plus NGF/NT3 or BDNF (D-F); with 20% fibronectin, plus NGF/NT3 or BDNF (G-I). Plots representing maximum neurite length in the different culture conditions (J). Quantification of the number of neurites grown at increasing distance from the cord slice (K). Plots of the quantified area under each curve of K graph (L). Data expressed as mean ± SEM. *p<0.05 and ***p<0.001.

muscle reinnervation found in group FN+MP.BDNF is of relevance considering the longer distance that have to be regenerated in injured human nerves.

3.4. Combination of LM and.NGF/NT3 promotes sensory functional recovery at long term

In parallel, we assessed sensory functional recovery to mechanical and thermal stimuli in the hindpaw. For the pinprick test, LM and LM+MP.NGF/NT3 groups presented the first positive response at 30 dpi, whereas no response was observed in the other groups at this time point. At later time points, all groups showed positive responses, being LM+MP.NGF/NT3 the only group with significantly higher scores compared to the control group ($p<0.05$; Fig. 4C)

Withdrawal responses to heat stimulation in the plantar test showed similar results than the ones observed for the pinprick. Denervated paws did not respond to the hot stimuli on the lateral region until 45 dpi and at this time point group LM+MP.NGF/NT3 showed a shorter latency compared to control, FN and FN+MP.BDNF groups ($p<0.01$; Fig. 4D), indicating that more sensory fibers arrived to the plantar skin of the paw. However, all the groups showed similar latency at 60 and 75 dpi.

To further corroborate the functional results, skin reinnervation of the lateral pawpads was analyzed by immunohistochemistry. In all the rats PGP immunolabeling showed regenerated nerve fibers that surrounded the SG tubules, reached the subepidermal nerve plexus, and extended to intraepidermal terminals and Meissner corpuscles at the papillae (Fig. 5E-J). Group LM+MP.NGF/NT3 had significantly higher number of IENF than all the other groups (Fig. 5K). Similarly, the number of reinnervated SGs was highest in group LM+MP.NGF/NT3, although only significantly from groups COL and LM (Fig. 5L).

Taken together, these results indicate that the combination of LM and NGF/NT3 enhances sensory axons regeneration and skin reinnervation by populations of sensory neurons that contribute to thermal and mechanical sensibility, and less markedly of sympathetic fibers innervating the SGs.

4. Discussion

The results of this study demonstrate that the combined addition of LM with NGF and NT3 into a collagen matrix produces a selective and synergistic effect enhancing only regeneration of sensory axons, whereas combining FN with BDNF particularly enhanced combining LM and NGF/NT3.

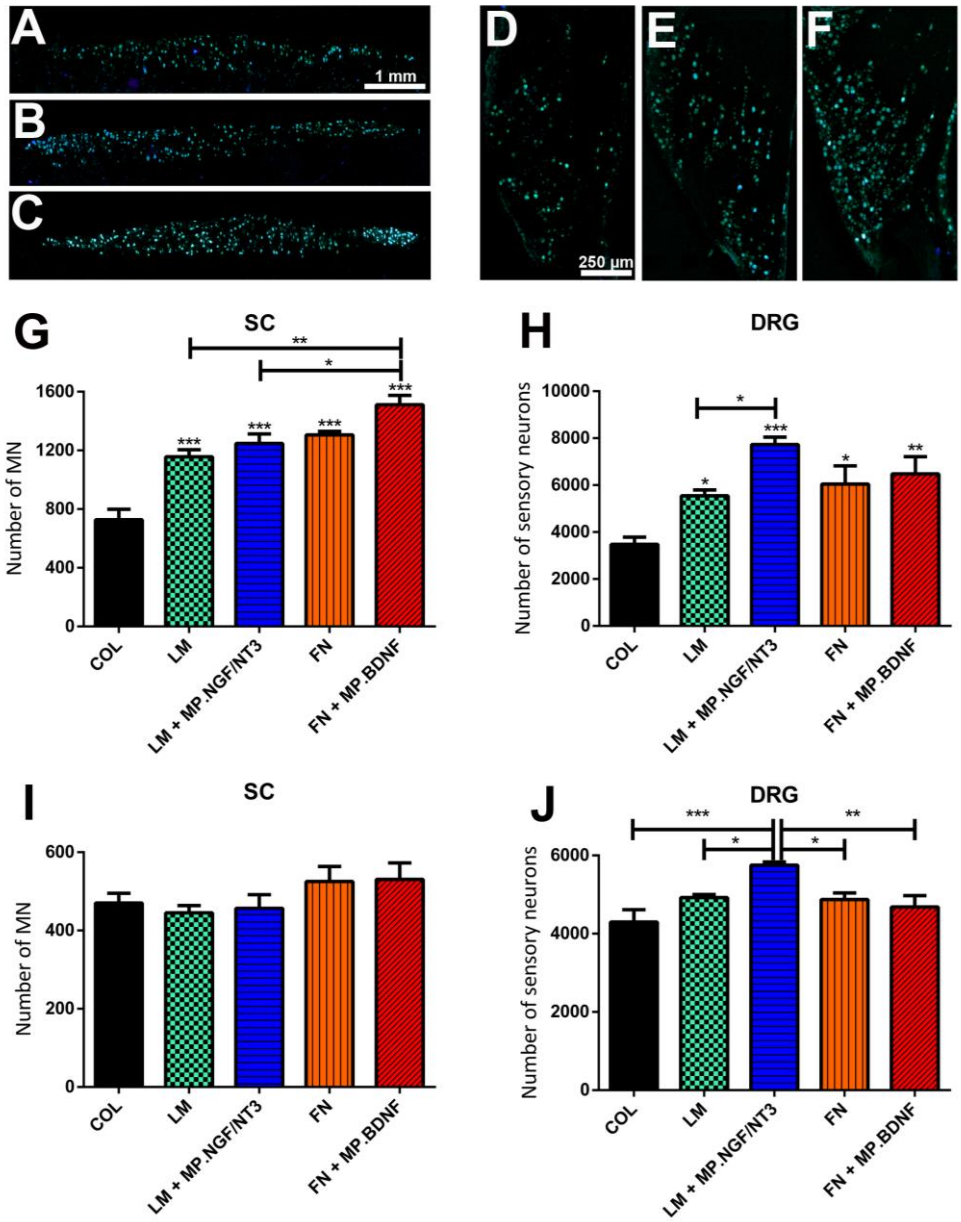

Figure 3. Representative micrographs of neurons retrolabeled with FG in the spinal cord (A-C) and DRG (D-F) of rats after sciatic nerve section and repair with a nerve conduit filled with COL (A, D), LM+MP.NGF/NT3 (B, E) or FN+MP.BDNF (C, F). Histogram of the number of regenerated motor neurons in the spinal cord (G) and sensory neurons in the DRG (H) in the short term study. Histogram of the number of regenerated motor neurons in the spinal cord (I) and sensory neurons in the DRG (J) after application of FG retrotracer at the ankle level 75 days after injury. Data expressed as mean ± SEM. *p<0.05, **p<0.01 and ***p<0.001.

Interestingly, these results were corroborated in a long term study, that showed earlier muscle reinnervation in the FN+MP.BDNF group, whereas functional and histological evidences of earlier and more extensive skin reinnervation was found in the LM+MP.NGF/NT3 group.

4.1. Mechanisms underlying the synergistic effects of combination of ECM molecules and NTFs

NTFs and ECM components both have important roles in nerve regeneration after injury, including effects on Schwann cell migration and differentiation, neuronal survival, cell adhesion and axonal growth (Allodi et al., 2012; Gordon, 2009). In vitro, using organotypic cultures of spinal cord and DRG, we corroborated the preferential effect of neurotrophins NGF and NT3 on sensory neurons and BDNF on motor neurons outgrowth, as previously reported (Allodi et al., 2011; Kemp et al., 2011; Lee et al., 2003; Sternel et al., 1997; Vögelin et al., 2006). Regarding ECM molecules, we previously found that sensory neurons extended longer neurites on collagen matrices enriched with laminin, whereas motoneurons extended longer neurites when the spinal cord slices were embedded in a fibronectin enriched matrix (Gonzalez-Perez et al., 2016). Thus, single addition of LM type I or NGF/NT3 containing substrate promoted DRG neurite outgrowth and density compared with the control collagen matrix, whereas no effect was observed on motor neuron outgrowth. On the other hand, the single addition of FN to the collagen matrix doubled the maximum length and density of motor neurites compared to LM containing substrate, and showed smaller effects on neurite length in DRG explants. Single addition of BDNF also increased motor neurons outgrowth, but had no effect on sensory neurons.

In order to investigate if such preferential effects of ECM components and NTFs could be synergistically added, we performed a screening of the possible combinations added to a collagen gel substrate. We observed a synergistic effect of LM and NGF+NT3 on neurite outgrowth in DRG explants, whereas this combination did not increase motor neurite length. On the other hand, BDNF combined with FN promoted a synergistic effect on motor neurite outgrowth with small effects on DRG explants, which can be attributed to the effect on regenerating proprioceptive neurites (Gonzalez-Perez et al., 2016). The synergistic effect can be exemplified for BDNF, that promotes sensory neurite outgrowth in the presence of LM but not when is added alone.

These proregenerative effects may be mediated by the differential expression of integrin and NTF receptors in regenerating neurons. It has been described that after injury integrin receptors α7β1 and α5β1 are upregulated in both motor and sensory neurons (Gonzalez-Perez et al., 2015; Werner et al., 2000), whereas high affinity TrkA and TrkC receptors are expressed in sensory neurons and TrKB is mainly expressed in motoneurons and in a low percentage of sensory neurons (Karchewski et al., 1999).

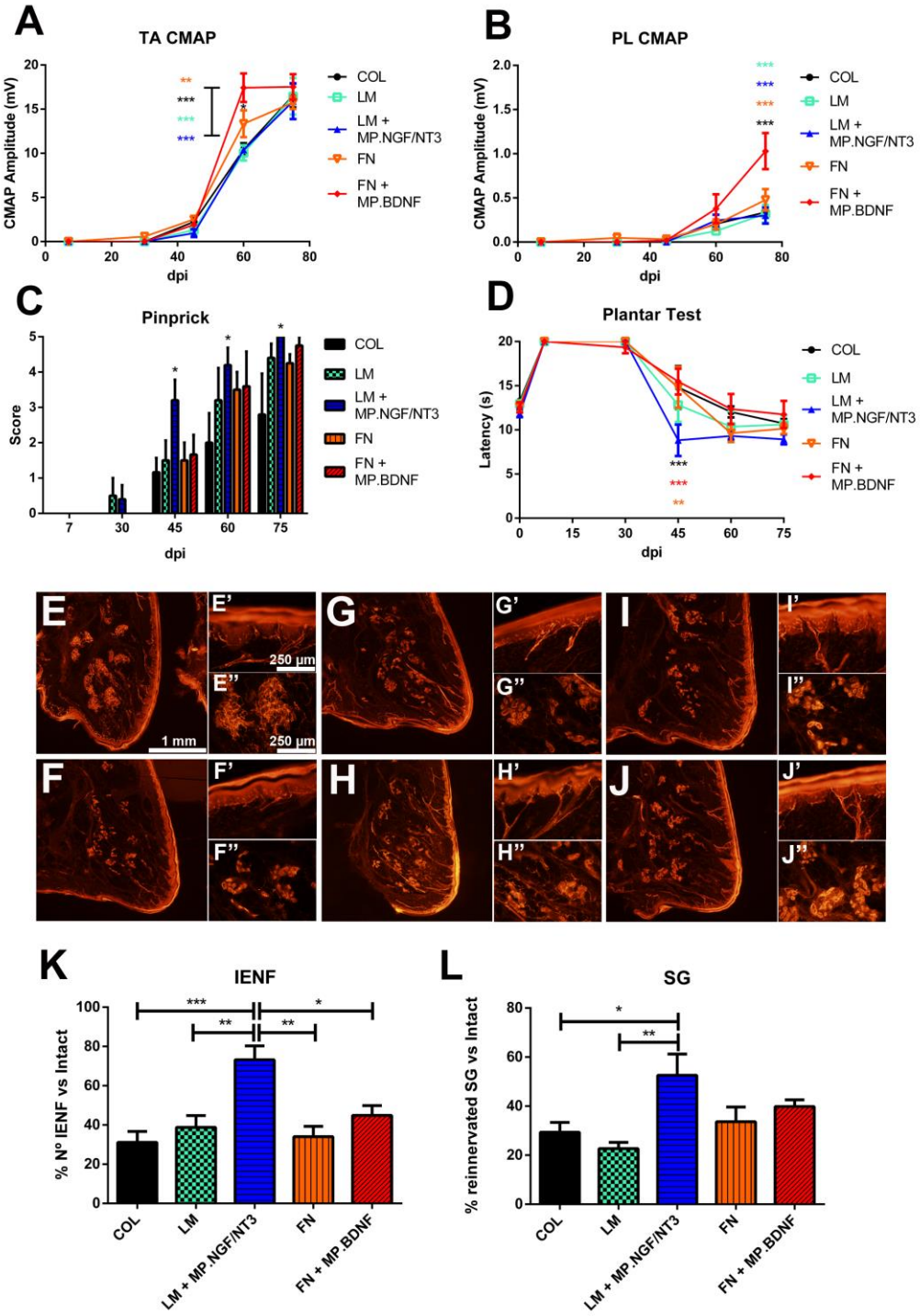

Figure 4. FN+MP.BDNF and LM+MP.NGF/NT3 enhance motor and sensory functional recovery, respectively. Mean amplitude of the CMAP in TA (A) and PL (B) muscles during follow-up. **p<0.01 and ****p*<0.001 FN+MP.BDNF vs all other groups referenced by the color of the star. Plot of the pinprick score in the different groups during follow-up (C). Latency of withdrawal response to thermal stimuli in the lateral part of the paw during follow-up (D). *p<0.05, **p<0.01 and ****p*<0.001 LM+MP.NGF/NT3 vs all other groups referenced by the color of the star. Representative images of plantar pads immunolabeled against PGP in an intact rat (E), COL (F), LM (G), LM+MP.NGF/NT3 (H), FN (I) and FN+MP.BDNF (J) treated animals. Scale bar 200 µm. Insets: Detail of axons stained with PGP innervating epidermis and SGs. Scale bar 50 µm. Percentage of reinnervated IENF (K) and reinnervated SGs (L) vs intact values. *p<0.05, **p<0.01 and ****p*<0.001. Data is presented as mean ± SEM.

It can be hypothetized that the partially selective in vitro effects of NTFs may be enhanced by the presence of certain ECM molecules in the substrate. In fact, it has been reported that the pro-regenerative effects of NGF and NT3 are reduced after blocking the α7 subunit of integrins in sensory neurons (Gardiner et al., 2005), and that synergistic actions between integrins and NTF receptors may be attributed to the sustained activation of Src and the downstream signaling Akt intermediate (Tucker and Mearow, 2008). On the other hand, NTFs may also modulate the expression of different integrin receptor subunits, whose upregulation is low in adult compared to their expression in early postnatal animals (Condic, 2001). Actually, NGF contributes to enhance ECM signaling by promoting axonal transport and accumulation of β1 integrin in growth cones, thus enhancing neurite outgrowth (Grabham et al., 2000).

.

4.2. FN+BDNF and LM+NGF/NT3 preferentially improve motor and sensory axons regeneration in vivo

We then tested in vivo if the introduction of a collagen matrix enriched with LM+NGF/NT3 or FN+BDNF also preferentially promoted regeneration of sensory and motor axons, respectively, after tube repair in adult rats. We encapsulated the NTFs in PLGA microspheres as we recently demonstrated that their slow release provided a more sustained suport and enhanced nerve regeneration with respect to free NFTs (Santos et al., 2016).

All the treated groups showed an increased number of retrogradely traced motor and sensory neurons that had regenerated their axons to the site of tracer application distal to the tube, compared to the control COL group. This is a positive indication that the design and the concentrations of encapsulated NTFs and ECM components did not cause detrimental effects such as the *candy store* effect (Tannemaat et al., 2008) or neuronal death induced by high concentration of NTFs (Mohiuddin et al., 1999). However, the preferential effect mediated by LM+NGF/NT3 and FN+BDNF treatments was more modest compared to the in vitro experiments. This comparative reduction may be explained because of the more complex environment present in the regenerating nerve. After nerve injury, ECM components are synthesized and secreted by non-neuronal cells such as Schwann cells and fibroblasts (Gonzalez-Perez et al., 2013), whereas NTFs are expressed by both neuronal and non-neuronal cells (Allodi et al., 2012; Boyd and Gordon, 2003; Brushart et al., 2013; Jesuraj et al., 2012). Furthermore, non-neuronal cells involved in Wallerian degeneration also express integrins and NTF receptors. Therefore, the in vivo implant of a matrix containing ECM components and NTFs in the nerve conduit does not only influence the injured neurons, but also acts on the migrating non-neuronal cells inside the

intratubular matrix. Hence, the activation of non-neuronal cells would contribute with proregenerative non specific cues and decrease the effects of the selective factors introduced in the exogenous matrix. Nevertheless, we still found in vivo a significant preferential regeneration of sensory neurons in animals treated with LM+MP.NGF/NT3 and of motor neurons in animals treated with FN+MP.BDNF.

Although retrolabeling of regenerating neurons is a useful tecnique to assess the differential effect of local treatments, functional restitution is the most important outcome after nerve injury (Navarro, 2016). Thus, in the long term in vivo study we evaluated functional recovery of both motor and sensory targets. Electrophysiological results demonstrated that muscle reinnervation started earlier and achieved higher levels in the FN+MP.BDNF group than in all the other groups. An increased regeneration rate improves muscle reinnervation, particularly of distal muscles in the limb, as shown in the foot muscles in this study, reducing the detrimental consequences of chronic denervation that occur in the long human nerves (Gordon et al., 2003). On the other hand, treatment with LM+MP.NGF/NT3 showed earlier sensory responses to both mechanical and thermal stimuli, confirming the results seen in the retrotracer study. We also demonstrated an increased number of sensory axons reinnervating the epidermis and of sympathetic axons reinnervating the SGs in the LM+MP.NGF/NT3 group. This parallel effect could be explained by the proregenerative role of NGF on sensory as well as on sympathetic neurons (Levi-Montalcini, 1987).

In conclusion, this study demonstrates that the interaction between FN+BDNF and between LM+NGF/NT3 has synergistic effects to preferentially enhance motor and sensory axon regeneration, respectively, in vitro. Furthermore, these effects are maintained in vivo in adult animals as motor and sensory axonal regeneration and functional recovery is enhanced after treating nerve injuries with the same combinations of NTFs and ECM components.

5. Acknowledgments

This research was supported by the European Union FP7-NMP project MERIDIAN under contract number 280778, and FPT-ICT project NEBIAS under contract number 611687, and TERCEL and CIBERNED funds from the Instituto de Salud Carlos III of Spain. The authors thank the technical help of Monica Espejo, Jessica Jaramillo and Marta Morell. The RT97 antibody was obtained from the Developmental Studies Hybridoma Bank developed under the auspices of the NICHD and maintained by the University of Iowa, Department of Biology.

6. Refferences

Aldskogius, H., Molander C., 1990. Specificity in regenerative outgrowth and target reinnervation by mammalian peripheral axons. Restor Neurol Neurosci 1: 275-280.

Allodi, I., Guzmán-Lenis, M.-S., Hernàndez, J., Navarro, X., Udina, E., 2011. In vitro comparison of motor and sensory neuron outgrowth in a 3D collagen matrix. J. Neurosci. Methods 198, 53–61.

Allodi, I., Udina, E., Navarro, X., 2012. Specificity of peripheral nerve regeneration : Interactions at the axon level. Prog. Neurobiol. 98, 16–37.

Boyd, J.G., Gordon, T., 2003. Neurotrophic Factors and Their Receptors in Axonal Regeneration and Functional Recovery After Peripheral Nerve Injury. Mol. Neurobiol. 27, 277–324.

Brushart, T.M., Aspalter, M., Griffin, J.W., Redett, R., Hameed, H., Zhou, C., Wright, M., Vyas, A., Höke, A., 2013. Schwann cell phenotype is regulated by axon modality and central-peripheral location, and persists in vitro. Exp. Neurol. 247, 272–81.

Clements, I.P., Mukhatyar, V.J., Srinivasan, A., Bentley, J.T., Andreasen, D.S., Bellamkonda, R. V, 2013. Peripheral nerve interfacing. IEEE Trans Neural Syst Rehabil Eng 21, 554–566.

Cobianchi, S., de Cruz, J., Navarro, X., 2014. Assessment of sensory thresholds and nociceptive fiber growth after sciatic nerve injury reveals the differential contribution of collateral reinnervation and nerve regeneration to neuropathic pain. Exp. Neurol. 255, 1–11.

Condic, M.L., 2001. Adult Neuronal Regeneration Induced by Transgenic Integrin Expression. J. Neurosci. 21, 4782–4788.

Gardiner, N.J., 2011. Integrins and the extracellular matrix: key mediators of development and regeneration of the sensory nervous system. Dev. Neurobiol. 71, 1054–72.

Gardiner, N.J., Fernyhough, P., Tomlinson, D.R., Mayer, U., von der Mark, H., Streuli, C.H., 2005. Alpha7 integrin mediates neurite outgrowth of distinct populations of adult sensory neurons. Mol. Cell. Neurosci. 28, 229–40.

Giudetti, G., del Valle, J., Navarro, X., Micera, S., 2014. NGF-loaded PLGA microparticles for advanced multifunctional regenerative electrodes. Conf Proc IEEE Eng Med Biol Soc. 1993–1995.

Gonzalez-Perez, F., Alé, A., Santos, D., Barwig, C., Freier, T., Navarro, X., Udina, E., 2016. Substratum preferences of motor and sensory neurons in postnatal and adult rats. Eur. J. Neurosci. 43:431-442.

Gonzalez-Perez, F., Udina, E., Navarro, X., 2013. Extracellular matrix components in peripheral nerve regeneration. Int. Rev. Neurobiol. 108, 257–275.

Gordon T, Sulaiman O, Boyd JG. Experimental strategies to promote functional recovery after peripheral nerve injuries. J Peripher Nerv Syst 2003; 8:236-50.

Gordon, T., 2009. The role of neurotrophic factors in nerve regeneration. Neurosurg. Focus 26, E3.

Grabham, P.W., Foley, M., Umeojiako, A., Goldberg, D.J., 2000. Nerve growth factor stimulates coupling of β 1 integrin to distinct transport mechanisms in the filopodia of growth cones. J. Cell Sci. 3012, 3003–3012.

Gundersen, H.J., 1986. Stereology of arbitrary particles. A review of unbiased number and size estimators and the presentation of some new ones, in memory of William R. Thompson. J. Microsc. 143, 3–45.

Hall, S., 2005. The response to injury in the peripheral nervous system. J. Bone Joint Surg. Br. 87, 1309–19.

Höke, A., Redett, R., Hameed, H., Jari, R., Zhou, C., Li, Z.B., Griffin, J.W., Brushart, T.M., 2006. Schwann cells express motor and sensory phenotypes that regulate axon regeneration. J. Neurosci. 26, 9646–55.

Jesuraj, N.J., Nguyen, P.K., Wood, M.D., Moore, A.M., Borschel, G.H., Mackinnon, S.E., Sakiyama-Elbert, S.E., 2012. Differential gene expression in motor and sensory Schwann cells in the rat femoral nerve. J. Neurosci. Res. 90, 96–104.

Karchewski, L.A., Kim, F.A., Johnston, J., Knight, R.M.M.C., Verge, V.M.K., 1999. Anatomical Evidence Supporting the Potential for Modulation by Multiple Neurotrophins in the Majority of Adult Lumbar Sensory Neurons 341, 327–341.

Kemp, S.W.P., Webb, A.A., Dhaliwal, S., Syed, S., Walsh, S.K., Midha, R., 2011. Dose and duration of nerve growth factor (NGF) administration determine the extent of behavioral recovery following peripheral nerve injury in the rat. Exp. Neurol. 229, 460–70.

Leary, S., Underwood, W., Lilly, E., Anthony, R., Cartner, S., Corey, D., Grandin, T., Collins, F., Greenacre, C., Gwaltney-brant, S., Mccrackin, M.A., Meyer, R., Miller, D., Shearer, J., Yanong, R., Golab, G.C., Patterson-kane, E., 2013. AVMA Guidelines for the Euthanasia of Animals : 2013 Edition.

Lee, A.C., Yu, V.M., Lowe, J.B., Brenner, M.J., Hunter, D. a, Mackinnon, S.E., Sakiyama-Elbert, S.E., 2003. Controlled release of nerve growth factor enhances sciatic nerve regeneration. Exp. Neurol. 184, 295–303. doi:10.1016/S0014-4886(03)00258-9

Lemons, M.L., Condic, M.L., 2008. Integrin signaling is integral to regeneration. Exp. Neurol. 209, 343–52.

Levi-Montalcini, R., 1987. The Nerve Growth Factor Thirty-Five Years Later. Biosci. Rep. 7, 681–699.

Lotfi, P., Garde, K., Chouhan, A.K., Bengali, E., Romero-Ortega, M.I., 2011. Modality-specific axonal regeneration: toward selective regenerative neural interfaces. Front. Neuroeng. 4, 1–11.

Lundborg, G., 2003. Nerve injury and repair -a challenge to the plastic brain. J. Peripher. Nerv. Syst. 226, 209–226.

Martini, R., Brushart, T.M., 1994. The L2 / HNK- 1 Carbohydrate Is Preferentially Expressed by Previously Motor Axon-associated Schwann Cells in Reinnervated Peripheral Nerves. J. Neurosci. 74, 7180–7191.

Mohiuddin, L., Delcroix, J.-D., Fernyhough, P., Tomlinson, D.R., 1999. Focally administered nerve growth factor suppresses molecular regenerative responses of axotomized peripheral afferents in rats. Neuroscience 91, 265–271.

Navarro, X., 2016. Functional evaluation of peripheral nerve regeneration and target reinnervation in animal models. A critical overview. Eur J Neurosci 43, 271-286.

Navarro, X., Verdú, E., Wendelschafer-Crabb, G., Kennedy, W.R., 1997. Immunohistochemical study of reinnervation by regenerative axons. J Comp Neurol 380, 164-174

Navarro, X., Vivó, M., Valero-Cabré, A., 2007. Neural plasticity after peripheral nerve injury and regeneration. Prog. Neurobiol. 82, 163–201. doi:10.1016/j.pneurobio.2007.06.005

Plantman, S., Patarroyo, M., Fried, K., Domogatskaya, A., Tryggvason, K., Hammarberg, H., Cullheim, S., 2008. Integrin-laminin interactions controlling neurite outgrowth from adult DRG neurons in vitro. Mol. Cell. Neurosci. 39, 50–62.

Richardson, P.M., Miao, T., Wu, D., Zhang, Y., Yeh, J., Bo, X., 2009. Responses of the nerve cell body to axotomy. Neurosurgery 65, A74–9.

Robinson, G.A., Madison, R.D., 2004. Motor neurons can preferentially reinnervate cutaneous pathways. Exp. Neurol. 190, 407–13.

Santos, D., Giudetti, G., Micera, S., Navarro, X., Del Valle, J., 2016. Focal release of neurotrophic factors by biodegradable microspheres enhance motor and sensory axonal regeneration in vitro and in vivo. Brain Res. 1636, 93–106.

Sternel, G.D., Brown, R.A., Green, C.J., Terenghi, G., 1997. Neurotrophin-3 Delivered Locally via Fibronectin Mats Enhances Peripheral Nerve Regeneration. Eur. J. Neurosci. 9, 1388–1396.

Tannemaat, M.R., Eggers, R., Hendriks, W.T., de Ruiter, G.C.W., van Heerikhuize, J.J., Pool, C.W., Malessy, M.J. a, Boer, G.J., Verhaagen, J., 2008. Differential effects of lentiviral vector-mediated overexpression of nerve growth factor and glial

cell line-derived neurotrophic factor on regenerating sensory and motor axons in the transected peripheral nerve. Eur. J. Neurosci. 28, 1467–79.

Torres-Espín, A, Santos, D., González-Pérez, F., del Valle, J., Navarro, X., 2014. Neurite-J: an image-J plug-in for axonal growth analysis in organotypic cultures. J. Neurosci. Methods 236, 26–39.

Torres-Espín, A., Allodi, I., Santos, D., González-Pérez, F., Udina, E., del Valle, J., Navarro, X., 2016. Analysis of axonal growth in organotypic neural cultures. Protocol Exchange

Tucker, B.A., Mearow, K.M., 2008. Peripheral Sensory Axon Growth: From Receptor Binding to Cellular Signaling. Can. J. Neurol. Sci. 35, 551–566.

Valero-Cabré, A., Navarro, X., 2002. Functional impact of axonal misdirection after peripheral nerve injuries followed by graft or tube repair. J Neurotrauma 19, 1475-1485.

Valero-Cabré, A., Tsironis, K., Skouras, E., Navarro, X. Neiss, W.F., 2004. Peripheral and spinal motor reorganization after nerve injury and repair. J. Neurotrauma 21, 95–108.

Valero-Cabré, A., Tsironis, K., Skouras, E., Perego, G., Navarro, X., Neiss, WF., 2001. Superior muscle reinnervation after autologous nerve graft and poly-l-lactide-e-caprolactone (PLC) tube implantation in comparison to silicone tube repair. J Neurosci Res 63, 214-223.

Verdú, E., Labrador, R.O., Rodríguez, F.J., Ceballos, D., Forés, J., Navarro, X., 2002. Alignment of collagen and laminin-containing gels improve nerve regeneration within silicone tubes. Restor Neurol Neurosci. 20, 169–180.

Vögelin, E., Baker, J.M., Gates, J., Dixit, V., Constantinescu, M.A., Jones, N.F., 2006. Effects of local continuous release of brain derived neurotrophic factor (BDNF) on peripheral nerve regeneration in a rat model. Exp. Neurol. 199, 348–53.

Werner, A., Willem, M., Jones, L.L., Kreutzberg, G.W., Mayer, U., 2000. Impaired Axonal Regeneration in α7 Integrin-Deficient Mice. J. Neurosci. 20, 1822–1830.

Xie, J., Jin, B., Li, D., Shen, B., Gong, N., Zhang, T., Dong, P., 2015. Effect of laminin-binding BDNF on induction of recurrent laryngeal nerve regeneration by miR-222 activation of mTOR signal pathway. Am J Transl Res 7, 1071–1080.

CHAPTER 3

Segregation of motor and sensory axons regenerating through bicompartmental tubes by combining extracellular matrix components with neurotrophic factors

Daniel Santos [1,2], Delgado-Martínez I [1,2], Guido Giudetti [3], Silvestro Micera [3,4], Jaume del Valle [1,2], Xavier Navarro [1,2]

[1] Institute of Neurosciences and Department of Cell Biology, Physiology and Immunology, Universitat Autònoma de Barcelona

[2] Centro de Investigación Biomédica en Red sobre Enfermedades Neurodegenerativas (CIBERNED), Bellaterra, Spain

[3] The BioRobotics Institute, Scuola Superiore Sant'Anna, Viale Rinaldo Piaggio 34, 56025 Pontedera, Italy

[4] Translational Neural Engineering Laboratory, Center for Neuroprosthetics and Institute of Bioengineering, School of Engineering, Ecole Polytechnique Federale de Lausanne (EPFL), Lausanne, Switzerland

Corresponding author: Dr. Xavier Navarro, Unitat de Fisiologia Mèdica, Facultat de Medicina, Universitat Autònoma de Barcelona, E-08193 Bellaterra, Spain. E-mail: xavier.navarro@uab.cat

Running title: Motor and sensory axon regeneration by combining ECM and NTFs

Abstract

The segregation of regenerating motor and sensory axons may be a good strategy to improve selective functionality of regenerative interfaces to provide close loop commands. Extracellular matrix (ECM) components and neurotrophic factors (NTFs) exert guidance effects on different neuronal populations. In the present study, we assessed in vivo the potential of separating sensory and motor axons regenerating in a Y-type tube, with each branch prefilled with an adequate combination of ECM and NTFs. For this purpose, we implanted a bicompartmental tube in the severed sciatic nerve of rats. In a control group both sides were filled with a collagen matrix with PLGA microspheres containing PBS (Col+MP.PBS). In another group, one compartment contained the collagen matrix enriched with fibronectin and BDNF encapsulated in PLGA microspheres (FN+MP.BDNF) in order to preferentially attract motor axons, whereas the other compartment was enriched with laminin and NGF/NT-3 encapsulated in PLGA microspheres (LM+MP.NGF/NT-3) for promoting sensory axons regeneration. By retrotracer labeling, we observed that LM+MP.NGF/NT-3 did not promote higher numbers of regenerated sensory axons regeneration compared to controls, and no differences were observed in sensory functional recovery. However, FN+MP.BDNF guided higher number of regenerating motor axons compared to controls, improving also motor recovery. These results demonstrate that motor axonal guidance can be modulated in vivo by the addition of fibronectin and BDNF.

Keywords: Y-tube, neurotrophic factors, extracellular matrix, motor axons, sensory axons, axonal guidance.

1. Introduction

Neuroprosthetic devices have been evolving in the last years in order to replace and restore limb functionality to amputee patients. Advanced neuroprotheses show high degrees of freedom (Carrozza et al., 2006), however, these robotic innovations are not matched by a suitable neural interface technology. Thus, there is still need for closed loop commands for precise execution of movements by incorporating readout from sensory neurons, i.e. the integration of both sensory neuron (SN) and motor neuron (MN) functions on the interface device, by providing access to high resolution neural signals. Therefore, the anatomical separation of regenerating axons from sensory and motor neurons in mixed nerves could be a good approach to selectively stimulate or record different neural signals by means of regenerative interfaces to obtain improved neuroprosthetic control.

Previous studies described the existence of a preferential motor reinnervation (PMR), in which motor axons tend to enter into muscle branches in higher proportion than into cutaneous branches (Brushart, 1988). Similarly, the muscle branch was also more prone to be reinnervated by muscular than by cutaneous sensory afferents (Madison et al., 1996). This phenomenon of preferential reinnervation has been attributed to the specific interactions between regenerating axons and the environment generated in the denervated distal nerve branches (T. Brushart, Gerber, Kessens, Chen, & Royall, 1998). Several studies have focused in elucidating different contributors for the PMR effect. Schwann cells have been suggested to have a specific identity that can be recognized by regenerating axons due to differential motor or sensory phenotypes and expression of particular surface receptors. Thus, the HNK-1 carbohydrate epitope is expressed strongly in Schwann cells of motor axons in the adult rodent, but rarely in those associated to sensory axons, whereas NCAM is present exclusively in sensory nerve fascicles and not in motor fascicles (Martini et al., 1992, 1994; Saito et al., 2005). However, Schwann cells de-differentiate during Wallerian degeneration and tend to loss that preferential marker expression within days after nerve transection in motor and sensory fascicles (Saito et al., 2005; Lago et al., 2007). Another point of view suggests that it is the relative level and type of trophic support provided by each nerve branch and the target organ that determine whether motor or sensory axons remain in that particular branch (Madison et al., 2007). Interestingly, Hoke et al. (2006) demonstrated that Schwann cells of sensory and motor nerves produce differing growth factors at baseline and respond differently during denervation and when reinnervated by cutaneous or motor axons. Thus, we hypothetized that by local sustained application of specific guidance and trophic factors might result in higher probability of directed regeneration of motor or sensory axons

than grafting different populations of Schwann cells, that loss their distinct phenotype after denervation and thus have a limited effect (Hoke et al., 2006; Lago et al., 2007)

Importantly, nerve growth factor (NGF) and neurotrophin-3 (NT-3) have predominant attractive properties for SN both in vitro and in vivo, mediated by their TrkA and TrkC receptors (Bloch, Fine, Bouche, Zurn, & Aebischer, 2001; Gallo, Lefcort, & Letourneau, 1997; Lotfi, Garde, Chouhan, Bengali, & Romero-Ortega, 2011; Moore et al., 2006), whereas BDNF promotes MN outgrowth in vitro (Allodi, Guzmán-Lenis, Hernàndez, Navarro, & Udina, 2011) and has attractive properties for regenerating MNs mediated by TrkB receptors (Henle et al., 2011; Li et al., 2005; Song et al., 1997; Yuan et al., 2003). In addition, different extracellular matrix components (ECM) constituents of the endoneurial tubes and the basal lamina play a role in the promotion of preferential axon outgrowth. For instance, laminin substrate mainly promotes sensory axon outgrowth in vitro (Gardiner, 2011; Plantman et al., 2008), whereas fibronectin enhances motor and proprioceptive axon outgrowth (Gonzalez-Perez et al., 2015). Therefore, the addition of different neurotrophic factors and ECM components in a Y tube model could be a interesting approach for segregating motor and sensory axons. In fact, a previous study used a Y-tube model to separate regenerating TrkC-expressing proprioceptive from TrkA-expressing nociceptive neurons by the addition of NT-3 and NGF, respectively (Lotfi et al., 2011).

In the present study, a sciatic nerve transection was repaired with a bicompartmental tube containing a different combination of ECM and neurotrophic factors in each distal branch. Based on our previous results, each branch was filled prior to implantation with a collagen matrix containing either fibronectin with PLGA microspheres releasing BDNF (FN+MP.BDNF) in one side of the chamber in close contact with the distal peroneal nerve (P), or laminin with PLGA microspheres releasing NGF and NT-3 (LM+MP.NGF/NT-3) at the other side in contact with tibial and sural nerves (T+S). We assessed whether regenerated motor axons preferentially grew in the first branch and sensory axons in the second branch, compared to control condition in which both branches contained the same collagen matrix and PLGA microspheres filled with PBS (Col+MP.PBS).

2. Materials and methods

2.1. Ethics statement

The experimental procedures were approved by the ethical committee of the Universitat Autonoma de Barcelona in accordance with the European Communities Council Directive 2010/63/EU. Female Sprague-Dawley rats (250–300 g) were used for the *in vivo* studies. They were kept on standard laboratory conditions with a light-dark

cycle of 12:12 h and *ad libitum* access to food and tap water. All efforts were made to minimize pain and animal discomfort during surgery and treatments.

2.2. Fabrication of the bicompartmental tube and implantation

The Y-tube consisted of a silicone tube divided in two sections by a flat polyimide film. Silicone tubes (8 mm long, 2 mm i.d.) were cut longitudinally along 4 mm and a polyimide film (8 mm long, 2 mm wide, 30 µm thick) were placed along the midline to divide the distal half tube into two separated chambers. To prevent distal axon reorganization, 4 mm of the polyimide film extended out of the tube (see Fig. 1A, B). The slit cut of the tube was closed by silicone adhesive to hold the film in place.

NGF, NT-3, and BDNF were encapsulated in Poly-lactic Co-Glycolic acid microspheres (MPs) as previously described (Giudetti et al., 2014). MPs containing NGF and NT-3 were added to a collagen type I solution (3 mg/ml; #354236, Corning) supplemented with laminin 20% (Sigma) to reach a final concentration of 1 µg/ml for each trophic factor. Similarly, BDNF containing MPs were added to a collagen solution supplemented with fibronectin 20% (BD Biosciences) to reach a final concentration of 2 µg/ml for BDNF. In the experimental group, each branch of the Y-tube was filled with one of the above solutions. In the control group, both distal branches were filled with collagen gel mixed with MPs containing PBS (Col+MP.PBS). Tubes were maintained vertically for 12 hours before surgery in order to promote fibril alignment during gel formation (Verdú et al., 2002).

Animals were anaesthetized with ketamine/xylacine (90/10 mg/kg i.p.), the sciatic nerve was exposed at the midthigh, transected and a portion of 3 mm resected. The proximal sciatic nerve stump was sutured to the proximal end of the bicompartmental tube. The distal stump was carefully dissected to separate the P, T and S nerve branches ; then, the distal P nerve was inserted in the compartment containing FN+MP.BDNF, whereas the T+S nerves were inserted in the compartment containing LM+MP.NGF/NT-3 (Fig. 1C). The nerve stumps were fixed with one 10-0 suture stitch, leaving a interstump distance of 6 mm. The wound was closed by planes with silk sutures. Animals were kept for 90 dpi to allow for axonal regeneration.

2.4. Assessment of skin sensory reinnervation.

The progression of nociceptive reinnervation of the hindpaw was assessed by means of the pinprick test and thermal algsimetry at 7, 30, 45, 60, 75 and 90 dpi. For the pinprick test, animals were gently kept in a cloth with the sole of the injured paw facing upward, and the skin was stimulated with a needle from proximal to distal at specific sites of the lateral side of the hindpaw plantar surface (Cobianchi, de Cruz, &

Navarro, 2014). Positive withdrawal responses were taken as sign of skin functional reinnervation and recorded only when clear pain reaction was triggered by the stimulation. A composite score was calculated as the mean number of responses per group at each day of testing.

Thermal sensitivity was assessed using a Plantar test algesimeter (Ugo Basile, Comerio, Italy). Rats were placed into a plastic box with an elevated plexiglass floor. The beam of a lamp was pointed to the lateral part in the hindpaw plantar surface. Intensity was set to low power (40 mW/cm^2) with a heating rate of 1°C/s to elicit activation of unmyelinated fibers as described before (Cobianchi et al., 2014). A cutoff time for the stimuli was set at 20 seconds to prevent tissue damage. Heat pain threshold was calculated as the mean of 3 trials per test site, with a 5-minute resting

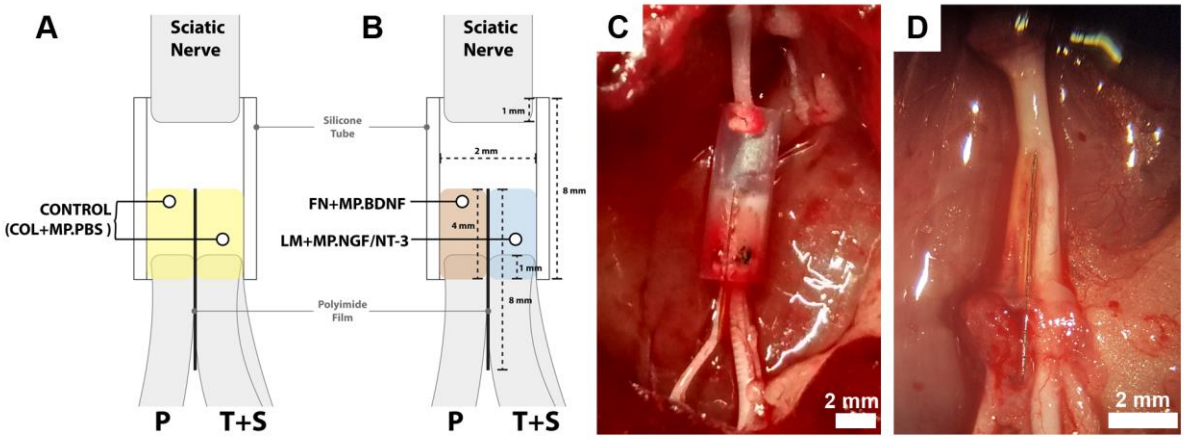

period between each trial, and expressed as the latency (in seconds) of paw withdrawal response.

Figure 1. Schematic drawing showing the design of the bicompartmental Y tube, and the contents of each branc in the control group and in the experiental group (A). Micrograph of the implanted Y tube filled with a collagen gel at both distal branches of the tube (B). Micrograph of a regenerated nerve after the extraction of the tube prior to retrotracer application (C). Scale bar: 2 mm.

2.5. Assessment of motor reinnervation

Functional reinnervation of target muscles was assessed at 90 dpi before the retrotracer application. Animals were anesthetized with ketamine/xylacine. The rat body temperature was maintained by means of a thermostated warming flat coil during the experiment. Sub-dermal steel needle electrodes were placed transcutaneously at the sciatic notch for electrical stimulation using a single monophasic pulses of 100 μs duration (Synergy Medelec, Viasys HealthCare). Elicited compound muscle action

potentials (CMAPs) for the tibialis anterior (TA), gastrocnemius medialis (GM) and plantar interosseus (PL) muscles were recorded using steel needles in monopolar configuration (Valero-Cabré and Navarro, 2001). The amplitude and latency of the M-wave were measured. The contralateral intact limb was used as control.

2.6. Retrograde labeling and neuronal counting

To quantify motor and sensory regenerated neurons, rats were anaesthetized with ketamine/xylacine, the sciatic nerve was carefully dissected and the silicone tube removed (Fig. 1D). The regenerated nerve branches were transected at the distal part, separated from the polyimde wall, and dipped in 5 µl of Fluorogold (FG; 5%; Fluorochrome Inc.) or True Blue (TB; 5%; Setareh Biotech) for 1 hr inside a vaseline well. Retrotracers application was counterbalanced in order to minimize possible differences between retrotracers efficacy (Zele, Sketelj, & Bajrović, 2010). After retrieval of the well, the area was rinsed with saline to clean any remnants of the tracer and the wound sutured. Animals were allowed to survive for 7 days for accumulation of the tracer in the soma of spinal motoneurons and DRG sensory neurons. Then, rats were deeply anesthetized and transcardially perfused with 4% paraformaldehyde in PBS. The lumbar segment (L3-L6) of the spinal cord and the L4 and L5 DRG were removed, postfixed at 4ºC in the same fixative solution for 1h and transferred to 30% sucrose in PBS. The cord and DRG were cut in a cryostat longitudinally into 40 and 20 µm thick sections respectively, mounted on slides, heated at 35ºC for 1h and stored at -20ºC in the dark. Finally, sections were observed with an Olympus BX51 fluorescence microscope under UV light and the number of labeled neurons were counted in every third section following the fractionator principle (Gundersen, 1986). Images were acquired at 4800x3600 resolution in RGB 24-bit format.

2.7. Morphometric analysis

The identification of labeled SNs was done using Fiji software (Schindelin, J et al., 2012). RGB pictures were converted to L*a*b* color space to extract the ‘a*’ channel, containing the information of the tracer fluorescence. The resulting image was smoothed using a median filter. A binary image was generated using a mid-grey adaptative local thresholding procedure. Soma clusters were extrapolated using a watershed algorithm. Neuron-like objects were then identified by the “Analyze particles” tool of the software and manually verified. The data about number of objects and their area and ‘a*’ value. were further analysed in SPSS 22.0 (IBM Corp., USA). Objects were clustered using a k-means procedure according to two independent features, area and mean value of the ‘a*’ channel. From the area, three groups were formed:

small, medium, and large size, according to defined size criteria (Fukuoka et al., 2001). From the value of the 'a*' channel, objects were separated into TB+, FG+, and double labeled (DL). TB+ and FG+ objects were assigned to the corresponding reinnervating branch based on the experimental settings.

2.8. Data analysis

Data are presented as mean ± SEM. Results were statistically analyzed by using GraphPad Prism (GraphPad Software, USA). A Student t-test and one and two-way ANOVA followed by Bonferroni's post hoc tests for comparison between groups were used. Statistical significance was considered when P value was <0.05.

3. Results

3.1. Effects on sensory and motor functional recovery

Sensory functional recovery, evaluated by mechanical and thermal tests, did not show differences between control and experimental groups. For pinprick test, the first responses were observed at 30 dpi, without significant differences at any time points (Fig. 2A). Similarly, withdrawal responses in the plantar test started to appear at 30 dpi and no differences were observed at during the follow-up between groups (Fig. 2B). These results indicate that the branch containing LM+MP.NGF/NT-3 did not promote higher regeneration of SNs to the T+S nerves in comparison with the Col+MP.PBS control condition.

Electrophysiological tests were performed to assess reinnervation of the TA, GM and PL muscles (Fig. 3). The amplitude of the TA CMAP was higher in FN+MP.BDNF than in the control group (27.5 ± 2.9 mV and 22.3 ± 2.7 mV, respectively, $p<0.05$). In contrast, the GM and PL CMAPs were higher in the control than in the LM+MP.NGF/NT-3 condition ($p<0.05$ for the GM CMAP. These results suggest that a higher number of MNs regenerated towards the P nerve by the addition of FN+MP.BDNF, but lower number towards the T+S nerves with LM+MP.NGF/NT-3 in comparison with the control condition.

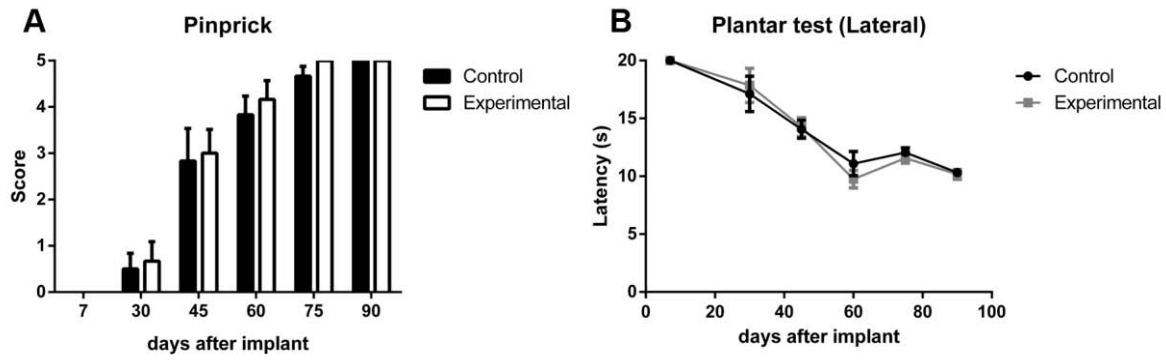

Figure 2. Plot of the pinprick score in the different groups during follow-up (A). Latency of withdrawal response to thermal algesimetry test in the lateral part of the paw during follow-up (B). Data expressed as mean ± SEM.

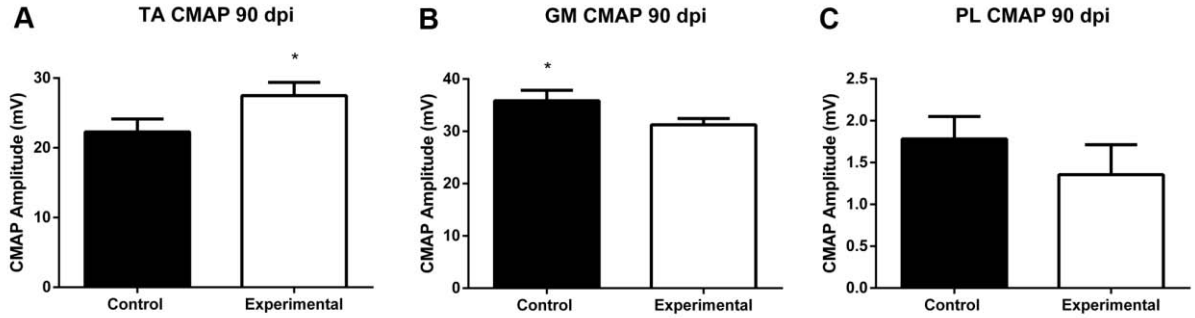

Figure 3. Histogram of the mean amplitude of the CMAP in TA (A), GM (B) and PL (C) muscles at 90 dpi. *p<0.05. Data expressed as mean ± SEM.

3.3. Effects on motor and sensory neuron directed regeneration

At the final time point, we observed that all the animals showed a regenerated nerve within the Y-tube that bifurcated in each compartment created by the polyimide film to distally reinnervate the P nerve at one side and T+S nerves at the other side (Fig. 1C).

Retrotracers application confirmed that in all the rats MNs and SNs had regenerated through the Y tube, as judged by the presence of TB+, FG+ and DL neurons (Fig. 4A-C) in SC and DRG sections (Fig. 4D-G). Data on the total number of retrolabeled neurons for each condition are shown in Table 1.

Table 1. Average number of motor and sensory neurons that regenerated axons within each branch of the Y tube towards the distal inserts of T+S or P nerves.

	COL+MP.PBS			COL+MP.ECM.NTF		
	T+S	P	DL	T+S	P	DL
MN	654.6 ± 11.4	88.6 ± 36.6	139.6 ± 56.9	339.6 ± 60.8	497.2 ± 60.1	91.4 ± 31.47
SN	5173.6 ± 343	1846.6 ± 864.1	698.3 ± 117.3	4263.2 ± 1069.7	2609.2 ± 700.5	633 ± 166.64

The number of regenerated neurons was about 8500 in both groups, but there were differences between branches and distribution. Thus, in the experimental group about 1200 more neurons regenerated their axons in the branch towards the P nerve and correspondingly less towards the T+S nerves than in the control group.

When counting the number of retrolabeled MNs, in the control group 74.1±1.2% of the MNs regenerated in T+S distal stump, whereas only 10.03±4.1% regenerated towards the P nerve. In addition, 15.8±6.45% of MNs appeared DL suggesting the formation of axonal sprouts that grew through both branches of the tube. On the other hand, in the experimental group 53.5±6.5% of regenerated MNs grew towards the FN+MP.BDNF branch connected to the P nerve ($p<0.001$ vs the control condition, Fig 4H). Consequently, less MNs regenerated through the LM+MP.NGF/NT-3 compartment (36.6±6.5%; $p<0.001$ vs the control condition). There were no differences in the number of DL MNs between the two groups.

With regard to retrolabeled SNs, in the control group 67.03±4.4% grew towards the T+S distal stump and only 23.9±9.0% towards the P distal nerve, whereas 9.04±1.5% were DL neurons. The addition of different combination of ECM and NTFs into separate branches of the Y tube had a slight but not significant influence on regeneration of sensory axons, since 56.8±14% were labeled from the LM+MP.NGF/NT-3 branch, 34.7±9.3% from the FN+MP.BDNF branch and 8.43±2.2 from both chambers (Fig. 4I).

These results demonstrate that the addition of LM+MP.NGF/NT-3 did not exert a significant effect attracting regenerating SNs, whereas the addition of FN+MP.BDNF significantly attracted more regenerating MNs compared to the control condition.

3.5. FN+BDNF preferentially attract large sensory neurons

Since SNs are constituted by a heterogeneous population (Usoskin et al., 2014), we performed a morphometric analysis to characterize differences in size of SNs that regenerated at different sites of the bichamber tube.

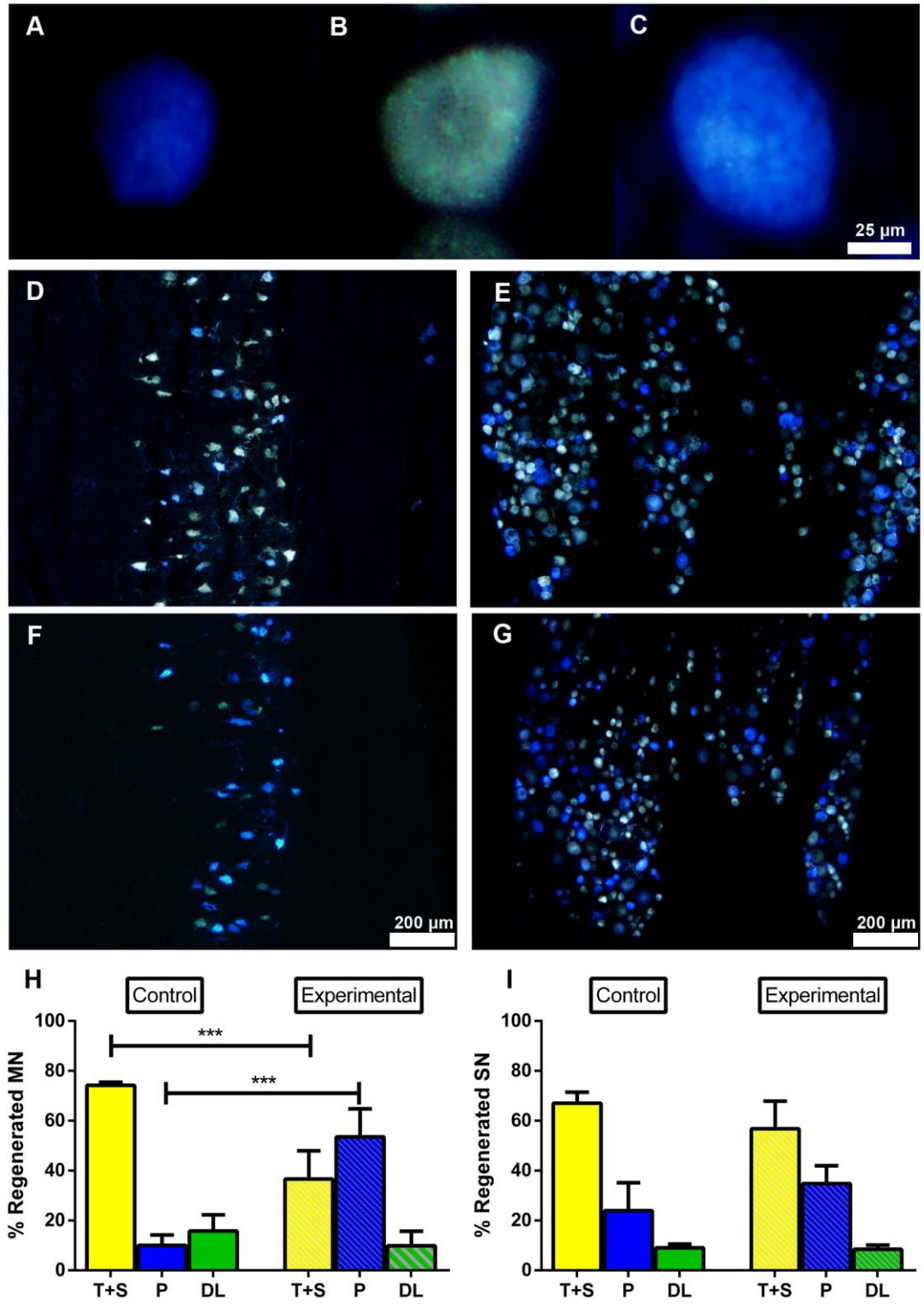

Figure 4. Representative micrographs of neurons retrolabeled with TB (A), FG (B) and DL (C). Representative micrographs of MNs retrolabeled in the spinal cord in control (D) and experimental conditions (F), and of SNs retrolabeled in DRG after control (E) and experimental conditions (G). In this case, FG was applied to the T+S distal nerve and TB to the P distal nerve. Histogram of the number of regenerated MNs in the spinal cord (H) and SNs in the DRG (I) in both control and experimental groups. Data expressed as mean ± SEM. ***p<0.001.

The frequency of distribution of regenerated SNs showed no differences in soma size of sensory neurons that regenerated in the LM+MP.NGF/NT-3 gel compared to the control gel (Fig. 5A). However, SNs that regenerated in the FN+MP.BDNF gel towards the P nerve showed a larger soma size than in the control gel ($p<0.05$, Fig. 5B). Then, we grouped the regenerated SNs in small, medium and large size to further characterize the composition of each regenerating branch (Fig. 5D-F). The only significant difference in size was observed between FN+MP.BDNF and Col+MP.PBS conditions for large SNs ($p<0.05$, Fig. 5F). These results demonstrate that the combination of FN and BDNF promoted the directed growth of large sensory axons, which are related with muscular afferents (Taylor, Holdeman, Weltmer, Ryals, & Wright, 2005).

4. Discussion

In this study we have used a bicompartmental tube model that forces the regenerating axons to grow along a different branch. When the axons regenerate within the tube, they may choose between two branches with a different milieu to grow. By manipulating the composition of the inside matrix of each branch we attempted to preferentially attract the regenerating motor and sensory axons and then selectively guide them towards different distal nerves and their corresponding targets. In accordance with similar studies with gap defects (Jerregård et al., 2001; Clements et al., 2009; Meyer et al., 2016), the division of the tube in two separated compartments did not suppose an obstacle for nerve regeneration as all the operated animals showed regeneration distal to the tube and evidence of functional reinnervation of skin and muscles. Tube repair leaving a short gap between proximal and distal nerve stumps was first presumed to allow axons to be guided towards their original distal fascicle by means of neurotropic diffusible factors (Evans et al., 1991; Rende et al., 1991). However, later studies proved that tube repair by itself did not improve the selectivity of regeneration with respect to direct suture when correct alignment between proximal and distal stumps was achieved (Bodine-Fowler et al., 1997; Valero-Cabré et al., 2001, 2004).

Therefore, we have evaluated here if the addition of a different combination of ECM molecules and NTFs into a collagen matrix was able to selectively guide the regeneration of motor and sensory neurons towards different distal fascicles.

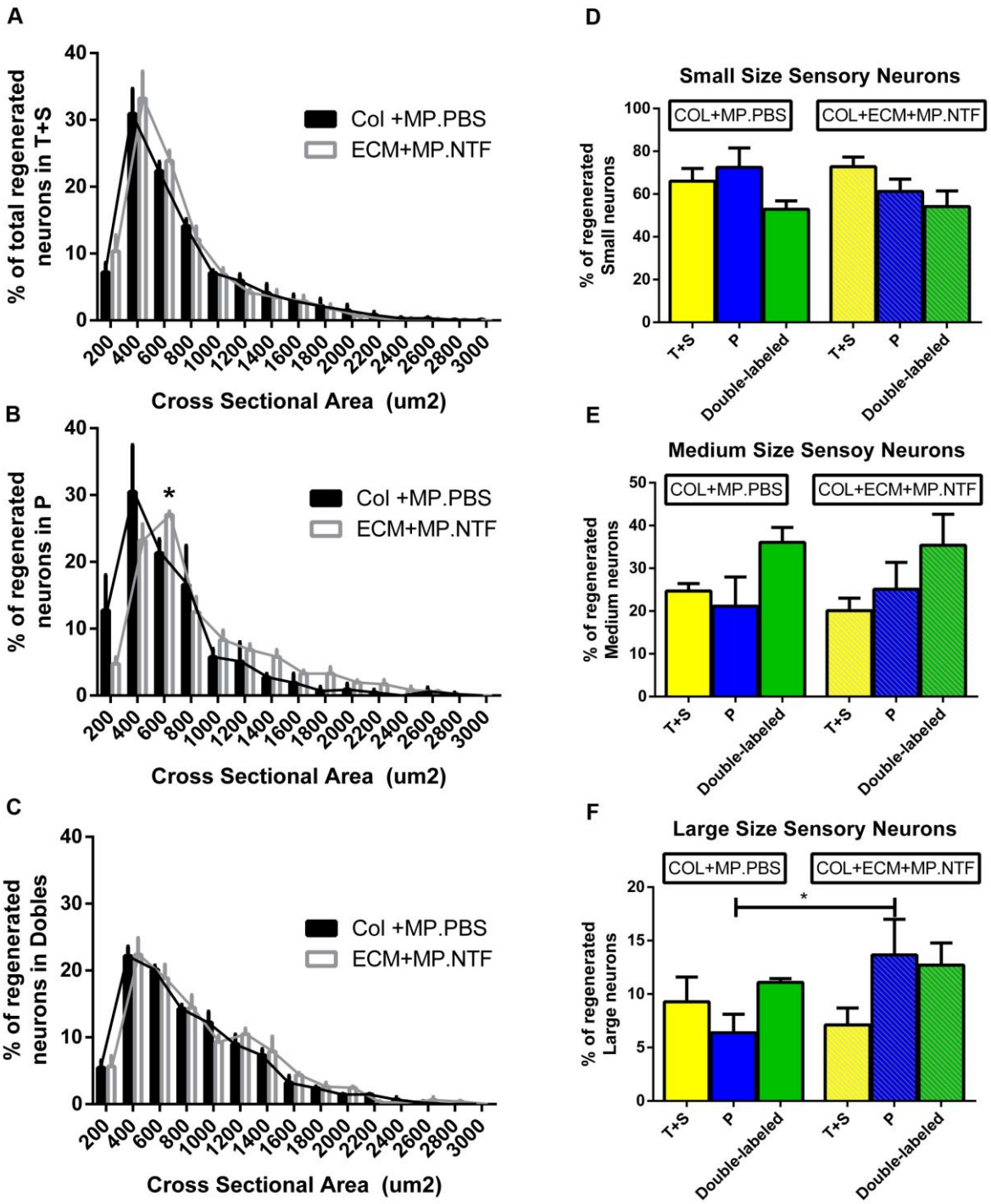

Figure 5. Morphometric analysis of regenerated SNs in the T+S nerves (A), P nerve (B) and in both branches (C) in the control (black bars) and experimental (white bars) groups. Histogram of regenerated small size (D), medium size (E) and large size sensory neurons (F) in the different branches of the Y tube in the two groups. Data expressed as mean ± SEM. *p<0.05.

We chose the two matrix combinations based on previous findings in vitro from our laboratory using organotypic cultures that demonstrated a preferential effect of fibronectin and BDNF to promote neurite growth from MNs and of laminin and NGF/NT-3 to promote neurite growth of SNs (Gonzalez-Perez et al., 2015; Santos et al 2016), and the synergistic effects reported in the previous chapter.

Retrotracer quantification of regenerated motor and sensory neurons when placing the control collagen matrix in the tube branches showed no significant differences between branches connected distally with the T+S nerves and the P nerve. Moreover, about 15% of motor and 9% of sensory neurons generated regenerative sprouts that grew towards both branches. Due to the fact that T, S and P are mixed nerves, no preferential motor or sensory neuron regeneration was expected (M. E. Brushart, 1993; T. Brushart et al., 1998). The higher percentage of motor and sensory neurons regenerating to the T+S branch than to the P branch can be attributed to the larger caliber of the former that contains larger number of Schwann cells that generate higher concentration of trophic and tropic factors (Robinson & Madison, 2004; Takahashi, Maki, Yoshizu, & Tajima, 1999; Uschold, Robinson, & Madison, 2007).

On the other hand, in the experimental group we found that adding FN+MP.BDNF at one branch of the tube and LM+MP.NGF/NT-3 to the other branch resulted in higher number of MNs that regenerated their axons towards the first condition compared to the control group. In accordance, higher CMAP amplitudes were recorded in TA muscles of animals treated with FN+MP.BDNF and lower CMAPS for the LM+MP.NGF/NT-3 indicating that more motor fibers had reinnervated the muscles provided by the P nerve than those by the T nerve. The addition of FN+MP.BDNF to the branch in contact with the P nerve was able to partially overcome the size attracting effect of the T+S nerves and attracted more than 50% of motor axons. In fact, BDNF is a potent neurotrophic factor for MNs regeneration both in vitro and in vivo (Allodi et al., 2011; Boyd & Gordon, 2002; Vögelin et al., 2006) and it has been also described that the same intracellular mechanisms that promote axonal growth and cell survival are related with axonal guidance (Henle et al., 2011; Yuan et al., 2003). Furthermore, fibronectin also preferentially promotes motor axon outgrowth in vitro (Gonzalez-Perez et al., 2015). In addition, it is possible that FN or BDNF act not only directly on the regenerating fibers but also they may promote the recruitment of motor-related Schwann cells (Jesuraj et al., 2012). The enhancing effect shown is of relevance given the reduced regeneration of motor fibers compared to sensory fibers in tube repair of mid to long gaps (Navarro et al., 1994; Madorsky et al 1998)

Contrary to our hypothesis, addition of laminin and NGF/NT-3 was not able to attract sensory axons, and in fact, a non significantly lower proportion of regenerating

SNs was labeled from the TS branch than with the control collagen gel. This result was corroborated by lack of differences in sensory functional recovery between both control and experimental groups. The lack of effect of LM+MP.NGF/NT-3 on SNs was not expected as previous studies described the guidance effect for laminin and NGF and NT-3 individually assessed (Gallo et al., 1997; Turney & Bridgman, 2005; Webber et al., 2008). One possible reason could be related with the heterogeneous populations of SNs (Usoskin et al., 2014) that reside in the DRG, in which approximately 70% of neurons express Trk receptors but of different subtypes whereas 30% are non-peptidergic neurons and respond to GDNF (Tucker & Mearow, 2008). Laminin substrate did not show effects on non-peptidergic neurons as they express α7 integrin receptor at low levels (Gardiner et al., 2005); but there are no studies assessing fibronectin for guidance of non-peptidergic axons. In addition, among the Trk+ SNs, a low percentage of neurons express only one type of Trk receptor (23%), whereas coexpression of different Trk receptors is more abundant (47%) (Karchewski LA et al., 1999). Then, the attracting effect mediated by the addition of LM+NGF/NT-3 could be masked by the heterogeneity of the DRG neuronal populations, which may be non responding to NGF and NT-3 or responding to BDNF, so that sorting sensory axons is a complex task. Hoke et al. (2006) reported that mRNA for NGF and also for BDNF, among others, were expressed vigorously by denervated cutaneous nerves. Therefore, it may be well considered that the increased supply of both factors one at each branch of the Y tube did not allow for an effective preferential guidance for sensory axons.

A first analysis of the differential growth of sensory axons was attempted by subdividing the regenerated SNs by soma size. Indeed, we observed a slight increase of medium and large SNs towards the FN+BDNF branch. It should be taken into account that proprioceptive neurons, characterized by their large size diameter (Taylor et al., 2005; Tucker & Mearow, 2008), respond to NT-3 (Lotfi et al., 2011) but also preferentially extend neurites on fibronectin containing substrates (Gonzalez-Perez et al., 2015). Taking into account that the FN+MP.BDNF branch attracted a high number of motor axons, it is plausible to think that such combination promotes also regeneration of large sensory neurons that are directed towards muscular targets. Indeed, during early development, muscle sensory axons grow slightly later and become adjacent to motor axons elongating along the muscular nerve to innervate the same muscle, reflecting specific attractions between them mediated by changes in expression of cell adhesion molecules. In contrast, developing cutaneous sensory axons bundle together, and project along individual cutaneous nerves (Honig et al 1998).

5. Conclusion

In this study we demonstrate that nerve regeneration is successful in a bicompartmental tube, in which the two branches may contain a matrix with different components. We found that motor axons regeneration was promoted preferentially in the branch containing fibronectin and BDNF. The same branch also attracted axons from large SNs, that might correspond mainly to proprioceptive neurons. On the other hand, the addition of laminin and NGF/NT-3 in the other branch did not promote the growth of sensory axons. Further studies are justified to enhance the effects obtained to segregate different functional populations of axons that may be of benefit for an advanced regenerative interface.

6. Acknowledgments

This research was supported by European Union FP7-NMP project MERIDIAN under contract number 280778, and FPT-ICT project NEBIAS under contract number 611687, TERCEL (RD12/0019/0011) and CIBERNED (CB06/05/1105) funds from the Instituto de Salud Carlos III of Spain, and FEDER funds. The authors thank the technical help of Monica Espejo and Jessica Jaramillo.

7. References

Abernethy, D. A., Rud, A., & Thomas, P. K. (1992). Neurotropic influence of the distal stump of transected peripheral nerve on axonal regeneration: absence of topographic specificity in adult nerve, 395–400.

Adams, D. N., Kao, E. Y., Hypolite, C. L., Distefano, M. D., Hu, W., & Letourneau, P. C. (2005). Growth Cones Turn and Migrate up an Immobilized Gradient of the Laminin IKVAV Peptide ABSTRACT : *Journal of Neurobiology*, *62*(1), 134–147.

Allodi, I., Guzmán-Lenis, M.-S., Hernàndez, J., Navarro, X., & Udina, E. (2011). In vitro comparison of motor and sensory neuron outgrowth in a 3D collagen matrix. *Journal of Neuroscience Methods*, *198*(1), 53–61.

Allodi, I., Udina, E., & Navarro, X. (2012). Specificity of peripheral nerve regeneration : Interactions at the axon level. *Progress in Neurobiology*, *98*, 16–37.

Bloch, J., Fine, E. G., Bouche, N., Zurn, a D., & Aebischer, P. (2001). Nerve growth factor- and neurotrophin-3-releasing guidance channels promote regeneration of the transected rat dorsal root. *Experimental Neurology*, *172*(2), 425–32.

Bodine-Fowler SC, Meyer RS, Moscowitz A, Abrams R, Botte M. 1997. Innaccurate projection of rat soleus motoneurons: a comparison of nerve repair techniques. Muscle Nerve 20:29-37.

Boyd, J. G., & Gordon, T. (2002). A dose-dependent facilitation and inhibition of peripheral nerve regeneration by brain-derived neurotrophic factor. *European Journal of Neuroscience*, *15*(4), 613–626.

Brushart, M. E. (1993). Motor Axons Preferentially Reinnervate Motor Pathways. *The Journal of Neuroscience*, *13*(6), 2730–2738.

Brushart, T. (1988). Preferential Axons Reinnervation of Motor Nerves by Regenerating Motor. *The Journal of Neuroscience*, *8*(3), 1026–1031.

Brushart, T., Gerber, J., Kessens, P., Chen, Y., & Royall, R. (1998). Contributions of Pathway and Neuron to Preferential Motor Reinnervation, *18*(21), 8674–8681.

Brushart, T. M., Aspalter, M., Griffin, J. W., Redett, R., Hameed, H., Zhou, C., Wright, M., Vyas, A., Höke, A. (2013). Schwann cell phenotype is regulated by axon modality and central-peripheral location, and persists in vitro. *Experimental Neurology*, *247*, 272–81.

Carrozza, M. C., Cappiello, G., Micera, S., Edin, B. ., Beccai, L., & Cipriani, C. (2006). Design of a cybernetic hand for perception and action. *Biol Cybern*, *95*, 629–644.

Clements, I. P., Kim, Y., English, A. W., Lu, X., Chung, A., & Bellamkonda, R. V. (2009). Thin-film enhanced nerve guidance channels for peripheral nerve repair. *Biomaterials*, *30*(23-24), 3834–46.

Cobianchi, S., de Cruz, J., & Navarro, X. (2014). Assessment of sensory thresholds and nociceptive fiber growth after sciatic nerve injury reveals the differential contribution of collateral reinnervation and nerve regeneration to neuropathic pain. *Experimental Neurology*, *255*, 1–11.

Evans PJ, Bain JR, Mackinnon SE, Makino AP, Hunter DA. 1991. Selective reinnervation: a comparison of recovery following microsuture and conduit nerve repair. Brain Res 559:315-321

Fukuoka T, Kondo E, Dai Y, Hashimoto N, Noguchi K (2001). Brain-derived neurotrophic factor increases in the uninjured dorsal root ganglion neurons in selective spinal nerve ligation model. J Neurosci 21: 4891–4900.

Gallo, G., Lefcort, F. B., & Letourneau, P. C. (1997). The trkA Receptor Mediates Growth Cone Turning toward a Localized Source of Nerve Growth Factor, *17*(14), 5445–5454.

Gardiner, N. J. (2011). Integrins and the extracellular matrix: key mediators of development and regeneration of the sensory nervous system. *Developmental Neurobiology*, *71*(11), 1054–72.

Gardiner, N. J., Fernyhough, P., Tomlinson, D. R., Mayer, U., von der Mark, H., & Streuli, C. H. (2005). Alpha7 integrin mediates neurite outgrowth of distinct populations of adult sensory neurons. *Molecular and Cellular Neurosciences*, *28*(2), 229–40.

Giudetti, G., del Valle Macià, J., Navarro Acebes, X., & Micera, S. (2014). NGF-loaded PLGA microparticles for advanced multifunctional regenerative electrodes. *Conf Proc IEEE Eng Med Biol Soc.*, 1993–1995.

Gonzalez-Perez, F., Alé, A., Santos, D., Barwig, C., Freier, T., Navarro, X., & Udina, E. (2015). Substratum preferences of motor and sensory neurons in postnatal and adult rats. *The European Journal of Neuroscience*, 1–12.

Gonzalez-Perez, F., Udina, E., & Navarro, X. (2013). Extracellular matrix components in peripheral nerve regeneration. *International Review of Neurobiology*, *108*, 257–275.

Gundersen, H. J. (1986). Stereology of arbitrary particles. A review of unbiased number and size estimators and the presentation of some new ones, in memory of William R. Thompson. *Journal of Microscopy*, *143*, 3–45.

Henle, S. J., Wang, G., Liang, E., Wu, M., Poo, M., & Henley, J. R. (2011). Asymmetric PI (3 , 4 , 5) P 3 and Akt Signaling Mediates Chemotaxis of Axonal Growth Cones. *The Journal of Neuroscience*, *31*(19), 7016–7027.

Höke, A., Redett, R., Hameed, H., Jari, R., Zhou, C., Li, Z. B., Griffin, J.W., Brushart, T. M. (2006). Schwann cells express motor and sensory phenotypes that regulate axon regeneration. *The Journal of Neuroscience*, *26*(38), 9646–55.

Honig MG, Frase PA, Camilli SJ. The spatial relationship among cutaneous, muscle sensory and motoneuron axons during development of the chick hindlimb. Development 1998, 125:995-1004.

Jerregård, H., Nyberg, T., & Hildebrand, C. (2001). Sorting of Regenerating Rat Sciatic Nerve Fibers with Target-Derived Molecules. *Experimental Neurology*, *306*, 298–306.

Jesuraj, N. J., Nguyen, P. K., Wood, M. D., Moore, A. M., Borschel, G. H., Mackinnon, S. E., & Sakiyama-Elbert, S. E. (2012). Differential gene expression in motor and sensory Schwann cells in the rat femoral nerve. *Journal of Neuroscience Research*, *90*(1), 96–104.

Kemp, S. W. P., Webb, A. A, Dhaliwal, S., Syed, S., Walsh, S. K., & Midha, R. (2011). Dose and duration of nerve growth factor (NGF) administration determine the extent of behavioral recovery following peripheral nerve injury in the rat. *Experimental Neurology*, *229*(2), 460–70.

Lago N, Rodríguez FJ, Guzmán MS, Jaramillo J, Navarro X. Effects of motor and sensory nerve transplants on amount and specificity of sciatic nerve regeneration. J Neurosci Res. 2007; 85(12):2800-12.

Lee, A. C., Yu, V. M., Lowe, J. B., Brenner, M. J., Hunter, D. A, Mackinnon, S. E., & Sakiyama-Elbert, S. E. (2003). Controlled release of nerve growth factor enhances sciatic nerve regeneration. *Experimental Neurology*, *184*(1), 295–303.

Li, Y., Jia, Y., Cui, K., Li, N., Zheng, Z., Wang, Y., & Yuan, X. (2005). Essential role of TRPC channels in the guidance of nerve growth cones by brain-derived neurotrophic factor. *Nature*, *434*(April), 1–5.

Lotfi, P., Garde, K., Chouhan, A. K., Bengali, E., & Romero-Ortega, M. I. (2011). Modality-specific axonal regeneration: toward selective regenerative neural interfaces. *Frontiers in Neuroengineering*, *4*(10), 1–11.

Madison RD, Robinson GA, Chadaram SR. The specificity of motor neurone regeneration (preferential reinnervation). Acta Physiol 2007; 189, 201–206.

Madison, R. D., Archibald, S. J., & Brushart, T. M. (1996). Reinnervation accuracy of the rat femoral nerve by motor and sensory Neurons. *The Journal of Neuroscience*, *16*(18), 5698–5703.

Madorsky SJ, Swett JE, Crumley RL. Motor versus sensory neuron regeneration through collagen tubules. Plast Reconstr Surg. 1998;102:430-6; discussion 437-8.

Martini R, Xin Y, Schmitz B, Schachner M. 1992. The L2/HNK-1 carbohydrate epitope is involved in the preferential outgrowth of motor neurons on ventral roots and motor nerves. Eur J Neurosci 4:628–639.

Martini R, Schachner M, Brushart TM. 1994. The L2/HNK-1 carbohydrate is preferentially expressed by previously motor axon associated Schwann cells in reinnervated peripheral nerves. J Neurosci 14:7180– 7191.

Meyer, C., Stenberg, L., Gonzalez-Perez, F., Wrobel, S., Ronchi, G., Udina, E., … Haastert-Talini, K. (2016). Chitosan-film enhanced chitosan nerve guides for long-distance regeneration of peripheral nerves. *Biomaterials*, *76*, 33–51.

Moore, K., Macsween, M., Shoichet, M. (2006). Immobilized Concentration Gradients of Neurotrophic Factors Guide Neurite Outgrowth of Primary Neurons in Macroporous Scaffolds. *Tissue Engineering*, *12*(2), 19–21.

Navarro X, Verdú E, Butí M. Comparison of regenerative and reinnervating capabilities of different functional types of nerve fibers. Exp Neurol 1994, 129:217-224.

Plantman, S., Patarroyo, M., Fried, K., Domogatskaya, A., Tryggvason, K., Hammarberg, H., & Cullheim, S. (2008). Integrin-laminin interactions controlling neurite outgrowth from adult DRG neurons in vitro. *Molecular and Cellular Neurosciences*, *39*(1), 50–62.

Rende M, Granato A, Manaco ML, Zelagno G, Toesca A. 1991. Accuracy of reinnervation by peripheral nerve axons regenerating across 10 mm gap within an impermeable chamber. Exp Neurol 111:332-339.

Robinson, G. A, & Madison, R. D. (2004). Motor neurons can preferentially reinnervate cutaneous pathways. *Experimental Neurology*, *190*(2), 407–13.

Saito H, Nakao Y, Takayama S, Toyama Y, Asou H. 2005. Specific expression of an HNK-1 carbohydrate epitope and NCAM on femoral nerve Schwann cells in mice. Neurosci Res 53:314-322

Schindelin, J., Arganda-Carreras, I., Frise, E., Kaynig, V., Longair, M., Pietzsch, T., Preibisch, S., Rueden, C., Saalfeld, S., Schmid, B., Tinevez, J-Y., White, D.J., Hartenstein, V., Eliceiri, K., Tomancak, P., Cardona, A. (2012). Fiji: open-source platform for biological-image analysis. Nat. Methods 9, 676–82.

Song, H., Ming, G., Poo, M., Shiro, M., Tomb, J., White, O., … Bergman, M. I. (1997). cAMP-induced switching in turning direction of nerve growth cones corrections Synthesis and X-ray structure of errata The complete genome sequence of the gastric pathogen Helicobacter pylori Measurements of elastic anisotropy due to solidification texturi. *Nature*, *389*(September), 1211–1212.

Sternel, G. D., Brown, R. A., Green, C. J., & Terenghi, G. (1997). Neurotrophin-3 Delivered Locally via Fibronectin Mats Enhances Peripheral Nerve Regeneration. *European Journal of Neuroscience*, *9*, 1388–1396.

Takahashi, Y., Maki, Y., Yoshizu, T., & Tajima, T. (1999). Both stump area and volume of distal sensory nerve segments influence the regeneration of sensory axons in rats. *Scand J Plast Reconstr Hand Surg*, (8), 177–180.

Taylor, M. D., Holdeman, A. S., Weltmer, S. G., Ryals, J. M., & Wright, D. E. (2005). Modulation of muscle spindle innervation by neurotrophin-3 following nerve injury. *Experimental Neurology*, *191*(1), 211–22.

Tucker, B. A., & Mearow, K. M. (2008). Peripheral Sensory Axon Growth: From Receptor Binding to Cellular Signaling. *The Canadian Journal of Neurological Sciences*, *35*(05), 551–566.

Turney, S. G., & Bridgman, P. C. (2005). Laminin stimulates and guides axonal outgrowth via growth cone myosin II activity. *Nature Neuroscience*, *8*(6), 717–719.

Uschold, T., Robinson, G. A, & Madison, R. D. (2007). Motor neuron regeneration accuracy: balancing trophic influences between pathways and end-organs. *Experimental Neurology*, *205*(1), 250–6.

Usoskin, D., Furlan, A., Islam, S., Abdo, H., Lönnerberg, P., Lou, D., … Ernfors, P. (2014). Unbiased classification of sensory neuron types by large-scale single-cell RNA sequencing. *Nature Neuroscience*, *18*(1), 145–153.

Valero-Cabré A, Navarro X. H reflex restitution and facilitation after different types of peripheral nerve injury and repair. Brain Res 2001, 919:302-312.

Valero-Cabré A, Tsironis K, Skouras E, Navarro X, Neiss WF. 2004. Peripheral and spinal motor reorganization after nerve injury and repair. J Neurotrauma 21:95-108

Valero-Cabré A, Tsironis K, Skouras E, Perego G, Navarro X, Neiss WF. 2001. Superior muscle reinnervation after autologous nerve graft or poly-l-lactide- γ-caprolactone (PLC) tube implantation in comparison to silicone tube repair. J Neurosci Res 63:214-223.

Verdú E, Labrador RO, Rodríguez FJ, Ceballos D, Forés J, N. X. (2002). Alignment of collagen and laminin-containing gels improve nerve regeneration within silicone tubes. *Restor Neurol Neurosci.*, *20*, 169–180.

Vögelin, E., Baker, J. M., Gates, J., Dixit, V., Constantinescu, M. A, & Jones, N. F. (2006). Effects of local continuous release of brain derived neurotrophic factor (BDNF) on peripheral nerve regeneration in a rat model. *Experimental Neurology*, *199*(2), 348–53.

Webber, C., Xu, Y., Vanneste, K., Martinez, J., Verge, V., & Zochodne, D. (2008). Guiding Adult Mammalian Sensory Axons During Regeneration. *J Neuropathol Exp Neurol.*, *67*(3), 212–222.

Yuan, X., Jin, M., Xu, X., Song, Y., Wu, C., Poo, M., & Duan, S. (2003). Signalling and crosstalk of Rho GTPases in mediating axon guidance. *Nature Cell Biology*, *5*, 1–8.

Zele, T., Sketelj, J., & Bajrović, F. F. (2010). Efficacy of fluorescent tracers in retrograde labeling of cutaneous afferent neurons in the rat. *Journal of Neuroscience Methods*, *191*(2), 208–14.

CHAPTER 4

Fascicular nerve stimulation and recording using a novel double-aisle regenerative electrode

Daniel Santos [1,2], Ignacio Delgado-Martinez [1], Martina Righi [3], Anarita Cutrone [3], Jordi Badia [1], Silvestro Micera [3,4,5], Jaume del Valle [1,2], Xavier Navarro [1,2]

[1] Institute of Neurosciences, Department of Cell Biology, Physiology and Immunology, Universitat Autònoma de Barcelona, Bellaterra, Spain
[2] Centro de Investigación Biomédica en Red sobre Enfermedades Neurodegenerativas (CIBERNED), Bellaterra, Spain
[3] The Biorobotics Institute, Scuola Superiore Sant'Anna, Viale Rinaldo Piaggio 34, I-56025, Pontedera(PI), Italy
[4] Bertarelli Chair in Translational NeuroEngineering, Institute of Bioengineering, School of Engineering, Ecole Polytechnique Federale de Lausanne, Lausanne, Switzerland
[5] Center for Neuroprosthetics, Ecole Polytechnique Federale de Lausanne (EPFL), Lausanne, Switzerland

Corresponding author: Dr. Xavier Navarro, Unitat de Fisiologia Mèdica, Facultat de Medicina, Universitat Autònoma de Barcelona, E-08193 Bellaterra, Spain. E-mail: xavier.navarro@uab.cat

Running title: Fascicular selectivity using a double-aisled regenerative electrode

Abstract

Neuroprosthetic devices are aimed to restore sensorimotor limb function of the amputee patients. However, high selective electrodes are needed to transduce all the signals generated by the nervous system and provide close loop commands to the user. In this study, we show the selective stimulation of different nerve fascicles using a novel double-channel regenerative electrode. The design consists on a polyimide thin-film layer inserted across a silicone tube, creating two separated aisles in which regenerating fascicles can regrowth independently after sciatic nerve transaction. Implantation of the electrodes in acutely transected nerves of rats showed the capability of selectively stimulating and recording different fascicles implanted in the aisles. Chronic implantation of the electrode as a bridge between fascicles ends showed high number of myelinated axons located near the electrode and reinnervation of distal target muscles indicating no impairment of the regeneration process and good biocompatibility. After 90 days post-implantation, we were able to stimulate and record independently from each of the regenerated fascicles in the separated aisles. Our results demonstrate the potential contribution of the doubled-aisled regenerative electrode to selectively interface different nerve fascicles with no deleterious effects in nerve regeneration.

Key words: regenerative electrode, selectivity, nerve regeneration, neural interface.

1. Introduction

Interest on peripheral neural prostheses has rapidly grown in the last years as a therapeutic tool for the restoration or replacement of neural function after peripheral nerve disorders. The aim is to enable a bi-directional communication establishing a direct link between the nerve tissue and an artificial device through the use of peripheral nerve electrodes (Oddo et al., 2016; Raspopovic et al., 2014). Since nerves contain thousands of nerve fibers, interfacing each one of them with a corresponding electrode is an unrealistic task. Therefore, different strategies in the design of electrodes have been used to tackle specific problems in neural interfacing. Higher selectivity of communication with individual nerve fibers implies higher invasivity and thus potential damage to the nerve (del Valle and Navarro, 2013). On the other way, a more respectful approach to the nerve implies a lower quality of the communication, since the distance from the electrode to individual axons must increase (Badia et al., 2011a).

Regenerative electrodes represent the most ambitious design in communication quality terms since they may provide the highest axon-to-electrode ratio, signal-to-noise ratio, and other quality parameters (Stieglitz et al., 1996; Thompson et al., 2016). They are thought to be implanted in a nerve that will undergo regeneration so that axons can be redirected to the vicinity of the active sites of the neural interface during the regrowth process (Dario et al., 1998). The earliest design of this kind of neural interfaces was the sieve electrode. Here, a laminar electrode is facing the transected nerve stump, forcing the axons to grow through the wholes, each containing an active site (Lago et al., 2005). As a result, each active site contacts a small number of axons (~10-40) (Ceballos et al., 2002; Lago et al., 2007b). However, since the electrode transparency (i.e. the easiness for the axons to grown across the electrode) is low, nerve regeneration may be compromised (Edell, 1986; Navarro et al., 1996; Zhao et al., 1997).

More recently, the regenerative electrodes have evolved into more sophisticated designs, such as the microchannel electrodes (Lacour et al., 2009). Axonal have to grow within embedded microchannels, allowing selective electrophysiological interfacing of different subpopulations of axons. However, the regeneration of miniature nerve fascicles is sharply reduced in implants with gap defects longer than 2 mm. Romero-Ortega and colleagues proposed a neural interface that would parcel axonal fibers toward target sites by incorporating chemical cues to select different axon types and improve selectivity, while allowing axons to regenerate in a more efficient and

natural way (Lotfi et al., 2011). Based in this concept, (I. Clements et al., 2013) designed the regenerated scaffold electrode (RSE) in which the regrowing nerve was bifurcated in two regenerating fascicles containing both myelinated and unmyelinated fibers of varying diameter and the rest of neural structures of a mature nerve. Despite the promising results of the RSE, the potential use for neuroprosthetic applications has not been proved.

In this work, we present a new design of regenerative electrode based on the RSE. Here we used a thin-film polyimide planar multi-contact electrode to serve as a "septum" to divide a tubular silicone graft into two ample "aisles", in which regenerating fascicles can grow independently. We show that this "double-aisle" regenerative electrode can be used to selectively record and stimulate fascicles in each of the aisles, acutely as well as chronically. More importantly, we prove the electrode does not impair fascicle regrowth. Multi-aisled regenerative electrodes may represent a significant advance in neuroprosthetic applications where sub-fascicular selectivity of an injured nerve is essential.

2. Materials and Methods

2.1. Development of the planar regenerative electrode

The double-aisle regenerative electrode (Fig. 1) is characterized by a planar multi-electrode septum and a nerve guidance aisle or compartment at each side. It is designed to be longitudinally inserted inside a 10 mm long silicone tube with an internal diameter of 2 mm.

The planar structure contains a total of 24 gold active sites, half at each side (Fig. 1A). The active sites have a circular shape with a diameter of 60 µm, and they are arranged around the center of the lumen of the tube. This distribution was chosen because of the nerve tendency to mainly regenerate along the central axis of the conduit while regeneration at the periphery of the tube is reduced. Consecutive sites have horizontal and vertical offset to ensure a greater coverage (0.8 x 4 mm^2) of the regeneration area: the pitch between active sites is 350 µm in horizontal and 380 µm in vertical plane. A reference electrode with the same dimension of the active sites is present on both the surfaces and located outside of the silicone tube. The double-aisle regenerative electrode was manufactured following standard lithographic techniques previously used for thin-film based electrodes (Cutrone et al. 2015; Boretius et al 2010,). Polyimide was used as the insulating and flexible polymer for the entire electrode layout, while the active parts (active sites, electrical tracks and pads) were obtained by using a thin film

of titanium coated with gold. The selected materials are well known for their biocompatibility, mechanical integrity and electrical efficacy (Rubehn and Stieglitz 2010).

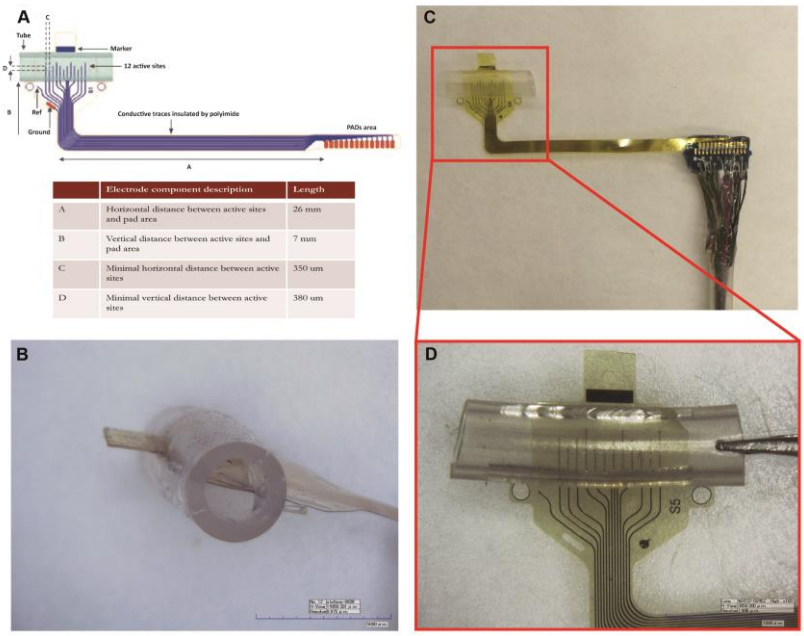

	Electrode component description	Length
A	Horizontal distance between active sites and pad area	26 mm
B	Vertical distance between active sites and pad area	7 mm
C	Minimal horizontal distance between active sites	350 um
D	Minimal vertical distance between active sites	380 um

Figure 1. A: Layout of the double-aisled regenerative electrode. **B:** Close view the two created aisles by the insertion of the polyimide septum **C:** Micrograph of the device with the AS sites area inserted into the silicone tube and the PCB connected to the pad area and to wires. **D:** Close view of the electrode inside a silicone tube of C image showing the distribution of the AS into the tube.

The packaging of the double-sided septum of the regenerative electrode (Fig. 1B) was obtained by sealing together two symmetric single-sided electrodes provided with a connection to PCB and wires and inserted through a silicone tube (length = 10 mm; external diameter = 3 mm; internal diameter = 2 mm) used as guidance channel for nerve regeneration. Using tweezers, the double-sided electrode was carefully inserted inside the tube and accurately placed to get a flat configuration and to divide the entire volume of the cylinder in two equal ones. The use of gold markers and the enlargements allowed to properly set the electrode inside the chamber so to get the best spatial distribution of the active sites inside the bi-chamber volume. A small amount of cyanoacrylate glue was used to seal the cut parts of the tube and to ensure electrode stability inside the channel. The wires for electrical connections were inserted into an additional clean flexible silicone tube and sealed with biocompatible UV glue (Dymax). A two component biocompatible silicone (Silbione-Bluestar Silicones) was

used to cover the electrical connections on the PCB, the gold marker area and the two cuts on the silicone tube previously glued together.

2.2. Surgical procedures

Female Sprague-Dawley rats (250–300 g) were used for the in vivo studies. All experimental procedures performed were approved by the Ethical Committee of the *Universitat Autònoma de Barcelona* in accordance with the European Communities Council Directive 2010/63/EU. Adequate measures were taken to minimize pain and animal discomfort during surgery and in the postoperative follow-up. After surgeries animals were left to recover under a warm environment for 24 hours and then were housed in peer groups at 22±2ºC under a 12:12h light cycle with food and water with amitriptyline to prevent autotomy *ad libitum*. All efforts were made to minimize animal suffering and to reduce the number of animals used.

All surgeries were performed under anesthesia with ketamine and xylacine (90 / 10 mg/kg i.p.). Under a dissecting microscope the sciatic nerve was surgically exposed at the midthigh, and a 3 mm nerve segment was resected. For the acute electrophysiological testing (n=4), the peroneal nerve was dissected and introduced in one aisle of the regenerative electrode, whereas the bundle containing the tibial and sural nerves was dissected and introduced in the other aisle, both in close contact with the active sites (AS) of the regenerative electrode. The nerve ends were fixed by an epineural 10-0 monofilament suture to the proximal edge of the corresponding aisle (Fig 3A) during the realization of the tests. Sectioned nerves were able to conduce action potentials during the experimental period as denervated axons begin to show some signs of degeneration 1 or 2 days post injury (Glass et al., 2002). Afterwards, the nerve ends were released and sutured separately again at the distal ends of both aisles of the regenerative electrode. The sciatic proximal nerve stump was then sutured to the proximal edge of the regenerative electrode leaving a 6 mm gap to allow for regeneration (n=4) (Fig. 2A). Next, the muscle plane was sutured with 6-0 sutures, leaving the PCB in the subdermal compartment. The wires were routed subcutaneously along the back of the animal. Finally, the skin was sutured with 3-0 silk sutures and the wound was disinfected.

2.3. Electrophysiological tests

During all the experiments, the animals were anesthetized and kept warm with a heating pad. Stimulation tests were done by applying monophasic rectangular pulses of 20 μs width using each of the 24 AS alternatively as anode and a steel needle placed

on the proximal segment of the sciatic nerve or the reference site as cathode, for monopolar or bipolar stimulation, respectively. The pulses were delivered by a Grass stimulator (S44, Grass; West Warwick, RI, USA). Compound muscle action potentials (CMAPs) of the Tibialis anterior (TA) and Gastrocnemius (GM) muscles were simultaneously recorded with steel monopolar needles inserted into the muscle belly. The signals were amplified at 200x to 2000x using P511 AC (Grass) amplifiers and digitally sampled with a PowerLab recording system at 20,000 Hz (PowerLab16SP, ADInstruments, Bella Vista, Australia) controlled by LabChart v7 (ADInstruments).

Acute and chronic recording tests were performed by recording compound nerve action potentials (CNAPs) after distal electrical stimulation or nerve signals after sensory stimulation. CNAPs were elicited by delivering monophasic rectangular pulses of 20 μs width through two needle electrodes placed at the ankle level and the paw for the stimulation of the tibial nerve. Sensory stimulation was performed as previously described (Raspopovic et al., 2010) by applying fast scratch and pressure stimuli to the skin of the sole of the rat. Electroneurography (ENG) signals were amplified at 5,000X and sampled at 20,000 Hz.

To assess nerve regeneration, nerve conduction tests were conducted 3 months after implantation. Briefly, under anesthesia, the sciatic nerve was stimulated with single electrical pulses (50 μs duration and supramaximal intensity) delivered by monopolar intradermal steel needles placed at the sciatic notch and CMAP of TA and GM muscles was recorded using monopolar needle electrodes placing the active one in the muscle belly and the reference in the fourth toe (Valero-Cabré and Navarro, 2002). The amplitude and the latency of the M-wave were measured. Values of the contralateral intact limb were used as control. During the tests, the rat body temperature was maintained by means of a thermostated warming flat coil.

2.4. Histological studies

Three months after implantation, the sciatic nerves were harvested to evaluate the morphology of the regenerated nerve. Rats were deeply anesthetized and perfused with 4% paraformaldehyde in PBS. The sciatic nerve segment including the electrode implant was collected and divided in two parts. The proximal half was postfixed in the same perfusion solution for 4 h. Then samples were washed and embedded in optimal cutting temperature (OCT) cryostat-embedding compound (*Tissue-Tek*; Torrance, CA, USA), cut into 15 μm thick transverse sections on a cryostat (Leica Microsystems, Germany), mounted in gelatin-coated slides, and stored upon further staining at -20ºC.

Slides were allowed to thaw at room temperature and then rehydrated with PBS for 5 min. Then, nerve sections were blocked and permeabilized with PBS containing 5% normal donkey serum (S30, Millipore) and 0.3% Triton-X-100 (Sigma–Aldrich) for 20 min. After washes in PBS, slides were incubated with primary antibodies for myelinated axons (RT97, 1:200, Developmental Studies Hybridoma Bank), Schwann cells (S100, 1:200, Immunostar) and macrophages (iba-1, 1:500, Wako) overnight at 4ºC diluted in 0.1% Triton-X-100 (Sigma–Aldrich). They were then washed again and incubated for 1 h at room temperature in the dark with Alexa 488 or Alexa 594-conjugated secondary antibodies (1:200; Life Technologies), or, for anti-S100 antibody, with biotinilated anti-mouse secondary antibody (1:200, Vector) and then for 1 hour with Alexa 594-conjugated streptavidin (1:200, Life Technologies). Finally, slides were washed, mounted using mowiol with DAPI (0.1 ng/ml, Sigma), allowed to dry overnight at room temperature and stored at 4ºC. Image acquisition was performed with a fluorescence microscope (BX51, Olympus).

The distal half of the nerve was postfixed in 3% glutaraldehyde-3% paraformaldehyde in buffer solution, and processed for embedding in epon. Semithin 0.5 µm thick sections were stained with toluidine blue, examined under microscope (BX51, Olympus) and pictures were taken using an Olympus DP50 digital camera. Sets of images for analysis obtained at 100x magnification were chosen by systematic random sampling of squares representing at least 30% of each fascicle cross-sectional area and measurements of cross-sectional area of the whole nerve and counts of the number of myelinated nerve fibers were conducted.

2.5. Data and statistical analysis

Analysis of the electrophysiological data was done using LabChart v7.0. Total power of the electrophysiological recordings was obtained by calculating the short-time Fourier transform in a window of 1 ms and an overlap of 87.5 %. Values are presented as mean ± SEM and results were statistically analyzed using GraphPad Prism software.

3. Results

3.1. The double-aisle regenerative electrode allows selective stimulation and recording of nerve fascicles

To test the fascicle selectivity of the regenerative electrode, we implanted a double-aisle regenerative electrode in the sciatic nerve of four rats. The peroneal and tibial fascicles were dissected and introduced each in one of the two aisles of the device for acute electrophysiological testing. To check for stimulation selectivity we applied a

series of stimuli in small increasing steps to each of the 12 AS at both sides of the septum while the CMAPs of TA muscle, innervated by the peroneal nerve, and GM muscle, innervated by the tibial nerve, were recorded. The results were compared to the pattern obtained by the combined stimulation of all the AS (from here on, control stimulation). The results show that selective stimulation of the two separate fascicles was possible from each of the aisles (Fig. 2B). However, the selectivity was variable between AS from the same side of the septum (Fig. 2C), probably due to the relative position between the active site and the fascicle axis. The maximum selectivity index (SI_{max}) of the AS was 0.93 ± 0.03 for the TA and 0.87 ± 0.07 for the GM (Fig. 2E), and the stimulation threshold to evoke the SI_{max} was 8.5 ± 2.33 V and 11.5 ± 1.79 V (Fig. 2D), respectively. As the stimulation intensity increased, cross-activation of the antagonist muscle increased as well (Badia et al., 2011a), leading to poorer selectivity. However, this phenomenon can ba also attributed at least in part to cross-talk between recording in the two closely located muscles, TA and GM (Valero-Cabré and Navarro, 2002). Overall, 70% of the ASs in the aisle in which the peroneal nerve was inserted elicited a TA CMAP of maximal amplitude similar to the control stimulation (39.8 ± 3.2 mV for single AS stimulation and 38.9 ± 3.0 mV for control stimulation), but with a GM CMAP significantly smaller than the control. Similarly, when using the aisle containing the tibial fascicle for stimulation, 50% of the AS evoked a GM CMAP undistinguishable from control stimulation (48.4 ± 5.4 mV for single AS stimulation and 47.9 ± 6.0 mV for control stimulation) with only a small TA CMAP (Fig. 2C).

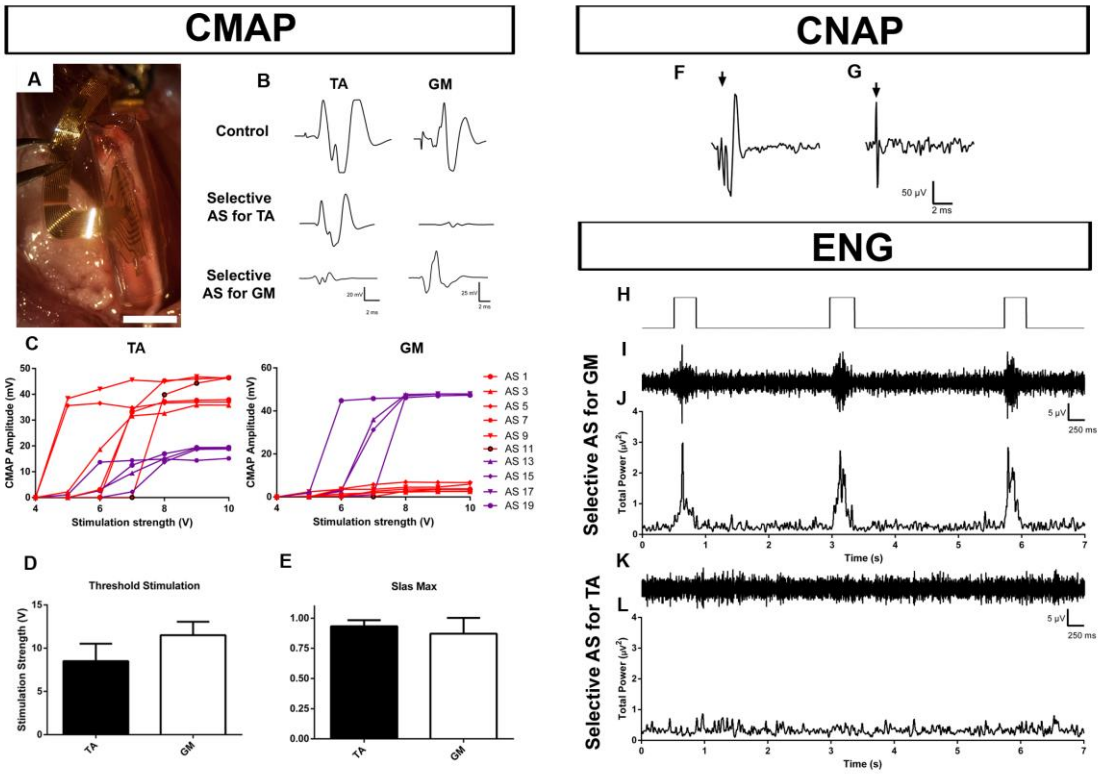

Figure 2. A: Micrograph of a transected peroneal, tibial and sural nerves fixed by an epineural 10-0 monofilament suture to the proximal edge of the corresponding aisle during the realization of the acute tests. **B:** Representative CMAP amplitudes recorded from the TA and GM muscles, evoked by electrical stimulation derived from selected AS. **C:** Recruitment curves for TA and GM muscles tested with stimulation delivered by selective AS of a regenerative electrode implanted in the sciatic nerve of a rat. Plots representing the threshold stimulation (**D**) and SIas Max (**E**) for TA and GM muscles. Representative CNAP amplitude recorded in AS situated in aisles containing the tibial nerve (**F**) and peroneal nerve (**G**). Raw signals recorded in the AS facing the tibial-sural bundle (**I**) or the peroneal nerve (**K**) after touch stimulation (fast scratch) during the intervals indicated in **H**. Total power spectrum analysis of the raw signals showed increased activity in the tibial-sural bundle (**J**) but not in the peroneal nerve (**L**). Scale bar: 3 mm

Similarly, nerve signals were recorded only from the AS located in the proximity of the corresponding nerve fascicle inside the aisle. CNAPs evoked by electrical stimulation at the ankle showed a peak-to-peak amplitude of 151.4 ± 13.7 μV (n=11) recorded from AS from the aisle containing the tibial-sural bundle and 9.3 ± 2.9 μV (n=15) from those in the aisle containing the peroneal nerve (Fig. 2F). Similarly, sensory stimulation of the foot produced an increase in the total power of the signal (Fig. 2L) recorded from the selected AS facing the tibial-sural bundle (during rest, 11.2 ± 1.3 pV^2; during stimulation, 171.6 ± 62.2 pV^2, n=20) but not from those in the aisle containing the peroneal nerve (during rest, 17.0 ± 3.2 pV^2, n=22; during stimulation, 26.4 ± 5.5 pV^2, n=20). This indicated that nerve signals originated from the selective stimulation of the tibial nerve sensory fibers (Navarro et al., 2007) were not incorrectly detected by the AS located in the aisle containing the peroneal nerve.

3.3. Chronically implanted electrodes allow for selective stimulation and recording

After 3-6 months chronical implantation, we tested if the double-aisle device was still able to interface the regenerated sciatic nerve following similar testing as above. Selective stimulation and recording of the regenerated tibial and peroneal fascicles was again possible (Fig. 3). Stimulation from AS of the aisle where the peroneal nerve was distally inserted elicited activation of the TA muscle similar to the one obtained by stimulation of the sciatic nerve proximal to the injury (CMAP amplitude 14.4 ± 0.1 mV, and 13.8 ± 0.7 mV, n=6, respectively) but very low or absent for the GM muscle (CMAP amplitude 2.6 ± 0.1 mV, and 18.4 ± 0.9 mV for control, n=6). Conversely, stimulation from the AS of the aisle containing the tibial-sural bundle provoked a contraction of the GM similar to the stimulation from the sciatic notch (CMAP amplitude 16.6 ± 0.9 mV, n=8) with little activation of the TA muscle (CMAP amplitude of 1.3 ± 0.3 mV, n=8) (Fig 3A).

Similarly to the acute testing, afferent signals were also selectively recorded from the aisle connecting to the tibial-sural bundle evoked by either electrical stimulation of the nerve at the ankle (Fig. 3B) or by mechanical stimuli on the paw (Fig. 3D-H) in the AS in contact with the tibial nerve. On the other hand, no signals were detected in the aisle where the peroneal nerve was sutured.

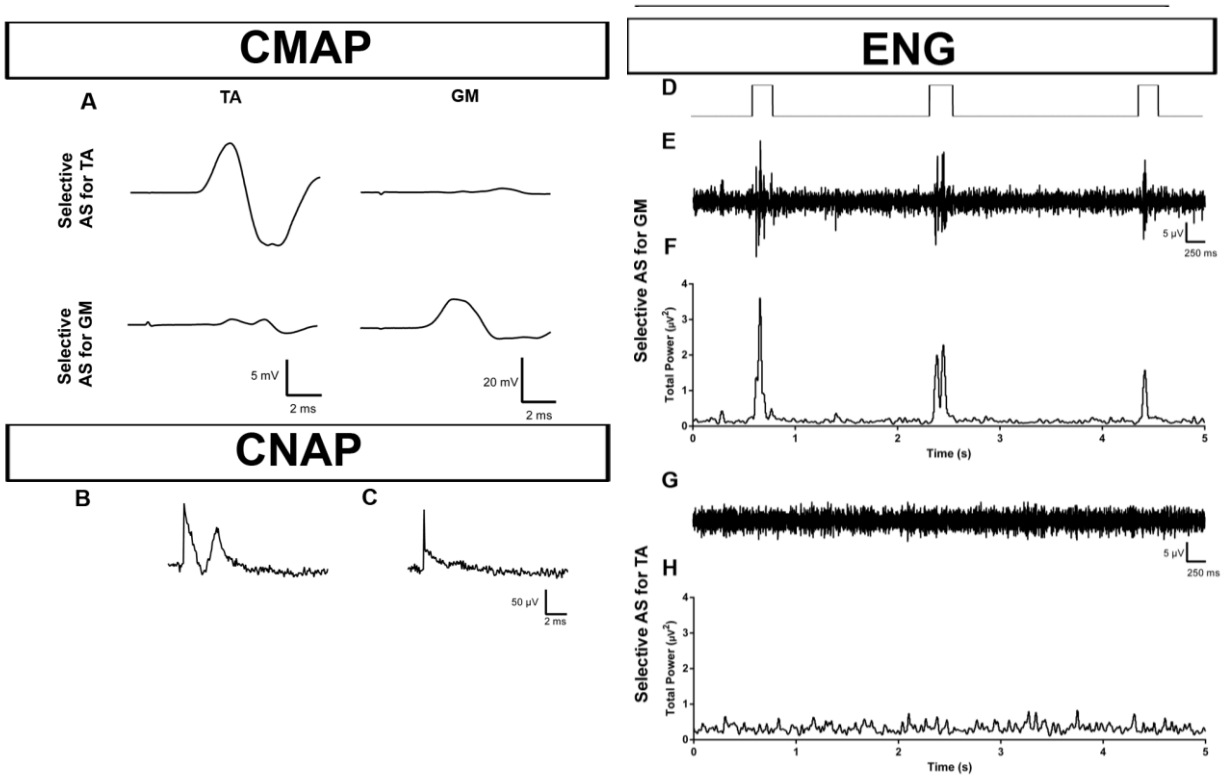

Figure 3. A: Representative CMAP from the TA and GM muscles, evoked by electrical stimulation derived from selected AS at 90 dpi. Representative CNAP recorded in AS placed in aisles containing the tibial nerve (**B**) and peroneal nerve (**C**). Raw signals recorded in the AS facing the tibial-sural bundle (**E**) or the peroneal nerve (**G**) after touch stimulation (fast scratch) during the intervals indicated in **D**. Total power spectrum analysis of the raw signals showed increased activity in the tibial-sural bundle (**F**) but not in the peroneal nerve (**I**)

CMAP was reduced by 35% in the case of the TA muscle and 45% in the case of the GM muscle in comparison to the contralateral leg. The latency of the CMAP was 83% longer in the TA muscle and 65% in the GM muscle compared to the contralateral leg.

Visual inspection of the implants showed a regenerated nerve along the tubular device, originating from the sciatic stump and ending separately in each of the distally reconnected branches (Fig. 4A,B). Toluidine blue staining of the regenerated segment inside the electrode showed a high number of myelinated axons, surrounded by a layer of connective tissue (Fig. 4C,D). The total number of myelinated axons from both aisles

at the midlevel of the regenerative electrode was 12,988 ± 3,938 (n=4). These data showed a proper regeneration process, similar to the nerve gap models using hollow silicone tubes (Lago et al., 2007a). Labeling of the different cell types in the regenerated branches by immunohistochemistry showed a pattern similar to those previously observed in chronic intraneural electrode implant (Badia et al., 2011b). Regrown axons were found in the middle portion of the regenerative branches (Fig. 4E,F). Schwann cells were associated to the axons and some of them in the connective external layer (Fig. 4G). Numerous macrophages were found in the external connective layer as well as in the regenerative area (Fig. 4H).

These results show that the regenerative process occurring within the double-aisle electrode was similar to the one described in studies using simple nerve conduits, and was not hampered by the presence of the polyimide septum containg the electrode AS.

4. Discussion

We presented in this work a new design of regenerative electrode and showed evidences of its functionality for neuroprosthetics applications. Similar to the RSE (Clements et al., 2013), the doubled-aisle regenerative electrode allows the regrowing nerve to bifurcate so separated fascicles travel along each aisle in close contact with the active sites located in the dual sides of the thin-film polyimide septum. This can provide an extra layer of selectivity to the neural interface. We proved that two independent branches can be selectively stimulated by the electrode when inserted in different aisles. For practical reasons, we used the two main terminal branches of the rat sciatic nerve: the peroneal nerve and the tibial-sural bundle. However, the design can be easily modified to target more branches or fascicles by increasing the number of aisles using different septa organization. This is important when the topological anatomy of the human nerve is taking into consideration. It is known that over 20 fascicles arrive at the carpal tunnel from the median nerve in humans (Delgado-Martínez et al., 2016). Whereas placing so many sieve or microchannel electrodes in the median nerve for a prosthetic limb does not seem feasible, a single regenerative electrode of 20 aisles appears, however, more practical and doable.

Compared to the sieve and microchannel regenerative electrodes, the double-aisle electrode is less aggressive to the nerve since it allows the regeneration of structured axonal bundles with connective tissue and vascular system. Nerve regeneration through sieve electrodes has been reported to be impaired on the long term, with signs of axonopathy due to the low transparency of this electrode (Ceballos et al., 2002; Lago et al., 2005).

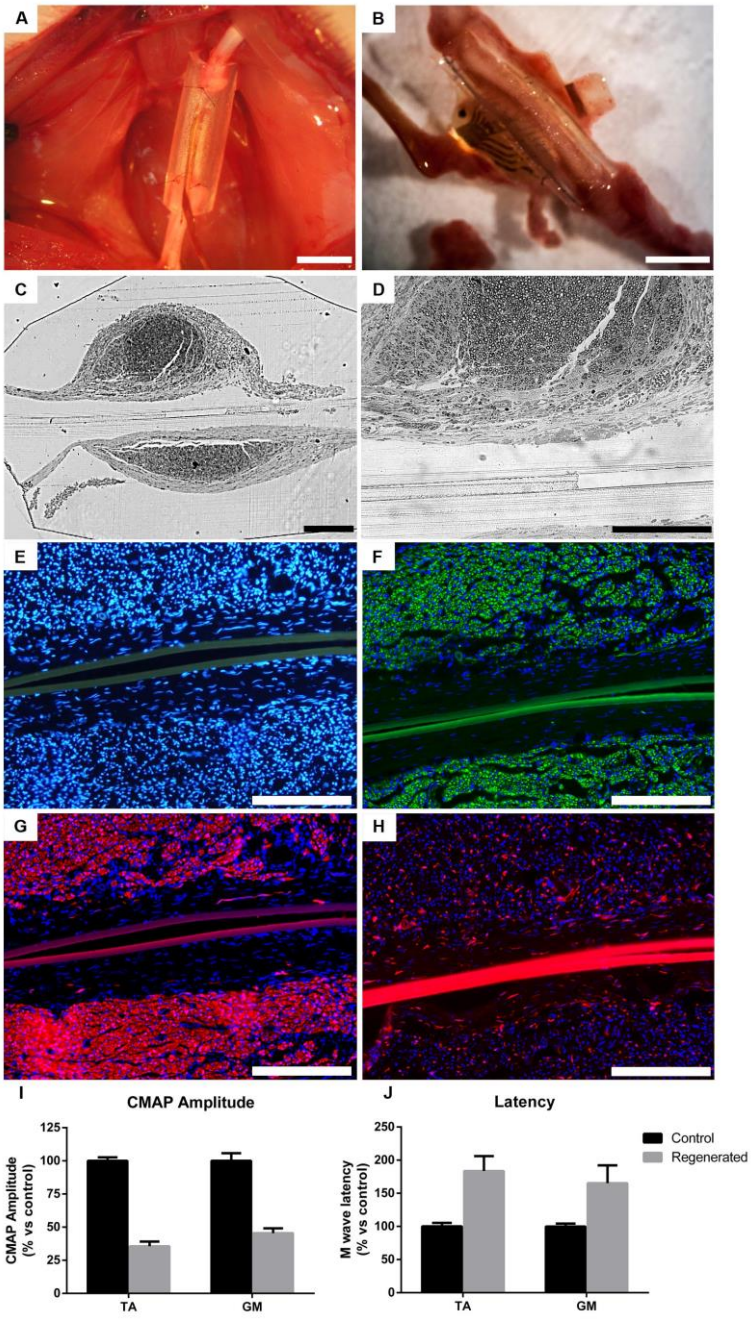

Figure 4. A: Micrograph of a regenerated rat sciatic nerve across the regenerative electrode. **B:** Close view of the regenerated nerve on a double-aisled regenerative electrode transversally implanted. **C:** Semithin transverse sections of the two branches of the regenerated nerve and the electrode. **D**: Higher magnification view of the regenerated nerve with endoneurium surrounded by a thick perineurial layer. **E:** Myelinated axons (green) distributed across the nerve section. **F:** Cell nuclei (blue) stained with DAPI indicating direct contact of the regenerated nerve and the polyimide interface. **G:** Schwann cells (red) occupying the same area as myelinated axons. **H:** Some macrophages (red) distributed homogenously through the section. Final values expressed as % of control contralateral values of the CMAP amplitude (**I**) and latency (**J**) of Tibialis Anterior (TA) and Gastrocnemius (GM) muscles obtained 90 days after regenerative electrode implant in rats. *p<0.001 vs regenerated. Scale bar: 3 mm (A-B), 200 µm (C-H).

Micro-channel electrodes attempt to increase the transparency by providing wider channels for the axons to grow in (Srinivasan et al., 2015). However, it is not to exclude that both designs produce neuropathic pain after chronic use. The double-aisle electrode, on the other hand, is virtually transparent to the nerve. The aisles are sufficiently wide for a regenerating nerve bundle to grow unimpaired and provide space for scar formation and vascularization, processes important for nerve repair. In fact, it has been described that a similar design is able to support nerve regeneration through critical gap defects of 14 mm (Clements et al., 2009), and it is very important as the functionality of regenerative electrodes is strongly dependent upon the success of axonal regeneration. In addition, our results showed higher number of myelinated axons at the electrode level compared with those present after the implant of sieve or microchannel electrodes (Fitzgerald et al., 2012; Lago et al., 2005).

Consequent with the electrode classification from Navarro et al., 2005, the lesser aggressiveness of the double-aisle electrode implies that it is less selective than those other electrodes. However, different designs of the more invasive regenerative electrode with higher numbers of AS do not ensure selective recordings (Fitzgerald et al., 2012; Lago et al., 2007b). These problems are related to the randomness produced in axonal regeneration, in which different motor or sensory axons that subsequently will reinnervate antagonistic muscles or different receptive fields can merge into a single AS creating a signal overlap and a loss of selectivity of stimulation and recordings. The septum of the double-aisled electrode presented here contains 12 active sites facing each of the two aisles. They are horizontally and vertically offset to cover an area of at least 3 mm^2. Thanks to this pattern, we increased the chances that an active site is in the vicinity of the regrowing nerve. Due to the unpredictability of nerve regrowth and the extent build-up of connective and scar tissue, we expect sub-optimal performance of the active site-nerve interface and, therefore, increasing the number of active sites will ensure a proper interface of regenerating nerves. The septum also acts as a physical separation of the regenerating fascicles and could minimize the passage of local currents (Wallman et al., 1999) from one aisle to the other aisle avoiding unspecific recording or stimulation. Another advantage of the planar structure is that no problems are related with a decay of nerve signals in function to the internodal length as it occupies a longer area (Fitzgerald et al., 2008)

Although the larger caliber of the fascicles and higher number of axons per contact site limits the selectivity of the double-aisle electrode, compared to the sieve electrode design, the fascicle regeneration into separate compartments may provide a way for functional selectivity, which cannot be achieved with other electrodes. Axonal regrowth

in sieve or micro-channel regenerative electrodes is random and uncontrolled. It is known, however, that using chemo-attractants may modulate the segregation of different populations of sensory neurons or segregate the regrowth of sensory and motor fibers into two different fascicles (Jerregård et al., 2001; Lotfi et al., 2011). A double-aisle regenerative electrode with separated sensory and a motor compartments might provide effective closed-loop commands to amputee patients for the use of advanced neuroprostheses (Micera et al., 2008)

5. Acknowledgments

This research was supported by European Union FP7-NMP project MERIDIAN under contract number 280778, and FPT-ICT project NEBIAS under contract number 611687, TERCEL (RD12/0019/0011) and CIBERNED (CB06/05/1105) funds from the Instituto de Salud Carlos III of Spain, and FEDER funds. The authors thank the technical help of Monica Espejo and Jessica Jaramillo.

6. References

Badia, J., Boretius, T., Andreu, D., Azevedo-Coste, C., Stieglitz, T., Navarro, X., 2011a. Comparative analysis of transverse intrafascicular multichannel, longitudinal intrafascicular and multipolar cuff electrodes for the selective stimulation of nerve fascicles. J. Neural Eng. 8, 036023. doi:10.1088/1741-2560/8/3/036023

Badia, J., Boretius, T., Udina, E., Stieglitz, T., Navarro, X., 2011b. Biocompatibility of Chronically Implanted Transverse Intrafascicular Multichannel Electrode (TIME) in the Rat Sciatic Nerve. IEEE Trans Biomed Eng 58, 2324–2332.

Ceballos D, Valero-Cabré A, Valderrama E, Schüttler M, Stieglitz T, Navarro X. Morphological and functional evaluation of peripheral nerve fibers regenerated through polyimide sieve electrodes over long term implantation. J Biomed Mat Res 2002, 60:517-528.

Clements, I.P., Kim, Y., English, A.W., Lu, X., Chung, A., Bellamkonda, R. V, 2009. Thin-film enhanced nerve guidance channels for peripheral nerve repair. Biomaterials 30, 3834–46. doi:10.1016/j.biomaterials.2009.04.022

Clements, I.P., Mukhatyar, V.J., Srinivasan, A., Bentley, J.T., Andreasen, D.S., Bellamkonda, R. V, 2013. Regenerative scaffold electrodes for peripheral nerve interfacing. IEEE Trans Neural Syst Rehabil Eng 21, 554–566.

Dario, P., Garzella, P., Toro, M., Micera, S., Member, S., Alavi, M., Meyer, U., Valderrama, E., Sebastiani, L., Ghelarducci, B., Mazzoni, C., Pastacaldi, P., 1998. Neural interfaces for regenerated nerve stimulation and recording. IEEE Trans Rehabil Eng. 6, 353–363.

Del Valle, J., Navarro, X., 2013. Interfaces with the peripheral nerve for the control of neuroprostheses. Int. Rev. Neurobiol. 109, 63–83. doi:10.1016/B978-0-12-420045-6.00002-X

Edell, D.J., 1986. A peripheral nerve information transducer for amputees: long-term multichannel recordings from rabbit peripheral nerves. IEEE Trans. Biomed. Eng. 33, 203–14. doi:10.1109/TBME.1986.325892

Fitzgerald, J.J., Lacour, S.P., McMahon, S.B., Fawcett, J.W., 2008. Microchannels as axonal amplifiers. IEEE Trans. Biomed. Eng. 55, 1136–46. doi:10.1109/TBME.2007.909533

Fitzgerald, J.J., Lago, N., Benmerah, S., Serra, J., Watling, C.P., Cameron, R.E., Tarte, E., Lacour, S.P., McMahon, S.B., Fawcett, J.W., 2012. A regenerative microchannel neural interface for recording from and stimulating peripheral axons in vivo. J. Neural Eng. 9, 016010. doi:10.1088/1741-2560/9/2/029601

Glass, J.D., Culver, D.G., Levey, A.I., Nash, N.R., 2002. Very early activation of m-calpain in peripheral nerve during Wallerian degeneration. J. Neurol. Sci. 196, 9–20. doi:10.1016/S0022-510X(02)00013-8

Jerregård, H., Nyberg, T., Hildebrand, C., 2001. Sorting of Regenerating Rat Sciatic Nerve Fibers with Target-Derived Molecules. Exp. Neurol. 306, 298–306. doi:10.1006/exnr.2001.7656

Lacour, S.P., Fitzgerald, J.J., Lago, N., Tarte, E., McMahon, S., Fawcett, J., 2009. Long micro-channel electrode arrays: a novel type of regenerative peripheral nerve interface. IEEE Trans. Neural Syst. Rehabil. Eng. 17, 454–60. doi:10.1109/TNSRE.2009.2031241

Lago, N., Ceballos, D., Rodríguez, F.J., Stieglitz, T., Navarro, X., 2005. Long term assessment of axonal regeneration through polyimide regenerative electrodes to interface the peripheral nerve. Biomaterials 26, 2021–31. doi:10.1016/j.biomaterials.2004.06.025

Lago, N., Rodríguez, F.J., Guzmán, M.S., Jaramillo, J., Navarro, X., 2007a. Effects of motor and sensory nerve transplants on amount and specificity of sciatic nerve regeneration. J. Neurosci. Res. 85, 2800–12. doi:10.1002/jnr.21286

Lago, N., Udina, E., Ramachandran, A., Navarro, X., 2007b. Neurobiological assessment of regenerative electrodes for bidirectional interfacing injured peripheral nerves. IEEE Trans. Biomed. Eng. 54, 1129–37. doi:10.1109/TBME.2007.891168

Lotfi, P., Garde, K., Chouhan, A.K., Bengali, E., Romero-Ortega, M.I., 2011. Modality-specific axonal regeneration: toward selective regenerative neural interfaces. Front. Neuroeng. 4, 1–11. doi:10.3389/fneng.2011.00011

Micera, S., Member, S., Navarro, X., Carpaneto, J., Citi, L., Tonet, O., Rossini, P.M., Carrozza, M.C., Hoffmann, K.P., Vivó, M., Yoshida, K., Dario, P., 2008. On the Use of Longitudinal Intrafascicular Peripheral Interfaces for the Control of Cybernetic Hand Prostheses in Amputees. IEEE Trans Neural Syst Rehabil Eng. 16, 453–472.

Navarro, X., Calvet, S., Butí, M., Gómez, N., Cabruja, E., Garrido, P., Villa, R., Valderrama, E., 1996. Peripheral nerve regeneration through microelectrode arrays based on silicon technology. Restor. Neurol. Neurosci. 9, 151–160. doi:10.3233/RNN-1996-9303.

Navarro X, Lago N, Vivó M, Yoshida K, Koch KP, Poppendieck W, Micera S. Neurobiological evaluation of thin-film longitudinal intrafascicular electrodes as a peripheral nerve interface. Proceedings of the IEEE 10th International Conference on Rehabilitation Robotics, pp. 643-649, 2007.

Oddo, C.M., Raspopovic, S., Artoni, F., Mazzoni, A., Spigler, G., Petrini, F., Giambattistelli, F., Vecchio, F., Miraglia, F., Zollo, L., Di Pino, G., Camboni, D., Carrozza, M.C., Guglielmelli, E., Rossini, P.M., Faraguna, U., Micera, S., 2016. Intraneural stimulation elicits discrimination of textural features by artificial fingertip in intact and amputee humans. Elife 5, 1–27. doi:10.7554/eLife.09148

Raspopovic, S., Capogrosso, M., Petrini, F.M., Bonizzato, M., Rigosa, J., Di Pino, G., Carpaneto, J., Controzzi, M., Boretius, T., Fernandez, E., Granata, G., Oddo, C.M., Citi, L., Ciancio, A.L., Cipriani, C., Carrozza, M.C., Jensen, W., Guglielmelli, E., Stieglitz, T., Rossini, P.M., Micera, S., 2014. Restoring natural sensory feedback in real-time bidirectional hand prostheses. Sci. Transl. Med. 6, 222ra19. doi:10.1126/scitranslmed.3006820

Raspopovic, S., Carpaneto, J., Udina, E., Navarro, X., Micera, S., 2010. On the identification of sensory information from mixed nerves by using single-channel cuff electrodes. J. Neuroeng. Rehabil. 7, 17. doi:10.1186/1743-0003-7-17

Srinivasan, A., Tahilramani, M., Bentley, J.T., Gore, R.K., Millard, D.C., Mukhatyar, V.J., Joseph, A., Haque, A.S., Stanley, G.B., English, A.W., Bellamkonda, R. V, 2015. Microchannel-based regenerative scaffold for chronic peripheral nerve interfacing in amputees. Biomaterials 41, 151–65. doi:10.1016/j.biomaterials.2014.11.035

Stieglitz, T., Navarro, X., Calvet, S., Blau, C., Meyer, J., 1996. Interfacing regenerating peripheral nerves with a Micromachined Polyimide Sieve Electrode. IEEE Eng. Med. Biol. Soc. 1, 365–366.

Thompson, C.H., Zoratti, M.J., Langhals, N.B., Purcell, E.K., 2016. Regenerative Electrode Interfaces for Neural Prostheses. Tissue Eng. Part B. Rev. 22, 125–35. doi:10.1089/ten.TEB.2015.0279

Valero-Cabré, A., Navarro, X., 2002. Functional impact of axonal misdirection after peripheral nerve injuries followed by graft or tube repair. J. Neurotrauma 19, 1475–85. doi:10.1089/089771502320914705

Valero-Cabré, A., Navarro, X., 2001. H reflex restitution and facilitation after different types of peripheral nerve injury and repair. Brain Res. 919, 302–312. doi:10.1016/S0006-8993(01)03052-9

Wallman, L., Levinsson, A., Schouenborg, J., Holmberg, H., Montelius, L., Danielsen, N., Laurell, T., 1999. Perforated Silicon Nerve Chips with Doped Registration Electrodes : in Vitro Performance and in Vivo Operation. IEEE Trans. Biomed. Eng 46, 1065–1073.

Zhao, Q., Drott, J., Laurell, T., Wallman, L., Lindstrijm, K., Bjursten, L.M., Montelius, L., Danielsent, N., 1997. Rat sciatic nerve regeneration through a micromachined silicon chip. Biomaterials 18, 75–80.

IV. DISCUSSION

DISCUSSION

During the last decades, the design and the preclinical use of advanced neuroprosthetic devices and hybrid bionic systems has been pursued by many research groups targeting neural injuries and proximal nerve transections as in amputees by developing neural interfaces between artificial devices and the PNS (Cogan, 2008). However, at the current state of the art, the improvement in robotic technologies is not matched by a suitable neural interface technology for reliable, widespread and affordable use. Moreover, with future generation prosthetic devices such as those with large degrees of freedom, the problems are still more complex. There is need for closed loop commands for precise execution of movements by incorporating readout from sensory neurons, i.e. the integration of both sensory neuron (SN) and motorneuron (MN) functions on the interfacial device. A second issue is the lack of techniques for providing access to high resolution MNs and SNs signals, targeting man-machine devices such as robotic arms.

Taking into account that regenerative electrodes are designed to interface a high number of axons as they regenerate, with a large number of efferent and afferent nerve fibres independently interfaced by individual micro-electrodes, we envisage that growth cones of regenerating nerve fibres can be chemically guided. Thus, the development of a high-resolution planar regenerative interface ensemble in which motor and sensory axons are specifically interfaced to solve issues related with closed loop commands for chronic implants are the main goals of the thesis.

Different components of such a high-resolution planar regenerative interface were studied in the experimental work made in this thesis separately in order to combine them in future studies.

First, we focused in the design of the tube that could be a good candidate to use as a scaffold for the regenerative interface. For this purpose, we studied the ability to sustain sciatic nerve regeneration of a synthetic tube made of electrospun fibers of poly(ethylene glycol terephthalate) and crystalline, hydrophobic poly(butylene terephthalate), named Polyactive (PA) in comparison with silicone tubes. Our results demonstrates that PA tubes enhance nerve regeneration in long gaps evidenced by the higher number of myelinated axons and better outcomes in motor, sensory and autonomic reinnervation.

Second, we focus on chapter 2 and 3 in studying the role of neurotrophic factors (NTFs) and extracellular matrix components (ECM) to selectively promote regeneration

of motor and sensory neurons and the effects these moleculas have in guidance of regenerating axons. As the maintenance of specific conditions inside the regenerative guides within the period of regeneration is a key factor to modulate neuronal regeneration, we characterized in chapter 2.1 how NTFs encapsulated in PLGA microspheres embedded in a collagen matrix could be a good approach to guarantee the maintenance and the optimal effect of NTFs in the regenerative environment. Then, in chapter 2.2, we studied the selective enhancement of sensory and motor regeneration of different NTFs at several doses. Our results demonstrate that in vitro NGF and NT-3 selectively increased sensory axon outgrowth while BDNF selectively enhanced motor axon outgrowth only at high doses. However, the effect of NGF and NT-3 was reduced in vivo after sciatic transection and tube repair and only BDNF showed similar results in vivo. In chapter 2.3, we tested whether selective effects mediated by BDNF for motor neurons and NGF and NT-3 for sensory neurons could be potentiated by the addition of ECM components. We observed both in vitro and in vivo a synergistic and selective effect for sensory neurons when laminin molecules were mixed with NGF and NT-3 (LM + NGF/NT-3) and parallel effects were observed for motor neurons when fibronectin was mixed with BDNF (FN + BDNF). Afterwards, once the selective and promoting effects of these conditions on motor and sensory neuronal regeneration had been characterized, we studied in chapter 3 the ability of FN + BDNF for guidin motor regenerating neurons and of LM + NGF/NT-3 for guiding sensory regenerating neurons after sciatic nerve transection and regeneration along a Y- tube, mimicking the scaffold of the planar regenerative electrode tested in chapter 4. Retrolabeling the regenered axons indicated that FN + BDNF exerted an attractive effect for motor axons, whereas LM + NGF/NT-3 did not show a significant effect for sensory axons, probably due to the variability of sensory neuronal population and the complexity to uniformly attract this heterogenous population (Usoskin et al., 2015).

Finally, in chapter 4 we studied the biocompatibility and functionality of the planar regenerative interface following an acute implantation and after 3 months of nerve regeneration. In acute implants, we observed that this device was able to perform selective stimulation on different fascicles and also record sensory afferent signals both after external electrical stimulation (CNAPs) or natural tactile stimuli (ENG). Although some limitations were detected in chronic implants, planar regenerative electrode maintained the capacity to perform selective stimulation of reinnervated muscles and to record afferent signals from distal targets.

Polyactive tube as a scaffold for planar regenerative electrode

After sciatic nerve transection, repairing by direct suture is not always possible because of tissue loss or nerve retraction (Georgeu et al., 2005; Hall, 2005). In this case, autograft repair is the standard choice but some disadvantatges such as the use of sensory-only nerves, mismatches in size and fascicular pattern regarding both proximal and distal stumps, donor site morbidity, and possible requirement of a second surgical procedure caused by painful neuroma formation or scarring (Daly et al., 2012; Johnson and Soucacos, 2008) makes it necessary to find better alternatives. Tube repair emerge thus as a possible option to promote nerve regeneration, but more efforts are needed to bridge long gap defects as regenerative outcomes are still far from those achieved after autograft repair (Navarro and Kennedy, 1991). Presently, numerous studies focus in improving nerve regeneration by using different innovative biomaterials that are associated with proregenerating properties, such as facilitating the influx of nutrients, enhancing cell adherent properties, increasing cell viability or decreasing foreign body reaction to implanted materials. However, while there is a wide range of nerve guides fabricated with natural or synthetic polymers and some of them have been approved by regulatory authorities for use in humans, there is still a long way to go as all these tubes only offer a limited capacity to repair even small-sized nerve gaps (Madduri and Gander, 2012).

On the other hand, the use of nerve guides is essential to immobilize and stabilize the regenerative electrodes over the period of nerve regeneration. In recent experiments, although some studies have used porous polysulfone tubes (Clements et al., 2013; Gore et al., 2015), silicone tubes are the most used to sustain regenerative electrodes (FitzGerald et al., 2012; Lacour et al., 2009; Lago et al., 2005; Srinivasan et al., 2015) because of their stability and flexible properties. However, while the nerve guide has usually been considered as a mere passive scaffold to hold the interface, the possibility to use it also as an added factor to promote nerve regeneration has not been explored in the last published reports.

For this purpose, we tested a new polymeric tube as a possible candidate to sustain the planar regenerative electrode and at the same time, enhance nerve regeneration in limiting (10 mm) and critical (15 mm) gap defects (Navarro and Verdú, 2004; Yannas and Hill, 2004). PA was chosen as it belongs to a family of biocompatible copolyethers approved by the FDA for its use in several biomedical applications. Moreover, PA can be readily processed by electrospinning and this technique represents an auspicious approach to enhance axon regeneration, with initial studies reporting moderate

success (Panseri et al., 2008; Yu et al., 2011). Indeed, nerve conduit fabrication with this technique offers the possibility not only to manipulate the conditions of the fibres of the tube but also to incorporate several cues within the walls that can interact with regenerating axons (Catrina et al., 2013; Townsend-Nicholson and Jayasinghe, 2006; Whitehead and Sundararaghavan, 2014) thus modulating the regenerating process on demand. Finally, the fabrication of a nerve guide with the electrospinning technique is envisioned to provide an automatical manufacture of PA tubes surrounding the regenerative electrode and then, automatizing the process of the whole electrode ensemble fabrication.

In chapter 1, we observed that PA tubes showed promising results supporting nerve regeneration of a high number of myelinated axons in both limiting and critical gaps that lead to improved motor, sensory and autonomic functional reinnervation compared with animals repaired with silicone tubes. The differences between both groups can be explained by the design of PA tubes and properties of the synthetic polymer. PA tubes were fabricated through an electrospinning process that generates an ideal combination of fiber size (1.44 μm ± 0.29 μm), fiber alignment (1.4 ± 0.37 degrees) and porosity (62.7 ± 1.3%) and pore diameters (average between 8.02 and 10.22 μm), which is within the recommended range, as it is considered optimal for the influx of nutrients while providing a sufficient barrier to minimize the invasion of detrimental inflammatory cells (Kehoe et al., 2012).

On the other hand, fiber alignment has also been shown to enhance *in vitro* Schwann cell migration and high oriented neurite elongation (Schnell et al., 2007). It should be taken into account that our results show that the general direction of neurite growth on PA (Chapter 1, Fig. 2B) differs from the underlying fiber orientation by an average of only 2.67 ± 3.61 degrees revealing a high oriented growth of neurite regeneration. On the other hand, after 4 months of implantation, PA tubes showed a higher area of regeneration with axons spread throughout the internal lumen and also in contact with the conduit wall, in contrast to the usual regenerated nerve centered in the silicone tube (Lundborg et al., 1982). Thus, it seems that PA fibers may provide a guiding longitudinal structure to the regenerating axons, serving as an additional ECM-like guidance structure for Schwann cell migration and neurite extension.

Importantly, PA tubes reached promising results in critical gap defects without the addition of matrix, NTFs or exogenous cells, which have been described to enhance nerve regeneration (Allodi et al., 2012). Then, integration of these factors within the nerve wall or inside the lumen can help to enhance the number of regenerating

neurons or even overcome nerve defects even longer than the 15mm reported here. In this sense, the possibility to bridge long nerve defects could be useful to improve the functionality of the planar regenerative electrode as expanded gaps allow the implant of longer electrodes with higher number of AS, thus improving the spatial resolution and increasing the probability to interface more regenerated axons. In addition, long gaps also give the opportunity to increase the distance between the proximal sutured stump and the proximal part of the planar regenerative electrode in order to facilitate the reorganization of regenerating motor and sensory axons, and facilitate the guidance of distinct populations of axons with the addition of different NTFs or ECM proteins. Finally, taking into account that nerve fibers grew in contact with the tube wall, it would also be possible to design a regenerative electrode ensemble made of PA tubes with embedded electronics similar to cuff electrodes (Badia et al., 2011). Hence, not only the axons that grow in contact with the planar regenerative electrode would be interfaced but also those far from the center of the tube and close to the walls, thus making available more signals to better control a neuroprosthesis and provide the patients with an enhanced sensory feed-back.

Carrier technologies for the creation of proregenerative environments

After nerve injury, NTFs exert positive effects on nerve regeneration through their ability to promote neuronal survival, to guide and increase axonal outgrowth and to improve target reinnervation (Allodi et al., 2012). However, NTFs added within a nerve conduit can be rapidly degraded (Ejstrup et al., 2010; Tria et al., 1994), diffuse outside the conduit or get diluted after liquid infiltration resulting in sub-optimal concentrations, and thus poor regeneration outcomes (de Boer et al., 2012; Wood et al., 2013).

Hence, to guarantee the bioactivity of NTF, several strategies such as immobilization of the factors, focal release, sustained delivery or a local production of these molecules will help to secure the presence of NTFs within the axon regeneration microenvironment throughout the regeneration process. However, some issues are associated to the use of these systems. For instance, the engraft of catheter ports or osmotic minipumps (Hontanilla et al., 2007; McDonald and Zochodne, 2003) are invasive approaches that require the chronic implantation of the devices, maintenance of the catheter in the correct position during nerve regeneration appears difficult and a second surgery is needed to explant the devices (Pfister et al., 2007). Furthermore, these strategies usually require daily administration of drugs that could lead to inhibitory effects on nerve regeneration (Boyd and Gordon, 2002) if high levels of NTF

are reached. On the other hand, genetically modified Schwann cells have also been used to perform a local production and a sustained secretion of the drugs. However, leaving aside that this option may need immunosupression therapy to avoid cell implant rejection, the high levels of NTFs secreted do not always lead to an enhanced nerve regeneration due to the "candy-store" effect (Tannemaat et al., 2008), in which axons stay in areas with high NTF concentration and withhold their regeneration towards distal target organs.

Taking all these premises into account, we focused in the characterization of PLGA MPs as an interesting candidate for a sustained and focal release of NTFs. PLGA MPs are biocompatible and reabsorbable thus eliminating the need of secondary surgeries. Moreover, MPs can be fabricated at different sizes, which may facilitate different release kinetics for one or several growth factors (Pfister et al., 2007). An important factor for the generation of a desirable environment with MPs is the selection of a proper scaffold to ensure that MPs remain inside the tube during the regeneration process. Collagen matrix has been widely used to fill nerve guides acting as 3D structure that sustains nerve regeneration allowing cellular migration and regeneration of the regrowing axons. However, it is important to take into account the density of the matrix, since axonal elongation may be hindered in a high density matrix, whereas low density may allow over diffusion of the added molecules (Labrador et al., 1998, 1995).

In chapter 2.1, we observed that 10 days after MP fabrication, only 30% of the encapsulated NTF had been already released, and that a slow and sustained release was maintained for more than a month. Furthermore, we also tested the bioactivity of the secreted NTF in organotypic cultures to ensure that physical stresses of MPs manufacturing and long periods of NTF encapsulation did not affect to their therapeutic effects. In this sense, organotypic DRG and SC slices showed an increased neurite outgrowth when cultured in collagen matrixes that had been embedded 1 week before with encapsulated NTFs in comparison with DRG and SC slices cultured in the same conditions but with no NTF encapsulation. Thus, it seems that MPs were still releasing NTFs at a concentration high enough to stimulate the growing response while NTFs in the non-encapsulated group had eluted out of the matrix.

Likewise, we also observed in vivo an increased number of motor and sensory neurons that regenerate distally to the nerve conduit in the groups with encapsulated NTFs. Then, the prolonged NTF release would extend the therapeutic window of these molecules (McDonald and Zochodne, 2003; Williams et al., 1983) enhancing the intrinsic mechanisms of axon regeneration and neuronal survival. Moreover, this

extended period of action would also have an indirect effect inducing endogenous Schwann cells to a proregenerative state (Gordon et al., 2003) during the time that axons are crossing the tube thus increasing regeneration outcomes after this treatment. Furthermore, our results also demonstrate that sustained release of NTF does not lead to higher deleterious concentrations that have been reported to interfere or even hinder the regeneration process (Boyd and Gordon, 2002; Eggers et al., 2013; Gold, 1997; Mohiuddin et al., 1999). Therefore, we conclude that MPs releasing NTF mixed with a collagen matrix is an appropriate strategy to create a desirable pro-regenerating environment for next studies.

Nevertheless, having in mind the double-aisle regenerative electrode we put forward here, the sole enhancement of nerve regeneration is not enough to create two specific conditions at each side of the electrode to enhance motor or sensory neuron regeneration. However, as NTFs and their receptors in nonneuronal cells show a specific temporal expression (Boyd and Gordon, 2003a), encapsulation of different NTF in different MPs would help to release these molecules with individual optimal kinetics creating thus specific environments to enhance distinct neuronal populations. In addition, microspheres have also been used for the generation of NTF gradients inside the tubes guiding axonal growth towards attractive molecular gradients (Roam et al., 2015). Thus, combination of these factors with the intrinsic capability of different NTFs and ECM molecules to specifically enhance motor or sensory axon regeneration discussed below can contribute to create a selective microenvironment to separate distinct neuron populations.

NTF and ECM components for the creation of motor and sensory pathways

The effects of NTFs have been widely described both in development and nerve regeneration for the stimulation of survival, differentiation and guidance of neurons and axons (Li et al., 2005; Richner et al., 2014). Characterization of the molecular motor and sensory pathways emerged as a possible solution to overcome the unaccurate reinnervation produced after nerve injury by misdirected regenerating axons which leads to poor functional recovery (Lundborg and Rosén, 2001; Valero-Cabré and Navarro, 2002). Therefore, the expression pattern of several NTF both in healthy conditions and after injury has been characterized in different parts of the peripheral nervous system such as in dorsal roots and ventral roots, among others (Brushart et al., 2013; Höke et al., 2006).

However, to selectively modulate motor or sensory axons regeneration and in order to predict which cell will respond or be guided by a certain condition, it is not only important to recognize the patterns of expression of NTFs but also to be aware of which receptors are expressed by each cell population, what expression pattern each follows after nerve injury and how are they regulated in response to exogenous addition of different NTFs.

Thus, in order to select a trophic factor able to selectively promote motor or sensory regeneration and having in mind that specific doses of trophic factors may be required, we characterized in vitro and in vivo the effect of GDNF, FGF-2, NGF, NT-3 and BDNF at different concentrations on axon regeneraton in chapter 2.2.

With regard to GDNF and FGF-2, they have been postulated as important factors to enhance motor neuron regeneration (Allodi et al., 2013; Boyd and Gordon, 2003b). However, after assessing their effects in DRG explants and SC slices we observed that both GDNF and FGF-2 stimulate not only motor but also sensory neurite outgrowth as well. Therefore, while these NTFs showed an increase in motor neurons outgrowth as it had been reported, they should not be defined as *motor* NTFs as they also promote sensory neurite outgrowth probably mediated by the activation of both GRF/Ret and FGFR receptors in sensory neurons (Allodi et al., 2013; Bennett et al., 1998).

On the other hand, we observed in vitro that all the tested doses of NGF and NT-3 selectively promoted sensory neurite outgrowth with no observable effect on motor neurons in agreement with previous studies (Terenghi, 1999). This selective effect is mediated by the restricted location of NGF receptor TrkA receptor to sensory neurons as well as the downregulation of NT-3 receptor TrkC in motor neurons after injury (Boyd and Gordon, 2003a).

Besides, in accordance with previous studies (Allodi et al., 2011), we observed that while maximal doses of BDNF did not increase motor axon outgrowth; low, medium and high doses of BDNF enhanced motor regeneration, an effect that is mediated by the upregulation of TrkB receptors in motor neurons after injury (Boyd and Gordon, 2003a). Unexpectedly, we observed that BDNF enhance sensory neurite outgrowth only at low doses, whereas high doses did not show any significant effect. Indeed, it has been demonstrated that BDNF inhibits sensory neurite outgrowth in PC12 cells by the exclusive activation of p75 receptor as these cells does not express TrkB (MacPhee and Barker, 1997). Then, it is possible that low doses of BDNF allow sensory neurite outgrowth, whereas high levels of this neurotrophin counteract the beneficial effects through p75 activation in TrkA and TrkC positive neurons, which

represent a 45% of total DRG population (Tucker and Mearow, 2008). Furthermore, very high levels of BDNF have been associated with a reduction of TrkB protein as well as of trkB and trkC mRNA both in vitro and in vivo (Frank, 1996), then activation of p75 in all neurons is facilitated thus explaining why sensory and motoneuron regeneration is inhibited in maximal doses. Consequently, we defined the high dose of BDNF as a potential candidate to potentiate motor pathways and NGF and NT-3 to induce regeneration of sensory pathways.

After that, we tested in vivo the effect of different doses of the selected NTFs on motor and sensory regeneration. In accordance to the in vitro results, BDNF enhanced motor neuron regeneration at all doses, whereas only the low dose promoted sensory neuron regeneration. However, the addition of NGF and NT-3 did not show a selective effect as we observed enhanced regeneration both in motor and sensory regeneration.

Due to the fact that the effect of NTF in vivo was not enough to generate straight motor and sensory pathways, we studied in chapter 2.3 whether the addition of ECM could synergistically contribute with NTF to improve a selective regeneration of motor and sensory neurons. Previous studies showed that laminin promoted sensory neuron regeneration mediated by their integrin receptor (Gardiner, 2011), whereas fibronectin promoted motor neuron regeneration (Gonzalez-Perez et al., 2015). Therefore, we combined NGF and NT-3 with laminin (LM) to achieve a pro-sensory regenerative environment and BDNF with fibronectin (FN) to create a pro-motor regenerative matrix. After organotypic DRG and SC slices, results revealed a selective and synergistic effect on sensory neurite outgrowth with the LM + NGF/NT-3 group, whereas FN + BDNF exhibited a preferential and synergistic effect on motor neurite outgrowth. However, when we tested these combinations in vivo we observed again that the selective effects of motor and sensory conditions were reduced.

This comparative reduction could be a result of a more complex environment in the regenerating nerve than in the organotypic culture. After nerve injury, ECM components are synthesized and secreted by non-neuronal cells such as Schwann cells and fibroblasts (Gonzalez-Perez et al., 2013), whereas NTFs and their receptors are expressed by both neuronal and non-neuronal cells (Brushart et al., 2013; Jesuraj et al., 2012). Furthermore, non-neuronal cells involved in Wallerian degeneration also express integrins and NTF receptors. Therefore, the in vivo implant of a matrix containing different ECM components and NTFs in the nerve conduit does not only influence the injured neurons, but also acts on the migrating non-neuronal cells inside the intratubular matrix. Hence, the activation of non-neuronal cells would contribute

with nonspecific proregenerative cues and decrease the effects of the selective factors introduced in the exogenous matrix. On the other hand, in organotypic cultures neurons are in contact with some Schwann cells and fibroblasts, which may remain in the root stump, but the amount of these cells is much lower than in in vivo conditions of nerve injury and the trophic influence is likely different (Allodi et al., 2011).

However, in spite of the pleiotrophic environment that takes place within the regenerative milieu in vivo, we observed a preferential and synergistic effect on sensory neurons regeneration and target reinnervation mediated by LM + NGF/NT-3 leading to an earlier sensory functional recovery, whereas FN + BDNF showed a preferentially and synergistic effect on motor neuron regeneration leading also to an earlier motor functional recovery.

Motor and sensory neuron guidance

After characterization in chapter 2 of the necessary conditions to promote sensory and motor axon regeneration, the final step towards a selective invasion of two different aisles in the regenerative ensemble was to challenge both treatments in the same conditions and compare directed versus random regeneration. To this end, we prefilled passive regenerative electrodes (i.e. double-aisle regenerative electrodes without PCB or wires) with the combinations of ECM and NTFs described before.

Neurotrophins play an important role during development to stimulate and guide axonal growth for the establishment of a correctly wired and functional neural system (Markus et al., 2002). Growth cone motility and navigation in response to NTFs is regulated by actin dynamics of the neuronal cytoskeleton after the activation of their cognate receptors. Indeed, NGF, BDNF and NT-3 have been reported to elicit increases in the amount of F-actin in growth cones of sensory neurons (Paves and Saarma, 1997). Particularly, it has been described that the same intracellular mechanisms that promote axonal growth and cell survival are related with axonal guidance (Henle et al., 2011; Ming et al., 1999; Yuan et al., 2003).

Evidence of these guidance effects has been mainly studied in vitro with different types of neurons. Early studies into the specific chemotropic effects of NGF found that microinjection of NGF into the brain ventricle of neonatal rats evoked a massive ingrowth of sympathetic fibres into brain tissue towards the source of NGF. Furthermore, this ectopic growth was shown to be dependent upon NGF because withdrawal of the neurotrophin led to retraction of the axons (Levi-Montalcini et al.,

1978; Menesini et al., 1978). Afterwards, several reports have described how gradients of NGF, NT-3, and BDNF induce turning of growth cones toward these neurotrophins (Moore et al., 2006).

On the other hand, NTFs are not the only molecules that promote axonal guidance. ECM components have also an important role in axonal guidance. Indeed, LM and FN, which bind to integrin receptors, were demonstrated to be two of the key molecules both in vitro and in vivo studies of peripheral and central neurons (Evercooren et al., 1982; Manthorpe et al., 1983; Orr and Smith, 1988; Rogers et al., 1987), with LM exerting the most significant effect on directional growth (Luckenbill-edds, 1997; Sanes, 1989). When compared, sources of laminin influenced growth cone directionality and advancement by the alteration of filopodial dynamics compared to the effect produced by fibronectin (Kuhn et al., 1995).

However, axonal guidance of different populations mediated by combined effects of both ECM and NTF is less studied in vivo after peripheral nerve injuries. In chapter 3, we observed after the implant of a bicompartmental tube filled only with collagen (i.e. without guidance cues) that sensory and motor regenerating neurons grew preferentially to the chamber with the distal nerve stump of a higher caliber. These results are in accordance with previous studies that described a major attracting effects by higher caliber of distal nerves (Abernethy et al., 1992; Takahashi et al., 1999; Uschold et al., 2007). Indeed, it has been hypothesized that neurons may sense the levels of trophic support from each of the branches and over time preferentially direct the axons towards the one that contains larger number of Schwann cells that generate higher concentration of trophic and tropic factors (Robinson and Madison, 2004). Therefore, our in vivo model intrinsically attracts more regenerating axons from one chamber and this may hinder the axonal guidance effects of our treatments in different neuronal populations.

With all this in consideration, we aimed to study the segregation effect of motor from sensory regenerating axons inside the same Y-shaped tube by challenging a pro-sensory matrix made of collagen with LM + MP.NGF/NT-3 in the branch with the bigger distal nerve with a pro-motor matrix prepared with collagen and FN + MP.BDNF with the disadvantage of a smaller distal nerve.

Similarly to what had been seen in chapter 2.3, LM + MP.NGF/NT-3 did not attract a higher number of regenerating sensory neurons compared to control tubes containing Col + MP.PBS in both branches. However, we can not conclude that LM + NGF/NT-3 did not pull their specific regenerating population of sensory neurons towards the pro-

regenerative environment as TrkA and TrkC receptors are expressed approximately in only 45% of the total lumbar DRG neurons (Tucker and Mearow, 2008). Furthermore, most sensory neurons coexpress more than one type of Trk receptor with different binding affinities in the growth cone (Usoskin et al., 2015). Then, it could be possible that LM + NGF/NT-3 attracted a number of target neurons but also other axons were attracted to the other aisle due to TrkB activation by BDNF. Thus, it remains unanswered which phenotype of the sensory neurons turned to LM + NGF/NT-3 medium to properly assess the effects of NGF and NT-3 on TrkA+ and TrkC+ neurons. On the other hand, we observed a switch of motor and large sensory neurons preferentially regenerating towards the FN + MP.BDNF indicating that this condition is able to partially overcome the attractive effect mediated by larger caliber distal stumps.

Finally, given that the control of the specific environment for motor and sensory neuron regeneration activates both neuronal and non-neuronal growth and guidance pathways contributing to the creation of an unspecific environment for regeneration, it could be interesting to seek new strategies to selectively avoid this non-neuronal activation.

One of the potential candidates are inhibitory molecules that have been widely studied in development and central nervous system. However, few studies have focused on their role in peripheral nervous system (Giger et al., 2010; Pasterkamp et al., 1998). Actually, it has been demonstrated that semaphorin 3A (Sema3A) exerts inhibitory effects on motor and sensory neurons (Molofsky et al., 2014; Vermeren et al., 2000) even when NTFs are present (McCormick et al., 2015). In addition, semaphorin 6A (Sema6A) selectively inhibits embryonic sensory neurite outgrowth in cultures (Curley et al., 2014) whereas no inhibitory effects were observed in motor neurite outgrowth (Mauti et al., 2007). Similarly, EphrinB1 selectively inhibited motor neurite outgrowth (Vermeren et al., 2000; Wang and Anderson, 1997). However, semaphorin and ephrin families are composed by a large number of different subtypes and few studies have focused on their role after peripheral nerve injury (Arvanitis and Davy, 2008; Serini and Bussolino, 2004; Worzfeld and Offermanns, 2014). Thus, although Sema6A and EphrinB1 could be good candidates for motor and sensory axon guidance after nerve injury, all the studies cited above have focused on their effect on development stages. Moreover, it is not known whether their receptors are differentially upregulated in adult animals after nerve injury or whether these molecules could interfere with Schwann cell activation, division or migration disrupting the regenerative process.

Contributions of double-aisle electrode in the field of neuroprosthetics

After the characterization of the different conditions to promote selective motor and sensory axons regeneration, the last part of this project was aimed at the design, optimization and testing in vivo the functionality of double-aisle regenerative electrodes.

The use of regenerative electrodes to control a neuroprothesis is intended to provide amputee patients with a bidirectional communication between the nervous system and the neuroprosthesis. Thus, motor signals could be used for the control of motor commands (Edell, 1986), whereas afferent signals should provide sensory afferent information to the patient by different tactile sensors (Riso, 1999) distributed in the neuroprothesis.In chapter 4, we present a new design based on the regenerative scaffold electrode (RSE) model (Clements et al 2013). We used a double-aisled electrode scaffolded by a silicone tube that was implanted to repair gap defects of 6 mm after sciatic nerve transection. Unlike the one-sided RSE design, a double-aisle electrode contains a higher number of AS distributed in both sides, being able to interface regenerated fascicles from the two aisles whereas RSE electrode only interfaced one aisle. In addition, Clements an colleagues (2013) did not fully characterize the functionality of the electrode as they show no data of muscle activation after stimulation from the electrode and they show only recording of CNAPS after external stimulation of the proximal nerve. Thus, it is not clear if the RSE allows reinnervation of distal targets and if this RSE is able to functionally interface regenerated axons to record afferent electrical signals and to induce activation of motor efferent fibers.

Despite previous designs of regenerative electrodes (FitzGerald et al., 2012; Meyer et al., 1995; Navarro et al., 1998) require nerve regeneration for their functional test, the wide compartments of the electrode and the transparency of the double-aisle electrode allowed functional testing acutely. Moreover, there is a latency period of at least one day after axotomy in which no degeneration of the nerve fibers occur and thus nerve conduction is still present (Glass et al., 2002; Lubińska, 1977). Thus, placing the tibial and peroneal branches in the two aisles of the electrode was useful for stimulation of efferent fiers and for recording of afferent nerve signals.

Indeed, in chapter 4 we demonstrate that this electrode is able to stimulate motor fibers from different AS to elicit contraction of two different muscles with maximum values of the selectivity index close to 1, higher than other intraneural electrodes (Badia et al., 2011). Moreover, results from acute experiments reveal that this electrode is able to record not only CNAPs after external electrical stimulation of nerve fibers at the ankle

but also to record afferent signals similar to those obtained in sieve electrodes (Lago et al., 2007) after the application of fast scratch stimuli on the plantar pads.

Next, we examined if the electrode would allow or hinder nerve regeneration and distal reinnervation after implant. Histological processing demonstrated successful regeneration of the sciatic nerve through the aisles, creating two fascicles in contact with the electrode with positive staining for axons and Schwann cells. Moreover, histology revealed that the sum of both chambers contained 12,988 ± 3,938 myelinated axons at the midlevel of the tube. These results demonstrate that implant of double-aisled electrode is not an obstacle for nerve regeneration, as previous studies showed similar values of myelinated axons in a tube without electrode (Lago et al 2007). In addition, these numbers of regenerated axons were higher than the 2000 axons seen in silicone tubes with sieve electrodes (Lago et al., 2007) or 1000 (FitzGerald, 2016) and 6000 (FitzGerald et al., 2012) reported for microchannel electrodes.

It has been described that axon growth in regenerative electrodes is determined by electrode transparency, which refers to the balance between electrode scaffold and open space for regeneration (Navarro et al., 1996; Wallman et al., 2001). And although axon regeneration has been reported from arrays with a 30% transparency factor (Wallman et al., 2001) up to 69% (Lacour et al., 2009), it is generally accepted that increasing transparency and thus minimizing structural obstruction of regeneration by the device scaffold improves axon regeneration (Gore et al., 2015). Then, the good outcomes on nerve regeneration seen in our electrode are in agreement with these reports as transparency of double-aisled electrodes (close to 100%) is higher compared with sieve or microchannels electrodes.

On the other hand, this high transparency could lead to poor selectivity compared with sieve and microchannels electrodes. However, neither sieve (Lago et al., 2007) nor microchannel electrodes (FitzGerald et al., 2012) were able to ensure selective recordings. Indeed, after 90 days post-implantation we were able to selectively stimulate regenerated fascicles to induce selective contraction of tibial and gastrocnemius muscles as well as record different afferent signals. Then, the double-aisle electrode ensures nerve regeneration in all the animals and it does not necessarily imply a substantial reduction of selectivity..

Finally, taken into account the selective stimulation and recordings obtained from regenerated fascicles by the double-aisled electrode, some improvements could be added to increase the selectivity of the electrode.

A first approximation would introduce the additional insertion of two MEAs crossing the tube scaffold within both aisles based on the design suggested by the group of Romero-Ortega (Fig. 10). Although this insertion would diminish the transparency, previous studies have not found an impaired regeneration (Garde et al., 2009).

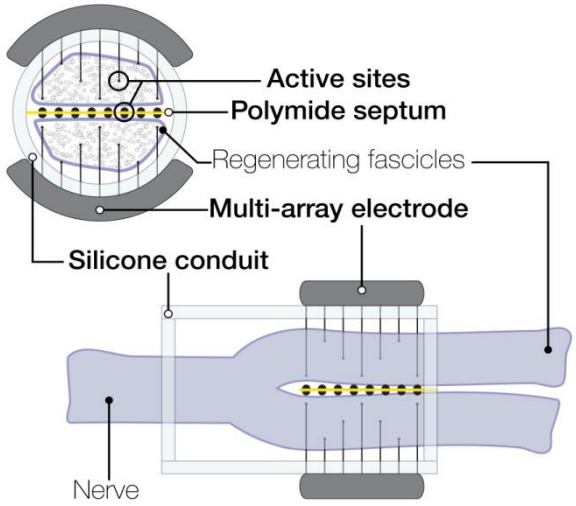

Figure 10. Prototype of double-aisle electrode. Transversal multi-array electrode (MEAs) are inserted in each aisle (based on Garde et al., 2009), to complement and increase the selectivity exerted by the AS located in the surface of the double-aisle electrode.

A further option would be to develop wireless systems with remote delivery and recordings of electrical pulses (Bredeson et al., 2015; Romero-Ortega et al., 2015) based on cochlear implants and functional stimulators (Chung, 2004). Indeed, it has been reported that wire and connector failures mainly caused by tissue response or the behavior of the animals compromise the long-term functionality of the electrodes (Biran et al., 2007; Desai et al., 2014). Then, elimination of this weak points would increase the long-term performance of the electrodes.

Another possible improvement could be the addition of extra aisles to our device, for instance adding two additional aisles at the distal part creating four aisles in total. Then, it could be possible to suture proximally tibial and peroneal nerves, and then further separate these two branches in motor and sensory subfascicles (Fig. 11A). Furthermore, considering the topological anatomy of median human nerves (Delgado-

Martínez et al., 2016), it is possible to identify more than 20 fascicles that innervate different targets in the hand. Then, more aisles would allow to suture the median nerve into a single device with a high amount of aisles able to provide a high selectivity in terms of stimulation and recording of different fascicles to improve the control of neuroprosthetics (Fig. 11B).

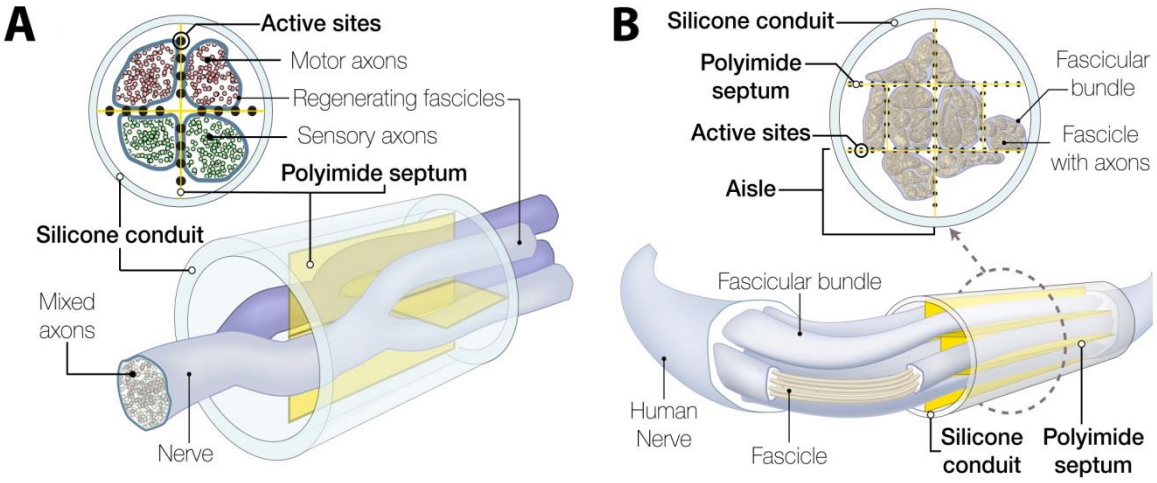

Figure 11. New prototypes of electrodes based on the double-aisle electrode. (A) Double-aisle electrode that distally forms a quad-aisle electrode for the segregation of motor and sensory axons of two different fascicles**.** (B) Proposed prototypes of multi-aisled electrode for use in the human median nerve, targeting 8 independent fascicle bundles with several in each of them.

V. CONCLUSIONS

CONCLUSIONS

1. Polyactive™ (PA) conduits are porous and contain aligned fibers in the longitudinal axis that promote aligned growing of neurites and Schwann cells in vitro. These properties also enhance axonal regeneration in vivo, in limiting (10 mm) and in critical (15 mm) nerve gap defects compared to standard silicone tubes, as well as functional reinnervation. Therefore, PA conduits are a potential candidate for use as scaffold of regenerative electrodes.

2. The sustained release of NTFs from PLGA MPs promotes neurite outgrowth in vitro and axonal regeneration in vivo:

a) NGF and BDNF encapsulated in MPs promote sensory and motor axon outgrowth in 1 week preconditioned medium, whereas free factors lose their effects and show similar results to control cultures.

b) After sciatic nerve transection, repair with tubes filled with collagen and MP encapsulated NTFs enhance motor and sensory axon regeneration compared with tubes filled with free NTFs.

3. Different NTFs show dose dependent and selective effects on motor and sensory axon outgrowth in organotypic cultures, but these effects are reduced when tested in vivo in transected peripheral nerves:

a) FGF-2 and GDNF promote both motor and sensory axon outgrowth at different doses in organotypic cultures.

b) NGF and NT-3 selectively enhance at different doses sensory axon outgrowth without effect on motor axons in organotypic cultures. However, this selective effect is lost when they are applied in vivo.

c) BDNF selectively promotes motor neuron outgrowth in vitro at doses of 50 ng/ml, without effect on sensory neurite outgrowth. BDNF also enhances motor axon regeneration in vivo at all tested doses but only high doses do not enhance sensory regeneration.

4. Combining selected ECM components with NTFs is an adequate strategy to selectively enhance motor and sensory neuron regeneration.

a) The combination of LM with NGF and NT-3 produces a selective and synergistic effect on sensory neurite outgrowth in vitro. Furthermore, this combination also enhances sensory axon regeneration in vivo, leading to an earlier sensory reinnervation and functional recovery.

b) Combining FN with BDNF promotes a preferential and synergistic effect on motor neurite outgrowth in vitro. In addition, motor regeneration is also preferentially enhanced by FN and BDNF in short and long term models compared with controls, and improves motor axon regeneration and functional recovery.

5. In vivo, the combination of FN and BDNF can be used as an attractive condition for motor and large sensory regenerating axons in a bicompartmental tube repair model. However, the combination of LM and NGF/NT-3 does not preferentially attract regenerating sensory neurons compared to the control condition.

6. After sciatic nerve transection, the double-aisle electrode developed allows for selective stimulation and neural signals recording from different nerve fascicles in both acute and chronic situations. In addition, the double-aisle electrode allows for effective axonal regeneration, improving nerve regeneration with regards to previous designs of regenerative electrodes, such as sieve and microchannels electrodes. Thus, the double-aisle electrode emerges as a promising interface for the peripheral nerve of amputee subjects for the control of neuroprostheses.

VI. ABBREVIATIONS

AS: Active sites

BDNF: brain-derived neurotrophic factor

C-domain: central domain

CNS: Central Nervous System

CSPGs: chondroitin sulfate proteoglycans

DRG: Dorsal Root Ganglia

ECM: Extracellular matrix

ERK: extracellular signal-regulated kinase

FDA: Food and Drug Administration

FGF-2: fibroblast growth factor-2

GAP-43: growth-associated protein 43

GDNF: glial cell-derived neurotrophic factor

HGF: hepatocyte growth factor

IGF-1: insulin growth factor 1

JNK: c-jun N-terminal kinase

LIF: leukaemia inhibitory factor

MPs: microspheres

MTs: microtubules

NC: nerve conduit

NGF: nerve growth factor

NT-3: neurotrophin-3

NTF: Neurotrophic Factor

P-domain: peripheral domain

PAN-MA: poly(acrylonitrile-co-methylacrylate

PCL: poly-caprolactone

PGA: poly-glycolic acid

PHB: poly(3-hydroxybutyric acid)

PI3K: phosphatidylinositol 3-kinase

PLA: poly-(lactic acid)

PLC-γ: phospholipase C-γ

PLGA: poly-(lactide-coglycolide)

PMR: preferential motor reinnervation

PNI: Peripheral Nerve Injury

PNS: Peripheral Nervous System

VEGF: vascular endothelial growth factor

T-zone: transition zone

TrkA: tropomyosin receptor kinase A

TrkB: tropomyosin receptor kinase B

TrkC: tropomyosin receptor kinase C

VI. REFERENCES

REFERENCES

Abernethy, D.A., Rud, A., Thomas, P.K., 1992. Neurotropic influence of the distal stump of transected peripheral nerve on axonal regeneration : absence of topographic specificity in adult nerve 395–400.

Acheson, A., Barker, P.A., Alderson, R.F., Miller, F.D., Murphy, R.A., 1991. Detection of brain-derived neurotrophic factor-like activity in fibroblasts and Schwann cells: inhibition by antibodies to NGF. Neuron 7, 265–275. doi:10.1016/0896-6273(91)90265-2

Agius, E., Cochard, P., 1998. Comparison of Neurite Outgrowth Induced by Intact and Injured Sciatic Nerves : A Confocal and Functional Analysis. J. Neurosci. 18, 328–338.

Airaksinen, M.S., Koltzenburg, M., Lewin, G.R., Masu, Y., Helbig, C., Wolf, E., Brem, G., Toyka, K. V, Thoenen, H., Meyer, M., 1996. Specific Subtypes of Cutaneous Mechanoreceptors Require Neurotrophin-3 Following Peripheral Target Innervation. Neuron 16, 287–295. doi:10.1016/S0896-6273(00)80047-1

Akin, T., Najafi, K., Smoke, R.H., Bradley, R.M., 1994. A micromachined silicon sieve electrode for nerve regeneration applications. IEEE Trans. Biomed. Eng. 41, 305–313. doi:10.1109/10.284958

Allodi, I., Casals-Díaz, L., Santos-Nogueira, E., Gonzalez-Perez, F., Navarro, X., Udina, E., 2013. FGF-2 low molecular weight selectively promotes neuritogenesis of motor neurons in vitro. Mol. Neurobiol. 47, 770–81. doi:10.1007/s12035-012-8389-z

Allodi, I., Guzmán-Lenis, M.-S., Hernàndez, J., Navarro, X., Udina, E., 2011. In vitro comparison of motor and sensory neuron outgrowth in a 3D collagen matrix. J. Neurosci. Methods 198, 53–61. doi:10.1016/j.jneumeth.2011.03.006

Allodi, I., Mecollari, V., González-Pérez, F., Eggers, R., Hoyng, S., Verhaagen, J., Navarro, X., Udina, E., 2014. Schwann cells transduced with a lentiviral vector encoding Fgf-2 promote motor neuron regeneration following sciatic nerve injury. Glia 62, 1736–46. doi:10.1002/glia.22712

Allodi, I., Udina, E., Navarro, X., 2012. Specificity of peripheral nerve regeneration : Interactions at the axon level. Prog. Neurobiol. 98, 16–37.

Alsmadi, N.Z., Patil, L.S., Hor, E.M., Lofti, P., Razal, J.M., Chuong, C.-J., Wallace, G.G., Romero-Ortega, M.I., 2015. Coiled polymeric growth factor gradients for multi-luminal neural chemotaxis. Brain Res. 1619, 72–83. doi:10.1016/j.brainres.2015.01.055

Archibald, S.J., Krarup, C., Shefner, J., Li, S.T., Madison, R.D., 1991. A collagen-based nerve guide conduit for peripheral nerve repair: an electrophysiological study of nerve regeneration in rodents and nonhuman primates. J. Comp. Neurol. 306, 685–696. doi:10.1002/cne.903060410

Arslantunali, D., Dursun, T., Yucel, D., Hasirci, N., Hasirci, V., 2014. Peripheral nerve conduits: Technology update. Med. Devices Evid. Res. 7, 405–424. doi:10.2147/MDER.S59124

Arvanitis, D., Davy, A., 2008. Eph / ephrin signaling : networks. Genes Dev. 22, 416–429. doi:10.1101/gad.1630408.416

Babington, E.J., Vatanparast, J., Verrall, J., Blackshaw, S.E., 2005. Three-dimensional culture of leech and snail ganglia for studies of neural repair. Invert. Neurosci. 5, 173–82. doi:10.1007/s10158-005-0006-7

Badia, J., Boretius, T., Andreu, D., Azevedo-Coste, C., Stieglitz, T., Navarro, X., 2011. Comparative analysis of transverse intrafascicular multichannel, longitudinal intrafascicular and multipolar cuff electrodes for the selective stimulation of nerve fascicles. J. Neural Eng. 8, 036023. doi:10.1088/1741-2560/8/3/036023

Bennett, D.L.H., Averill, S., Clary, D., Priestleyl, J. V, McMahon, S.B., 1996. SHORT COMMUNICATION Postnatal Changes in the Expression of the trkA High- affinity NGF Receptor in Primary Sensory Neurons. Eur. J. Neurosci. 8, 2204–2208.

Bennett, D.L.H., Michael, G.J., Ramachandran, N., Munson, J.B., Averill, S., Yan, Q., Mcmahon, S.B., Priestley, J. V, 1998. A Distinct Subgroup of Small DRG Cells Express GDNF Receptor Components and GDNF Is Protective for These Neurons after Nerve Injury. J. Neurosci. 18, 3059–3072.

Bibel, M., Hoppe, E., Barde, Y., 1999. Biochemical and functional interactions between the neurotrophin receptors trk and p75 NTR. EMBO J. 18, 616–622.

Biran, R., Martin, D.C., Tresco, P. a, 2007. The brain tissue response to implanted silicon microelectrode arrays is increased when the device is tethered to the skull. J Biomed Mater Res A. 82, 169–78. doi:10.1002/jbm.a.31138

Bixby, J.L., Harris, W. a, 1991. Molecular mechanisms of axon growth and guidance. Annu. Rev. Cell Biol. 7, 117–59. doi:10.1146/annurev.cb.07.110191.001001

Bodine-Fowler, S., Meyer, R., Moskovitz, A., Abrams, R., Botte, M., 1997. Inaccurate projection of rat soleus motoneurons: a comparison of nerve repair techniques. Muscle Nerve 20, 29–37.

Bouquet, C., Nothias, F., 2007. Molecular mechanisms of axonal growth. Adv. Exp. Med. Biol. doi:10.1007/978-0-387-76715-4_1

Boyd, J.G., Gordon, T., 2003a. Glial cell line-derived neurotrophic factor and brain-derived neurotrophic factor sustain the axonal regeneration of chronically axotomized motoneurons in vivo. Exp. Neurol. 183, 610–619. doi:10.1016/S0014-4886(03)00183-3

Boyd, J.G., Gordon, T., 2003b. Neurotrophic Factors and Their Receptors in Axonal Regeneration and Functional Recovery After Peripheral Nerve Injury. Mol. Neurobiol. 27, 277–324.

Boyd, J.G., Gordon, T., 2002. A dose-dependent facilitation and inhibition of peripheral nerve regeneration by brain-derived neurotrophic factor. Eur. J. Neurosci. 15, 613–626. doi:10.1046/j.1460-9568.2002.01891.x

Boyd, J.G., Gordon, T., 2001. The neurotrophin receptors, trkB and p75, differentially regulate motor axonal regeneration. J. Neurobiol. 49, 314–25. doi:10.1002/neu.10013

Braun, S., Croizat, B., Lagrange, M.-C., Warter, J.-M., Poindron, P., 1996. Neurotrophins increase motoneurons' ability to innervate skeletal muscle fibers in rat spinal cord-human muscle cocultures. J. Neurol. Sci. 136, 17–23. doi:10.1016/0022-510X(95)00315-S

Bredeson, S., Kanneganti, A., Deku, F., Cogan, S., Romero-Ortega, M., Troyk, P., 2015. Chronic in-vivo testing of a 16-channel implantable wireless neural stimulator. Conf Proc IEEE Eng Med Biol Soc. 1017–20. doi:10.1109/EMBC.2015.7318537

Brushart, T., Gerber, J., Kessens, P., Chen, Y., Royall, R., 1998. Contributions of Pathway and Neuron to Preferential Motor Reinnervation 18, 8674–8681.

Brushart, T., Seiler, W., 1987. Selective Reinnervation by Peripheral of Distal Motor Stumps Motor Axons '. Exp. Neurol. 97, 289–300.

Brushart, T.M., 1993. Motor axons preferentially reinnervate motor pathways. J. Neurosci. 13, 2730–2738.

Brushart, T.M., 1988. Preferential Axons Reinnervation of Motor Nerves by Regenerating Motor 8.

Brushart, T.M., Aspalter, M., Griffin, J.W., Redett, R., Hameed, H., Zhou, C., Wright, M., Vyas, a, Höke, a, 2013. Schwann cell phenotype is regulated by axon modality and central-peripheral location, and persists in vitro. Exp. Neurol. 247, 272–81. doi:10.1016/j.expneurol.2013.05.007

Buj-Bello, A., Buchman, V.L., Horton, A., Rosenthal, A., Davies, A.M., 1995. GDNF is an age-specific survival factor for sensory and autonomic neurons. Neuron 15, 821–828. doi:10.1016/0896-6273(95)90173-6

Bunge, M., Williams, A., Wood, P., 1982. Neuron-Schwann in Basal Lamina Formation. Dev. Biol. 460, 449–460.

Burnett, M.G., Zager, E.L., 2004. Pathophysiology of peripheral nerve injury: a brief review. Neurosurg. Focus 16, E1. doi:10.3171/foc.2004.16.5.2

Butí, M., Verdú, E., Labrador, R.O., Vilches, J., Forés, J., Navarro, X., 1996. Influence of Physical Parameters of Nerve Chambers on Peripheral Nerve Regeneration and Reinnervation. Exp. Neurol. 33, 26–33.

Caissie, R., Gingras, M., Champigny, M.-F., Berthod, F., 2006. In vivo enhancement of sensory perception recovery in a tissue-engineered skin enriched with laminin. Biomaterials 27, 2988–93. doi:10.1016/j.biomaterials.2006.01.014

Campbell, W.W., 2008. Evaluation and management of peripheral nerve injury. Clin. Neurophysiol. 119, 1951–65. doi:10.1016/j.clinph.2008.03.018

Chao, M. V, 2003. Neurotrophins and their receptors: a convergence point for many signalling pathways. Nat. Rev. Neurosci. 4, 299–309. doi:10.1038/nrn1078

Chernousov, M., Carey, D., 2000. Schwann cell extracellular matrix molecules and their receptors. Histol. Histopathol. 15, 593–601.

Chew, S., Mi, R., Höke, A., Leong, K., 2008. Aligned Protein–Polymer Composite Fibers Enhance Nerve Regeneration: A Potential Tissue-Engineering Platform. Adv Funct Mater. 17, 1288–1296.

Chiono, V., Tonda-Turo, C., 2015. Trends in the design of nerve guidance channels in peripheral nerve tissue engineering. Prog. Neurobiol. 1–18. doi:10.1016/j.pneurobio.2015.06.001

Cho, Y., Sloutsky, R., Naegle, K.M., Cavalli, V., 2013. Injury-induced HDAC5 nuclear export is essential for axon regeneration. Cell 155, 894–908. doi:10.1016/j.cell.2013.10.004

Chung, K., 2004. Challenges and Recent Developments in Hearing Aids: Part II. Feedback and Occlusion Effect Reduction Strategies, Laser Shell Manufacturing Processes, and Other Signal Processing Technologies. Trends Amplif. 8, 125–164. doi:10.1177/108471380400800402

Clements, I., Mukhatyar, V., Srinivasan, A., Bentley, J.T., Andreasen, D., Bellamkonda, R. V., 2013. Regenerative scaffold electrodes for peripheral nerve interfacing. Neural Syst. … 21, 554–566.

Clements, I.P., Kim, Y., Andreasen, D., Bellamkonda, R. V., 2007. A regenerative electrode scaffold for peripheral nerve interfacing. 2007 3rd Int. IEEE/EMBS Conf. Neural Eng. 390–393. doi:10.1109/CNE.2007.369691

Cogan, S.F., 2008. Neural stimulation and recording electrodes. Annu. Rev. Biomed. Eng. 10, 275–309. doi:10.1146/annurev.bioeng.10.061807.160518

Cohen, S., Levi-Montalcini, R., 1956. A NERVE GROWTH-STIMULATING FACTOR ISOLATED FROM SNAKE VENOM. Proc. Natl. Acad. Sci. 42, 571–574.

Curley, J., Catig, G., Horn-Ranney, E., Moore, M., 2014. Sensory axon guidance with semaphorin 6A and nerve growth factor in a biomimetic choice point model. Biofabrication 6, 1–26. doi:10.1088/1758-5082/6/3/035026

Curtis, R., Adryan, K., Zhu, Y., Harkness, P., Lindsay, R., DiStefano, P.S., 1993. Retrograde axonal transport of ciliary neurotrophic factor is increased by peripheral nerve injury. Nature 365, 253–255.

Curtis, R., Scherer, S.S., Somogyi, R., Adryan, K.M., Ip, N.Y., Zhu, Y., Lindsay, R.M., DiStefano, P.S., 1994. Retrograde axonal transport of LIF is increased by peripheral nerve injury: Correlation with increased LIF expression in distal nerve. Neuron 12, 191–204. doi:10.1016/0896-6273(94)90163-5

Curtis, R., Tonra, J.R., Stark, J.L., Adryan, K.M., Park, J.S., Cliffer, K.D., Lindsay, R.M., DiStefano, P.S., 1998. Neuronal injury increases retrograde axonal transport of the neurotrophins to spinal sensory neurons and motor neurons via multiple receptor mechanisms. Mol. Cell. Neurosci. 12, 105–18. doi:10.1006/mcne.1998.0704

Cutrone, A., del Valle, J., Santos, D., Badia, J., Filippeschi, C., Micera, S., 2015. A three-dimensional self-opening intraneural peripheral interface (SELINE). J. Neural Eng. 0, 0. doi:10.1088/1741-2560/0/0/000000

Daly, W., Yao, L., Zeugolis, D., Windebank, A., Pandit, A., 2012. A biomaterials approach to peripheral nerve regeneration : bridging the peripheral nerve gap and enhancing functional recovery. J.R.Soc.Interface 9, 202–221.

Davis, J., Stroobant, P., 1990. Platelet-derived Growth Factors and Fibroblast Growth Factors Are Mitogens for Rat Schwalm Cells. J. Cell Biol. 110, 1353–1360.

Davis, T.S., Wark, H. a C., Hutchinson, D.T., Warren, D.J., O'Neill, K., Scheinblum, T., Clark, G. a, Normann, R. a, Greger, B., 2016. Restoring motor control and sensory feedback in people with upper extremity amputations using arrays of 96 microelectrodes implanted in the median and ulnar nerves. J. Neural Eng. 13, 036001. doi:10.1088/1741-2560/13/3/036001

De Boer, R., Borntraeger, A., Knight, A.M., Hébert-Blouin, M.-N., Spinner, R.J., Malessy, M.J. a, Yaszemski, M.J., Windebank, A.J., 2012. Short- and long-term peripheral nerve regeneration using a poly-lactic-co-glycolic-acid scaffold containing nerve growth factor and glial cell line-derived neurotrophic factor releasing microspheres. J. Biomed. Mater. Res. A 100, 2139–46. doi:10.1002/jbm.a.34088

Del Valle, J., Navarro, X., 2013. Interfaces with the peripheral nerve for the control of neuroprostheses. Int. Rev. Neurobiol. 109, 63–83. doi:10.1016/B978-0-12-420045-6.00002-X

Delivopoulos, E., Chew, D.J., Minev, I.R., Fawcett, J.W., Lacour, S.P., 2012. Concurrent recordings of bladder afferents from multiple nerves using a microfabricated PDMS microchannel electrode array. Lab Chip 12, 2540–51. doi:10.1039/c2lc21277c

Desai, V.H., Anand, S., Tran, M., Kanneganti, A., Vasudevan, S., Seifert, J.L., Cheng, J., 2014. Chronic Sensory - Motor Activity in Behaving Animals using Regenerative Multi - electrode Interfaces. Conf Proc IEEE Eng Med Biol Soc. 1973–1976.

Deumens, R., Bozkurt, A., Meek, M.F., Marcus, M. a E., Joosten, E. a J., Weis, J., Brook, G. a, 2010. Repairing injured peripheral nerves: Bridging the gap. Prog. Neurobiol. 92, 245–76. doi:10.1016/j.pneurobio.2010.10.002

Diamond, J., Coughlin, M., Macintyre, L., Holmes, M., 1987. Evidence that endogenous BETA nerve growth factor is responsible for the collateral sprouting , but not the regeneration , of nociceptive axons in adult rats. Proc. Nati. Acad. Sci. USA 84, 6596–6600.

Dickson, B.J., 2002. Molecular Mechanisms of Axon Guidance. Science (80-.). 298, 1959–1964.

Dinis, T.M., Elia, R., Vidal, G., Dermigny, Q., Denoeud, C., Kaplan, D.L., Egles, C., Marin, F., 2015. 3D multi-channel bi-functionalized silk electrospun conduits for peripheral nerve regeneration. J. Mech. Behav. Biomed. Mater. 41, 43–55. doi:10.1016/j.jmbbm.2014.09.029

Ebendal, T., Tomac, a, Hoffer, B.J., Olson, L., 1995. Glial cell line-derived neurotrophic factor stimulates fiber formation and survival in cultured neurons from peripheral autonomic ganglia. J. Neurosci. Res. 40, 276–84. doi:10.1002/jnr.490400217

Edell, D.J., 1986. A peripheral nerve information transducer for amputees: long-term multichannel recordings from rabbit peripheral nerves. IEEE Trans. Biomed. Eng. 33, 203–14. doi:10.1109/TBME.1986.325892

Eggers, R., de Winter, F., Hoyng, S. a, Roet, K.C.D., Ehlert, E.M., Malessy, M.J. a, Verhaagen, J., Tannemaat, M.R., 2013. Lentiviral vector-mediated gradients of GDNF in the injured peripheral nerve: effects on nerve coil formation, Schwann cell maturation and myelination. PLoS One 8, e71076. doi:10.1371/journal.pone.0071076

Ejstrup, R., Kiilgaard, J.F., Tucker, B. a, Klassen, H.J., Young, M.J., La Cour, M., 2010. Pharmacokinetics of intravitreal glial cell line-derived neurotrophic factor: experimental studies in pigs. Exp. Eye Res. 91, 890–5. doi:10.1016/j.exer.2010.09.016

Erlanger, J., Gasser, H.S., 1937. Electrical signs of nervous activity.

Ernfors, P., Rosario, C.M., Grant, G., Aldskogius, H., Persson, H., 1993. Expression of mRNAs for neurotrophin receptors in the dorsal root ganglion and spinal cord during development and following peripheral or central axotomy. Mol. Brain Res. 17, 217–226.

Evercooren, A.B., Kleinman, H.K., Ohno, S., Schwa-, J.P., Dubois-dalcq, M.E., 1982. Nerve Growth Factor , Laminin , and Fibronectin Promote Neurite Growth in Human Fetal Sensory Ganglia Cultures. J. Neurosci. Res. 193, 179–193.

Evercooren, B., Gansmüller, A., Gumpel, M., Baumann, N., Kleinman, H., 1986. Schwann cell differentiation in vitro: extracellular matrix deposition and interaction. Dev Neurosci 8, 182–196.

Faroni, A., Mobasseri, S.A., Kingham, P.J., Reid, A.J., 2015. Peripheral nerve regeneration: Experimental strategies and future perspectives. Adv. Drug Deliv. Rev. 82, 160–167. doi:10.1016/j.addr.2014.11.010

Fields, R.D., Le Beau, J.M., Longo, F.M., Ellisman, M.H., 1989. Nerve regeneration through artificial tubular implants. Prog. Neurobiol. 33, 87–134. doi:10.1016/0301-0082(89)90036-1

Fine, E., Decosterd, I., Papaloïzos, M., Zurn, A., Aebischer, P., 2002. GDNF and NGF released by synthetic guidance channels support sciatic nerve regeneration across a long gap. Eur. J. Neurosci. 15, 589–601.

Fitzgerald, J.J., Lago, N., Benmerah, S., Serra, J., Watling, C.P., Cameron, R.E., Tarte, E., Lacour, S.P., McMahon, S.B., Fawcett, J.W., 2012. A regenerative microchannel neural interface for recording from and stimulating peripheral axons in vivo. J. Neural Eng. 9, 016010. doi:10.1088/1741-2560/9/2/029601

Fox, M. a, 2008. Novel roles for collagens in wiring the vertebrate nervous system. Curr. Opin. Cell Biol. 20, 508–13. doi:10.1016/j.ceb.2008.05.003

Frank, L., Ventimiglia, R., Anderson, K., Lindsay, R., Rudge, J., 1996. BDNF down-regulates neurotrophin responsiveness, TrkB protein and TrkB mRNA levels in cultured rat hippocampal neurons. Eur. J. Neurosci. 8, 1220–1230. doi:10.1111/j.1460-9568.1996.tb01290.x

Franz, C.K., Rutishauser, U., Rafuse, V.F., 2005. Polysialylated neural cell adhesion molecule is necessary for selective targeting of regenerating motor neurons. J. Neurosci. 25, 2081–91. doi:10.1523/JNEUROSCI.4880-04.2005

Freeman, R.S., Burch, R.L., Crowder, R.J., Lomb, D.J., Schoell, M.C., Straub, J.A., Xie, L., 2004. NGF deprivation-induced gene expression: after ten years, where do we stand? Prog. Brain Res. 146, 111–126. doi:10.1016/S0079-6123(03)46008-1

Funakoshi, H., Frisén, J., Barbany, G., Timmusk, T., Zachrisson, O., Verge, V., Persson, H., 1993. Differential expression of mRNAs for neurotrophins and their receptors after axotomy of the sciatic nerve. J. cell … 123, 455–465.

Garde, K., Keefer, E., Botterman, B., Galvan, P., Romero, M.I., 2009. Early interfaced neural activity from chronic amputated nerves. Front. Neuroeng. 2, 5. doi:10.3389/neuro.16.005.2009

Gardiner, N.J., 2011. Integrins and the extracellular matrix: key mediators of development and regeneration of the sensory nervous system. Dev. Neurobiol. 71, 1054–72. doi:10.1002/dneu.20950

Gardiner, N.J., Moffatt, S., Fernyhough, P., Humphries, M.J., Streuli, C.H., Tomlinson, D.R., 2007. Preconditioning injury-induced neurite outgrowth of adult rat sensory neurons on fibronectin is mediated by mobilisation of axonal alpha5 integrin. Mol. Cell. Neurosci. 35, 249–60. doi:10.1016/j.mcn.2007.02.020

Georgeu, G. a, Walbeehm, E.T., Tillett, R., Afoke, a, Brown, R. a, Phillips, J.B., 2005. Investigating the mechanical shear-plane between core and sheath elements of peripheral nerves. Cell Tissue Res. 320, 229–34. doi:10.1007/s00441-004-1031-2

Ghosh, A., Greenberg, M., 1995. Calcium signaling in neurons: molecular mechanisms and cellular consequences. Science (80-.). 268, 239–247.

Giger, R.J., Ii, E.R.H., Tuszynski, M.H., 2015. Guidance Molecules in Axon Regeneration. Cold Spring Harb Perspect Biol. 7, 1–22.

Giordano, S., Sherman, L., Lyman, W., Morrison, R., 1992. Multiple molecular weight forms of basic fibroblast growth factor are developmentally regulated in the central nervous system. Dev. Biol. 152, 293–303. doi:10.1016/0012-1606(92)90136-5

Gloster, A., Diamond, J., Ln, C., 1992. Sympathetic Nerves in Adult Rats Regenerate Normally and Restore Pilomotor Function During an Anti-NGF Treatment That Prevents Their Collateral Sprouting. J. Comp. Neurol. 326, 363–374.

Gluck, T., 1880. Ueber neuroplastik auf dem wege der transplantation. Arch Klin Chir 25, 606–616.

Godinho, M.J., Teh, L., Pollett, M. a, Goodman, D., Hodgetts, S.I., Sweetman, I., Walters, M., Verhaagen, J., Plant, G.W., Harvey, A.R., 2013. Immunohistochemical, ultrastructural and functional analysis of axonal

regeneration through peripheral nerve grafts containing Schwann cells expressing BDNF, CNTF or NT3. PLoS One 8, e69987. doi:10.1371/journal.pone.0069987

Gold, B.., 1997. Axonal regeneration of sensory nerves is delayed by continuous intrathecal infusion of nerve growth factor. Neuroscience 76, 1153–1158. doi:10.1016/S0306-4522(96)00416-2

Goldberg, J.L., 2003. How does an axon grow ? Genes Dev. 941–958. doi:10.1101/gad.1062303.GENES

Gómez, N., Cuadras, J., Butí, M., Navarro, X., 1996. Histologic assessment of sciatic nerve regeneration following resection and graft or tube repair in the mouse. Restor Neurol Neurosci. doi:10.3233/RNN-1996-10401; 10.3233/RNN-1996-10401

Gonzalez-Perez, F., Alé, A., Santos, D., Barwig, C., Freier, T., Navarro, X., Udina, E., 2015. Substratum preferences of motor and sensory neurons in postnatal and adult rats. Eur. J. Neurosci. 1–12. doi:10.1111/ejn.13057

Gonzalez-Perez, F., Udina, E., Navarro, X., 2013. Extracellular matrix components in peripheral nerve regeneration. Int. Rev. Neurobiol. 108, 257–275. doi:10.1016/B978-0-12-410499-0.00010-1

Gordon, T., Hegedus, J., Tam, S.L., 2004. Adaptive and maladaptive motor axonal sprouting in aging and motoneuron disease. Neurol. Res. 26, 174–85. doi:10.1179/016164104225013806

Gordon, T., Sulaiman, O., Boyd, J.G., 2003. Experimental strategies to promote functional recovery after peripheral nerve injuries. J. Peripher. Nerv. Syst. 8, 236–250. doi:10.1111/j.1085-9489.2003.03029.x

Gordon, T., Tyreman, N., Raji, M. a, 2011. The basis for diminished functional recovery after delayed peripheral nerve repair. J. Neurosci. 31, 5325–34. doi:10.1523/JNEUROSCI.6156-10.2011

Grothe, C., Heese, K., Meisinger, C., Wewetzer, K., Kunz, D., Cattini, P., Otten, U., 2000. Expression of interleukin-6 and its receptor in the sciatic nerve and cultured Schwann cells: relation to 18-kD fibroblast growth factor-2. Brain Res. 885, 172–181. doi:10.1016/S0006-8993(00)02911-5

Grothe, C., Meisinger, C., Hertenstein, A., Kurz, H., Wewetzer, K., 1997. EXPRESSION OF FIBROBLAST GROWTH FACTOR-2 AND FIBROBLAST GROWTH FACTOR RECEPTOR 1 MESSENGER RNAS IN SPINAL GANGLIA AND SCIATIC NERVE : REGULATION AFTER PERIPHERAL NERVE LESION 76, 123–135.

Grothe, C., Nikkhah, G., 2001. The role of basic fibroblast growth factor in peripheral nerve regeneration. Anat. Embryol. (Berl). 204, 171–177. doi:10.1007/s004290100205

Groves, M.J., An, S.F., Giometto, B., Scaravilli, F., 1999. Inhibition of sensory neuron apoptosis and prevention of loss by NT-3 administration following axotomy. Exp. Neurol. 155, 284–94. doi:10.1006/exnr.1998.6985

Guan, W., Puthenveedu, M.A., Condic, M.L., 2003. Sensory Neuron Subtypes Have Unique Substratum Preference and Receptor Expression before Target Innervation. J. Neurosci. 23, 1781–1791.

Gutmann, E., Guttmann, L., Medawar, P.B., Young, J.Z., 1942. The rate of regeneration of nerve. J. Exp. Biol. 19, 14–44.

Haastert, K., Lipokatic, E., Fischer, M., Timmer, M., Grothe, C., 2006. Differentially promoted peripheral nerve regeneration by grafted Schwann cells over-expressing

different FGF-2 isoforms. Neurobiol. Dis. 21, 138–53. doi:10.1016/j.nbd.2005.06.020

Hall, S., 2005. Mechanisms of repair after traumatic injury, in: Peripheral Neuropathy. Elsevier, pp. 1403–1433. doi:10.1016/B978-0-7216-9491-7.50061-2

Hausott, B., Schlick, B., Vallant, N., Dorn, R., Klimaschewski, L., 2008. Promotion of neurite outgrowth by fibroblast growth factor receptor 1 overexpression and lysosomal inhibition of receptor degradation in pheochromocytoma cells and adult sensory neurons. Neuroscience 153, 461–73. doi:10.1016/j.neuroscience.2008.01.083

Hempstead, B., Martin-Zanca, D., Kaplan, D., 1991. High-affinity NGF binding requires coexpression of the trk proto-oncogene and the low-affinity NGF receptor. Nature 350, 678–683.

Henderson, C.E., Phillips, H.S., Pollock, R.A., Davies, A.M., Lemeulle, C., Armanini, M., Simpson, L.C., Moffet, B., Vandlen, R.A., Koliatsos, V.E., Rosenthal, A., 1994. GDNF : Potent Survival Present in Peripheral Motoneurons Muscle. Science (80-.). 266, 1062–1064.

Henle, S.J., Wang, G., Liang, E., Wu, M., Poo, M., Henley, J.R., 2011. Asymmetric PI (3 , 4 , 5) P 3 and Akt Signaling Mediates Chemotaxis of Axonal Growth Cones. J. Neurosci. 31, 7016–7027. doi:10.1523/JNEUROSCI.0216-11.2011

Heumann, R., Korsching, S., Bandtlow, C., Thoenen, H., 1987a. Changes of Nerve Growth Factor Synthesis in Nonneuronal Cells in Response to Sciatic Nerve Transection. J. Cell Biol. 104, 1623–1631.

Heumann, R., Lindholm, D., Bandtlow, C., Meyer, M., Radeke, M., Misko, T., Shooter, E., Thoenen, H., 1987b. Differential regulation of mRNA enconding nerve growth factor and its receptor in rat sciatic nerve during development, degeneration, and regeneration: Role of macrophages. Proc. Nati. Acad. Sci. USA 84, 8735–8739.

Hoffman, P.N., Cleveland, D.O.N.W., Griffint, J.W., Landes, P.W., I, N.J.C., Price, D.L., 1987. Neurofilament gene expression: A major determinant of axonal caliber. Proc. Nati. Acad. Sci. USA 84, 3472–3476.

Höke, A., Cheng, C., Zochodne, D.W., 2000. Expression of glial cell line-derived neurotrophic factor family of growth factors in peripheral nerve injury in rats. Neuroreport 11, 1651–1654. doi:10.1097/00001756-200006050-00011

Höke, A., Gordon, T., Zochodne, D., Sulaiman, O., 2002. A decline in glial cell-line-derived neurotrophic factor expression is associated with impaired regeneration after long-term Schwann cell denervation. Exp. Neurol. 173, 77–85. doi:10.1006/exnr.2001.7826

Höke, A., Ho, T., Crawford, T., Lebel, C., Hilt, D., Griffin, J.W., 2003. Glial cell line-derived neurotrophic factor alters axon schwann cell units and promotes myelination in unmyelinated nerve fibers. J. … 23, 561–567.

Höke, A., Redett, R., Hameed, H., Jari, R., Zhou, C., Li, Z.B., Griffin, J.W., Brushart, T.M., 2006. Schwann cells express motor and sensory phenotypes that regulate axon regeneration. J. Neurosci. 26, 9646–55. doi:10.1523/JNEUROSCI.1620-06.2006

Höke, A., Sun, H.S., Gordon, T., Zochodne, D.W., 2001. Do denervated peripheral nerve trunks become ischemic? The impact of chronic denervation on vasa nervorum. Exp. Neurol. 172, 398–406. doi:10.1006/exnr.2001.7808

Hökfelt, T., Broberger, C., Xu, Z.D., Sergeyev, V., Ubink, R., Diez, M., 2000. Neuropeptides — an overview Tomas Ho. Neuropharmacology 39, 1337–1356.

Hökfelt, T., Zhang, X., 2006. Central consequences of peripheral nerve damage. Wall Melzack's … 60, 947–960.

Hontanilla, B., Aubá, C., Gorría, O., 2007. Nerve regeneration through nerve autografts after local administration of brain-derived neurotrophic factor with osmotic pumps. Neurosurgery 61, 1268–1274. doi:10.1227/01.neu.0000306106.70421.ed

Huang, E.J., Reichardt, L.F., 2001. Neurotrophins: roles in neuronal development and function. Annu. Rev. Neurosci. 24, 677–736. doi:10.1146/annurev.neuro.24.1.677

Ito, M., Kudo, M., 1994. Reinnervation by axon collaterals from single facial motoneurons to multiple muscle targets following axotomy in the adult guinea pig. Acta Anat 151, 124–130.

Jain, R.A., 2000. The manufacturing techniques of various drug loaded biodegradable poly (lactide- co -glycolide) (PLGA) devices. Biomaterials 21, 2475–2490.

Jaquet, J., Shreuders, T., Kalmijn, S., Ruys, a. C.J., Coert, H., Hovius, S.E.R., 2006. Median and Ulnar Nerve Injuries: Prognosis and Predictors for Clinical Outcome, Journal of Reconstructive Microsurgery. doi:10.1055/s-2006-949697

Jayasinghe, S.N., 2013. Cell electrospinning: a novel tool for functionalising fibres, scaffolds and membranes with living cells and other advanced materials for regenerative biology and medicine. Analyst 138, 2215–23. doi:10.1039/c3an36599a

Jesuraj, N.J., Nguyen, P.K., Wood, M.D., Moore, A.M., Borschel, G.H., Mackinnon, S.E., Sakiyama-Elbert, S.E., 2012. Differential gene expression in motor and sensory Schwann cells in the rat femoral nerve. J. Neurosci. Res. 90, 96–104. doi:10.1002/jnr.22752

Johnson, E.O., Charchanti, A., Soucacos, P.N., 2008. Nerve repair: Experimental and clinical evaluation of neurotrophic factors in peripheral nerve regeneration. Injury 39, 34–37. doi:10.1016/j.injury.2008.06.015

Johnson, E.O., Soucacos, P.N., 2008. Nerve repair: experimental and clinical evaluation of biodegradable artificial nerve guides. Injury 39 Suppl 3, S30–6. doi:10.1016/j.injury.2008.05.018

K.M Rich, J.R Luszczynski, P.A Osborne, E.. J., 1987. Nerve growth factor protects adult sensory neurons from cell death and atrophy caused by nerve injury. J. Neurocytol. 268, 261–268.

Kang, H., Lichtman, J.W., 2013. Motor Axon Regeneration and Muscle Reinnervation in Young Adult and Aged Animals. J. Neurosci. 33, 19480–19491. doi:10.1523/JNEUROSCI.4067-13.2013

Kehoe, S., Zhang, X.F., Boyd, D., 2012. FDA approved guidance conduits and wraps for peripheral nerve injury: a review of materials and efficacy. Injury 43, 553–72. doi:10.1016/j.injury.2010.12.030

Kerrebijn, J., Freeman, J., 1998. Facial nerve reconstruction: outcome and failures. J. Otolaryngol. … 27, 183–186.

Kimura, J., Rodnitzky, R.L., Okawara, S.H., 1975. Electrophysiologic analysis of aberrant regeneration after facial nerve paralysis. Neurology 25, 989–93.

Koh, H.S., Yong, T., Teo, W.E., Chan, C.K., Puhaindran, M.E., Tan, T.C., Lim, a, Lim, B.H., Ramakrishna, S., 2010. In vivo study of novel nanofibrous intra-luminal guidance channels to promote nerve regeneration. J. Neural Eng. 7, 046003. doi:10.1088/1741-2560/7/4/046003

Kokai, L.E., Bourbeau, D., Weber, D., McAtee, J., Marra, K.G., 2011. Sustained growth factor delivery promotes axonal regeneration in long gap peripheral nerve repair. Tissue Eng. Part A 17, 1263–75. doi:10.1089/ten.TEA.2010.0507

Konofaos, P., 2013. Nerve Repair by Means of Tubulization : Past , Present , Future.

Kuhn, T.B., Schmidt, M.F., Kater, S.B., 1995. Laminin and fibronectin guideposts signal sustained but opposite effects to passing growth cones. Neuron 14, 275–285. doi:10.1016/0896-6273(95)90285-6

Kwok, R., 2013. Once more, with feeling. Nature 497, 176. doi:10.1038/497176a

Labrador, R.O., Butí, M., Navarro, X., 1998. Influence of collagen and laminin gels concentration on nerve regeneration after resection and tube repair. Exp. Neurol. 149, 243–252. doi:10.1006/exnr.1997.6650

Labrador, R.O., Butí, M., Navarro, X., 1995. Peripheral nerve repair: role of agarose matrix density on functional recovery. Neuroreport 6, 2022–2026.

Lacour, S.P., Fitzgerald, J.J., Lago, N., Tarte, E., McMahon, S., Fawcett, J., 2009. Long micro-channel electrode arrays: a novel type of regenerative peripheral nerve interface. IEEE Trans. Neural Syst. Rehabil. Eng. 17, 454–60. doi:10.1109/TNSRE.2009.2031241

Lago, N., Ceballos, D., Rodríguez, F.J., Stieglitz, T., Navarro, X., 2005. Long term assessment of axonal regeneration through polyimide regenerative electrodes to interface the peripheral nerve. Biomaterials 26, 2021–31. doi:10.1016/j.biomaterials.2004.06.025

Lago, N., Udina, E., Ramachandran, A., Navarro, X., 2007. Neurobiological assessment of regenerative electrodes for bidirectional interfacing injured peripheral nerves. IEEE Trans. Biomed. Eng. 54, 1129–37. doi:10.1109/TBME.2007.891168

Lee, S.E., Shen, H., Taglialatela, G., Chung, J.M., Chung, K., 1998. Expression of nerve growth factor in the dorsal root ganglion after peripheral nerve injury. Brain Res. 796, 99–106. doi:10.1016/S0006-8993(98)00335-7

Lefcort, F., Venstrom, K., Mcdonald, J.A., Reichardt, L.F., 1992. Regulation of expression of fibronectin and its receptor , development and regeneration of peripheral nerve during. Development 782, 767–782.

Letourneau, P.C., Shattuck, T. a, 1989. Distribution and possible interactions of actin-associated proteins and cell adhesion molecules of nerve growth cones. Development 105, 505–519.

Li, H., Terenghi, G., Hall, S.M., 1997. Effects of delayed re-innervation on the expression of c-erbB receptors by chronically denervated rat Schwann cells in vivo. Glia 20, 333–47.

Li, Y., Jia, Y., Cui, K., Li, N., Zheng, Z., Wang, Y., Yuan, X., 2005. Essential role of TRPC channels in the guidance of nerve growth cones by brain-derived neurotrophic factor. Nature 434, 1–5.

Lieberman, A., 1971. The axon reaction: a review of the principal features of perikaryal responses to axon injury. Int. Rev. Neurobiol. 14, 49–124.

Lindholm, D., Heumann, R., Meyer, M., Thoenen, H., 1987. Interleukin-1 regulates synthesis of nerve growth factor in non-neuronal cells of rat sciatic nerve. Nature 330, 658–659.

Lotfi, P., Garde, K., Chouhan, A.K., Bengali, E., Romero-Ortega, M.I., 2011. Modality-specific axonal regeneration: toward selective regenerative neural interfaces. Front. Neuroeng. 4, 1–11. doi:10.3389/fneng.2011.00011

Luckenbill-edds, L., 1997. Laminin and the mechanism of neuronal outgrowth. Brain Res. Rev. 23, 1–27.

Lundborg G, Dahlin LB, D.N., Gelberman RH, Gelberman RH, Longo FM, P.H. and V.S., 1982. Nerve regeneration in silicone chambers: Influence of gap length and of distal stump components. Exp. Neurol. 76, 361–375. doi:10.1016/0014-4886(82)90215-1

Lundborg, G., Rosén, B., 2001. Sensory relearning after nerve repair. Lancet 358, 809–810. doi:10.1016/S0140-6736(01)06001-9

Lundborg, G., Rosen, B., Dahlin, L., Danielsen, N., Holmberg, J., 1997. Tubular versus conventional repair of median and ulnar nerves in the human forearm: Early results from a prospective, randomized, clinical study. J. Hand Surg. Am. 22, 99–106. doi:10.1016/S0363-5023(05)80188-1

Lundborg, G., Rosén, B., Dahlin, L., Holmberg, J., Rosén, I., 2004. Tubular repair of the median or ulnar nerve in the human forearm: A 5 - Year follow - Up. J. Hand Surg. Am. 29 B, 100–107. doi:10.1016/j.jhsb.2003.09.018

Mackinnon, S.E., Dellon, A.L., O'Brien, J.P., 1991. Changes in nerve fibers distal to a nerve reapir in the rat sciatic nerve model. Muscle Nerve 14, 1116–1122.

MacPhee, I.J., Barker, P. a., 1997. Brain-derived Neurotrophic Factor Binding to the p75 Neurotrophin Receptor Reduces TrkA Signaling While Increasing Serine Phosphorylation in the TrkA Intracellular Domain. J. Biol. Chem. 272, 23547–23551. doi:10.1074/jbc.272.38.23547

Madduri, S., Feldman, K., Tervoort, T., Papaloïzos, M., Gander, B., 2010. Collagen nerve conduits releasing the neurotrophic factors GDNF and NGF. J. Control. release 143, 168–74. doi:10.1016/j.jconrel.2009.12.017

Madison, R.D., Archibald, S.J., Brushart, T.M., 1996. Reinnervation Accuracy of the Rat Femoral Nerve by Motor and Sensory Neurons. J. Neurosci. 16, 5698–5703.

Madison, R.D., Robinson, G. a, Chadaram, S.R., 2007. The specificity of motor neurone regeneration (preferential reinnervation). Acta Physiol. (Oxf). 189, 201–6. doi:10.1111/j.1748-1716.2006.01657.x

Makwana, M., Raivich, G., 2005. Molecular mechanisms in successful peripheral regeneration. FEBS J. 272, 2628–38. doi:10.1111/j.1742-4658.2005.04699.x

Manthorpe, M., Engvall, E.V.A., Ruoslahti, E., Longo, F.M., Davis, G.E., Varon, S., 1983. Laminin Promotes Neuritic Regeneration from Cultured Peripheral and Central Neurons. J. Cell Biol. 97.

Mao, Y., Schwarzbauer, J.E., 2005. Stimulatory effects of a three-dimensional microenvironment on cell-mediated fibronectin fibrillogenesis. J. Cell Sci. 118, 4427–36. doi:10.1242/jcs.02566

Markus, A., Patel, T.D., Snider, W.D., 2002. Neurotrophic factors and axonal growth. Curr. Opin. Neurobiol. 12, 523–531. doi:10.1016/S0959-4388(02)00372-0

Martini, R., Xin, Y., Schmitz, B., Schachner, M., 1992. The L21HNK-1 Carbohydrate Epitope is Involved in the Preferential Outgrowth of Motor Neurons on Ventral Roots and Motor Nerves. Eur. J. Neurosci. 4, 628–639.

Mauti, O., Domanitskaya, E., Andermatt, I., Sadhu, R., Stoeckli, E.T., 2007. Semaphorin6A acts as a gate keeper between the central and the peripheral nervous system. Neural Dev. 2, 28. doi:10.1186/1749-8104-2-28

McCormick, A.M., Jarmusik, N. a, Leipzig, N.D., 2015. Co-immobilization of semaphorin3A and nerve growth factor to guide and pattern axons. Acta Biomater. 28, 33–44. doi:10.1016/j.actbio.2015.09.022

Mcdonald, D.S., Zochodne, D.W., 2003. An injectable ner v e regeneration chamber for studies of unstable soluble growth factors. J Neurosci Methods 122, 171–178.

Meier, C., Parmantier, E., Brennan, A., Mirsky, R., Jessen, K.R., 1999. Developing Schwann Cells Acquire the Ability to Survive without Axons by Establishing an Autocrine Circuit Involving Insulin-Like Growth Factor , Neurotrophin-3 , and Platelet-Derived Growth Factor-BB. J. Neurosci. 19, 3847–3859.

Meisinger, C., Zeschnigk, C., Grothe, C., 1996. In Vivo and in Vitro Effect of Glucocorticoids on Fibroblast Growth Factor (FGF) -2 and FGF Receptor 1 Expression *. J. Biol. Chem. 271, 16520–16525.

Menei, P., Pean, J.M., Nerrière-Daguin, V., Jollivet, C., Brachet, P., Benoit, J.P., 2000. Intracerebral implantation of NGF-releasing biodegradable microspheres protects striatum against excitotoxic damage. Exp. Neurol. 161, 259–72. doi:10.1006/exnr.1999.7253

Meyer, C., Stenberg, L., Gonzalez-Perez, F., Wrobel, S., Ronchi, G., Udina, E., Suganuma, S., Geuna, S., Navarro, X., Dahlin, L.B., Grothe, C., Haastert-Talini, K., 2016. Chitosan-film enhanced chitosan nerve guides for long-distance regeneration of peripheral nerves. Biomaterials 76, 33–51. doi:10.1016/j.biomaterials.2015.10.040

Meyer, M., Matsuoka, I., Wetmore, C., Olson, L., Thoenen, H., 1992. Enhanced synthesis of brain-derived neurotrophic factor in the lesioned peripheral nerve: Different mechanisms are responsible for the regulation of BDNF and NGF mRNA. J. Cell Biol. 119, 45–54. doi:10.1083/jcb.119.1.45

Micera, S., 2016. Staying in Touch: Toward the Restoration of Sensory Feedback in Hand Prostheses Using Peripheral Neural Stimulation. IEEE Pulse 7, 16–19. doi:10.1109/MPUL.2016.2539760

Micera, S., Navarro, X., 2009. Bidirectional interfaces with the peripheral nervous system., 1st ed, International review of neurobiology. Elsevier Inc. doi:10.1016/S0074-7742(09)86002-9

Ming, G., Song, H., Berninger, B., Inagaki, N., Tessier-lavigne, M., Poo, M., 1999. Phospholipase C- □ and Phosphoinositide 3-Kinase Mediate Cytoplasmic Signaling in Nerve Growth Cone Guidance University of California at San Diego. Neuron 23, 139–148.

Mohiuddin, L., Delcroix, J.-D., Fernyhough, P., Tomlinson, D.R., 1999. Focally administered nerve growth factor suppresses molecular regenerative responses of axotomized peripheral afferents in rats. Neuroscience 91, 265–271. doi:10.1016/S0306-4522(98)00582-X

Molliver, D.., Wright, D.., Leitner, M.., Parsadanian, A.S., Doster, K., Wen, D., Yan, Q., Snider, W.., 1997. IB4-Binding DRG Neurons Switch from NGF to GDNF Dependence in Early Postnatal Life. Neuron 19, 849–861. doi:10.1016/S0896-6273(00)80966-6

Molofsky, A. V, Kelley, K.W., Tsai, H.-H., Redmond, S. a, Chang, S.M., Madireddy, L., Chan, J.R., Baranzini, S.E., Ullian, E.M., Rowitch, D.H., 2014. Astrocyte-encoded

positional cues maintain sensorimotor circuit integrity. Nature 509, 189–94. doi:10.1038/nature13161

Mortimer, D., Fothergill, T., Pujic, Z., Richards, L.J., Goodhill, G.J., 2008. Growth cone chemotaxis. Trends Neurosci. 31, 90–8. doi:10.1016/j.tins.2007.11.008

Mueller, B.K., 1999. Growth cone guidance: first steps towards a deeper understanding. Annu. Rev. Neurosci. 22, 351–88. doi:10.1146/annurev.neuro.22.1.351

Mukhopadhyay, G., Doherty, P., Walsh, F.S., Cracker, P.R., Filbin, M., 1994. A Novel Role for Myelin-Associated G lycoprotein as an Inhibitor of Axonal Regeneration. Neuron 13, 757–767.

Musick, K.M., Rigosa, J., Narasimhan, S., Wurth, S., Capogrosso, M., Chew, D.J., Fawcett, J.W., Micera, S., Lacour, S.P., 2015. Chronic multichannel neural recordings from soft regenerative microchannel electrodes during gait. Sci. Rep. 5, 14363. doi:10.1038/srep14363

Navarro, X., Calvet, S., Rodriguez, F., Stieglitz, T., Blau, C., Buti, M., Valderrama, E., Meyer, J., 1998. Stimulation and recording from regenerated peripheral nerves through polyimide sieve electrodes. J. Peripher. Nerv. Syst. 3, 91–101.

Navarro, X., del Valle, J., 2014. Regenerative neural interfaces for neuroprosthetic applications. Front. Neuroeng. doi:10.3389/conf.fneng.2014.11.00003

Navarro, X., Krueger, T.B., Lago, N., Micera, S., Stieglitz, T., Dario, P., 2005. A critical review of interfaces with the peripheral nervous system for the control of neuroprostheses and hybrid bionic systems. J. Peripher. Nerv. Syst. 10, 229–58. doi:10.1111/j.1085-9489.2005.10303.x

Navarro, X., Udina, E., Ceballos, D., Gold, B.G., 2001. Effects of FK506 on nerve regeneration and reinnervation after graft or tube repair of long nerve gaps. Muscle and Nerve 24, 905–915. doi:10.1002/mus.1088

Navarro, X., Verdú, E., 2004. Cell transplants and artificial guides for nerve repair, in: J.M, H.T. and D.-G. (Ed.), Brain Damage and Repair. From Molecular Research to Clinical Therapy. pp. 451–471.

Navarro, X., Vivó, M., Valero-Cabré, A., 2007. Neural plasticity after peripheral nerve injury and regeneration. Prog. Neurobiol. 82, 163–201. doi:10.1016/j.pneurobio.2007.06.005

Nectow, A.R., Marra, K.G., Kaplan, D.L., 2012. Biomaterials for the development of peripheral nerve guidance conduits. Tissue Eng. Part B. Rev. 18, 40–50. doi:10.1089/ten.TEB.2011.0240

Nerlich, A.G., Zink, A., Szeimies, U., Hagedorn, H.G., 2000. Ancient Egyptian prosthesis of the big toe. Lancet 356, 2176–2179. doi:10.1016/S0140-6736(00)03507-8

Oddo, C.M., Raspopovic, S., Artoni, F., Mazzoni, A., Spigler, G., Petrini, F., Giambattistelli, F., Vecchio, F., Miraglia, F., Zollo, L., Di Pino, G., Camboni, D., Carrozza, M.C., Guglielmelli, E., Rossini, P.M., Faraguna, U., Micera, S., 2016. Intraneural stimulation elicits discrimination of textural features by artificial fingertip in intact and amputee humans. Elife 5, 1–27. doi:10.7554/eLife.09148

Ornitz, D., Itoh, N., 2001. Fibroblast growth factors. Genome Biol 2, 1–12.

Ornitz, D.M., Xu, J., Colvin, J.S., Mcewen, D.G., Macarthur, C.A., Gao, G., Goldfarb, M., 1996. Receptor Specificity of the Fibroblast Growth Factor Family. J. Biol. Chem. 271, 15292–15297.

Orr, D.J., Smith, R.A., 1988. Neuronal maintenance and neurite extension of adult mouse neurones in non-neuronal cell-reduced cultures is dependent on substratum coating. J. Cell Sci. 555–561.

Palkovits, M., 1995. Neuropeptide messenger plasticity in the CNS neurons following axotomy. Mol. Neurobiol. 10, 91–103. doi:10.1007/BF02740669

Panetsos, F., Avendaño, C., Negredo, P., Castro, J., Bonacasa, V., 2008. Neural Prostheses : Electrophysiological and Histological Evaluation of Central Nervous System Alterations Due to Long-Term Implants of Sieve Electrodes to Peripheral Nerves in Cats. IEEE Trans Neural Syst Rehabil Eng. 16, 223–232.

Papalia, I., Geuna, S., Stagno D'Alcontres, F., Tos, P., 2007. Origin and history of end-to-side neurorrhaphy. Microsurgery. doi:10.1002/micr.20303

Pasterkamp, R.J., Giger, R.J., Verhaagen, J., 1998. Regulation of semaphorin III/collapsin-1 gene expression during peripheral nerve regeneration. Exp. Neurol. 153, 313–27. doi:10.1006/exnr.1998.6886

Paves, H., Saarma, M., 1997. Neurotrophins as in vitro growth cone guidance molecules for embryonic sensory neurons. Cell Tissue Res. 290, 285–297. doi:10.1007/s004410050933

Péan, J., Menei, P., Morel, O., Montero-Menei, C., Benoit, J., 2000. Intraseptal implantation of NGF-releasing microspheres promote the survival of axotomized cholinergic neurons. Biomaterials 21, 2097–2101.

Pfister, L. a, Papaloïzos, M., Merkle, H.P., Gander, B., 2007. Nerve conduits and growth factor delivery in peripheral nerve repair. J. Peripher. Nerv. Syst. 12, 65–82. doi:10.1111/j.1529-8027.2007.00125.x

Raivich, G., Hellweg, R., Kreutzberg, G.W., 1991. NGF receptor-mediated reduction in axonal NGF uptake and retrograde transport following sciatic nerve injury and during regeneration. Neuron 7, 151–164. doi:10.1016/0896-6273(91)90083-C

Ramer, M.S., Thompson, S.W.N., McMahon, S.B., 1999. Causes and consequences of sympathetic basket formation in dorsal root ganglia. Pain 82, S111–S120. doi:10.1016/S0304-3959(99)00144-X

Raspopovic, S., Capogrosso, M., Petrini, F.M., Bonizzato, M., Rigosa, J., Di Pino, G., Carpaneto, J., Controzzi, M., Boretius, T., Fernandez, E., Granata, G., Oddo, C.M., Citi, L., Ciancio, a. L., Cipriani, C., Carrozza, M.C., Jensen, W., Guglielmelli, E., Stieglitz, T., Rossini, P.M., Micera, S., 2014. Restoring Natural Sensory Feedback in Real-Time Bidirectional Hand Prostheses. Sci. Transl. Med. 6, 222ra19–222ra19. doi:10.1126/scitranslmed.3006820

Ray, W.Z., Mackinnon, S.E., 2010. Management of nerve gaps: Autografts, allografts, nerve transfers, and end-to-side neurorrhaphy. Exp. Neurol. 223, 77–85. doi:10.1016/j.expneurol.2009.03.031

Reichardt, L.F., 2006. Neurotrophin-regulated signalling pathways. Philos. Trans. R. Soc. Lond. B. Biol. Sci. 361, 1545–64. doi:10.1098/rstb.2006.1894

Reyes, O., Sosa, I., Kuffler, D., 2005. Promoting neurological recovery following a traumatic peripheral nerve injury. P. R. Health Sci. J. 24, 215–23.

Rich, M., Lichtman, J.W., 1989. In Vivo Visualizaton of Pre- and Postsynaptic Changes During Synapse Elimination in Reinnervated Mouse Muscle. J. Neurosci. 9, 1781–1805.

Richner, M., Ulrichsen, M., Elmegaard, S.L., 2014. Peripheral Nerve Injury Modulates Neurotrophin Signaling in the Peripheral and Central Nervous System. Mol. Neurobiol. 50, 945–970. doi:10.1007/s12035-014-8706-9

Rishal, I., Fainzilber, M., 2014. Axon-soma communication in neuronal injury. Nat. Rev. Neurosci. 15, 32–42. doi:10.1038/nrn3609

Riso, R.R., 1999. Strategies for providing upper extremity amputees with tactile and hand position feedback – moving closer to the bionic arm. Technol Heal. Care. 7, 401–409.

Roam, J.L., Yan, Y., Nguyen, P.K., Kinstlinger, I.S., Leuchter, M.K., Hunter, D. a, Wood, M.D., Elbert, D.L., 2015. A modular, plasmin-sensitive, clickable poly(ethylene glycol)-heparin-laminin microsphere system for establishing growth factor gradients in nerve guidance conduits. Biomaterials 72, 112–24. doi:10.1016/j.biomaterials.2015.08.054

Robinson, G. a, Madison, R.D., 2004. Motor neurons can preferentially reinnervate cutaneous pathways. Exp. Neurol. 190, 407–13. doi:10.1016/j.expneurol.2004.08.007

Rogers, S.L., Letourneau, P.C., Furcht, L.T., 1987. Selective Interaction of Peripheral and Central Nervous System Cells with Two Distinct Cell-binding Domains of Fibronectin. J. Cell Biol. 105, 1435–1442.

Romero-Ortega, M., Kanneganti, A., Bendale, G., Seifert, J., Bredeson, S., Troyk, P., Deku, F., Cogan, S., 2015. Chronic and low charge injection wireless intraneural stimulation in vivo. Conf Proc IEEE Eng Med Biol Soc. 1013–6. doi:10.1109/EMBC.2015.7318536

Rosberg, H.-E., Carlsson, K.S., Dahlin, L.B., 2005. Prospective study of patients with injuries to the hand and forearm: costs, function, and general health. Scand. J. Plast. Reconstr. Surg. Hand Surg. 39, 360–9. doi:10.1080/02844310500340046

Rosner, B.I., Siegel, R. a., Grosberg, a., Tranquillo, R.T., 2003. Rational Design of Contact Guiding, Neurotrophic Matrices for Peripheral Nerve Regeneration. Ann. Biomed. Eng. 31, 1383–1401. doi:10.1114/1.1626118

Rossini, P.M., Micera, S., Benvenuto, A., Carpaneto, J., Cavallo, G., Citi, L., Cipriani, C., Denaro, L., Denaro, V., Di Pino, G., Ferreri, F., Guglielmelli, E., Hoffmann, K.-P., Raspopovic, S., Rigosa, J., Rossini, L., Tombini, M., Dario, P., 2010. Double nerve intraneural interface implant on a human amputee for robotic hand control. Clin. Neurophysiol. 121, 777–83. doi:10.1016/j.clinph.2010.01.001

Rutten, W.L.C., 2002. Selective electrical interfaces with the nervous system. Annu. Rev. Biomed. Eng. 4, 407–452. doi:10.1146/annurev.bioeng.4.020702.153427

Sahenk, Z., Oblinger, J., Edwards, C., 2008. Neurotrophin-3 deficient Schwann cells impair nerve regeneration. Exp. Neurol. 212, 552–6. doi:10.1016/j.expneurol.2008.04.015

Sahenk, Z., Seharaseyon, J., Mendell, J.R., 1994. CNTF potentiates peripheral nerve regeneration. Brain Res. 655, 246–250. doi:10.1016/0006-8993(94)91621-7

Sakiyama-Elbert, S.E., Hubbell, J. a., 2000. Controlled release of nerve growth factor from a heparin-containing fibrin-based cell ingrowth matrix. J. Control. Release 69, 149–158. doi:10.1016/S0168-3659(00)00296-0

Salonen, V., Aho, H., Peltonen, J., 1988. Quantitation of Schwann cells and endoneurial fibroblast-like cells after experimental nerve trauma. Acta Neuropathol 75, 331–336.

Sameem, M., Wood, T.J., Bain, J.R., 2011. A systematic review on the use of fibrin glue for peripheral nerve repair. Plast. Reconstr. Surg. 127, 2381–2390. doi:10.1097/PRS.0b013e3182131cf5

Sanes, J.R., 1989. Extracellular matrix molecules that influence neural development. Ann. Rev. Neurosci. 491–516.

Santos, X., Rodrigo, J., Hontanilla, B., Bilbao, G., 1998. Evaluation of peripheral nerve regeneration by nerve growth factor locally administered with a novel system. J. Neurosci. Methods 85, 119–127. doi:10.1016/S0165-0270(98)00130-7

Schnell, E., Klinkhammer, K., Balzer, S., Brook, G., Klee, D., Dalton, P., Mey, J., 2007. Guidance of glial cell migration and axonal growth on electrospun nanofibers of poly-epsilon-caprolactone and a collagen/poly-epsilon-caprolactone blend. Biomaterials 28, 3012–25. doi:10.1016/j.biomaterials.2007.03.009

Schultz, A.E., Kuiken, T. a, 2011. Neural interfaces for control of upper limb prostheses: the state of the art and future possibilities. PM R 3, 55–67. doi:10.1016/j.pmrj.2010.06.016

Seddon, H.J., 1943. Three types of nerve injury. Brain 66, 237–288. doi:10.1093/brain/66.4.237

Serini, G., Bussolino, F., 2004. Common cues in vascular and axon guidance. Physiology 19, 348–354.

Singh, P., Carraher, C., Schwarzbauer, J.E., 2010. Assembly of fibronectin extracellular matrix. Annu. Rev. Cell Dev. Biol. 26, 397–419. doi:10.1146/annurev-cellbio-100109-104020

Skene, J.H., 1989. Axonal growth-associated proteins. Annu. Rev. Neurosci. 12, 127–56. doi:10.1146/annurev.ne.12.030189.001015

Song, H., Ming, G., Poo, M., Shiro, M., Tomb, J., White, O., Kerlavage, A.R., Clayton, R.A., Sutton, G.G., Fleischmann, R.D., Ketchum, K.A., Klenk, H.P., Gill, S., Dougherty, B.A., Nelson, K., Quackenbush, J., Zhou, L., Kirkness, E.F., Peterson, S., Loftus, B., Richardson, D., Dodson, R., Khalak, H.G., Glodek, A., Mckenney, K., Fitzegerald, L.M., Lee, N., Adams, M.D., Hickey, E.K., Berg, D.E., Gocayne, J.D., Utterback, T.R., Peterson, J.D., Kelley, J.M., Cotton, M.D., Weidman, J.M., Fujii, C., Bowman, C., Watthey, L., Wallin, E., Hayes, W.S., Borodovsky, M., Karp, P.D., Smith, H.O., Fraser, C.M., Venter, J.C., Bergman, M.I., 1997. cAMP-induced switching in turning direction of nerve growth cones corrections Synthesis and X-ray structure of errata The complete genome sequence of the gastric pathogen Helicobacter pylori Measurements of elastic anisotropy due to solidification texturi. Nature 389, 1211–1212.

Song, H.J., Poo, M.M., 1999. Signal transduction underlying growth cone guidance by diffusible factors. Curr. Opin. Neurobiol. doi:10.1016/S0959-4388(99)80052-X

Sperry, R.W., 1963. Chemoaffinity in the orderly growth of nerve fiber patterns and connections. Proc Natl Acad Sci U S A 50, 703–710.

Srinivasan, A., Guo, L., Bellamkonda, R., 2011. Regenerative Microchannel Electrode Array for Peripheral Nerve Interfacing 253–256.

Srinivasan, A., Tahilramani, M., Bentley, J.T., Gore, R.K., Millard, D.C., Mukhatyar, V.J., Joseph, A., Haque, A.S., Stanley, G.B., English, A.W., Bellamkonda, R. V, 2015. Microchannel-based regenerative scaffold for chronic peripheral nerve interfacing in amputees. Biomaterials 41, 151–65. doi:10.1016/j.biomaterials.2014.11.035

Stankus, J.J., Guan, J., Fujimoto, K., Wagner, W.R., 2006. Microintegrating smooth muscle cells into a biodegradable, elastomeric fiber matrix. Biomaterials 27, 735–44. doi:10.1016/j.biomaterials.2005.06.020

Sterne, G.D., Coulton, G.R., Brown, R. a., Green, C.J., Terenghi, G., 1997. Neurotrophin-3–enhanced Nerve Regeneration Selectively Improves Recovery of Muscle Fibers Expressing Myosin Heavy Chains 2b. J. Cell Biol. 139, 709–715. doi:10.1083/jcb.139.3.709

Sternel, G.D., Brown, R.A., Green, C.J., Terenghi, G., 1997. Neurotrophin-3 Delivered Locally via Fibronectin Mats Enhances Peripheral Nerve Regeneration. Eur. J. Neurosci. 9, 1388–1396.

Stoll, G., Müller, H.W., 1999. Nerve Injury, Axonal Degeneration and Neural Regeneration: Basic Insights. Brain Pathol. 9, 313–325. doi:10.1111/j.1750-3639.1999.tb00229.x

Sunderland, S., 1990. The anatomy and physiology of nerve injury. Muscle Nerve 13, 771–784. doi:10.1002/mus.880130903

Tajdaran, K., Gordon, T., Wood, M.D., Shoichet, M.S., Borschel, G.H., 2015. A glial cell line-derived neurotrophic factor delivery system enhances nerve regeneration across acellular nerve allografts. Acta Biomater. doi:10.1016/j.actbio.2015.10.001

Takahashi, Y., Maki, Y., Yoshizu, T., Tajima, T., 1999. BOTH STUMP AREA AND VOLUME OF DISTAL SENSORY NERVE SEGMENTS INFLUENCE THE REGENERATION OF SENSORY AXONS IN RATS. Scand J Plast Reconstr Hand Surg 177–180.

Tan, D.W., Schiefer, M.A., Keith, M.W., Anderson, J.R., Tyler, J., Tyler, D.J., 2014. NEUROPROSTHETICS A neural interface provides long-term stable natural touch perception. Sci Transl Med 6, 1–11.

Tanaka, K., Zhang, Q.-L., Webster, H. deF., 1992. Myelinated fiber regeneration after sciatic nerve crush: Morphometric observations in young adult and aging mice and the effects of macrophage suppression and conditioning lesions. Exp. Neurol. 118, 53–61. doi:10.1016/0014-4886(92)90022-I

Tang, B.L., 2003. Inhibitors of neuronal regeneration: mediators and signaling mechanisms. Neurochem. Int. 42, 189–203. doi:10.1016/S0197-0186(02)00094-3

Tannemaat, M.R., Eggers, R., Hendriks, W.T., de Ruiter, G.C.W., van Heerikhuize, J.J., Pool, C.W., Malessy, M.J. a, Boer, G.J., Verhaagen, J., 2008. Differential effects of lentiviral vector-mediated overexpression of nerve growth factor and glial cell line-derived neurotrophic factor on regenerating sensory and motor axons in the transected peripheral nerve. Eur. J. Neurosci. 28, 1467–79. doi:10.1111/j.1460-9568.2008.06452.x

Taylor, C. a, Braza, D., Rice, J.B., Dillingham, T., 2008. The incidence of peripheral nerve injury in extremity trauma. Am. J. Phys. Med. Rehabil. 87, 381–385. doi:10.1097/PHM.0b013e31815e6370

Tessier-Lavigne, M., Goodman, C., 1996. The molecular biology of axon guidance. Science (80-.). 274, 1123–33.

Tetzlaff, W., Leonard, C., Krekoski, C. a, Parhad, I.M., Bisby, M. a, 1996. Reductions in motoneuronal neurofilament synthesis by successive axotomies: a possible explanation for the conditioning lesion effect on axon regeneration. Exp. Neurol. 139, 95–106. doi:10.1006/exnr.1996.0084

Theeuwes, F., Yum, S.., 1976. Principles of the design and operation of generic osmotic pumps for the delivery of semisolid or liquid drug formulations. Ann. Biomed. Eng. 4, 343–53.

Tofaris, G.K., Patterson, P.H., Jessen, K.R., Mirsky, R., 2002. Denervated Schwann Cells Attract Macrophages by Secretion of Leukemia Inhibitory Factor (LIF) and

Monocyte Chemoattractant Protein-1 in a Process Regulated by Interleukin-6 and LIF. J. Neurosci. 22, 6696–6703.

Tria, M.A., Fusco, M., Vantini, G., Mariot, R., 1994. Pharmacokinetics of nerve growth factor (NGF) following different routes of administration to adult rats. Exp. Neurol. 127, 178–183. doi:10.1006/exnr.1994.1093

Tucker, B. a., Mearow, K.M., 2008. Peripheral Sensory Axon Growth: From Receptor Binding to Cellular Signaling. Can. J. Neurol. Sci. 35, 551–566. doi:10.1017/S0317167100009331

Uschold, T., Robinson, G. a, Madison, R.D., 2007. Motor neuron regeneration accuracy: balancing trophic influences between pathways and end-organs. Exp. Neurol. 205, 250–6. doi:10.1016/j.expneurol.2007.02.005

Usoskin, D., Furlan, A., Islam, S., Abdo, H., Lönnerberg, P., Lou, D., Hjerling-leffler, J., Haeggström, J., Kharchenko, O., Kharchenko, P. V, Linnarsson, S., Ernfors, P., 2014. r e so u r c e Unbiased classification of sensory neuron types by large-scale single-cell RNA sequencing. Nat. Neurosci. 18, 145–153. doi:10.1038/nn.3881

Vaegter, C.B., 2014. Neurotrophins and their receptors in satellite glial cells following nerve injury. Neural Regen. Res. 9, 2039–2039. doi:10.4103/1673-5374.147924

Valero-Cabré, A., Navarro, X., 2002. Functional impact of axonal misdirection after peripheral nerve injuries followed by graft or tube repair. J. Neurotrauma 19, 1475–85. doi:10.1089/089771502320914705

Vanlair, C., 1882. De la régénération des nerfs périphériques par le procédé de la suture tubulaire. Arch Biol Paris 3, 379–496.

Vermeren, M.M., Cook, G.M., Johnson, a R., Keynes, R.J., Tannahill, D., 2000. Spinal nerve segmentation in the chick embryo: analysis of distinct axon-repulsive systems. Dev. Biol. 225, 241–52. doi:10.1006/dbio.2000.9820

Vleggeert-Lankamp, C.L. a M., de Ruiter, G.C.W., Wolfs, J.F.C., Pêgo, a P., Feirabend, H.K.P., Lakke, E. a J.F., Malessy, M.J. a, 2005. Type grouping in skeletal muscles after experimental reinnervation: another explanation. Eur. J. Neurosci. 21, 1249–56. doi:10.1111/j.1460-9568.2005.03954.x

Vögelin, E., Baker, J.M., Gates, J., Dixit, V., Constantinescu, M. a, Jones, N.F., 2006. Effects of local continuous release of brain derived neurotrophic factor (BDNF) on peripheral nerve regeneration in a rat model. Exp. Neurol. 199, 348–53. doi:10.1016/j.expneurol.2005.12.029

Wallquist, W., Patarroyo, M., Thams, S., Carlstedt, T., Stark, B., Cullheim, S., Hammarberg, H., 2002. Laminin chains in rat and human peripheral nerve: distribution and regulation during development and after axonal injury. J. Comp. Neurol. 454, 284–93. doi:10.1002/cne.10434

Wang, G.-Y., Hirai, K.-I., Shimada, H., 1992. The role of laminin, a component of Schwann cell basal lamina, in rat sciatic nerve regeneration within antiserum-treated nerve grafts. Brain Res. 570, 116–125. doi:10.1016/0006-8993(92)90571-P

Wang, H.U., Anderson, D.J., 1997. Repulsive Guidance of Trunk Neural Crest Migration and Motor Axon Outgrowth. Neuron 18, 383–396.

Warwick, K., Gasson, M., Hutt, B., Goodhew, I., Kyberd, P., Abdrews, B., Teddy, P., Shad, A., 2003. The application of implant technology for cybernetic systems. Arch. Neurol. 60, 1369–1373. doi:10.1001/archneur.60.10.1369

Wasserschaff, M., 1990. Coordination of reinnervated muscle and reorganization of spinal cord motoneurons after nerve transection in mice. Brain Res. 515, 241–246. doi:10.1016/0006-8993(90)90602-8

Weber, R. a, Breidenbach, W.C., Brown, R.E., Jabaley, M.E., Mass, D.P., 2000. A randomized prospective study of polyglycolic acid conduits for digital nerve reconstruction in humans. Plast. Reconstr. Surg. 106, 1036–1045; discussion 1046–1048. doi:10.1097/00006534-200109150-00056

Werner, A., Willem, M., Jones, L.L., Kreutzberg, G.W., Mayer, U., 2000. Impaired Axonal Regeneration in ␣ 7 Integrin-Deficient Mice. J. Neurosci. 20, 1822–1830.

Whitehead, T.J., Sundararaghavan, H.G., 2014. Electrospinning Growth Factor Releasing Microspheres into Fibrous Scaffolds. J. Vis. Exp. 1–9. doi:10.3791/51517

Wilhelm, J.C., Xu, M., Cucoranu, D., Chmielewski, S., Holmes, T., Lau, K.S., Bassell, G.J., English, A.W., 2012. Cooperative roles of BDNF expression in neurons and Schwann cells are modulated by exercise to facilitate nerve regeneration. J. Neurosci. 32, 5002–9. doi:10.1523/JNEUROSCI.1411-11.2012

Williams, L.R., Longo, F.M., Powell, H.C., Lundborg, G., Varon, S., 1983. Spatial-temporal progress of peripheral nerve regeneration within a silicone chamber: parameters for a bioassay. J. Comp. Neurol. 218, 460–470. doi:10.1002/cne.902180409

Witzel, C., Rohde, C., Brushart, T.M., 2005. Pathway sampling by regenerating peripheral axons. J. Comp. Neurol. 485, 183–90. doi:10.1002/cne.20436

Wong, J., Oblinger, M., 1990. A comparison of peripheral and central axotomy effects on neurofilament and tubulin gene expression in rat dorsal root ganglion neurons. J. Neurosci. 10, 2215–2222.

Wood, M.D., Gordon, T., Kim, H., Szynkaruk, M., Phua, P., Lafontaine, C., Kemp, S.W., Shoichet, M.S., Borschel, G.H., 2013. Fibrin gels containing GDNF microspheres increase axonal regeneration after delayed peripheral nerve repair. Regen. Med. 8, 27–37. doi:10.2217/rme.12.105

Worzfeld, T., Offermanns, S., 2014. Semaphorins and plexins as therapeutic targets. Nat. Rev. Drug Discov. 13, 603–21. doi:10.1038/nrd4337

Wright, D.E., Snider, W.D., 1995. Neurotrophin receptor mRNA expression defines distinct populations of neurons in rat dorsal root ganglia. J. Comp. Neurol. 351, 329–38. doi:10.1002/cne.903510302

Xiang, Z., Sheshadri, S., Lee, S.-H., Wang, J., Xue, N., Thakor, N. V., Yen, S.-C., Lee, C., 2016. Mapping of Small Nerve Trunks and Branches Using Adaptive Flexible Electrodes. Adv. Sci. n/a–n/a. doi:10.1002/advs.201500386

Xu, X., Yu, H., Gao, S., Mao, H.-Q., Leong, K.W., Wang, S., 2002. Polyphosphoester microspheres for sustained release of biologically active nerve growth factor. Biomaterials 23, 3765–3772. doi:10.1016/S0142-9612(02)00116-3

Yang, Y., Chen, X., Ding, F., Zhang, P., Liu, J., Gu, X., 2007. Biocompatibility evaluation of silk fibroin with peripheral nerve tissues and cells in vitro. Biomaterials 28, 1643–1652. doi:10.1016/j.biomaterials.2006.12.004

Yannas, I. V., Hill, B.J., 2004. Selection of biomaterials for peripheral nerve regeneration using data from the nerve chamber model. Biomaterials 25, 1593–1600. doi:10.1016/S0142-9612(03)00505-2

Yuan, X., Jin, M., Xu, X., Song, Y., Wu, C., Poo, M., Duan, S., 2003. Signalling and crosstalk of Rho GTPases in mediating axon guidance. Nat. Cell Biol. 5, 1–8. doi:10.1038/ncb895

Zhang, J.-Y., Luo, X.-G., Xian, C.J., Liu, Z.-H., Zhou, X.-F., 2000. Endogenous BDNF is required for myelination and regeneration of injured sciatic nerve in rodents. Eur. J. Neurosci. 12, 4171–4180. doi:10.1111/j.1460-9568.2000.01312.x

Zhao, Z., Alam, S., Oppenheim, R.W., Prevette, D.M., Evenson, A., Parsadanian, A., 2004. Overexpression of glial cell line-derived neurotrophic factor in the CNS rescues motoneurons from programmed cell death and promotes their long-term survival following axotomy. Exp. Neurol. 190, 356–72. doi:10.1016/j.expneurol.2004.06.015